APPENDIX 3-F

IWV ARSENIC DATA

(Page Intentionally Left Blank)

Compiled IWV Arsenic Data

Unique Well Name	Alternative Well Name	Sample Date	Arsenic (mg/L)	Analysis Type	Arsenic Reference
24S38E16J02	Sawmill Well #1	6/16/1982	0.011		B
24S38E21A01	USBR-10-S	9/1/1992	0.016		USBR
24S38E21A02	USBR-10-S/M	9/1/1992	0.003		USBR
24S38E21A03	USBR-10-M/D	9/1/1992	0.008		USBR
24S38E21A04	USBR-10-D	9/2/1992	0.010		USBR
24S38E33J02	Pearsonville Well	6/15/1982	0.008		B
24S40E21K01	TTIWV-MW14	2/17/2002	0.056	Est	TTEMI
24S40E21K01	TTIWV-MW14	8/22/2002	0.058		Tri
24S40E36A	TTIWV-MW13	2/16/2002	0.076	Est	TTEMI
24S40E36A	TTIWV-MW13	2/16/2002	0.090	Est	TTEMI
24S40E36A	TTIWV-MW13	12/17/2002	0.085		Tri
25S10E11K01		6/9/1982	0.230		B
25S38E12L01	USBR-06-S	1/10/1992	0.195		USBR
25S38E12L02	USBR-06-M	1/10/1992	0.135		USBR
25S38E12L03	USBR-06-D	1/10/1992	0.075		USBR
25S38E13L01		6/15/1982	0.002		B
25S38E25J01	NR1-S (Neal Ranch-1-S)	2/2/1991	0.010		USBR
25S38E25J02	NR1-M (Neal Ranch-1-M)	2/26/1991	0.028		USBR
25S38E25J03	NR1-D (Neal Ranch-1-D)	2/26/1991	0.130		USBR
25S38E34G02	USBR-05-M	1/6/1992	0.080		USBR
25S38E34G03	USBR-05-D	1/6/1992	0.025		USBR
25S38E36G01	NR2-S (Neal Ranch-2-S)	2/26/1991	0.010		USBR
25S38E36G02	NR2-M (Neal Ranch-2-M)	2/26/1991	0.012		USBR
25S38E36G03	NR2-D (Neal Ranch-2-D)	2/26/1991	0.460		USBR
25S40E08A01	USGS-354658117411201	5/16/1979	0.150		B
25S40E08A01	USGS-354658117411201	5/20/1980	0.170		B
25S40E08A01	USGS-354658117411201	6/9/1982	0.170		B
25S40E14H01	TTIWV-MW12	2/16/2002	0.099	Est	TTEMI
25S40E14H01	TTIWV-MW12	2/16/2002	0.104	Est	TTEMI
25S40E14H01	TTIWV-MW12	2/16/2002	0.135	Est	TTEMI
25S40E14H01	TTIWV-MW12	2/16/2002	0.127	Est	TTEMI
25S40E14H01	TTIWV-MW12	8/23/2002	0.126		Tri
25S40E18R01	TTBK-MW12	5/16/1979	0.220		B
25S40E18R01	TTBK-MW12	5/20/1980	0.088		B
25S40E18R01	TTBK-MW12	6/9/1982	0.054		B
25S40E18R01	TTBK-MW12	11/5/1989	0.027		Tri
25S40E20F01	USGS-354450117415301	5/16/1979	0.044		B
25S40E20F01	USGS-354450117415301	5/20/1980	0.079		B
25S40E20F01	USGS-354450117415301	6/9/1982	0.042		B
25S40E30E01	TTBK-MW14	5/11/1999	0.042		Tri
25S40E33L01	USGS-354258117403901	5/21/1980	2.000		B
25S40E33L01	USGS-354258117403901	6/9/1982	2.900		B

Compiled IWV Arsenic Data

Unique Well Name	Alternative Well Name	Sample Date	Arsenic (mg/L)	Analysis Type	Arsenic Reference
25S40E33L02	USGS-354258117403902	5/31/1979	0.002		B
25S40E33L02	USGS-354258117403902	5/22/1980	0.003		B
25S40E33L02	USGS-354258117403902	6/9/1982	0.007		B
25S40E35D01	TTBK-MW13	2/16/2002	0.500	Est	TTEMI
25S40E35D01	TTBK-MW13	2/16/2002	0.052	Est	TTEMI
25S40E35D01	TTBK-MW13	2/16/2002	0.500	Est	Tri
26S38E35B01		6/15/1982	0.005		B
26S39E26A01	USBR-04	10/30/1990	0.015		USBR
26S39E26A02-D	TTIWV-MW01 (D)	2/17/2002	0.015	Est	TTEMI
26S39E26A02-D	TTIWV-MW01 (D)	2/17/2002	0.005	ND	TTEMI
26S39E26A02-I	TTIWV-MW01 (I)	2/17/2002	0.005	ND	TTEMI
26S39E27D01	MW 32-S	10/17/1991	0.026		USBR
26S39E27D02	MW 32-S/M	10/18/1991	0.036		USBR
26S39E27D03	MW 32-M/D	10/21/1991	0.010		USBR
26S39E27D04	MW 32-D	10/21/1991	0.061		USBR
26S40E01A02		6/9/1982	0.640		B
26S40E01J01	USGS-354155117370201	5/16/1979	0.028		B
26S40E01J01	USGS-354155117370201	5/21/1980	0.180		B
26S40E01J01	USGS-354155117370201	6/10/1982	0.180		B
26S40E01Q01		5/16/1979	0.005		B
26S40E01Q01		5/20/1980	0.001		B
26S40E01Q02		5/15/1979	0.009		B
26S40E01Q02		5/20/1980	0.008		B
26S40E01Q02		6/11/1982	0.020		B
26S40E06D02		6/18/1996	0.050		H96
26S40E10F01	USGS-354125117393701	6/5/1979	0.009		B
26S40E10F01	USGS-354125117393701	5/20/1980	0.008		B
26S40E10F01	USGS-354125117393701	6/9/1982	0.003		B
26S40E11J01	USGS-354108117380801	5/28/1980	0.029		B
26S40E12A01		6/29/1978	0.016		B
26S40E12A01		5/17/1979	0.001		B
26S40E12A01		5/21/1980	0.001		B
26S40E12D01		5/24/1996	1.100		H96
26S40E12G01		6/29/1978	0.004		B
26S40E12G01		5/27/1980	0.001		B
26S40E12G01		6/11/1982	0.020		B
26S40E12Q01	USGS-354101117372201	6/29/1978	0.004		B
26S40E12Q01	USGS-354101117372201	5/15/1979	0.005		B
26S40E12Q01	USGS-354101117372201	5/27/1980	0.018		B
26S40E12R01		6/29/1978	0.003		B
26S40E12R01		6/6/1979	0.002		B
26S40E12R01		5/27/1980	0.002		B

Compiled IWV Arsenic Data

Unique Well Name	Alternative Well Name	Sample Date	Arsenic (mg/L)	Analysis Type	Arsenic Reference
26S40E13C01	USGS-354037117373201	6/29/1978	0.003		B
26S40E13C01	USGS-354037117373201	6/6/1979	0.002		B
26S40E13C01	USGS-354037117373201	5/21/1980	0.002		B
26S40E13C01	USGS-354037117373201	6/11/1982	0.001		B
26S40E13M01	USGS-354010117375601	5/21/1980	0.001		B
26S40E14B01	USGS-354039117382801	5/15/1979	0.230		B
26S40E14B01	USGS-354039117382801	5/20/1980	0.310		B
26S40E14B01	USGS-354039117382801	6/9/1982	0.230		B
26S40E14B01	USGS-354039117382801	5/24/1996	1.200		H96
26S40E14L01	USGS-354020117384201	5/15/1979	0.011		B
26S40E14L01	USGS-354020117384201	5/20/1980	0.042		B
26S40E15E01	USGS-354036117400701	5/31/1979	0.013		B
26S40E15E01	USGS-354036117400701	5/22/1980	0.018		B
26S40E15E02	USGS-354033117400601	6/10/1982	0.014		B
26S40E15N01	USGS-354002117400601	5/31/1979	0.006		B
26S40E15N01	USGS-354002117400601	5/22/1980	0.033		B
26S40E15N01	USGS-354002117400601	5/22/1980	0.008		B
26S40E15N02	USGS-354011117400001	6/14/1982	0.006		B
26S40E16K	TTIWV-MW06	2/17/2002	0.062	Est	TTEMI
26S40E16K	TTIWV-MW06	2/17/2002	0.036	Est	TTEMI
26S40E19N	TTIWV-MW02 (s)	2/18/2002	0.011	Est	TTEMI
26S40E19N	TTIWV-MW02 (S)	8/22/2002	0.012		Tri
26S40E20A	TTBK-MW04	11/6/1998	0.006	Est	Tri
26S40E22H01	USGS-353942117390801	5/15/1979	0.910		B
26S40E22H01	USGS-353942117390801	5/20/1980	0.990		B
26S40E22H01	USGS-353942117390801	6/8/1982	0.880		B
26S40E22H01	USGS-353942117390801	5/24/1996	0.050		H96
26S40E22H02	USGS-353942117390802	5/15/1979	0.019		B
26S40E22H02	USGS-353942117390802	5/20/1980	0.094		B
26S40E22H02	USGS-353942117390802	6/8/1982	0.100		B
26S40E22H03	USGS-353942117390803	5/15/1979	0.091		B
26S40E22H03	USGS-353942117390803	5/20/1980	0.190		B
26S40E22H03	USGS-353942117390803	6/8/1982	0.130		B
26S40E22N01	USGS-353913117400601	5/31/1979	0.170		B
26S40E22N01	USGS-353913117400601	5/23/1980	0.250		B
26S40E22P01	USGS-353908117395201	5/17/1979	0.008		B
26S40E22P01	USGS-353908117395201	5/28/1980	0.013		B
26S40E22P02	USGS-353908117394001	5/29/1996	0.030		H96
26S40E23A01	USGS-353948117381001	5/17/1979	0.081		B
26S40E23A01	USGS-353948117381001	5/21/1980	0.084		B
26S40E23A01	USGS-353948117381001	6/10/1982	0.080		B
26S40E23A02	USGS-353948117381002	5/17/1979	0.016		B

Compiled IWV Arsenic Data

Unique Well Name	Alternative Well Name	Sample Date	Arsenic (mg/L)	Analysis Type	Arsenic Reference
26S40E23A02	USGS-353948117381002	5/21/1980	0.019		B
26S40E23A02	USGS-353948117381002	6/10/1982	0.006		B
26S40E23G01	USGS-353942117383101	5/29/1996	1.400		H96
26S40E24C01	USGS-353953117373701	5/21/1980	0.004		B
26S40E24C01	USGS-353953117373701	6/10/1982	0.036		B
26S40E25C	TT64-MW01	6/7/2002	0.540		Tri
26S40E26F01		6/14/1982	0.013		B
26S40E26N02	TTBK-MW02	2/18/2002	0.005	Est	TTEMI
26S40E26N02	TTBK-MW02	8/24/2002	0.014		Tri
26S40E26N02	TTBK-MW02	2/18/2020	0.009	Est	TTEMI
26S40E28J01	USGS-353828117401301	6/29/1978	0.001		B
26S40E28J01	USGS-353828117401301	6/1/1979	0.001		B
26S40E28J01	USGS-353828117401301	5/27/1980	0.008		B
26S40E35H02		8/5/1996	0.040		H96
26S40E36A01	USGS-353801117370701	6/29/1978	0.024		B
26S40E36A01	USGS-353801117370701	6/6/1979	0.013		B
26S40E36A01	USGS-353801117370701	5/27/1980	0.013		B
26S40E36A01	USGS-353801117370701	6/14/1982	0.034		B
26S41E06P01	TTIWV-MW09	2/16/2002	0.022	Est	TTEMI
26S41E06P01	TTIWV-MW09	5/28/2002	0.035	St. Add	Tri
26S41E06P01	TTIWV-MW09	5/28/2002	0.031	St. Add	Tri
26S41E07D01		6/29/1978	0.008		B
26S41E07D01		5/17/1979	0.001		B
26S41E07D01		5/21/1980	0.003		B
26S41E07E01		6/29/1978	0.022		B
26S41E07E01		5/17/1979	0.016		B
26S41E07E01		5/20/1980	0.017		B
26S41E07E01		6/10/1982	0.008		B
26S41E07G01		6/29/1978	0.018		B
26S41E07G01		5/17/1979	0.018		B
27S38E02C02	USBR-02-M	10/30/1990	0.017		USBR
27S38E02C03	USBR-02-D	10/30/1990	0.014		USBR
27S38E23F01	USBR-01-S	3/2/1991	0.010		USBR
27S38E23F02	USBR-01-S/M	3/18/1991	0.010		USBR
27S38E23F03	USBR-01-M/D	3/18/1991	0.010		USBR
27S38E23F04	USBR-01-D	3/18/1991	0.010		USBR
27S39E11D01	USBR-03-S	3/18/1991	0.010		USBR
27S39E11D02	USBR-03-M	3/18/1991	0.010		USBR
27S39E11D03	USBR-03-D	3/18/1991	0.010		USBR
27S40E01G01		5/29/1996	0.090		H96
27S40E02J01	DMP Cemetery	6/28/1978	0.026		B
27S40E02J01	DMP Cemetery	6/1/1979	0.024		B

Compiled IWV Arsenic Data

Unique Well Name	Alternative Well Name	Sample Date	Arsenic (mg/L)	Analysis Type	Arsenic Reference
27S40E02J01	DMP Cemetery	5/23/1980	0.038		B
27S40E03R01	USGS-353630117390901	6/29/1978	0.026		B
27S40E03R01	USGS-353630117390901	6/6/1979	0.013		B
27S40E03R01	USGS-353630117390901	5/27/1980	0.025		B
27S40E03R01	USGS-353630117390901	6/15/1982	0.012		B
27S40E10R01	USGS-353540117390601	6/28/1978	0.003		B
27S40E10R01	USGS-353540117390601	5/28/1980	0.001		B
ITC02-MW21	ITC02-MW21	5/11/1999	0.006	Est	Tri
JMM12-MW08	JMM12-MW08	2/19/2002	0.022	Est	TTEMI
JMM12-MW08	JMM12-MW08	2/19/2002	0.025	Est	TTEMI
MK12-MW12	MK12-MW12	11/12/1999	0.011		Tri
MK12-MW16	MK12-MW16	11/14/1999	0.012		Tri
MK29-MW13	MK29-MW13	2/15/2002	0.028	Est	TTEMI
MK29-MW13	MK29-MW13	2/15/2002	0.025	Est	TTEMI
MK29-MW13	MK29-MW13	6/6/2002	0.047	St. Add	Tri
MK69-MW01	MK69-MW01	11/15/1999	0.087		Tri
MK69-MW01	MK69-MW01	2/18/2002	0.053		TTEMI
MK69-MW01	MK69-MW01	2/18/2002	0.055		TTEMI
MK69-MW02	MK69-MW02	2/18/2002	0.041		TTEMI
MK69-MW02	MK69-MW02	2/18/2002	0.029		TTEMI
MKFL-MW01	MKFL-MW01	2/20/2002	0.058		TTEMI
MKFL-MW01	MKFL-MW01	2/20/2002	0.075	St. Add	TTEMI
MKFL-MW01	MKFL-MW01	4/1/2005	0.348		Tri
MKFL-MW02	MKFL-MW02	2/20/2002	0.023	Est	TTEMI
MKFL-MW02	MKFL-MW02	2/20/2002	0.020	Est	TTEMI
RLS12-MW04	RLS12-MW04	2/19/2002	0.012	Est	TTEMI
RLS12-MW04	RLS12-MW04	2/19/2002	0.015	Est	TTEMI
RLS13-MW05	RLS13-MW05	2/28/1999	0.146		Tri
RLS15-MW03	RLS15-MW03	4/15/1999	0.170		Tri
RLS22-MW08	RLS22-MW08	5/13/1996	0.156		Tri
RLS29-MW01	RLS29-MW01	2/21/1992	0.076		Tri
RLS29-MW01	RLS29-MW01	2/16/2002	0.065	Est	TTEMI
RLS29-MW01	RLS29-MW01	2/16/2002	0.043	Est	TTEMI
RLS43-MW06	RLS43-MW06	4/14/2000	0.343		Tri
TT37-MW01	TT37-MW01	7/11/2001	0.111		Tri
TT37-MW02	TT37-MW02	7/10/2001	0.186		Tri
TT37-MW03	TT37-MW03	7/11/2001	0.173		Tri
TTBK-MW03	TTBK-MW03	8/6/1999	0.074		Tri
TTBK-MW06	TTBK-MW06	2/11/1999	0.002	Est	Tri
TTBK-MW08	TTBK-MW08	2/10/1999	0.017		Tri
TTBK-MW09	TTBK-MW09	5/13/1999	0.089	Est	Tri
TTBK-MW10	TTBK-MW10	8/4/1999	0.024		Tri

Compiled IWV Arsenic Data

Unique Well Name	Alternative Well Name	Sample Date	Arsenic (mg/L)	Analysis Type	Arsenic Reference
TTIWV-MW02-D	TTIWV-MW02 (D)	2/18/2002	0.013	Est	TTEMI
TTIWV-MW02-D	TTIWV-MW02 (D)	2/18/2002	0.018	Est	TTEMI
TTIWV-MW02-I	TTIWV-MW02 (I)	2/18/2002	0.007	Est	TTEMI
TTIWV-MW02-I	TTIWV-MW02 (I)	2/18/2002	0.011	Est	TTEMI
TTIWV-MW04	TTIWV-MW04	2/20/2002	0.035		TTEMI
TTIWV-MW04	TTIWV-MW04	2/20/2002	0.037		TTEMI
TTIWV-MW07	TTIWV-MW07	2/21/2002	0.028		TTEMI
TTIWV-MW07	TTIWV-MW07	2/21/2002	0.031		TTEMI
TTIWV-MW08	TTIWV-MW08	2/18/2002	0.007	Est	TTEMI
TTIWV-MW08	TTIWV-MW08	2/18/2002	0.008	Est	TTEMI
TTIWV-MW10	TTIWV-MW10	2/16/2002	0.022	Est	TTEMI
TTIWV-MW10	TTIWV-MW10	2/16/2002	0.014	Est	TTEMI
TTIWV-MW15	TTIWV-MW15	2/17/2002	0.022	Est	TTEMI
TTIWV-MW16	TTIWV-MW16	2/16/2002	0.010	Est	TTEMI
TTIWV-MW16	TTIWV-MW16	2/16/2002	0.008	Est	TTEMI
	RLS15-MW01	4/13/1999	0.360		Tri
	RLS15-MW02	4/13/1999	0.193		Tri
	VSI15-MW04	4/14/1999	0.058		Tri
	VSI15-MW03	4/15/1999	0.204		Tri
	RLS15-MW04	4/16/1999	0.286		Tri
	VSI15-MW01	4/16/1999	0.221		Tri
	VSI15-MW02	4/16/1999	0.214		Tri
	TTBK-MW11	5/19/1999	0.066		Tri
	RLS03-MW02	5/27/1999	0.018		Tri
	RLS03-MW03	5/27/1999	0.015		Tri
	RLS16-MW01	6/26/1999	0.184		Tri
	RLS17-MW01	6/26/1999	0.196		Tri
	TTBK-MW01	8/5/1999	0.056		Tri
	TTBK-MW05	8/5/1999	0.031		Tri
	TTBK-MW07	8/5/1999	0.004	ND	Tri
	RLS22-MW01	11/12/1999	0.174		Tri

APPENDIX 3-G

LAND SUBSIDENCE ANALYSIS

(Page Intentionally Left Blank)

Groundwater Sustainability Plan: Land subsidence conditions

Steven N. Bacon, P.G., C.E.G., Desert Research Institute, Reno, Nevada
Jenny Chapman, Desert Research Institute, Las Vegas, Nevada

I. Subsidence Environment

I.1 Aquifer materials and conditions in IWV

The Indian Wells Valley (IWV) groundwater basin includes up to about 610 m of water-bearing valley fill originating primarily from the Sierra Nevada Mountains. The valley fill consists of interbedded clay, silt, sand, and gravel deposited in alluvial, fluvial, and lacustrine environments typical for basins in the "Basin and Range Province" of the western United States (Fig. 1). Four general hydrogeologic units have been identified in the IWV groundwater basin, corresponding to unconsolidated sediment deposited in alluvial, lacustrine, playa, and sand dune environments, and these are underlain and bounded by consolidated and indurated basement rock (e.g., Kunkel and Chase, 1969, McGraw et al., 2016). The unconsolidated hydrogeologic units have variable degrees of permeability and are distributed across the valley based on their depositional environments. The distribution and depths of the hydrogeologic units are also structurally controlled by faults. The characteristics of the four hydrogeologic units in the IWV groundwater basin are summarized below from previous studies (e.g., Kunkel and Chase, 1969; Berenbrock and Martin, 1991; McGraw et al., 2016):

- The "alluvial hydrogeologic unit" (i.e., coarse-grained sediment) consists of interbedded, moderately to well-sorted gravel, sand, silt, and clay of Pleistocene and Holocene age having relatively high permeability. The percentage of interbedded silt and clay layers increase towards the depocenter of China Lake playa and commonly form thin and discontinuous aquitards of reduced relative permeability. These sediments include both older and younger alluvium, alluvial fan, and stream terrace deposits, plus elevated pediments (i.e., eroded bedrock). Alluvium extends across the IWV groundwater basin and is thickest along the westerly and southerly edges of the IWV groundwater basin along the range-front of the Sierra Nevada and low relief hills, respectively.

- The “lacustrine hydrogeologic unit” (i.e., fine-grained sediment) includes relatively thick deposits of silt and silty clay of Pleistocene age that have low permeability. The lacustrine unit is underlain by alluvium and is interbedded with deeper alluvium in the central portion of the basin. The extent of the clayey lacustrine unit coincides with the depocenter of China Lake basin and past water levels of China Lake and high stands of coalesced China-Searles Lake during the Pleistocene (Fig. 2).

- The “playa hydrogeologic unit” (i.e., fine-grained sediment) consists of low permeability silt and clay deposits with minor thin sand lenses of Holocene age.

- The “sand dune hydrogeologic unit” (i.e., coarse-grained sediment) is composed of surficial windblown sand deposits and/or fan delta deposits of Holocene to late Pleistocene age. This unit is typically less than about 30 m thick and occurs above the water table, thereby being unsaturated.

Cross sections developed by Kunkel and Chase (1969) across the IWV groundwater basin show the distribution and thickness of highly permeable alluvial gravel and interbedded alluvial (clay to gravel) hydrogeologic units at, and near, the land surface along the westerly and southerly margins of the IWV groundwater basin, as well as the extent and thickness of low-permeability lacustrine and playa hydrogeologic units near the center of the valley (Fig. 3). In addition, the westerly and southerly lateral margins of the lacustrine hydrogeologic unit are either in fault contact (Transects B-B’ and C-C’; Figs. 2 and 3) or form a facies sequence (i.e., interfinger relation) between overlapping and wedged shaped alluvial and lacustrine layers associated with Pleistocene paleolake fluctuations (Transect A-A’; Figs. 2 and 3).

I.2 Susceptibility of aquifer materials to subsidence

The weight of materials overlying an aquifer (e.g., sediment, water, vegetation, and structures on the land surface) is supported within an aquifer system by both the water in the pore spaces and by the clay, silt, sand, and gravel that form the granular mineral skeleton of the aquifer. When pumping lowers groundwater levels and thus fluid pressure in the pores (i.e., pore pressure), the weight of overlying materials must be increasingly supported by the mineral skeleton of the aquifer. Consequently, the increased pressure or stress on the mineral grains (i.e.,

effective stress) is equal to the support lost by decreased pore pressure. Increased effective stress may cause some compression of the aquifer system skeleton and, if the stresses are large enough, then some compaction of the aquifer system may occur. The cumulative result of the aquifer response to compaction over the full thickness of the aquifer system is expressed as subsidence at the land surface (e.g., Galloway et al., 1999; Borchers and Carpenter, 2014; Faunt et al., 2015) (Fig. 4). Aquifer-system deformation can range from fully reversible (elastic) to largely permanent (inelastic). Elastic deformation occurs when sediments compress as pore pressure decreases, and expand equally as pore pressure increases. The consequent cycles of subsidence and rebound of the land surface commonly occur seasonally, coincident with cyclic groundwater discharge and recharge. The compressibility of clayey aquitards typically is several times larger than that of coarser-grained aquifers.

Elastic deformation does not permanently alter the water storage properties of an aquifer, that is, the same volume of water can be stored in an aquifer after many cycles of solely elastic compression and expansion. If water-levels decline over large areas, broad and shallow (about 8 cm-deep) subsidence bowls commonly form at the land surface, but then soon disappear when water-levels recover and land surface rebounds. The rebound occurs because the aquifer system has not been permanently reconfigured into a denser, more closely packed arrangement (e.g., Borchers and Carpenter, 2014).

In contrast, permanent compaction results when the sediments are compressed inelastically beyond their previous maximum effective stress (pre-consolidation stress). Pre-consolidation stress is the effective stress threshold at which inelastic compaction begins, and generally is exceeded when groundwater levels decline past historical low levels. At these stress ranges, the materials compress inelastically, and the inelastic compaction and consequent land subsidence are largely permanent and irreversible. Because silt- and clay-rich sediment are often highly compressible and subject to rearrangement of grains, depressurization results in more compaction and land subsidence in fine-grained deposits than depressurization of less compressible, coarser-grained deposits of sand and gravel (Galloway et al., 1999; Borchers and Carpenter, 2014; Faunt et al., 2015).

The hydrogeologic units in the IWV groundwater basin have variable degrees of susceptibility to compaction. The inelastic compaction of the coarse-grained alluvial hydrogeologic units generally is negligible unless very large decreases in pore pressure increase effective stress to levels that fracture mineral grains (such as what occurs in oil and gas fields;

e.g., Galloway et al., 1999), which is unlikely to occur in the IWV groundwater basin. In contrast, the fine-grained lacustrine and playa hydrogeologic units, as well as the fine-grained aquitard interbeds in the alluvial hydrogeologic units, are prone to inelastic compaction. As a result, the land surface in areas underlain by the extensive fine-grained hydrogeologic units have high to very high susceptibility to land subsidence when the groundwater table is lowered below historically low levels (e.g., Fig. 4). Furthermore, the relative magnitude of potential land subsidence across the IWV groundwater basin is not expected to be uniform because of the heterogeneous nature of the alluvial hydrogeologic unit, overlapping lateral margins between the alluvial and lacustrine hydrogeologic units, and abrupt fault contacts. As a result, there is also high to very high susceptibility to differential land subsidence (i.e., subsidence occurring at different rates) across the valley.

I.3 Tectonic setting and implications for subsidence

The IWV groundwater basin is located within a tectonically active area of California referred to as the northern Eastern California shear zone or southern Walker Lane (e.g., Dokka and Travis, 1990; Monastero et al., 2002; Wesnousky, 2005). The valley floor of IWV is cross-cut by a northerly trending mosaic of fault segments with a wide-range of fault activity that merge towards the north with the Sierra Nevada frontal fault system and Coso volcanic center (e.g., Hauksson et al., 1995) (Fig. 5). The active faults in the valley include the Little Lake fault zone (LLFZ) and Airport Lake fault zone (ALFZ) (Bryant and Hart, 2007). The LLFZ is considered the principal fault system in the IWV and is characterized as an oblique, right-lateral (horizontal) fault with down-to-the-east normal (vertical) displacement, whereas the ALFZ is an oblique, right-lateral fault with down-to-the-west normal displacement that bifurcates from LLFZ in the north-central part of the IWV (Zellmer and Roquemore, 1997) (Fig. 5). Both fault zones are expressed at the surface as a distributed zone of short, en echelon scarps that have experienced two historical ground-rupturing earthquakes, the first in 1982 and the second in 1995 (Fig. 5). Although the surface rupture traces were relatively short (about 2 to 3 kilometers (km)) showing little displacement, they were associated with earthquakes with magnitudes (M) of up to M 4.9 and 5.4, respectively (Hauksson et al., 1995). Recently, significant ground rupture events on July 4 and 5, 2019 occurred during the M6.4 and M7.1 Searles Valley and Ridgecrest earthquakes, respectively. The main M7.1 earthquake rupture occurred in the eastern sector of China Lake basin and defined a broad zone of distributive faulting associated with the LLFZ and

ALFZ system (Fig. 5). In addition to the active LLFZ and ALFZ, a northerly trending series of unnamed fault segments that cross the eastern margin of El Paso Valley within the southwestern sector of the groundwater basin are mapped having an activity of less than 15,000 years (USGS, 2016) (Fig. 5). The zone of unnamed faults are informally referred to as the El Paso fault (EPF). The surface expression of the EPF appears as a well-defined fault lineament with vertical east-side-down separation that displaces a broad and relatively older alluvial fan associated with the axial drainage of El Paso Valley. All of these faults collectively control groundwater levels in the IWV groundwater basin by acting as groundwater barriers (Garner et al., 2017).

In general, land subsidence primarily, can occur as a result of groundwater extraction, but can also result from collapse of underground cavities, tectonic activity, natural consolidation of sediment, oxidation and compaction of organic deposits, hydrocompaction of moisture deficient soil and sediments, development of geothermal energy, and extraction of hydrocarbons (Borchers and Carpenter, 2014). The IWV is located in a tectonically and volcanically active area of California. Consequently, it is prudent to consider the tectonic effects on the land surface elevation in subsiding areas when evaluating subsidence in alluvial basins related to groundwater production. In contrast to other groundwater basins in the Mojave Desert that have a relationship between groundwater production and land subsidence (e.g., Motts et al., 1969; Galloway et al., 1999; Stamos et al., 2001, 2007; Sneed et al., 2003; Solt et al., 2014), the IWV groundwater basin is crossed by the active LLFZ and ALFZ and has experienced historical ground rupturing earthquakes (e.g., 1982, 1995, 2019) and continuous seismic activity. As a result, the hydrogeologic setting of the IWV groundwater basin is relatively more complex than most other groundwater basins in the western U.S. (e.g., Motts et al., 1969), and interpretation of observed land subsidence across the groundwater basin needs to be made in the context of a seismically active basin to differentiate between land subsidence from groundwater production and from tectonic activity.

II. Historical Observations of Subsidence

II.1 Public observations of valley subsidence

Historical information from anecdotal reports has been used in California to provide estimates of the location and magnitude of land subsidence due to groundwater extraction prior to extensive land-subsidence monitoring (e.g., Borchers and Carpenter, 2014). Isolated areas of land subsidence associated with early agricultural groundwater pumping were observed through

the 1970s in the greater Ridgecrest area. Two specific areas of land subsidence were observed centered at the old Bowman Ranch (near presented day Walmart) and in the vicinity of North Brown Road between Leliter and Neal Ranch Roads. These isolated areas of subsidence are reported to be evident today in the form of about 0.5 mi diameter depressions that are nearly 15 ft below the surrounding ground level (these depressions require greater vertical resolution than current 2-meter digital elevation models to observe). Additional evidence for the magnitude of subsidence in the two areas is from several groundwater pump wells that showed well-head protrusion (Don Decker, 2019, personal commun.). The isolated areas of subsidence coincide with an extensive organic-rich clay that is about 1600 ft thick and located west of the LLFZ (Don Decker, 2019, personal commun.). The organic-rich clay unit was commonly observed during well construction in the area, however, the clay unit was not included in the Kunkel and Chase (1969) hydrogeologic cross sections of the IWV groundwater basin. These anecdotal accounts of subsidence associated with groundwater pumping demonstrate that land subsidence from groundwater extraction has historically occurred in the IWV groundwater basin.

II.2 Level-line surveys showing tectonic ground deformation

In some seismically active areas, ground deformation is commonly associated with discrete movements on faults during coseismic slip (i.e., slip during earthquake) or interseismic creep (i.e., slip during no earthquakes). The area of IWV that the LLFZ and APFZ cross is actively deforming based on historical surface rupturing events, as well as from land-based geodetic data from repeat, high-resolution level-line surveys of the 6.55-km (4.07-miles (mi)) long Supersonic Naval Ordnance Research Track (SNORT) alignment within Naval Air Weapons Station China Lake (NAWSCL) (Zellmer and Roquemore, 1997) (Fig. 5). The style and magnitude of historical surface deformation of the SNORT alignment reflects complex fault geometry between the LLFZ and ALFZ, and an underlying shallow (about 3-km deep) magma body. The intersection of the LLFZ and ALFZ occurs about 2.1 km (1.3 mi) east of the northern end (muzzle end) of SNORT. Here, the LLFZ exhibits a large left-step and forms a localized graben (pull-apart basin) that distributes strain in a northwest-southeast direction, whereas the western ALFZ bifurcates to the north and transfers strain along the eastern margin of the graben (Fig. 5). The dominant style of coseismic deformation within the left-step during surface rupturing events is permanent surface subsidence, whereas interseismic deformation is reflected by cyclic strain accumulation in the form of uplift (Zellmer and Roquemore, 1997).

Active ground deformation attributed to cyclic strain accumulation up to about 50 millimeters (mm) of uplift (positive values) and up to about 40 mm of subsidence (negative values) near the LLFZ is shown by geodetic level-line surveys of the SNORT alignment from five survey intervals between 1952 and 1986 (Zellmer and Roquemore, 1997) (Fig. 6). The elevation differences between the surveys were computed as relative elevation changes along the track based on a fixed elevation of the initial survey's base station at the south end of SNORT (monument SF-0). This procedure removes the complications resulting from local and regional elevation changes, as well as possible surveying errors in determining absolute elevations of SF-0 over the period of record (Zellmer and Roquemore, 1997). The use of relative elevation survey data also resolves only ground deformation associated with tectonic deformation. The data demonstrates that the intervals of time with no seismic activity (i.e., interseismic periods) are predominantly characterized by uplift of the northern half of the alignment closest to the LLFZ, whereas the intervals of time between surveys that had seismic activity (i.e., coseismic periods) are mostly characterized by subsidence in the same general area (Zellmer and Roquemore, 1997) (Fig. 6). The observed ground deformations that occurred between the 1957 and 1977 surveys and the 1978 and 1984 surveys resulted from mostly tectonic stress buildup and subsequent release associated with approximately M5 earthquakes near SNORT in 1961 and 1982 (Fig. 6).

Evaluation of SNORT survey data for the period 1986–2000 was performed in this study to extend the period of record by 14 years. High-resolution, differential global positioning system (GPS) data acquired in 4 October to 6 November, 2000 by NAWSCL was compared with SNORT survey data collected in 1986 using the same methods of Zellmer and Roquemore (1997). To resolve the data to be fixed to the SNORT base station (SF-0), an offset of +33.7 mm was applied. This offset, and perhaps other offsets previously used by Zellmer and Roquemore (1997), could be a signal of land subsidence associated groundwater-related compaction of aquifer materials or errors between individual survey methods that included ground-based geodetic techniques and more recently GPS. Comparison of the relative elevation changes for the 1986–2000 dataset, however, shows similar trends with previous survey intervals where there was a large tectonic stress buildup during the period 1984–1986 and subsequent release associated with the 1995 M5.4 Ridgecrest earthquake sequence that was centered within the ALFZ northeast of SNORT in China Lake basin (Fig. 7).

II.3 InSAR data showing ground deformation from seismicity and groundwater production

Ground deformation at a valley-wide scale within the IWV groundwater basin has been previously characterized for the periods 1992–2000 and 2005–2010 using satellite-based Interferometric Synthetic Aperture Radar (InSAR) techniques (Peltzer et al., 2001; Katzenstein, 2013; 2015). The InSAR data analyzed between 1992 and 2000 shows three discrete areas of subsidence that correspond with the locations of seismic activity and mapped faults, geothermal production, and fine-grained aquifer materials (Fig. 7). Two of the three areas of subsidence in the IWV groundwater basin include a locus of subsidence within the depocenter of China Lake basin referred to as the northern subsidence area (SB N) and a locus of subsidence in the greater Ridgecrest area referred to as the southern subsidence area (SB S) (Fig. 7). In addition, the third locus of subsidence overlaps with the northern groundwater model domain boundary in the vicinity of the Coso geothermal field (COSO; Fig. 7). The extent of subsidence in the northern subsidence area and Coso geothermal field was previously identified by Peltzer et al. (2001) to correspond with the epicenters of the M5.4 Ridgecrest earthquake sequence beginning on 17 August 1995 and with the Coso volcanic center, respectively (e.g., Hauksson et al., 1995). The northern subsidence area shows the greatest amount of surface change during the period 1992–2000 with up to 35 to 38 mm of subsidence (Fig. 7). The extent of subsidence in the southern subsidence area near Ridgecrest was identified by Katzenstein (2015) to have up to 20 to 25 mm of subsidence that appeared to be associated with the surface trace of the LLFZ and ALFZ, and bounded by northwesterly striking bedrock faults (Fig. 7).

The InSAR data evaluated from 2005 to 2010 shows an example of 5 years of surface change during a period with no significant seismic activity. The area of the Coso geothermal field had the greatest amount of surface change during the period 2005–2010 with up to about 20 to 24 mm of subsidence (Coso; Fig. 8). The northern subsidence area (SB N) during this period shows mostly negligible to slightly positive surface change within the area of the 1995 Ridgecrest earthquake sequence. The southern subsidence area (SB S), however, exhibited continued subsidence of up to 10 to 15 mm that was narrowly distributed along the southern LLFZ and bounded by bedrock faults similar to the earlier period (Fig. 8).

The broad distribution of surface change from the InSAR analysis appears to show cyclic strain accumulation within the IWV groundwater basin similar to the geodetic survey data measured along the SNORT alignment in areas proximal to faults and earthquake epicenters.

During the period 1992–2000, the area where the ALFZ bifurcates from the LLFZ near the northern end of the SNORT alignment shows mostly negative surface change (subsidence), indicating the occurrence of a tectonic stress drop in this area during the 1995 Ridgecrest earthquake sequence (Fig. 7). The same area during the period 2005–2010, however, shows relatively less negative surface change, indicating tectonic stress buildup during 15 years after the earthquake sequence (Fig. 8). In contrast, the southern subsidence area (SB S) during the period 2005–2010 shows continued subsidence that is more narrowly distributed than during the 1992–2000 period with the Ridgecrest earthquake (Figs. 7 and 8). This indicates processes not entirely associated with tectonic cyclic strain accumulation.

An evaluation of how surface change is distributed along a about 6.55-km transect was performed by intersecting the InSAR data for the periods 1992–2000 and 2005–2010 with the location of monuments along the SNORT alignment to better understand cyclic strain accumulation associated with faults in the IWV. The georeferenced points of each SNORT monument along the alignment were intersected with the InSAR raster datasets using ArcGIS to determine the magnitude of surface change during the two periods at monument sites. Direct analysis between the SNORT level-line surveys and InSAR data cannot be made because the SNORT data are processed as relative elevation changes to identify only tectonic deformation. The absolute elevations of the base station F0 reported in the 1986 and 2000 surveys, however, were used to measure surface change for the period 1986–2000 to compare with InSAR measurements. The results of the analysis show subsidence of up to 10 and 11 mm during the 1992–2000 and 2005–2010 periods, respectively. This resulted in up to 20.5 mm of cumulative subsidence along the SNORT alignment from 1992 to 2010, which is considered a minimum because a 5-year gap was not analyzed between 2000 and 2005 (Fig. 9A). In addition, the absolute elevation difference of the SNORT base station F0 shows that 8.8 mm of subsidence occurred between 1986 and 2000 at the south end of the alignment, which is similar to the 10 mm estimate from InSAR for the period 1992–2000. (Fig. 9A) The 8.8 and 10 mm subsidence values are likely within the uncertainties of the ground- and satellite-based survey methods, respectively, thereby providing confidence in both types of measurements.

Estimates of the rate of subsidence during the two periods from the InSAR data and the absolute elevations of the SNORT base station F0 during 1986–2000 were also made to characterize land subsidence in the area. The rate of subsidence along the SNORT alignment has increased over the period between 1986 and 2010. Rates of subsidence during the 2005–2010

period range from up to 2.2 mm/yr in the south end to 1.3 mm/yr at the north end of the alignment (Fig. 9B). Furthermore, the effects of cyclic strain release reflected by subsidence during 1992–2000 and accumulation in the form of rebound during 2005–2010 following the 1995 Ridgecrest earthquake sequence is also evident in the InSAR data. This supports the Zellmer and Roquemore (1997) model of tectonic deformation associated with the LLFZ at the northern end of the SNORT alignment from repeat, high-resolution level-line surveys (Fig. 9).

II.4 Spatiotemporal correspondence between simulated groundwater-level and InSAR land-surface changes

An evaluation of groundwater drawdown and InSAR datasets was performed in this study to characterize potential spatiotemporal correspondence between groundwater level and land surface changes across the IWV groundwater basin. Simulation of drawdown from the IWV groundwater model (McGraw et al., 2016; Garner et al., 2017) were compared to InSAR datasets (Katzenstein, 2015) for the periods 1992–2000 and 2005–2010. The evaluation also included the location of faults used in the groundwater model and the extent of the clay-rich lacustrine/playa unit, along with the location of wells with greater than 900 acre-feet of production during each period noted above (Figs. 10 and 11). Collectively, all the data were used to examine potential explanations for non-tectonic subsidence in IWV.

Simulated drawdown during the period 1992–2000 shows three primary cones of depression with 5 to 10 ft of groundwater lowering. The southern cones of depression coalesce in areas of the LLFZ and southern subsidence area (Fig. 10). The effects of ground rupture and seismicity from the 1995 Ridgecrest earthquake is widely distributed in the northern subsidence area with corresponding simulated drawdown of less than 1 ft. The southern subsidence area, however, shows 10 to 25 mm of subsidence in areas with about 5 to 8 ft of drawdown (Fig. 10). In addition, the distribution of subsidence of 0.5 to 1.0 mm closely corresponds with the southwestern cone of depression with up to 10 ft of simulated drawdown (Fig. 10).

Simulated drawdown during the period 2005–2010 was relatively less in the southern subsidence area compared to the earlier period, and the distribution of subsidence of 10 to 15 mm is narrow (Fig. 11). Simulated drawdown during this period shows 3 to 8 ft of groundwater lowering at two well-defined cones of depression and two areas with poorly defined areas of drawdown. Three of the four drawdown features are located outside the southern subsidence area (Fig. 11).

Simulated drawdown for the entire period 1992–2010 displays two primary cones of depression with 18–28 ft of groundwater lowering in areas northwest and southwest of the southern subsidence area (Fig. 12). The area of the Coso geothermal field along the northern groundwater model domain boundary had the greatest amount of surface change during the period 1992–2010 with up to 40 to 46 mm of subsidence. The southern subsidence area had the second highest cumulative amount of surface change measured in IWV between 1992 and 2010 with up to 35–40 mm of subsidence that corresponded with 10–18 ft of simulated drawdown (Fig. 12). The magnitude of subsidence measured in the northern subsidence area is attributed to the 1995 Ridgecrest earthquake sequence with corresponding simulated drawdown of less than two ft. The magnitude and extent of measured subsidence on the northeastern boundary of the southern subsidence area appears to be controlled by the southern margin of the clay-rich unit and location of the LLFZ. In addition, the southwestern boundary of the southern subsidence area appears to parallel nearby bedrock faults and the distribution of densely placed wells with variable production volumes of 4,000 to 20,000 acre-feet during the period 1992–2010 (Figs. 7 and 12).

Georeferenced points of production wells were intersected with the InSAR raster datasets using ArcGIS to determine the magnitude of potential surface changes in areas of drawdown from groundwater production. Plots were constructed that show the elevation of simulated drawdowns on the primary y-axis and surface change on the secondary y-axis versus the year during the period of the model simulation from 1920 to 2017. The InSAR surface change values for the periods 1992–2000 and 2005–2010 are plotted on the x-axis as the midpoint for each time interval (e.g., 1996 and 2007.5, respectively). There is apparent temporal correspondence between the magnitude of simulated drawdown and land-surface changes at the well sites. A subset of three wells (Wells 8, 18, and 26) were used to show relations between drawdown and land surface change in different hydrogeologic settings relative to the southern subsidence area (Fig. 12). The wells have been categorized into sites that are: (1) proximal to faults within the southern subsidence area (Fig. 13); (2) in areas with greater than 20,000 acre-feet of groundwater pumping (Fig. 14); and (3) in areas with agriculture along the Sierra Nevada range front (Fig. 15).

Well 26 is situated on the boundary of the southern subsidence area within distal alluvial fans and playa margins (Fig. 12). Areas of the well 26 site have had up to about 58 ft of groundwater lowering over the past about 100 years (Fig. 13). In addition, there has been up to

about 12 ft of simulated drawdown and 19.0 mm of total subsidence at the well site during the period 1992–2010 (Fig. 13). The rate of subsidence at the well 26 site during this period is 1.1 mm/yr. This subsidence rate corresponds to variable rates of groundwater lowering ranging from about 80 mm/yr between 1992 and 2010 to about 396 mm/yr between 2000 and 2007.5 (Fig. 13).

Well 18 is situated outside of the western boundary of the southern subsidence area and is the site of greater than 20,000 acre-feet of groundwater production during the period 1992–2010 (Fig. 12). The well 18 site is also adjacent to other wells that produced groundwater greater than 4,000 and up to 20,000 acre-feet on medial to distal alluvial fans. Areas of the well 18 site have had up to about 70 ft of groundwater lowering over the past about 100 years. In addition, there has been up to about 18 ft of simulated drawdown and 16.1 mm of total subsidence at the well site during the period 1992–2010 (Fig. 14). The rate of subsidence at the well 18 site during this period is 0.9 mm/yr. The subsidence rate corresponds to a nearly constant rate of groundwater lowering of about 300 mm/yr between 1992 and 2010 (Fig. 14).

Well 8 is situated outside of the southern subsidence area and is the site of groundwater production of greater than 10,000 acre-feet during the period 1992–2010 (Fig. 12). The well 8 site is also adjacent to numerous wells that produced groundwater greater than 10,000 acre-feet in agricultural areas on medial to distal alluvial fans along the Sierra Nevada range front. Areas of the well 8 site have had up to about 68 ft of groundwater lowering over the past 100 years with most production beginning in the mid-1970s (Fig. 15). In addition, there has been up to about 19 ft of simulated drawdown and 5.0 mm of total subsidence at the well site during the period 1992–2010 (Fig. 15). The rate of subsidence at the well 8 site during this period is 0.3 mm/yr. The subsidence rate corresponds to a nearly constant rate of groundwater lowering of about 322 mm/yr between 1992 and 2010 (Fig. 15).

II.5 Subsidence modeling with MODFLOW

Potential subsidence in the IWV groundwater basin were previously estimated using the IWV groundwater model of McGraw et al., (2016). Simulations of subsidence were made with the Subsidence and Aquifer-System Compaction Package for Water-Table Aquifers in the USGS MODFLOW groundwater program. The results of the simulations were compared to the distribution of InSAR surface change of Katzenstein (2015). Comparisons between the two datasets yielded moderate to poor spatiotemporal correspondence because the MODFLOW simulations showed greater areas of subsidence than the measured amounts in the area west of

the southern subsidence area. McGraw et al. (2016) attribute the disparity to large uncertainty in parameterization of the subsurface properties. Specifically, the location and compressibility of the fine-grained interbeds within the alluvial hydrogeologic unit are largely unknown. Therefore, the distribution of specific yield in the upper aquifer layer in the MODFLOW groundwater model was used as a general indicator of compressibility for the calibration process. Furthermore, during this initial stage of the development of the IWV groundwater model, faults were not included in the model. The newer version of the IWV groundwater model (Garner et al., 2017) now includes faults, which may produce different results if subsidence modeling was to be performed again.

III. Assessment of Subsidence in Indian Wells Valley

III.1 Summary of rate, extent, and likely cause of historically observed subsidence

The hydrogeologic information, high-resolution level-line surveys of the SNORT alignment, InSAR remote sensing data, and simulated drawdown are integrated to assess subsidence in the IWV groundwater basin. Previous studies of the hydrogeology of IWV describe extensive fine-grained sediment in the central part of the valley in fault contact with the active Little Lake fault zone (LLFZ) and other bedrock faults, whereas discontinuous, interbedded fine-grained layers are present within alluvial sediment west of the LLFZ. These fine-grained layers have high to very high susceptibility to compaction when groundwater levels are lowered below historical levels. Ground- and satellite-based techniques have previously been used to measure land surface change across IWV. Site-specific, ground-based level-line surveys along the SNORT alignment at NAWSCL show active tectonic ground deformation in areas nearest to the LLFZ from cyclic strain accumulation of as much as about 50 mm of uplift and about 40 mm of subsidence between 1952 and 2000.

IWV-wide surface changes have also been documented based on remote sensing techniques for the periods 1992–2000 and 2005–2010. The InSAR analysis showed up to –38 and +64 mm of surface change between 1992 and 2000, as well as up to –24 to +19 mm between 2005 and 2010. The InSAR analysis measured two loci of subsidence near Ridgecrest, a northern subsidence area associated with the 1995 Ridgecrest earthquake sequence and a southern subsidence area in the vicinity of the southern LLFZ, bedrock faults, and production wells. The southern subsidence area during the 1992–2000 period had up to 25 mm of subsidence with a corresponding rate of 3.1 mm/yr. The same general area during the 2005–2010 period had up to

15 mm of subsidence with a corresponding rate of 3.0 mm/yr. The different periods of InSAR measurement yielded similar subsidence rates in the southern subsidence area even with the occurrence of the 1995 Ridgecrest earthquake sequence during the earlier period and relatively less groundwater drawdown during the latter period. The southern subsidence area also had the highest total amount of surface change compared to areas affected by the 1995 Ridgecrest earthquake sequence with up to 35 to 40 mm of subsidence that corresponded with 10 to 18 ft of simulated groundwater drawdown during the 1992–2010 period. The subsidence rate of the southern subsidence area over the entire 18-year period is up to 2.2 mm/yr.

The spatiotemporal distribution of the InSAR surface change was previously interpreted by Katzenstein (2013; 2015) to be controlled by the location of faults and historical seismicity, plus groundwater production. Additional analysis of the InSAR dataset with other information also indicates the southern subsidence area is geologically controlled by bounding conditions that include the southern margin of a clay-rich hydrogeologic unit and southern LLFZ on the northeast and a linear field of production wells and bedrock faults on the southeast.

Analysis of InSAR data along the SNORT alignment confirmed cyclic strain accumulation from tectonic processes, but showed the SNORT alignment has also been affected by non-tectonic subsidence. Measurements indicate that the magnitude and rates of subsidence in areas of SNORT have increased over the period between 1986 and 2010 with the largest values along the southern end of the alignment. InSAR measurements along the southern alignment show up to 20.5 mm of cumulative subsidence between 1992 and 2010. In addition, subsidence rates increased from up to 2.2 mm/yr in the south end to 1.3 mm/yr at the north end of the alignment during the 2005–2010 period. The south to north decreasing gradient of subsidence coincides with the northwest margin of the southern subsidence area and a northward migrating cone of depression from production wells west and south of SNORT from simulations of drawdown from the IWV groundwater model (e.g., McGraw et al., 2016; Garner et al., 2017).

The southern locus of subsidence is primarily in an area with no production wells in the immediate vicinity. Most of the production wells in IWV are located outside the area with the highest subsidence. It is likely that the locus of subsidence has developed from compaction of the thickly interbedded fine-grained lacustrine hydrologic units between coarse-grained alluvial units. Furthermore, the spatial configuration of the subsidence area also appears to be structurally controlled by two northwest-striking bedrock faults that are bisected by the active LLFZ. The structural configuration of these faults control the local flow paths by producing groundwater

barriers based on simulations of groundwater drawdown. Given these factors, the southern subsidence area appears to be associated with differential compaction of a laterally extensive and fault bounded interbedded clay-rich hydrogeologic unit experiencing drawdown from groundwater production areas to the west. In addition, historical seismicity and moderate M5 earthquakes could have also produced some of the measured subsidence in IWV by producing soft-sediment deformation and compaction of previously dewatered fine-grained aquifer materials. Continued subsidence in the southern subsidence area during the period 2005–2010 at a similar subsidence rate of ~3 mm/yr compared to the earlier period that included the 1995 Ridgecrest earthquake implies processes not entirely associated with tectonic ground deformation.

III.2 Risk of groundwater withdrawal-related subsidence in Indian Wells Valley

Sustained groundwater production in current areas will continue to lower water levels. The greater Ridgecrest area, especially in the vicinity of the southern subsidence area, have high to very high susceptibility to land subsidence because of the hydrogeologic and tectonic setting of IWV. With continued groundwater withdrawal, the spatial extent of aquifer materials that are prone to compaction will increase. This in turn will increase the risk of environmental consequences from significant or unreasonable land subsidence caused by compaction of aquifer systems. Some of the more costly consequences include damage to engineered structures, such as buildings, bridges, roadways, runways, sewerages, and well casings (Hoffman et al., 2003; Borchers and Carpenter, 2014). The magnitude of "significant or unreasonable" land subsidence depends on the engineered structure of concern. The above examples have a wide-range of allowable tolerances of vertical and horizontal displacements. It's only when the allowable tolerances are exceeded that the risk of damage increases.

The magnitude of land subsidence during the period 1992–2010 ranged from 0 to 0.5 to 35 to 40 mm in the vicinity of production wells and simulated cones of depression in the greater Ridgecrest area. The magnitudes of land subsidence during the 18-year period corresponded to subsidence rates of up to 2.2 mm/yr. In comparison to other areas in California, such as the San Joaquin Valley that had subsidence rates in excess of about 300 mm/yr (1 ft/yr) related to groundwater extraction (e.g., Borchers and Carpenter, 2014), the magnitude of subsidence and associated rates measured in IWV is relatively small.

III.3 Land subsidence monitoring in Indian Wells Valley

Land subsidence monitoring in groundwater basins of the Mojave Desert is commonly used to determine the location, extent, and magnitude of vertical land surface changes associated with groundwater extraction for domestic, agricultural, and municipal water supplies. Common land monitoring techniques include ground-based level-line surveys and space-based GPS and InSAR measurements (e.g., Sneed et al., 2003). In addition, subsurface methods including borehole extensometers are commonly used to directly quantity aquifer compaction by measuring the continuous change in vertical distance between the land surface and a subsurface reference point in the borehole (e.g., Borchers and Carpenter, 2014). The methods previously used in IWV to monitor potential land surface changes associated with groundwater extraction included level-line surveys at the SNORT alignment and InSAR surveys during 1992–2000 and 2005–2010. Possible future monitoring approaches could also include additional SNORT and InSAR surveys, as well as developing a GPS monitoring network that is integrated with established survey benchmarks and continuous GPS stations. The surveying effort can be made in coordination with NAWSCL since there is a long history of repeat measurements of numerous survey bench marks on base.

Nearly 10 years have passed since the last analysis of SNORT and InSAR survey data. Since this time, there has been continued groundwater extraction and the occurrences of the July 2019 M6.4 and M7.1 Searles Valley and Ridgecrest earthquakes that produced large surface ruptures and severe seismic shaking in the IWV groundwater basin. Additional land surface monitoring in areas of the southern subsidence area and production wells in lieu of continued groundwater lowering and recent seismic activity since 2010 will provide additional data to better understand the land subsidence potential in the greater Ridgecrest area associated with either tectonic or non-tectonic process, which in turn can be used to assist in making informed decisions of the water resources of the IWV groundwater basin. The California DWR in cooperation with NASA have recently published InSAR analyses between 6/13/2015 and 3/1/2018 - 6/1/2018 for high-use and populated groundwater basins across California, including the IWV groundwater basin. The InSAR analysis shows the total vertical displacement across the IWV groundwater basin ranged from -0.25 to 0.25 feet during this period. The DWR InSAR analysis, however, is processed at 100 m resolution, compared to the 50 m resolution InSAR survey data used between 1992–2000 and 2005–2010 in this study; and the DWR categories of total vertical displacement are categorized at 0.25 feet intervals. As a result, the DWR analysis is

too coarse of resolution to identify the spatiotemporal changes of land subsidence associated with either tectonic or non-tectonic processes. The DWR analysis does demonstrate that the magnitude of subsidence across the groundwater basin between 6/13/2015 and 3/1/2018 - 6/1/2018 has been no more than -0.25 feet.

References

Borchers, J. W., and Carpenter, M. (2014). Land subsidence from groundwater use in California, Full Report of Findings, report, California Water Foundation, 151 pp.

Bryant, W.A., and Hart, E.W. (2007). Fault rupture hazard zones in California: Alquist-Priolo earthquake fault zoning act with index to earthquake fault zones maps. California Geological Survey Special Publication 42, 42 p.

Bullard, T.F., Bacon, S.N., Adams, K.D., and Decker, D.L., 2018. Phase II: Geomorphic map of China Lake basin below 700 m in support of cultural resource management at NAWS China Lake. Final report prepared for Naval Air Warfare Center, Weapons Division by Naval Earth Sciences and Engineering Program, Desert Research Institute. Dated October 12, 2018, 31 p. plus appendices.

Danskin, W.R. (1998). Evaluation of the hydrologic system and selected water-management alternatives in the Owens Valley, California: U.S. Geological Survey Water-Supply Paper 2370-H, 175 p.

Dokka, R.K., and Travis, C.J. (1990). The role of the Eastern California shear zone in accommodating Pacific–North American plate motion. Geophysical Research Letters 17, 1323–1326.

dePolo, C.M., Clark, D.G., Slemmons, D.B., and Ramelli, A.R. (1991). Historic surface faulting in the Basin and Range Province, western North America: Implications for fault segmentation. Journal of Structural Geology 13, 123–136

Faunt, C.C., Sneed, M., Traum, J., and Brandt, J.T. (2015). Water availability and land subsidence in the Central Valley, California, USA. Hydrogeology Journal, DOI 10.1007/s10040-015-1339-x.

Galloway D.L., Jones D.R., and Ingebritsen S.E. (1999). Land subsidence in the United States. U.S. Geological Survey Circular 1182, 175 pp.

Garner, C., Bacon, S., Pohll, G., and Chapman, J. (2017). RE: Indian Wells Valley Groundwater Model Update. Technical Memorandum to Stetson Engineers from Desert Research Institute dated November 17, 2017, p. 28, plus figures and appendices.

Hauksson, E., Hutton, K., Kanamori, H., Jones, L., Mori, J., Hough, S., and Roquemore, G. (1995). Preliminary report on the 1995 Ridgecrest earthquake sequence in eastern California. Seismological Research Letters 66, 54–60.

Hoffmann, J., Galloway, D.L., and Zebker, H.A. (2003). Inverse modeling of interbed storage parameters using land subsidence observations, Antelope Valley, California. Water Resources Research 39, 1–13.

Katzenstein, K. (2013). Evaluation potential land subsidence induced by ground water withdrawal from the Indian Wells Valley, CA using InSAR. Geological Society of America Abstracts with Programs. Vol. 45, No. 7, p.775.

Katzenstein, K. (2015). InSAR analysis of aquifer-system response to pumping in the Indian Wells Valley, Kern County, California. Final Technical Report prepared for Desert Research Institute. January 21, 2015. 23 p.

McGraw, D., R. Carroll, G. Pohll, J. Chapman, S. Bacon, and R. Jasoni, 2016. Groundwater Resource Sustainability: Modeling Evaluation for the Naval Air Weapons Station, China Lake, California, Prepared by Desert Research Institute for the Naval Air Warfare Center Weapons Division, China Lake, CA, NAWCWD TP 8811.

Monastero, F.C., Walker, J.D., Katzenstein, A.M., and Sabin, A.E., 2002. Neogene Evolution of the Indian Wells Valley, East-Central California, In:Glazner, A.F., Walker, J.D., and Bartley, J.M., (eds.), Geologic Evolution of the Mojave Desert and Southwestern Basin and Range, Boulder, Colorado, Geological Society of America Memoir 195, p. 199–228.

Motts, W.S., ed., (1969). Geology and hydrology of selected playas in Western United States: Amherst, University of Massachusetts, 305 p.

Peltzer, G., Crampé, F., Hensley, S., and Rosen, P. (2001). Transient strain accumulation and fault interaction in the eastern California shear zone. Geology 29, 975–978.

Sneed, M. and Galloway, D.L. (2000). Aquifer-system compaction and land subsidence: measurements, analyses, and simulations—the Holly site, Edwards Air Force Base, Antelope Valley, California. U.S. Geological Survey Water-Resources Investigations Report 00-4015, p. 91–97.

Sneed, Michelle, Ikehara, M.E., Stork, S.V., Amelung, Falk, and Galloway, D.L. (2003). Detection and measurement of land subsidence using interferometric synthetic aperture radar and global positioning system, San Bernardino County, Mojave Desert, California: U.S. Geological Survey Water-Resources Investigations Report 03-4015, 60 p.

Solt, M., and Sneed, M. (2014). Subsidence (2004–2009) in and near lakebeds of the Mojave River and Morongo groundwater basins, southwest Mojave Desert, California: U.S. Geological Survey Scientific Investigations Report 2014-5011, unpaginated, http:// dx.doi.org/10.3133/sir20145011.

Stamos, C.L., Glockhoff, C.S., McPherson, K.R., and Julich, R.J. (2007), Water-level and land-subsidence studies in the Mojave River and Morongo groundwater basins: U.S. Geological Survey Scientific Investigations Report 2007-5097, unpaginated, http://pubs.usgs.gov/ sir/2007/5097/.

Stamos, C.L., Martin, Peter, Nishikawa, Tracy, and Cox, B.F. (2001). Simulation of ground-water flow in the Mojave River Basin, California (ver. 3, September 2001): U.S. Geological Survey Water- Resources Investigations Report 2001-4002, 137 p.

USGS [U.S. Geological Survey and California Geological Survey] (2006). Quaternary fault and fold database for the United States, accessed April 14, 2009, from USGS web site: http//earthquake.usgs.gov/hazards/qfaults/.

Wesnousky, S.G. (2005). Active faulting in the Walker Lane. Tectonics, 24, TC3009, doi: 10.1029/2004TC001645.

Zellmer, J.T., and Roquemore, G.R. (1997). Tectonic deformation of a Supersonic Naval Ordnance Research Track, Indian Wells Valley, California. Environmental and Engineering Geoscience 3, 205–215.

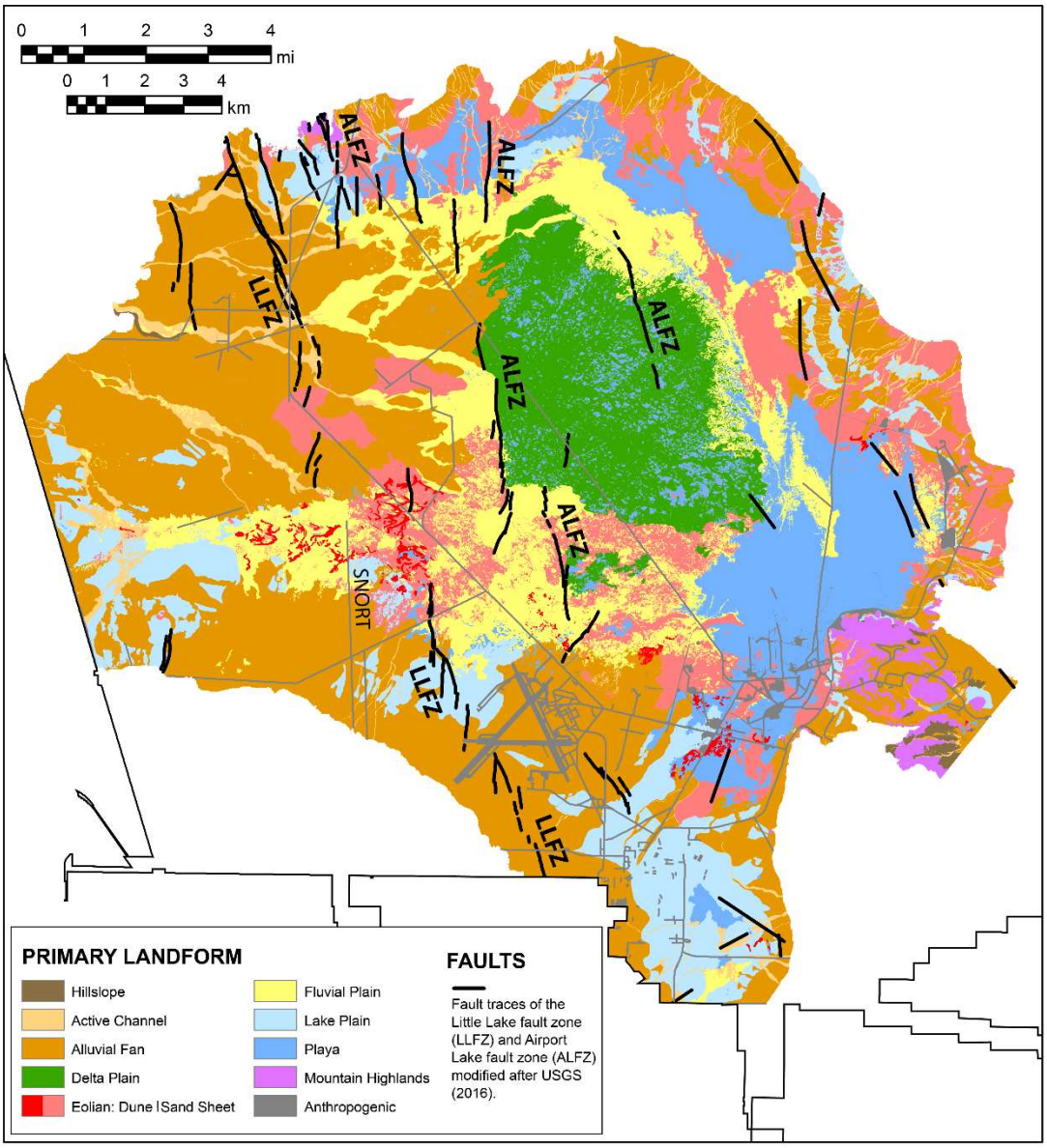

Figure 1. Geomorphic map of China Lake basin below ~2300 ft (700 m) elevation contour showing the distribution of primary landform types and major fault zones in the vicinity of the depocenter of Indian Wells Valley. LLFZ – Little Lake fault zone; ALFZ – Airport Lake fault zone. (from Bullard et al., 2018).

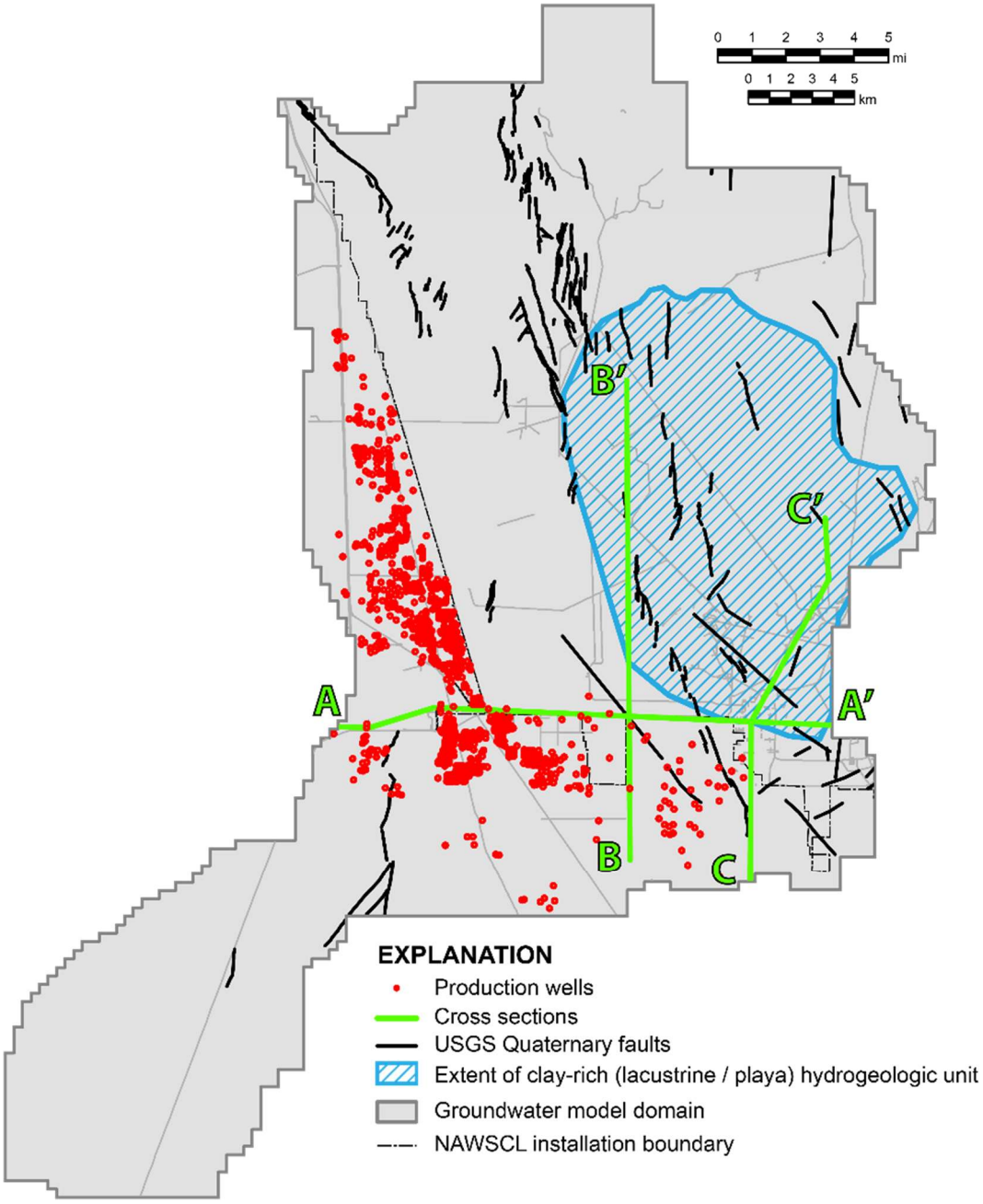

Figure 2. Spatial extent of fine-grained lacustrine and playa hydrogeologic units in Indian Wells Valley. Transects A-A', B-B', and C-C' of hydrogeologic cross sections in Figure 3 are shown. Adapted from Kunkel and Chase (1969) and McGraw et al. (2016).

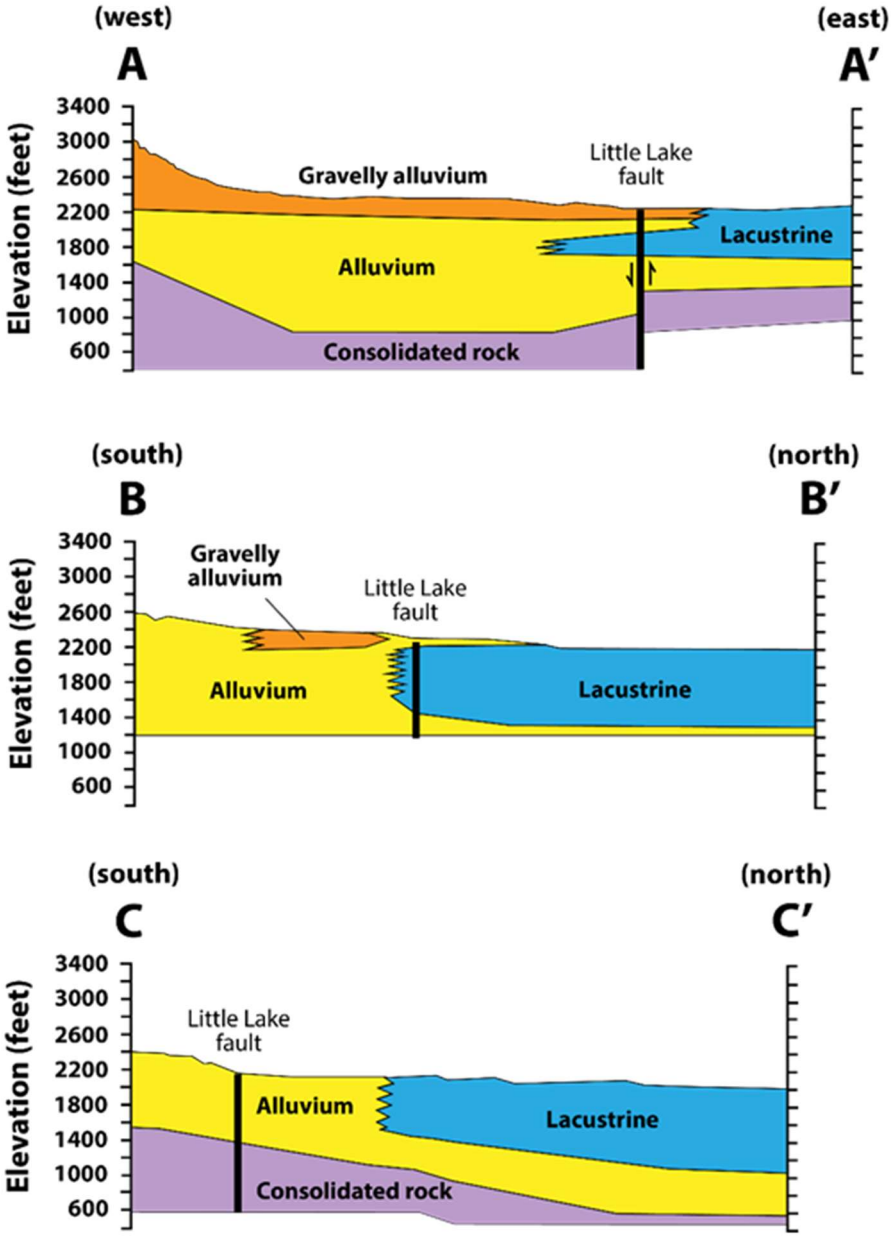

Figure 3. Cross sections of the primary hydrogeologic units in the IWV groundwater basin showing the distribution and depth of coarse-grained (gravel and alluvium) and fine-grained (lacustrine) deposits, as well as consolidated basement rocks. Also shown are the general locations of the active Little Lake fault (LLF). Modified after Kunkel and Chase (1969) and McGraw et al. (2016).

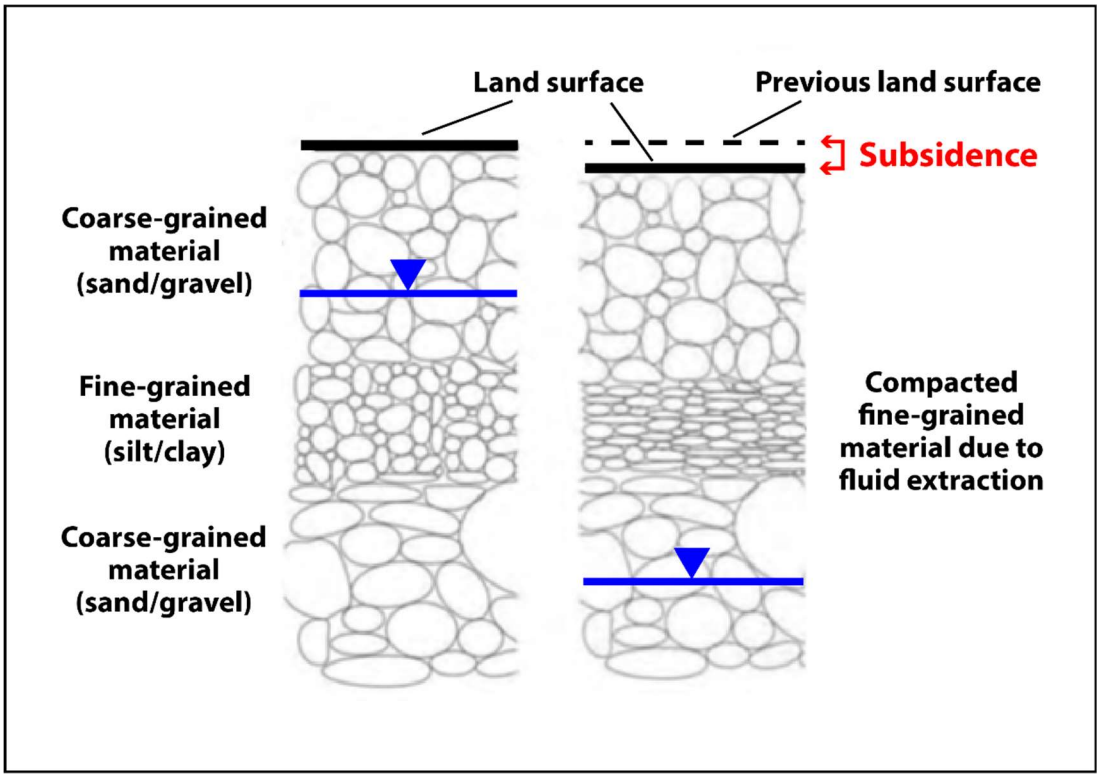

Figure 4. Conceptual model of land subsidence due to compaction of an interbedded fine-grained layer after fluid extraction from groundwater drawdown. (adapted from Sneed and Galloway, 2000; Borchers and Carpenter, 2014)

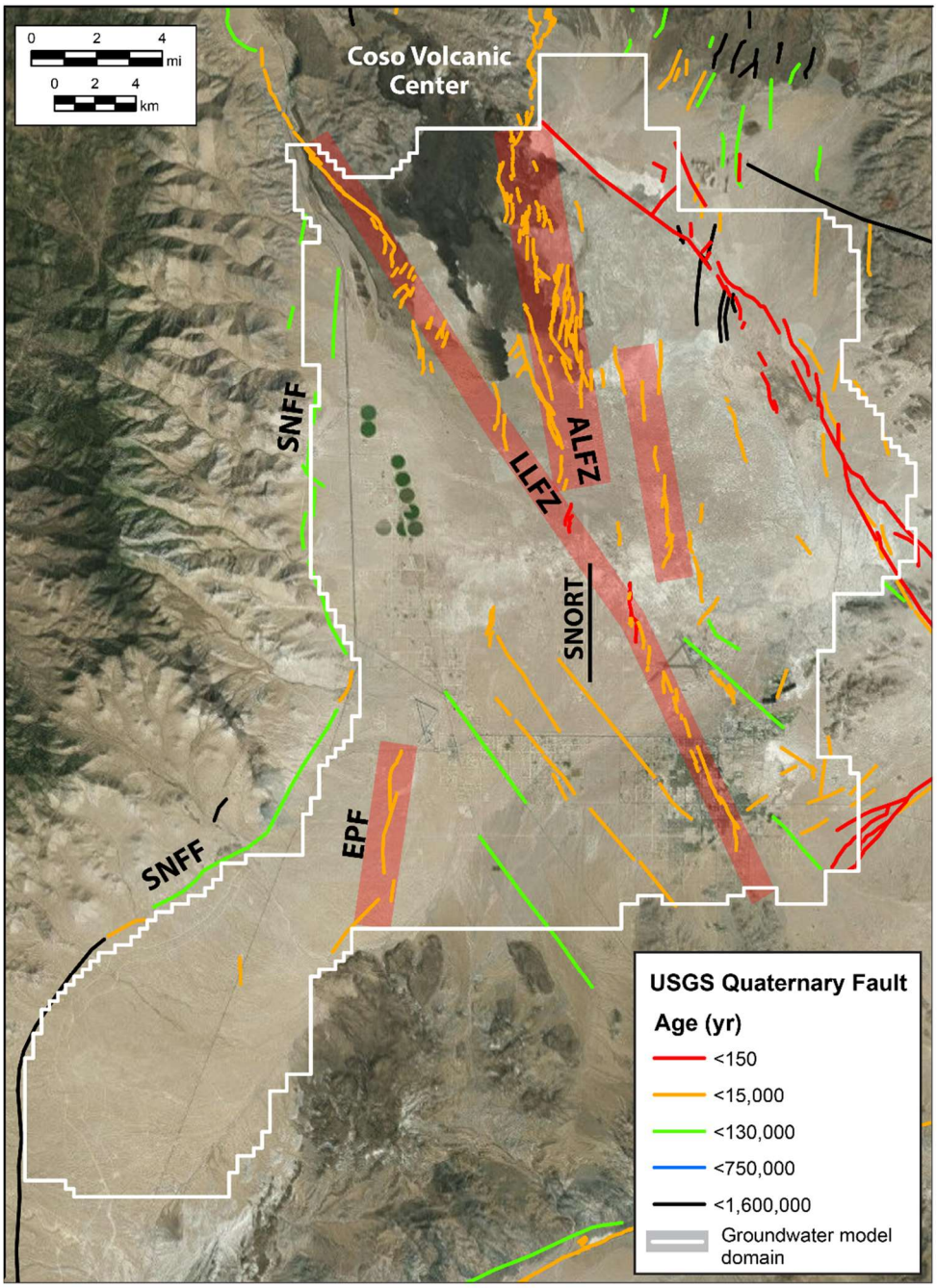

Figure 5. Map of the Indian Wells Valley groundwater model domain showing the location of the Supersonic Naval Ordnance Research Track (SNORT) alignment and faults of USGS (2016). The active Little Lake and Airport Lake fault zones (LLFZ and ALFZ, respectively), a well-defined series of faults informally referred to as the El Paso fault (EPF) are shown with red boxes. The Sierra Nevada Frontal fault (SNFF) system and the Coso Volcanic center are also

shown. The July 4 and 5, 2019 fault ruptures associated with the M6.4 Searles Valley and M7.1 Ridgecrest earthquakes, respectively, are shown as red faults, but without red boxes.

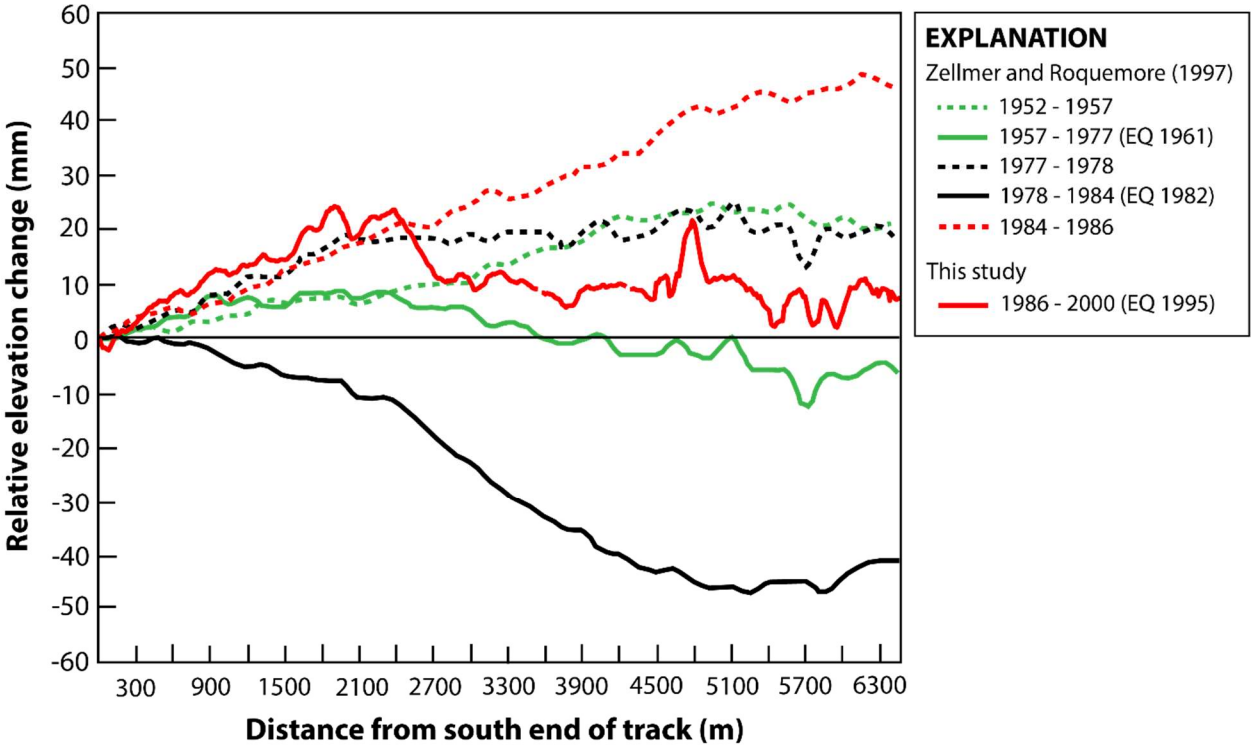

Figure 6. Plots of relative elevation change in the vertical directions of the SNORT alignment for the periods 1952–1957, 1957–1977, 1977–1978, 1978–1984, and 1984–1986 (Zellmer and Roquemore, 1997). The period 1986–2000 is from processing of SNORT GPS data of this study. Survey stations are spaced 15.2 m apart along the south to north oriented alignment. Positive values indicate an increase in relative elevation and negative values a decrease with respect to the zero-base station. Survey data reflect vertical and horizontal cyclic-strain accumulation along the LLFZ from stress build up (uplift) during periods with no seismic activity and a stress drop (subsidence) after notable nearby ~M5 earthquakes (EQ) in 1961, 1982, and 1995.

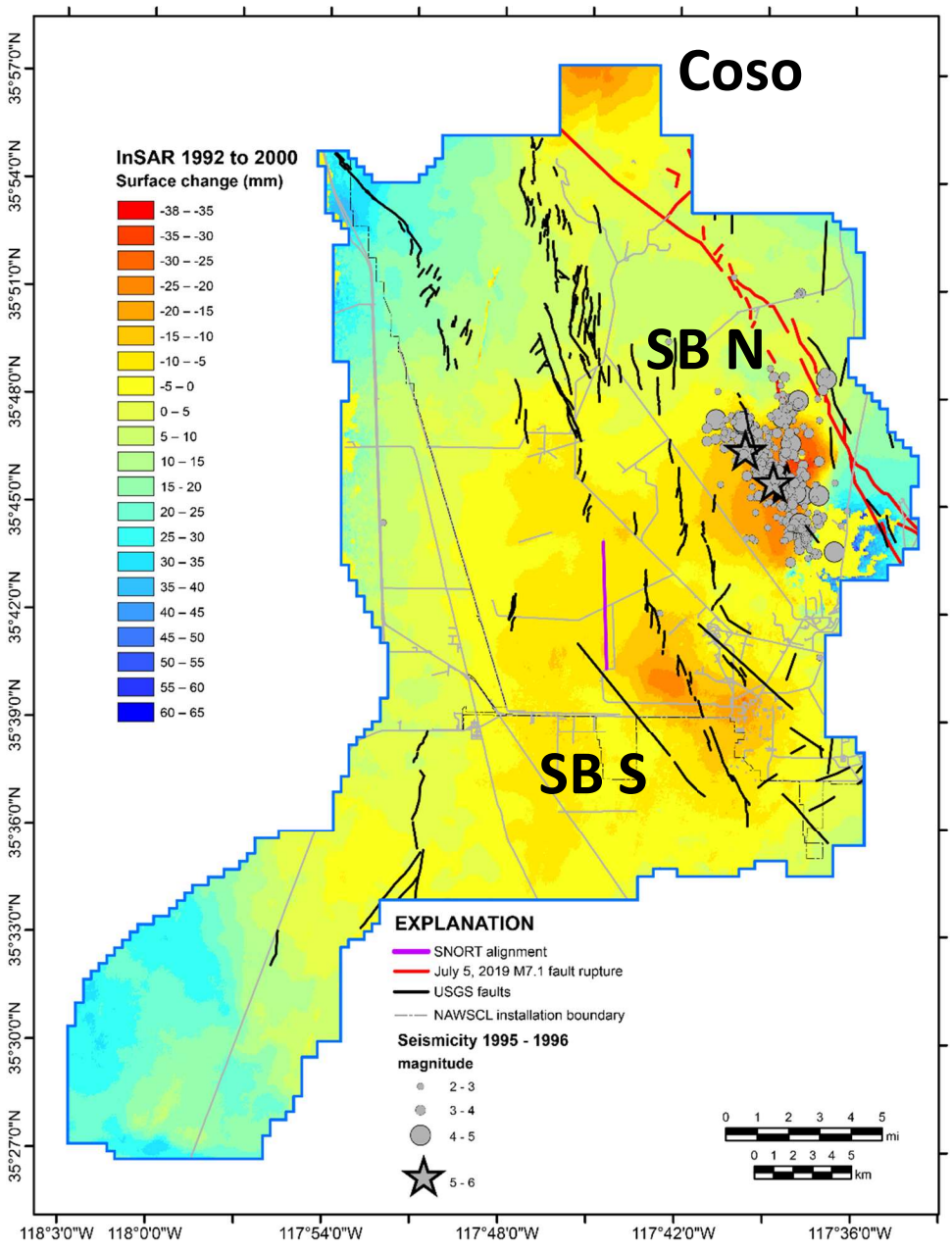

Figure 7. Map showing 8 years of surface change within the Indian Wells Valley (IWV) groundwater model domain from Interferometric Synthetic Aperture Radar (InSAR) data between 1992 and 2000 (Katzenstein, 2015). The location of faults from USGS (2016), the epicenters of the 1995 M5.4 Ridgecrest earthquake sequence, and SNORT alignment near the Little Lake fault zone are also shown. The SB N and SB S delineate the northern and southern subsidence areas, respectively; and Coso is a subsidence area related to the Coso geothermal field.

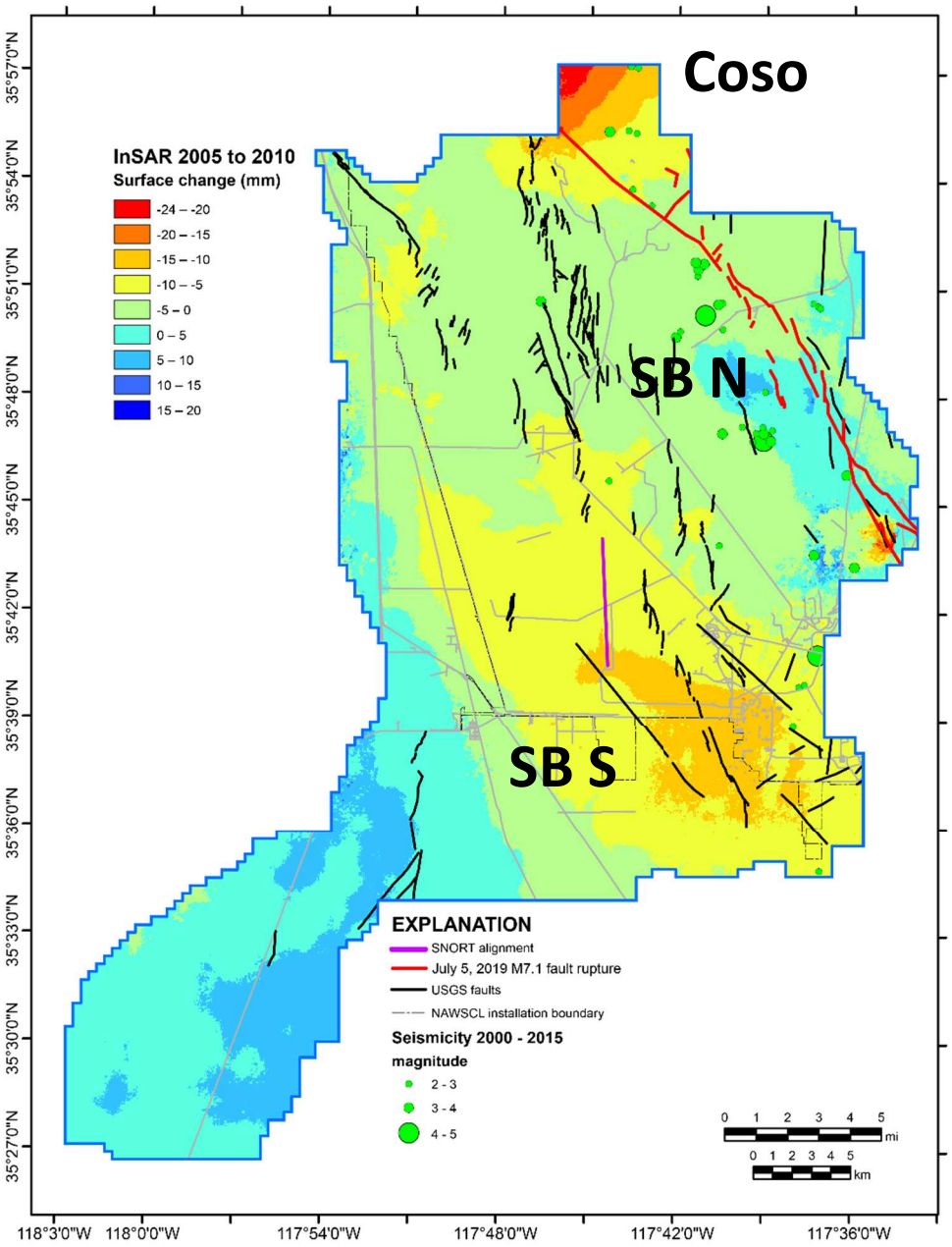

Figure 8. Map showing 5 years of surface change within the Indian Wells Valley (IWV) groundwater model domain from Interferometric Synthetic Aperture Radar (InSAR) data between 2005 and 2010 processed by Katzenstein (2015). The location of faults from USGS (2016), seismicity from 2000–2015, and SNORT alignment near the LLFZ is shown. The SB N and SB S delineate the northern and southern subsidence areas, respectively; and Coso is a subsidence area related to the Coso geothermal field.

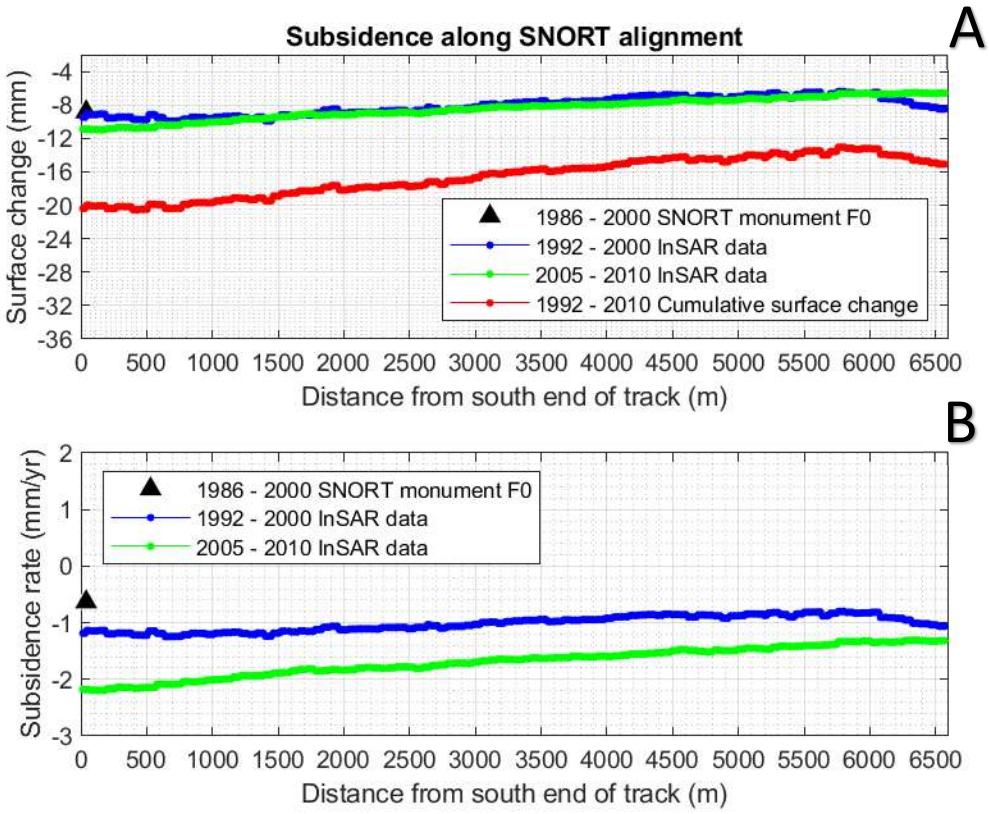

Figure 9. Plots showing discrete and cumulative subsidence (A) and subsidence rate (B) along the SNORT alignment from Interferometric Synthetic Aperture Radar (InSAR) data for the periods 1992–2000, 2005–2010, and 1992–2010. The amount of subsidence and rate of the SNORT base station (monument F0) from the difference of reported absolute elevations for the period 1986–2000 are also shown.

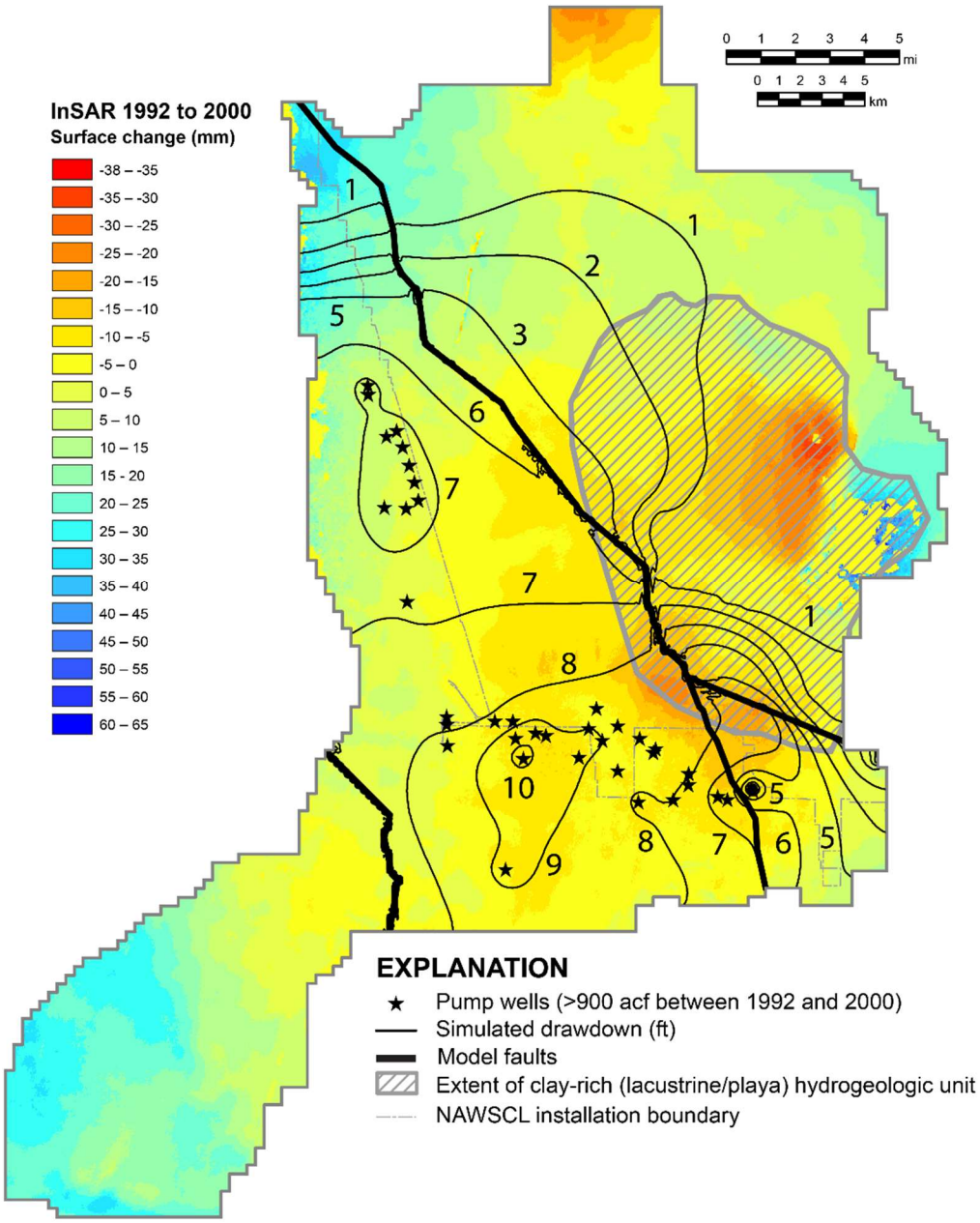

Figure 10. Map showing 8 years of surface change within the Indian Wells Valley (IWV) groundwater model domain from Interferometric Synthetic Aperture Radar (InSAR) data between 1992 and 2000 (Katzenstein, 2015). The location of modeled faults, simulated drawdown from the IWV groundwater model, and the extent of a clay-rich hydrogeologic unit

are shown. The distribution of wells with greater than 900 acre-feet of groundwater extraction during the period are also shown.

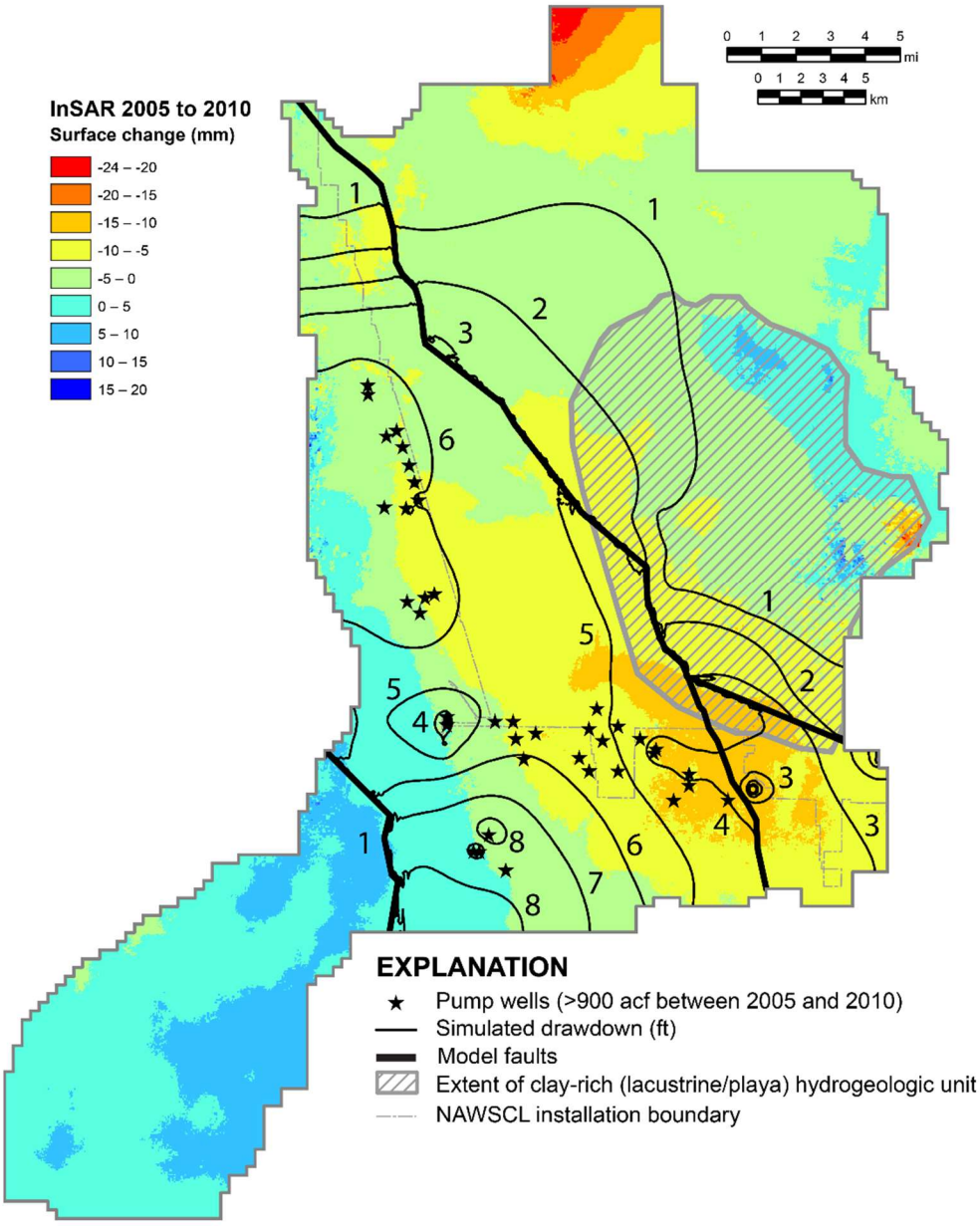

Figure 11. Map showing 5 years of surface change within the Indian Wells Valley (IWV) groundwater model domain from Interferometric Synthetic Aperture Radar (InSAR) data

between 2005 and 2010 (Katzenstein, 2015). The location of modeled faults, simulated drawdown from the IWV groundwater model, and the extent of a clay-rich hydrogeologic unit are shown. The distribution of wells with greater than 900 acre-feet of groundwater extraction during the period are also shown.

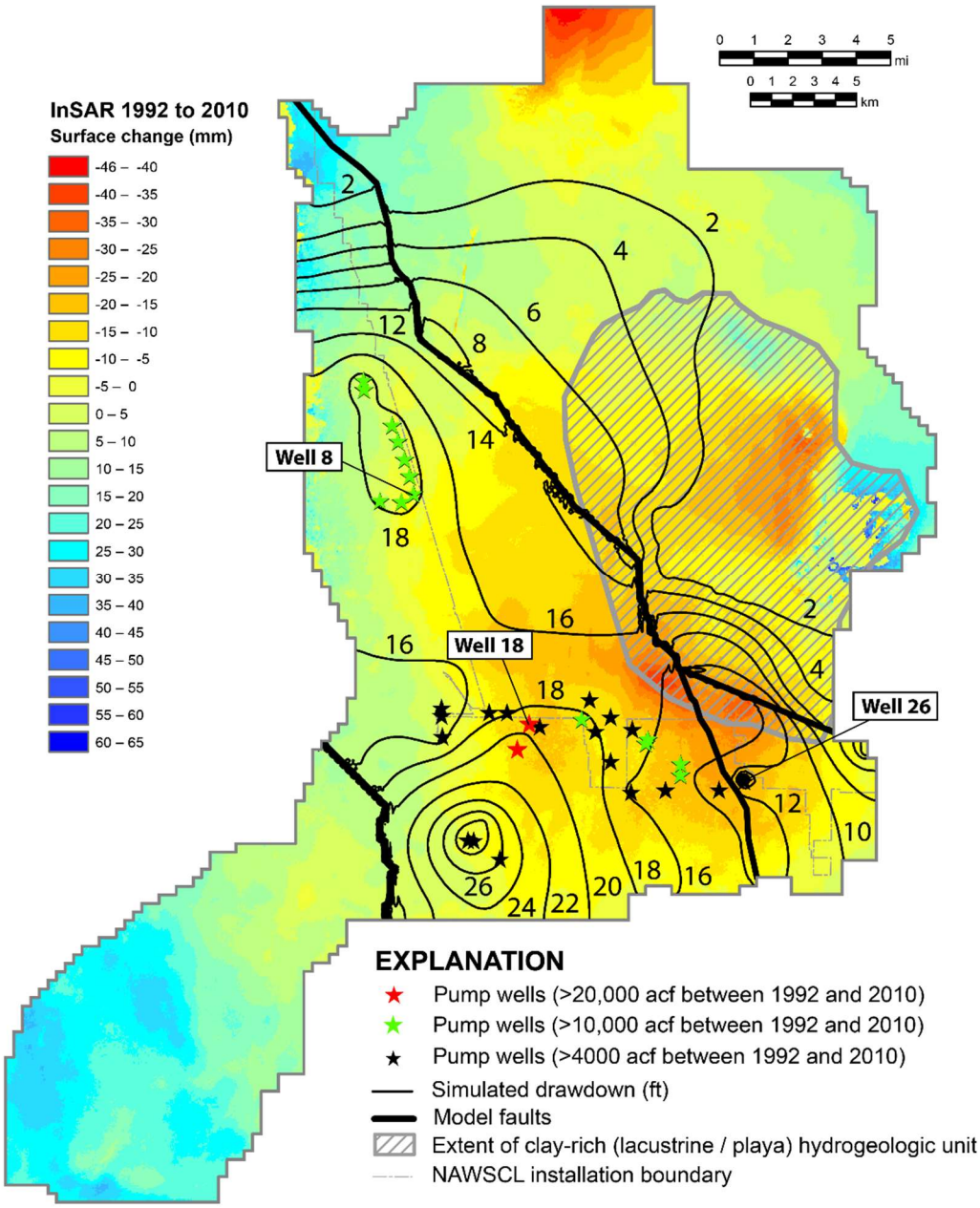

Figure 12. Map showing 18 years of surface change within the Indian Wells Valley (IWV) groundwater model domain from Interferometric Synthetic Aperture Radar (InSAR) data between 1992 and 2010 (Katzenstein, 2015). The location of modeled faults, simulated drawdown from the IWV groundwater model, and the extent of a clay-rich hydrogeologic unit

are shown. The distribution of wells with greater than 4000, 10,000, and 20,000 acre-feet of groundwater extraction during the period are also shown. The location of wells (8, 18, and 26) referred to in text are shown.

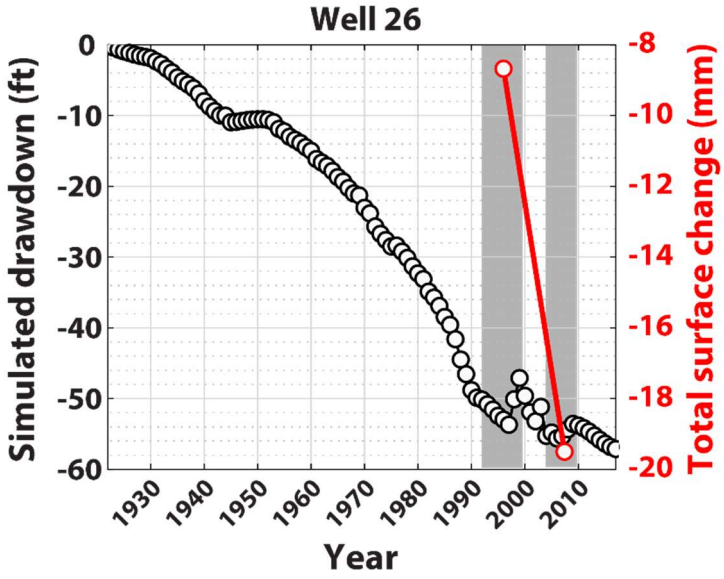

Figure 13. Plots showing temporal correspondence between simulated drawdown from the IWV groundwater model and land surface changes at well site 26 in areas of the southern subsidence area on distal alluvial fans and playa margins. Total surface change measured by Interferometric Synthetic Aperture Radar (InSAR) at the well site between the periods 1992–2000 (midpoint 1996) and 2005–2010 (midpoint 2007.5) are also shown. Well location and corresponding InSAR surface change value are on Figure 12.

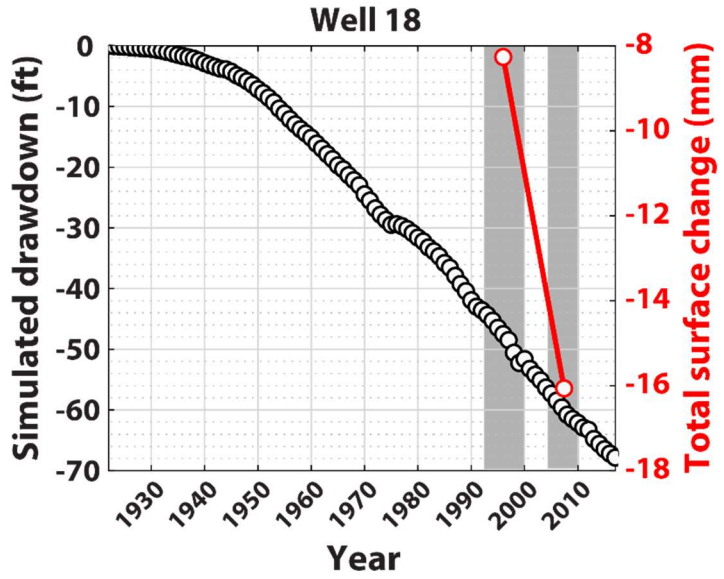

Figure 14. Plots showing temporal correspondence between simulated drawdown from the IWV groundwater model and land surface changes at well site 18 in areas of groundwater extraction of greater than 20,000 acre-feet on medial to distal alluvial fans during the period 1992–2010. Total surface change measured by Interferometric Synthetic Aperture Radar (InSAR) at the well site between the periods 1992–2000 (midpoint 1996) and 2005–2010 (midpoint 2007.5) are also shown. Well location and corresponding InSAR surface change value are on Figure 12.

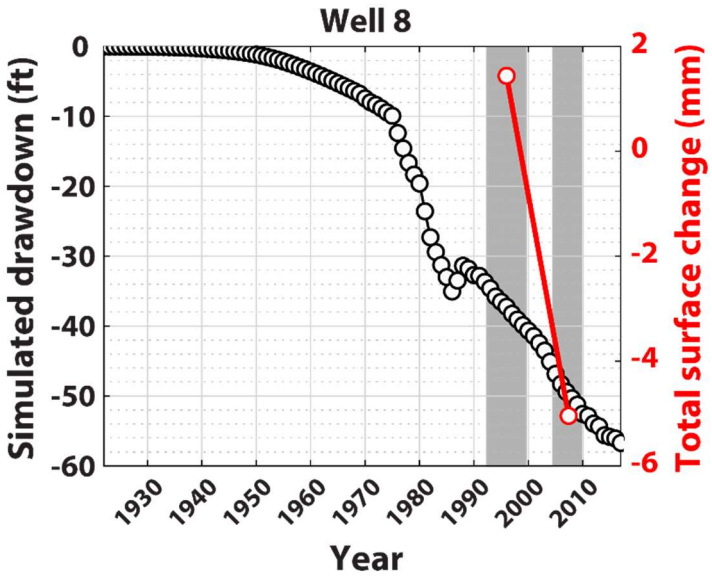

Figure 15. Plots showing temporal correspondence between simulated drawdown from the IWV groundwater model and land surface changes at well site 8 in areas of agricultural fields on medial to distal alluvial fans. Total surface change measured by Interferometric Synthetic Aperture Radar (InSAR) at the well site between the periods 1992–2000 (midpoint 1996) and 2005–2010 (midpoint 2007.5) are also shown. Well location and corresponding InSAR surface change value are on Figure 12.

APPENDIX 3-H

MODEL DOCUMENTATION

(Page Intentionally Left Blank)

Indian Wells Valley GSP Model Documentation
DRAFT

Karl Pohlmann, Chris Garner, Jenny Chapman, and Greg Pohll
Desert Research Institute
Nevada System of Higher Education

January 2020

THIS PAGE LEFT INTENTIONALLY BLANK

CONTENTS

List of Figures ii
List of Tables iv
1. Introduction 1
2. Flow Model 1
2.1 Strategy and Assumptions 1
2.2 Code Selection and Documentation 1
2.3 Configuration 2
2.4 Boundary Conditions 4
2.4.1 Perimeter Boundaries 4
2.4.2 Internal Boundaries 4
2.4.3 Recharge 5
2.4.4 Evapotranspiration 7
2.4.5 Groundwater Pumping 12
2.4.6 Basin Outflow 15
2.5 Calibration 16
2.5.1 Steady-State Model 16
2.5.2 Transient-Historical Model 24
2.6 Sensitivity Analysis 36
2.7 Predictive Flow Models 42
3. Transport Model 43
3.1 Introduction 43
3.2 Code Selection and Documentation 43
3.3 Configuration 43
3.4 Initial and Boundary Conditions 44
3.5 Calibration 53
3.6 Transport Results 55
4. Model Limitations 58
References 59
Appendix A: Plots of Simulated and Measured Groundwater Level Hydrographs for Calibration of the Transient-Historical Model A-1

List of Figures

1. Domain of the Indian Wells Valley groundwater flow model showing perimeter boundary conditions. 3
2. East-West cross-section A-A' through model mesh showing the configuration of the six computational layers. 4
3. Locations of the eight fault segments simulated as hydrologic barriers. 5
4. Mountain-block recharge zones surrounding Indian Wells Valley and their associated flux values (shown in blue) on the model boundary. 6
5. Annual variability of recharge forecasted for the predictive simulations. 7
6. Distribution of vegetation and bare ground (denoted as Barren in the legend) within the area of evapotranspiration (ET) (from McGraw et al. [2016]). 8
7. Map of evapotranspiration zones used for the Evapotranspiration Segments (ETS) package in the GSP model. 10
8. The ETS segmented curve that relates the proportion of evapotranspiration extinction depth (PXDP) to the proportion of the maximum evapotranspiration rate (PETM). 11
9. Spatial distribution of two ET zones in the model and their annual ET rates as estimated from EVI values from Landsat imagery using the method of Beamer et al. (2013). 12
10. Annual groundwater withdrawals for all use categories for the period 1920 through 2016. 14
11. Groundwater-pumping wells included in the transient models 15
12. Locations of groundwater level targets for the steady-state pre-development model (from Garner et al. [2017]). 17
13. Locations of pilot points in (a) Layer 1 and (b) Layers 2 and 3 that were used for calibration of the steady-state flow model. 18
14. Calibrated hydraulic conductivity in (a) Layer 1, (b) Layers 2 and 3, and (c) Layers 3, 4, and 5 of the steady state model. 20
15. Cross sections showing examples of the distribution of calibrated hydraulic conductivity within the layers of the steady state model. 21
16. Residuals between simulated and observed groundwater levels for the calibrated steady-state model. 22
17. Plot of simulated heads to observed heads in the calibrated steady-state model. 23
18. Groundwater flow directions and hydraulic heads simulated on Layer 1 of the pre-development steady-state model. 24
19. Locations of groundwater level targets used for calibration of the transient-historical flow model. 25
20. Example of the hydrograph slope-fitting method used for calibration of the transient-historical flow model. 27
21. Results of calibration metrics Drawdown Slope and MAE of All Heads used for calibration of the transient-historical flow model. 28

22. Spatial distribution of specific yield obtained by kriging in the calibrated transient-historical model. 29
23. Mean residuals between simulated and observed groundwater levels for the calibrated transient-historical model. 30
24. Plot of simulated heads to observed heads in the calibrated transient-historical model. 31
25. Simulated and observed heads at well 27S38E02C01 near the El Paso fault zone. 32
26. Mean residuals between simulated and observed drawdown slopes in the transient-historical model. 33
27. Comparison of water levels simulated by the transient-historical model to observed water levels for the year 2016. 34
28. Evapotranspiration (ET) simulated by the transient-historical model plotted against ET estimated by the empirical relationship established by Beamer et al. (2013) between EVI and ET. 35
29. Locations of wells used for water-level observations in the sensitivity analysis. 38
30. Results of sensitivity analysis for constant recharge rates (a) and specific yield (b). 39
31. Results of sensitivity analysis for specific storage (a) and hydraulic conductivity (b). 40
32. Results of sensitivity analysis for annually variable recharge rate. 41
33. Comparison of the sensitivity coefficients for the five parameters adjusted during the sensitivity analysis. 41
34. Annual rates of groundwater withdrawal and artificial recharge included in the Baseline and Scenario 6.2 models. 42
35. Examples of TDS temporal trends and the selection of the most recent TDS concentration for wells having multiple measurements. 45
36. Locations of wells and the most recent TDS concentrations in the three TDS zones used to develop the TDS initial conditions for the transport model. 46
37. Example of calculation of mean TDS values at wells having multiple measurements in a single TDS zone. 47
38. An example North-South cross section through the transport model illustrating the relationship between of the Shallow, Intermediate, and Deep TDS zones to the six computational layers in the flow model. 48
39. Locations of wells having multiple screens and TDS measurements in the Shallow and Deep TDS zones. 49
40. Spatial distributions of TDS concentration in the three TDS zones that are used for initial conditions in the transport model. 51
41. TDS concentrations assigned to groundwater recharge areas in the transport model. 52
42. Comparison of annual rate of change in TDS (mg/L/yr) forecasted for the years 2020 to 2070 in the Shallow TDS Zone to historical annual rates of change observed in wells. 54
43. Comparison of the spatial distributions of simulated TDS concentration in the shallow TDS zone in the year 2020 (left), and the year 2070 for the baseline model (center) and the scenario 6.2 model (right). 56

44. Areas where the forecasted annual rate of change in TDS concentration exceeds 5 mg/L/yr for the years 2020 to 2070 for the baseline model (left) and scenario 6.2 model (right). 57

List of Tables

1. Values of evapotranspiration rate used to develop the segmented ETS curve for the Evapotranspiration Segments (ETS) package. 9
2. Summary of ranges of parameter values and calibrated values estimated during calibration of the steady-state model. 19
3. Groundwater budget simulated by the steady-state model. 23
4. Groundwater budget simulated by the transient-historical model for the year 2016 36
5. Values of constant parameters used in the sensitivity analysis. 37
6. Wells used for comparison of observed to simulated TDS concentration trends 55

1. Introduction

A three-dimensional groundwater flow and salinity transport model of the groundwater system in Indian Wells Valley Groundwater Basin was developed for this Groundwater Sustainability Plan (GSP). This model was utilized to:

- develop a quantitative framework for synthesizing data and conceptualizing hydrogeologic processes,
- provide a common foundation for developing and testing conceptual models,
- testing of options for groundwater resources management, and
- evaluate compliance with the Sustainable Groundwater Management Act (SGMA).

This appendix documents how the conceptual model of the Indian Wells Valley Groundwater Basin (IWVGB) described in Section 3.3 is represented in the flow and salinity transport models. Also described here are the modeling strategy and assumptions, model simulation codes, model configuration, boundary conditions, calibration processes, and sensitivity analysis.

The IWVGB flow model is based on a groundwater flow model developed by Desert Research Institute (DRI) (McGraw et al., 2016) for the U.S. Navy to support their planning for the China Lake Naval Air Weapons Station (NAWS) in response to declining groundwater levels in Indian Wells Valley and concerns about water quality degradation and subsidence. The 2016 model was subsequently revised by DRI to include regional faults as internal hydrologic barriers and then recalibrated (Garner et al., 2017). The 2017 model was further revised and enhanced by DRI for the Indian Wells Valley GSP. This documentation provides an overview of the model construction and application, but ultimately focuses on the components and approaches incorporated for this GSP that differ from the previous versions.

2. Flow Model

2.1 Strategy and Assumptions

The primary assumptions of the model include the following:

- The groundwater system is in a transient state based on observed water level changes and the conceptualization of the groundwater budget.
- Groundwater flow can be described by the continuum approach, although several discrete hydrologic features are included to represent faults.
- Hydrogeologic units are internally heterogeneous, with variations established by calibration to local hydraulic data and conceptualizations of lithologic and structural features.
- The shallow zone of the groundwater system is unconfined below most of the basin, though discontinuous clay layers confine lower zones in some locations.

Additional model assumptions are described in subsequent sections of this documentation.

2.2 Code Selection and Documentation

The flow model utilizes the public-domain and widely-accepted MODFLOW-NWT finite-difference groundwater modeling code developed by the U.S. Geological Survey (version 1.1.3) (Niswonger et al., 2011) and its supporting modular flow packages. MODFLOW-NWT is a formulation of the MODFLOW-2005 code (Harbaugh, 2005) that provides improved solutions for complex, unconfined groundwater

flow systems. The model was constructed using the Groundwater Modeling System (GMS) environment (version 10.2) developed by Aquaveo, LLC. GMS serves as a database for all of the hydrogeologic information in the model and provides an easy to use graphical pre- and post-processor interface to MODFLOW. Although developed within GMS, the MODFLOW input and output files are in standard MODFLOW format and the model can be run without the use of GMS.

2.3 Configuration

The active domain of the IWVGB groundwater flow model encompasses 460 square miles on the valley floor of Indian Wells Valley (Figure 1). The model is aligned with and georeferenced to the Universal Transverse Mercator (UTM) coordinate system Zone 11 North, North American Datum (NAD) 1983, and is discretized on a uniform mesh of 231 rows and 207 columns. Cell dimensions are 820.2 feet (250 m) in both the easting and northing directions, corresponding to a cell area of 15.4 acres. Land surface elevations from a digital elevation model (DEM) having a resolution of 10 m were resampled to the model mesh to represent the top surface of the numerical model. The length unit is meters, but the output is converted to U.S. customary units for reporting purposes.

Six computational layers (Figure 2) vary in thickness from 100 to 500 ft to allow representation of the observed vertical and horizontal heterogeneity in hydraulic properties of unconsolidated alluvium, lacustrine, and playa deposits within the basin. Values of these properties were estimated during model calibration (Section 2.5). The model reaches its maximum thickness of 2,544 feet in the El Paso sub-basin.

The primary flux simulated on the perimeter boundary is mountain-block recharge and underflow of recharge in Rose Valley in the far northwestern corner of the model (McGraw et al., 2016) (described in Section 2.4.3). In terms of outflow, the IWVGB is considered to be a nearly hydrologically closed basin; the only interbasin groundwater discharge is thought to be a small quantity of flow toward Salt Wells Valley to the southeast (McGraw et al., 2016) (described in Section 2.4.1).

Three distinct intervals within the time period 1920 to 2070 are simulated in the GSP models to maximize the utility of available hydraulic data in the IWVGB and effectively predict changes in the groundwater system through time. A steady-state stress period, based on models constructed by DRI for the U.S. Navy (McGraw et al., 2016; Garner et al., 2017), represents hydrologic conditions prior to large-scale groundwater pumping that began in 1921 (McGraw et al., 2016) and was used for calibration. Groundwater conditions during the 96-year interval from 1921 through 2016 are simulated by the GSP transient-historical model that uses stress periods of one-year length and the results from the steady-state stress period as initial conditions. The GSP transient-predictive model predicts changes in groundwater levels and storage for the 54-year interval from 2017 through 2070 using stress periods of one-month length and the results of the 96-year transient-historical simulation as initial conditions.

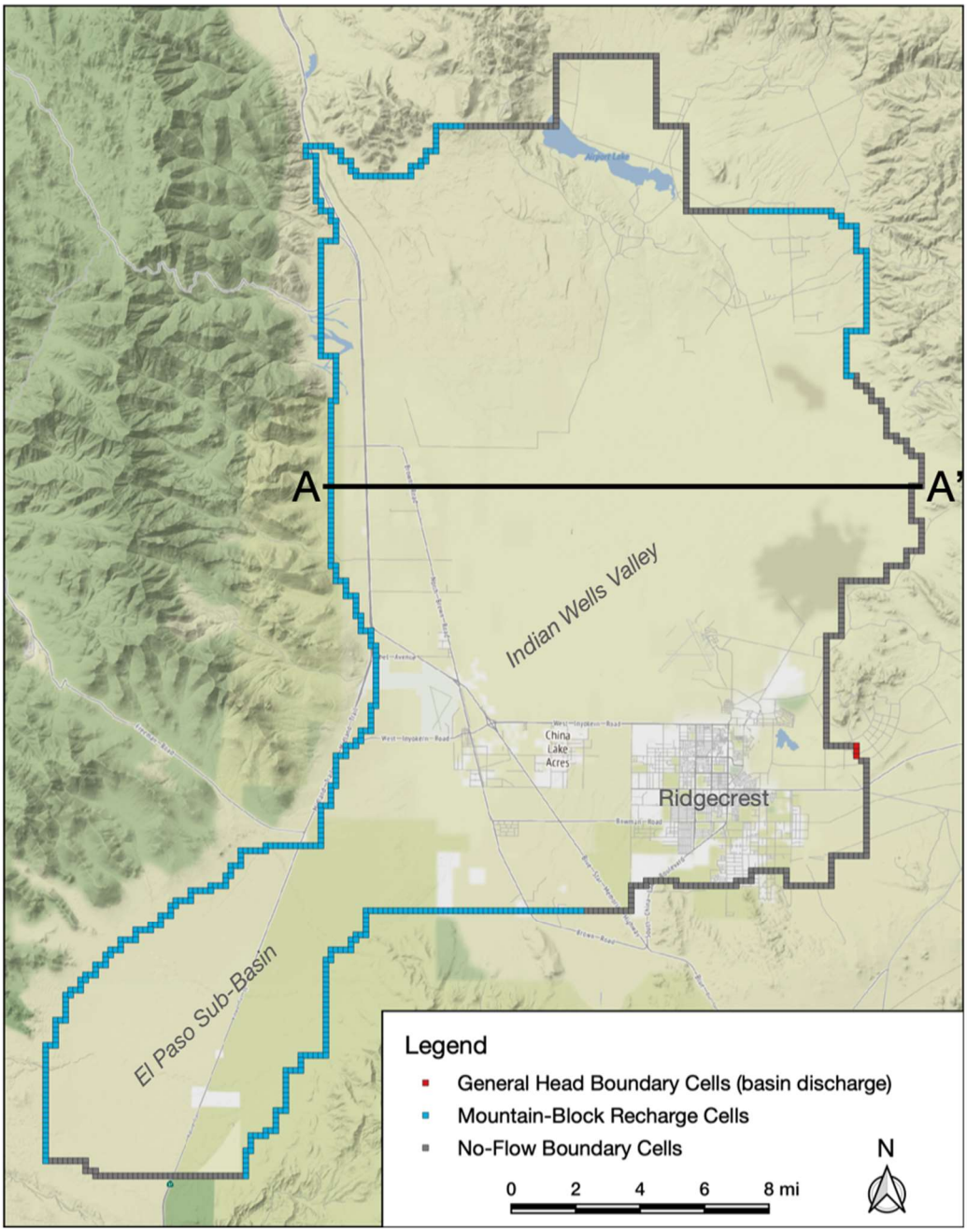

Figure 1. Domain of the Indian Wells Valley groundwater flow model showing perimeter boundary conditions. Cross-section A-A' through the model mesh is shown in Figure 2.

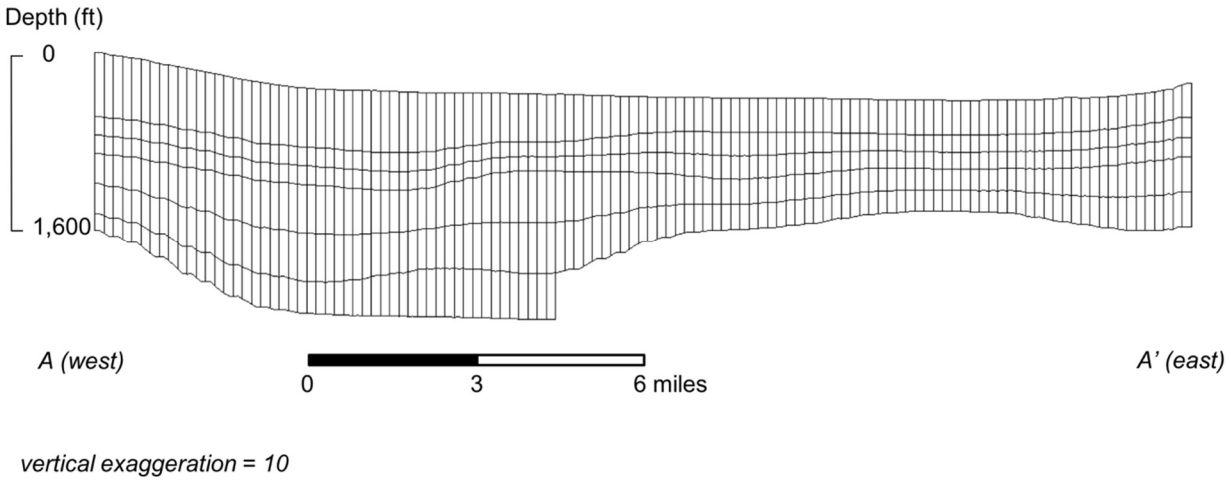

Figure 2. East-West cross-section A-A' through model mesh showing the configuration of the six computational layers.

2.4 Boundary Conditions

2.4.1 Perimeter Boundaries

The perimeter of the model is configured as interbasin flow, recharge, or no-flow boundary segments. Interbasin flow is simulated only toward Salt Wells Valley to the east using an assumed boundary head of 2,152 ft assigned to three adjoining boundary cells in Layer 1 (shown in Figure 1). Interbasin flow is only allowed to leave the model domain at this location and only in Layer 1 (Section 2.4.6).

Recharge from adjacent mountain blocks is simulated on selected perimeter boundary segments in Layers 1, 2, and 3 (shown in Figure 1) and is described further in Section 2.4.3. The remaining boundary segments are configured as no-flow in all six layers.

2.4.2 Internal Boundaries

Active faults in the IWVGB that are known to act as groundwater barriers include the Little Lake fault zone (LLFZ) and a fault that crosses the eastern margin of the El Paso Valley in the southwestern portion of IWV, informally referred to here as the El Paso fault (EPF) (Lancaster et al., 2019; Garner et al., 2017). These faults increase horizontal gradients, particularly in the vicinity of the EPF where a large groundwater gradient is present on the order of 100 ft/mile. Observations in Owens Valley, the next major hydrographic basin to the north, also find that fault systems can reduce transmissivity of aquifer materials in fault zones by a factor of 20 (Danskin, 1998).

The LLFZ and EPF are simulated as eight individual fault segments using MODFLOW's Horizontal Flow Barrier (HFB) package (Figure 3). These faults are assumed to extend vertically through all six model layers. Note that a splay of the LLFZ suggested by fault maps and water level patterns (Lancaster et al., 2019) was added to the 2017 model (Garner et al., 2017) to improve the fit of simulated head gradients in the southeastern area of the basin. Values of the fault hydraulic characteristic parameter for each fault segment were estimated during model calibration (Section 2.5).

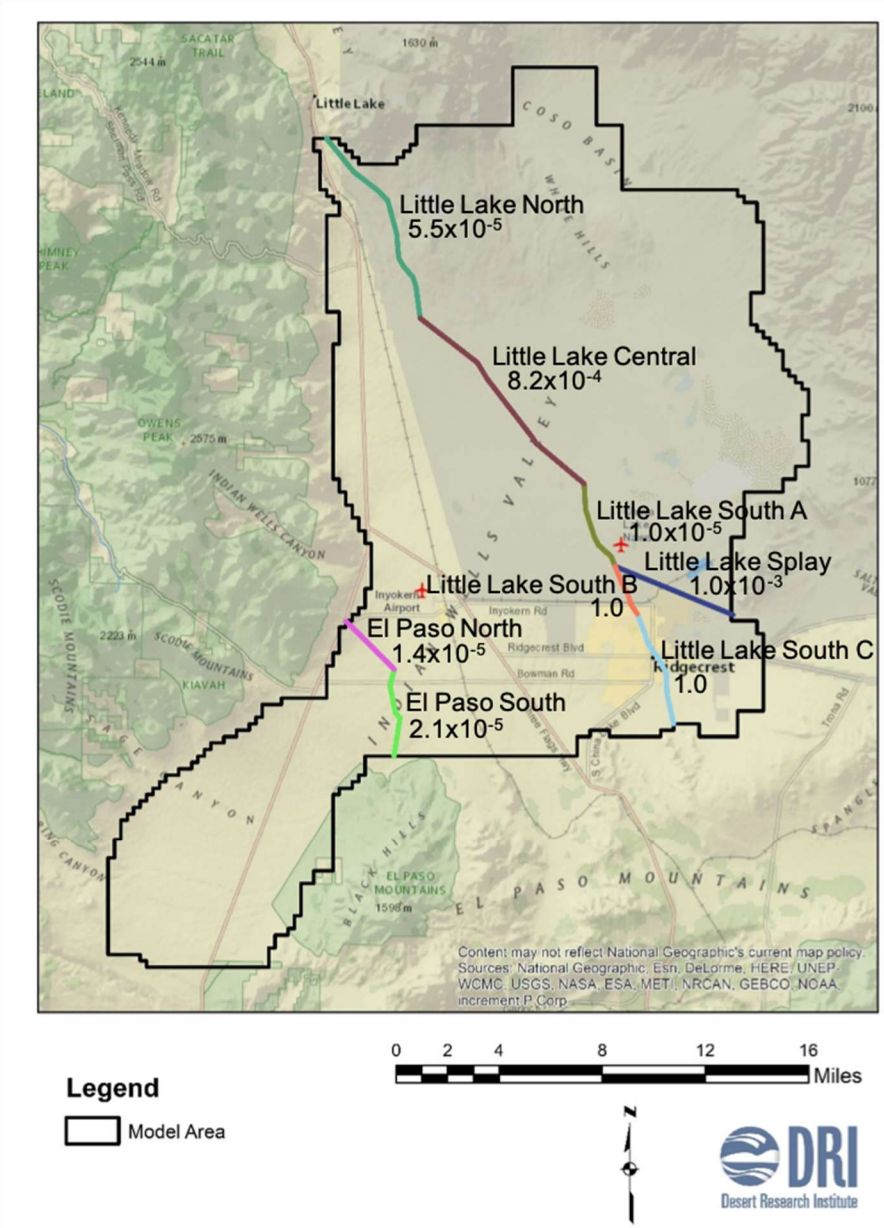

Figure 3. Locations of the eight fault segments simulated as hydrologic barriers. Values of the calibrated hydraulic characteristic parameter are shown for each segment. Units are day^{-1}.

2.4.3 Recharge

Mountain-block recharge is the primary inflow to the groundwater system and is simulated on selected segments of the perimeter boundary as a specified-flux boundary condition using the MODFLOW WEL package. Total mountain-block recharge is simulated as a constant flux of 7,650 AFY in the steady-state and transient models. This value was developed from analysis of fourteen previous recharge studies in the basin and a two-dimensional flow model constructed to assess the recharge estimates and their spatial distribution (McGraw et al., 2016). The range in estimates of total mountain-block recharge of

4,100 to 11,000 AFY from these previous studies was discussed with the Model Ad Hoc Group of the IWV Technical Advisory Committee and the best estimate value of 7,650 AFY presented by McGraw et al. (2016) was confirmed for use in the GSP model.

The recharge boundaries and their associated flux values are shown in Figure 4. Recharge flux from each recharge zone is distributed among the cells on the adjacent model boundary and is applied only to cells in Layers 1, 2, and 3 where permeabilities of the range-front and basin-fill sediments are expected to be highest. Below these recharge boundary segments, boundary cells in Layers 4, 5, and 6 are configured as no-flow. Recharge rates are constant in the steady-state and transient-historical simulations, and vary temporally in the transient-predictive simulations.

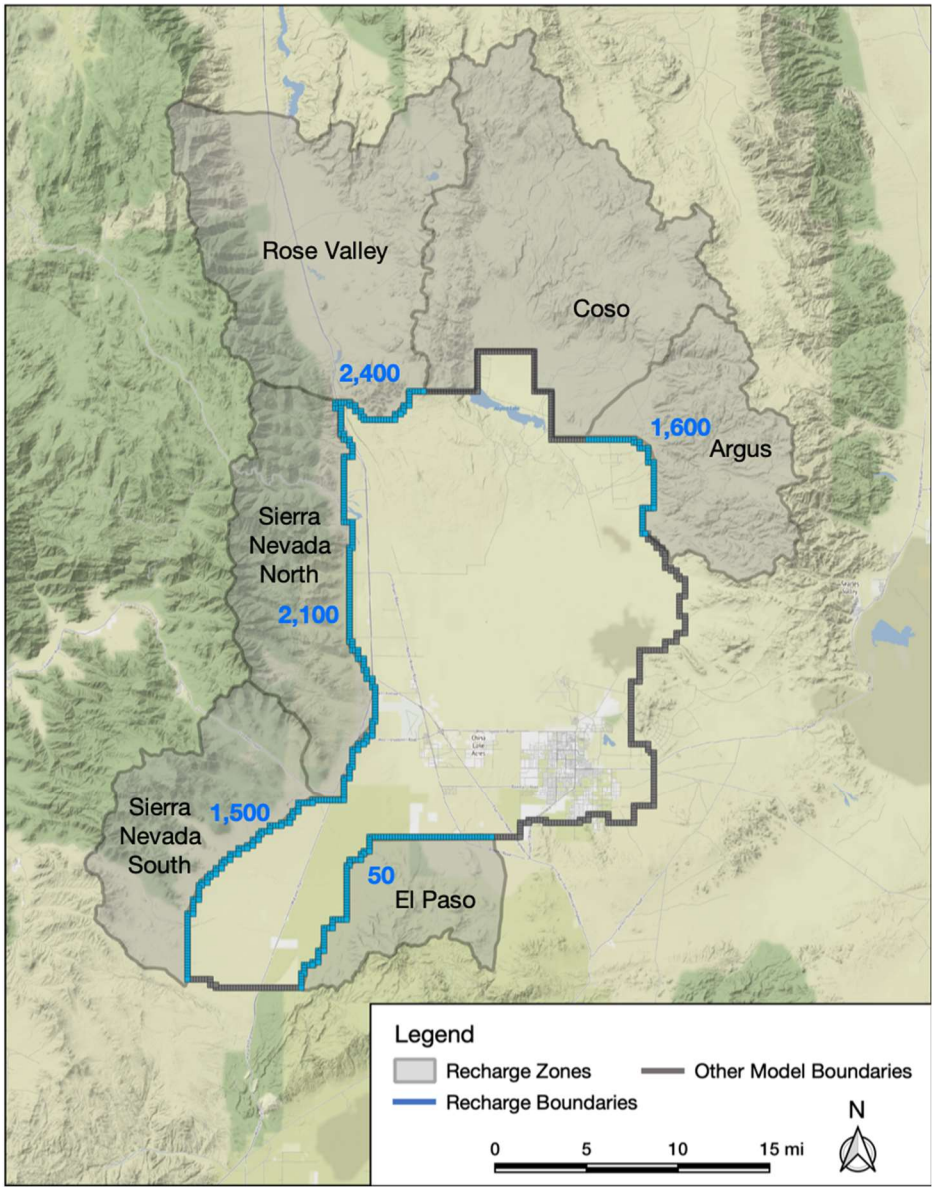

Figure 4. Mountain-block recharge zones surrounding Indian Wells Valley and their associated flux values (shown in blue) on the model boundary. Recharge units are acre-ft/year.

Annual variations in recharge rate were developed for the transient-predictive model by scaling the constant rate by the annual precipitation amounts observed in and near Indian Wells Valley over a balanced hydrologic period from 1990 through 2014 (Stetson Engineers, 2018). This 26-year period was then repeated to obtain the 51-year record (the last year of the repeated period was not included). The mean of these variations over the prediction period is equal to the annual recharge rate of 7,650 AF used for the steady-state and transient stress models (Figure 5).

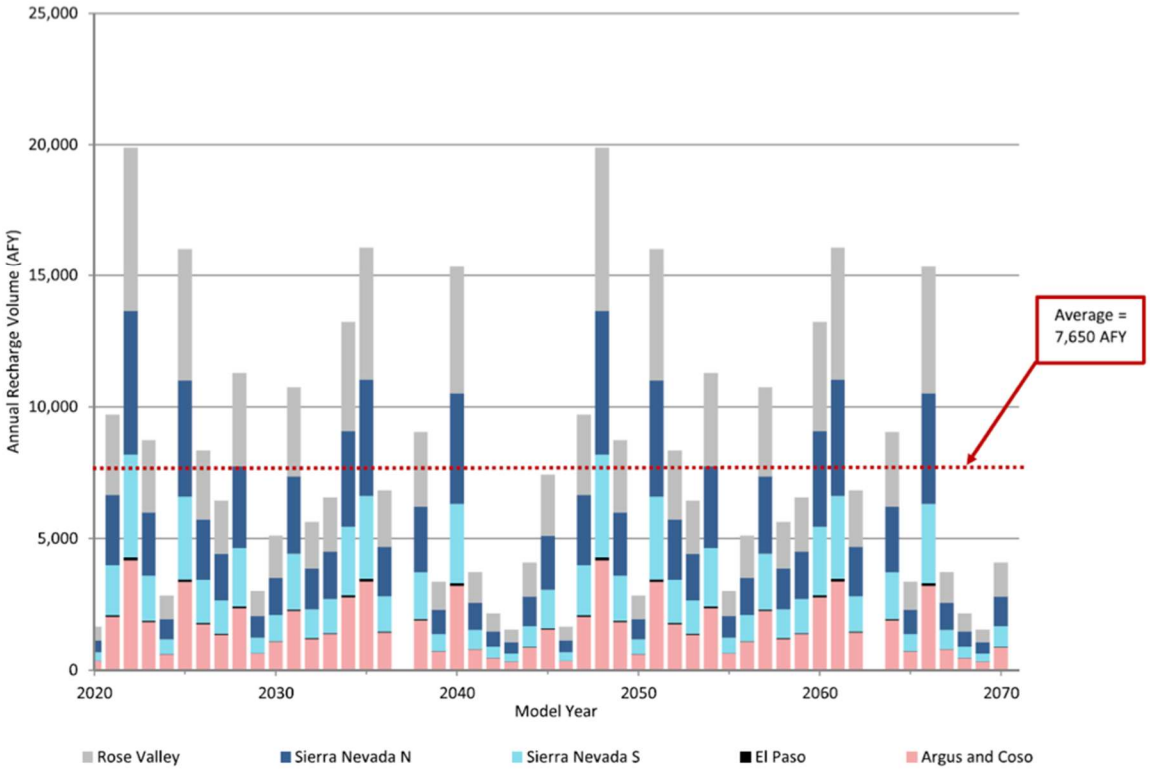

Figure 5. Annual variability of recharge forecasted for the predictive simulations. The mean of the annual recharge values is 7,650 AFY.

Other sources of groundwater recharge have been considered, such as fluid sources from deep geothermal upwelling (Bean, 1989), subsurface inflow from Sierra Nevada bedrock (Thyne et al., 1999), leakage from the Los Angeles Aqueduct (Todd Engineers, 2014), and percolation from wastewater ponds (Todd Engineers, 2014), but these have been either refuted or found to be insignificant when compared to the overall basin groundwater budget (Todd Engineers, 2014; McGraw et al., 2016).

2.4.4 Evapotranspiration

Evapotranspiration (ET) is focused in the area of the China Lake Playa where shallow groundwater levels support phreatophyte vegetation. Prior to 1921, when groundwater pumping began, ET was the predominant outflow from the IWVGB (McGraw et al., 2016), though no ET measurements are available from that time.

ET is simulated in the model using the Evapotranspiration Segments (ETS) package (Banta, 2000) that computes the volumetric ET rate in every model cell based on an input function that relates evapotranspiration to maximum ET flux at the ET surface, extinction depth, and hydraulic head. Based on the results of earlier studies in the IWVGB, McGraw et al. (2016) delineated two phreatophyte vegetation zones and estimated their associated ET rates (Figure 6) to establish a relationship of ET rate to depth to groundwater for the steady-state model. In that model, several smaller areas together represent a greasewood zone with a maximum ET rate of 2.4 ft/yr that terminates when groundwater levels are below an extinction depth of 33 ft. The second and much larger zone in the McGraw et al. (2016) model represents bare playa soil and all vegetation types outside of the greasewood zone (primarily pickleweed and saltgrass). This larger zone was assigned a maximum ET rate of 5.7 ft/yr and terminates when groundwater levels are below an extinction depth of 10 ft. The larger zone was expanded westward for the GSP model to incorporate phreatophyte vegetation mapped during subsequent hydrogeomorphic studies (Lancaster et al., 2019).

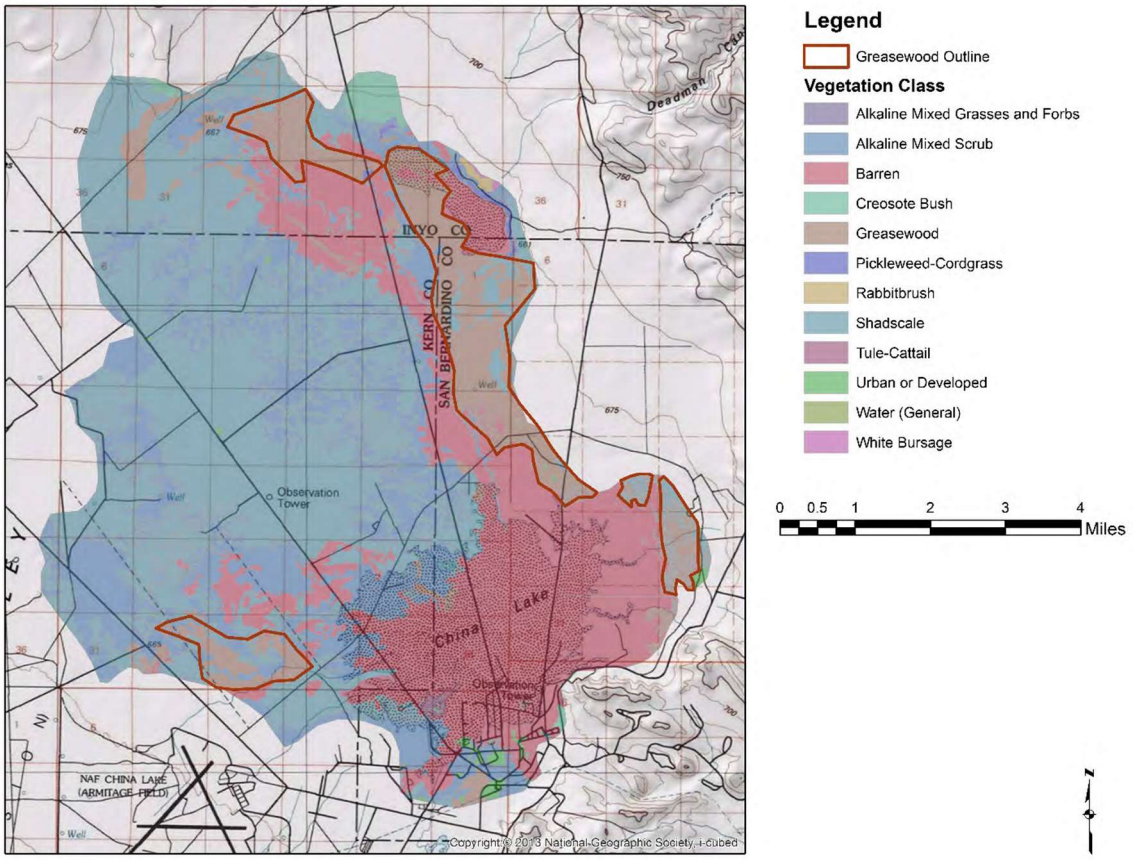

Figure 6. Distribution of vegetation and bare ground (denoted as Barren in the legend) within the area of evapotranspiration (ET) (from McGraw et al. [2016]). The two ET zones in the model are (1) greasewood (outlined in red) and (2) combination of bare playa and all other vegetation zones other than greasewood. Mapping is based on the 2013 vegetation survey of Menke et al. (2013) and correlation to geomorphic map units of Lancaster et al. (2019) in Bullard et al. (2019).

The extinction depth parameters in the GSP model were revised during calibration of the transient-historical model to better fit simulated heads to observed groundwater levels in the playa area. The final values used for the ETS package are listed in Table 1 and the associated ET zones are show in Figure 7. The ETS segmented curve that relates ET rate to hydraulic head is shown in Figure 8. ET is computed during the flow simulation by interpolating the proportion of the maximum ET rate (PETM) at the point on the appropriate segment defined by the hydraulic head (proportion of ET extinction depth, PXDP) for each cell where ET is simulated (Banta, 2000).

Table 1. Values of evapotranspiration rate used to develop the segmented ETS curve for the Evapotranspiration Segments (ETS) package.

ET Zone	Maximum ETS Rate (ft/yr)	ETS Extinction Depth (ft)
Greasewood	2.4	16.4
Dune Phreatophytes	7.2	16.4
Other Phreatophytes	7.2	4.9
Bare Playa	7.2	4.9

Rates of ET are likely to vary in relation to declines in groundwater levels and changes in the sizes and compositions of areas of phreatophyte vegetation. The results of two additional studies were employed to refine ET estimates during calibration of the transient models. Utilizing data from an eddy covariance station installed in 2014 on the southern edge of China Lake Playa, McGraw et al. (2016) estimate that ET rates for bare soil range from 0.2 to 0.4 ft/yr. The lower value accounts for removal of elevated ET measurements that often occur after precipitation events. Although these results are specific to Indian Wells Valley, they are limited to a one-year time period.

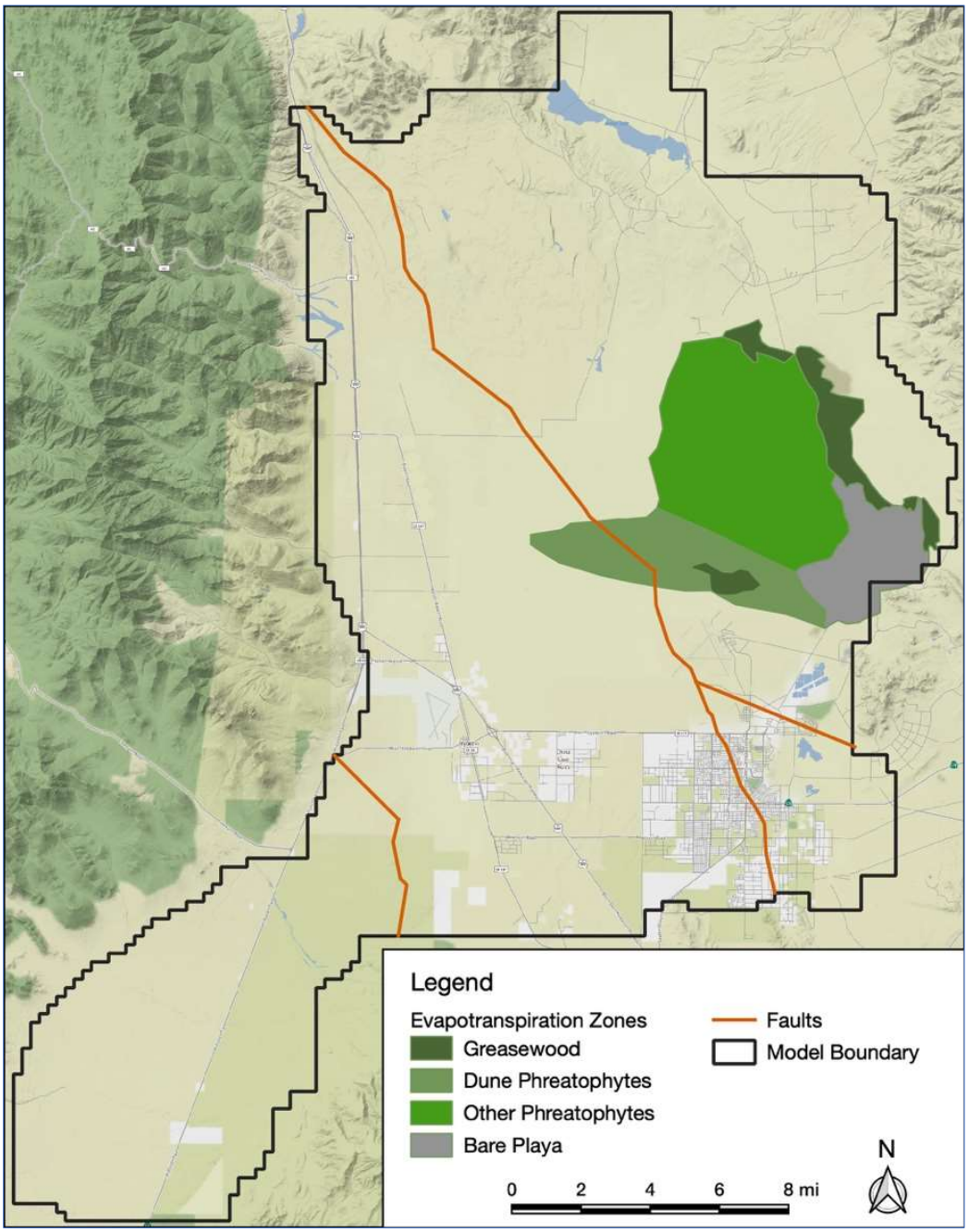

Figure 7. Map of evapotranspiration zones used for the Evapotranspiration Segments (ETS) package in the GSP model. Refer to Figure 3 for the names of the fault segments.

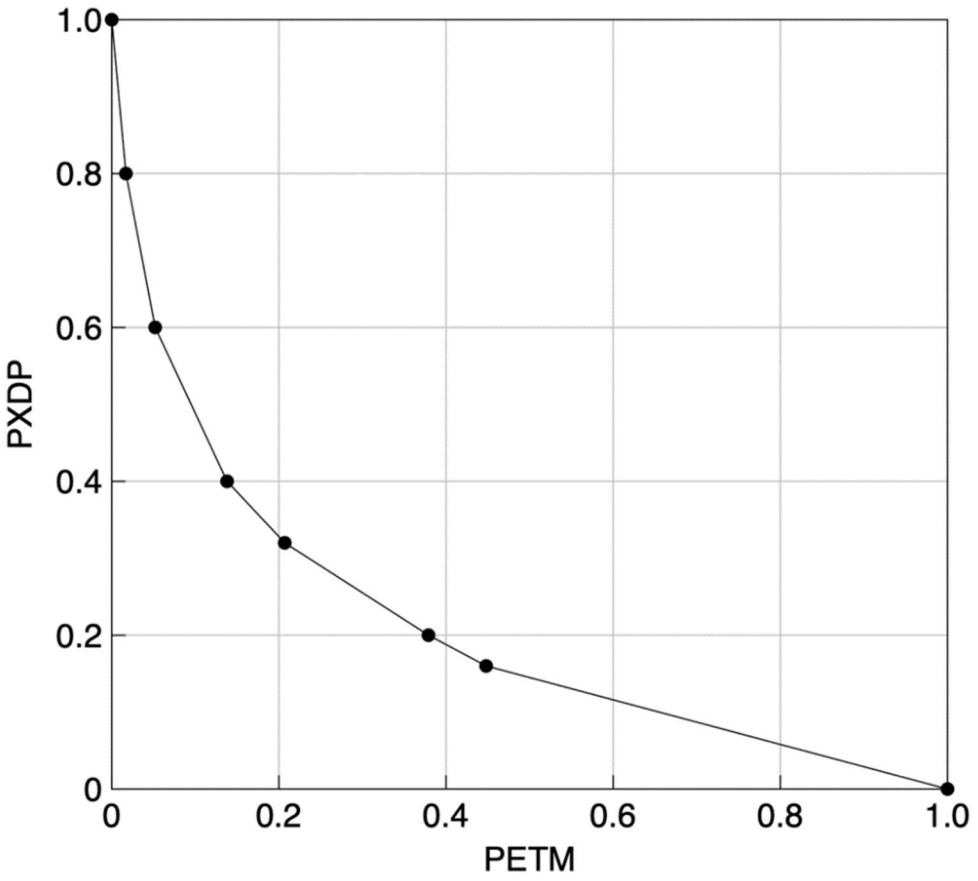

Figure 8. The ETS segmented curve that relates the proportion of evapotranspiration extinction depth (PXDP) to the proportion of the maximum evapotranspiration rate (PETM).

Beamer et al. (2013) compiled ET rates measured over the period 1997 to 2008 at 40 flux tower systems (eddy covariance and Bowen ratio) located throughout the Great Basin. By correlating the measured ET rates and enhanced vegetation index (EVI) values obtained from Landsat imagery for the same areas, Beamer developed an empirical relationship that is transferable to similar ET settings. Using EVI values from Landsat imagery covering the phreatophyte area in eastern Indian Wells Valley and the empirical relationship of Beamer et al. (2013), ET rates were estimated for the GSP model (Figure 9). The results are presented as part of model calibration in Section 2.5.

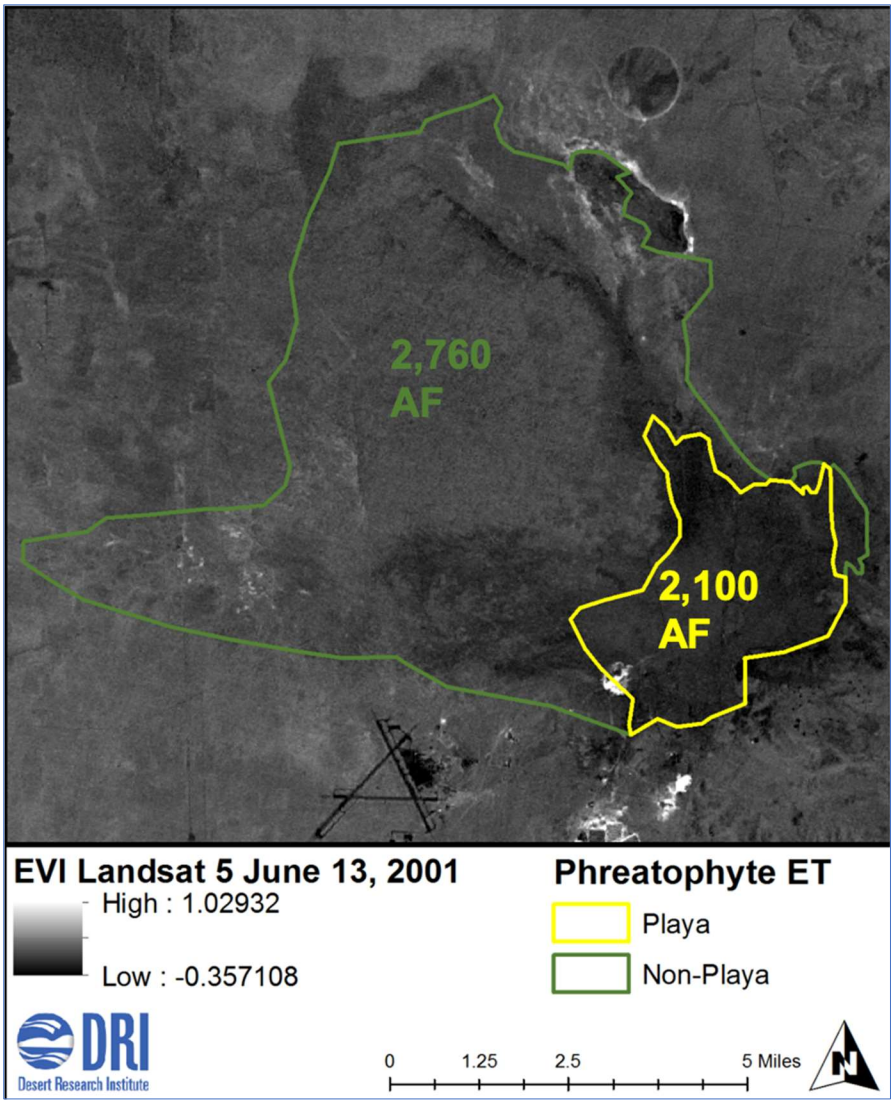

Figure 9. Spatial distribution of two ET zones in the model and their annual ET rates as estimated from EVI values from Landsat imagery using the method of Beamer et al. (2013).

2.4.5 Groundwater Pumping

Groundwater-pumping wells are simulated in the model using the MODFLOW WEL package. McGraw et al. (2016) compiled a groundwater-pumping database for the years 1920 through 2013 for use in the original transient-historical model. Pumping wells were evaluated and assigned by McGraw et al. (2016) to one of five use categories: private domestic, municipal, agriculture, Searles Valley Minerals (SVM), or NAWS. Wells were then compared to existing databases (Brown and Caldwell, 2009) and to aerial photographs to verify their use. Total annual withdrawals for each use category were digitized from Todd Engineers (2014, Figure 9) who summarized pumping data from Berenbrock and Martin (1991) and the Indian Wells Valley Cooperative Groundwater Management Group (IWVCGMG) Production Data (https://iwvgroundwater.org/iwv-production-data). Annual withdrawals were assigned to individual wells in the database when this relationship could be established. For other non-agriculture wells, the

remaining total annual withdrawal for each use category was divided equally among the wells in that category. Wells in the agriculture use category are assigned annual withdrawal rates determined by whether they are used for irrigation of alfalfa or pistachios. Pumping rates for these crops are based on estimates by Todd Engineers (2014) and the irrigated area of each crop type calculated from a geographic information system maintained by NAWS. Pumping rates for pistachio orchards increase over the 12-year period to maturity and then are held constant to account for changing water demands during their growth and mature stages (McGraw et al., 2016).

Garner et al. (2017) re-evaluated the groundwater-pumping database as part of the updates for the 2017 transient-historical model. Using annual withdrawal records for the period 1975 through 2015 available from the IWVCGMG, annual withdrawals in the model database were found to be in good agreement with the IWVCGMG data for the municipal, agriculture, SVM, and NAWS use categories. The annual rate in the database for private domestic wells of approximately 1 AF was found to be lower than the 2.5 AF rate prescribed by IWVCGMG, but is more consistent with the analysis of Todd Engineers (2014) that suggested the rate is generally less than 1 AF, with only a few parcels exceeding this amount.

Annual withdrawals in the database were updated through 2016 (Garner et al., 2017) utilizing records for individual IWCWD municipal wells and NAWS wells. Total annual withdrawals reported for private domestic wells; City of Inyokern, Ridgecrest Heights, and City of Ridgecrest municipal wells; and SVM wells were divided equally among the wells in their respective use categories. Annual withdrawals for agricultural wells were updated using estimates of alfalfa and pistachio production following the methods of McGraw et al. (2016). The domestic pumping rate of 1 AFY was used as described above. The annual groundwater withdrawals for all use categories are shown in Figure 10. Withdrawals were obtained from Berenbrock and Martin (1991) for 1920 through 1974 and from IWVCGMG estimates from 1975 through 2016. In addition, withdrawals at NAWS significantly declined in 1975. From 1980 through 2016, an annual average of approximately 25,000 AF was withdrawn from the basin. The total withdrawal for the year 2016, the last year simulated by the transient-historical model, is 24,473 AF. The locations, 2016 annual volumetric production, and use categories of the pumping wells are shown in Figure 11. Wells withdraw water from depths of up to 1,200 ft below land surface and from all six model layers.

The transient-predictive model simulations begin in the year 2020 and extend through 2070 using annual groundwater withdrawals associated with management scenarios developed by the Indian Wells Valley Groundwater Authority. The predictive flow models are described in Section 2.7.

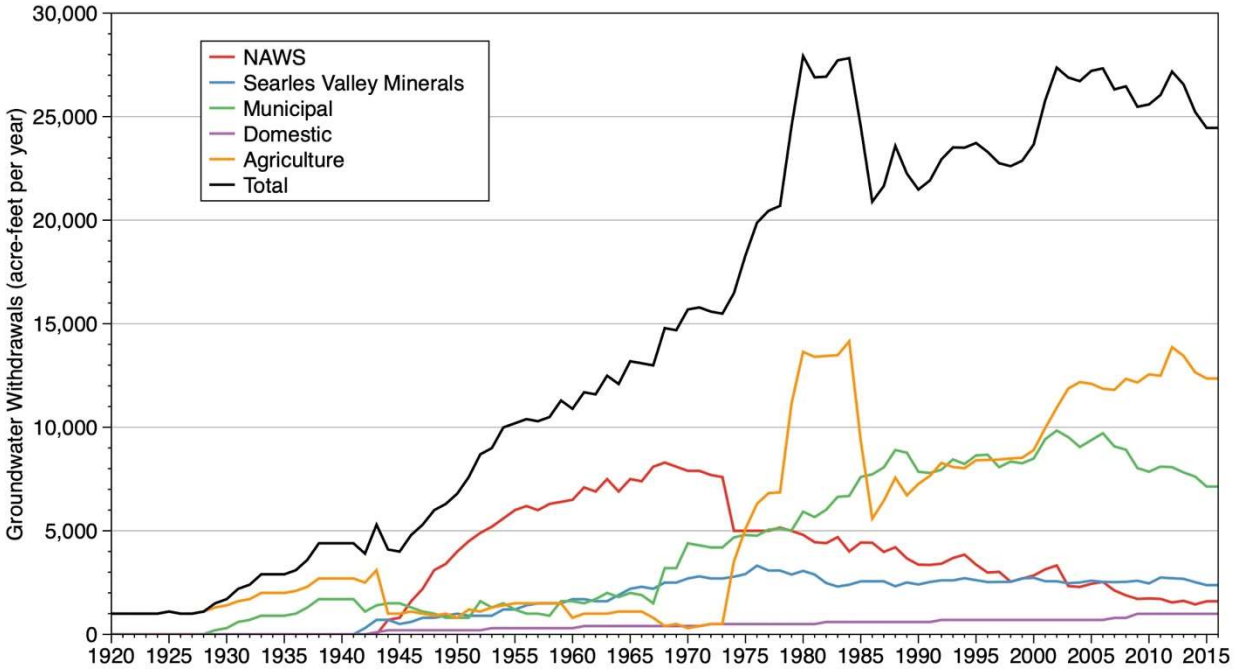

Figure 10. Annual groundwater withdrawals for all use categories for the period 1920 through 2016.

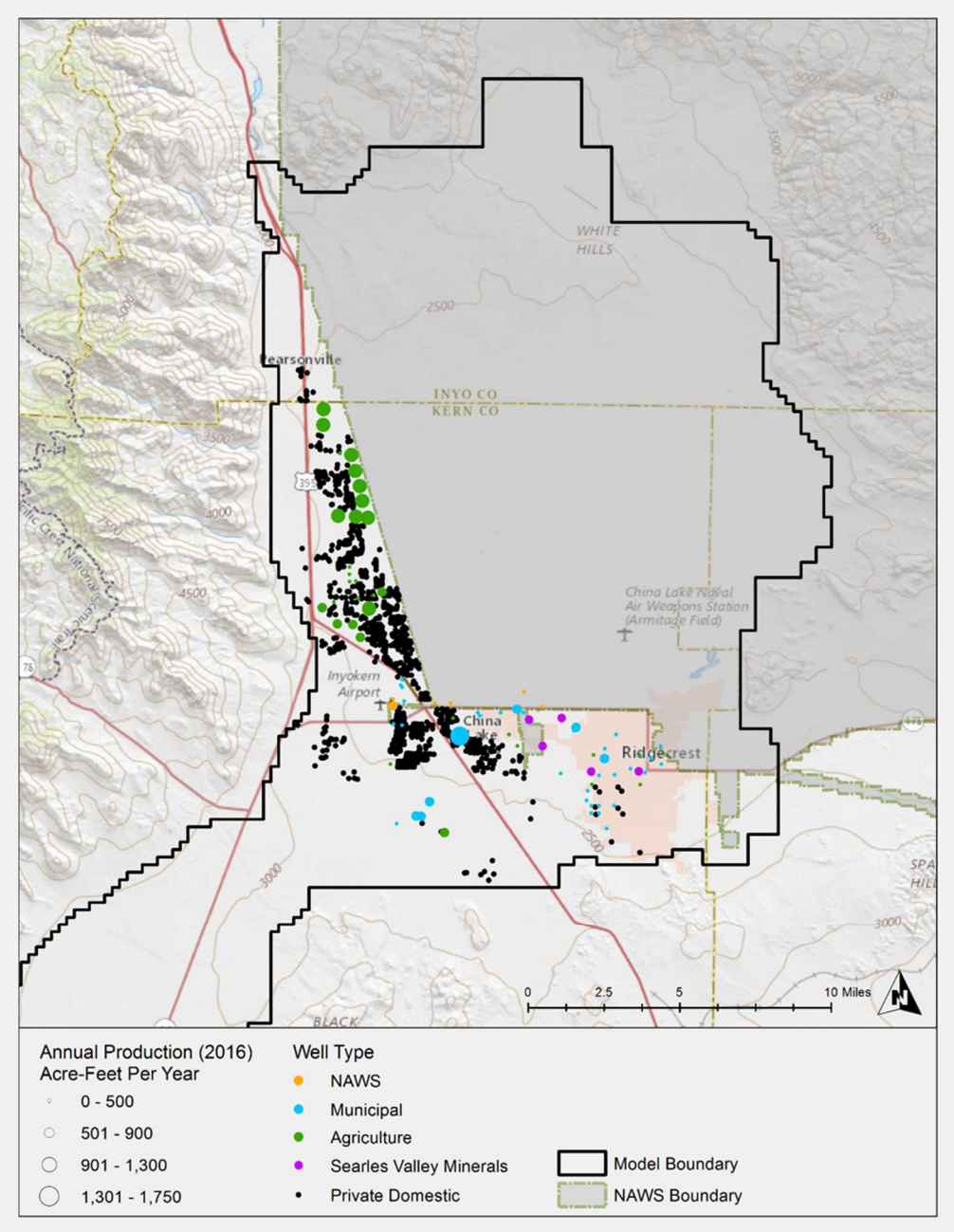

Figure 11. Groundwater-pumping wells included in the transient models.

2.4.6 Basin Outflow

Tertiary igneous and metamorphic rocks bound the IWVGB and Miocene basalts are present near the El Paso Mountains. Unless they are highly fractured, these rocks typically have low permeability and for the purposes of this and previous basin-fill groundwater models, they are not considered to be water-bearing. As a result, most studies of the IWVGB consider the pre-developed basin to be nearly hydrologically closed, with only very small or negligible underflow eastward toward Salt Wells Valley

(McGraw et al., 2016). Mass balance calculations of total dissolved solids suggest that the absence of large accumulations of salinity in the IWVGB (other than in the playa area where salinity increases through the ET process) may be indicative of interbasin groundwater outflow (McGraw et al., 2016). The possible annual magnitude of this flow was approximated as 200 AF by McGraw et al. (2016) using two-dimensional calculations incorporating hydraulic and geometric information from TriEcoTt (2012). This value was used in the original steady-state model and was adjusted downward during calibration of the transient-historical model as described in Section 2.5.

Basin outflow is simulated toward Salt Wells Valley using MODFLOW's General-Head Boundary (GHB) package with an assumed boundary head of 2,152 ft assigned to three adjoining boundary cells in Layer 1 (shown in Figure 1). This head value is revised in the GSP model from the value of 2,182 ft used by McGraw et al. (2016) based on further evaluation of water levels in this area of the basin. Interbasin flow is only allowed to leave the model domain at this location and only in Layer 1, based on the assumption that basin-fill deposits are most permeable in this area and at shallow depths.

2.5 Calibration

The general approach to GSP model calibration has been to adjust the values of selected parameters using manual and automated calibration processes until the model's simulated results are consistent with observed historic trends in Indian Wells Valley and the El Paso sub-basin. The flow model was calibrated in two stages, steady state and transient-historical, with comparisons made to observed water levels and water budgets in both cases.

2.5.1 Steady-State Model

The steady-state groundwater flow model represents hydrologic conditions before large-scale groundwater pumping began in 1921. This model is calibrated to steady-state water levels measured in 132 wells in Indian Wells Valley in 1920 and four wells in the El Paso sub-basin (Figure 12). Because pre-development water levels are not available in the El Paso sub-basin, the mean values of recent stable water levels in four wells were used (Garner et al., 2017). One artificial point, with an assigned water level elevation of 2,280 ft was added in the northwest basin (indicated in blue in Figure 12) to constrain simulated water levels to a range that would be expected in that area.

The values of two model parameters were optimized during steady-state calibration using the PEST (Parameter Estimation) software (Doherty and Hunt, 2010), (1) horizontal hydraulic conductivity (K) of the six model layers and (2) hydraulic characteristic (fault transmissivity divided by barrier width) of the fault segments identified in Figure 3. These parameters were chosen because in general they have significant effects on simulated water levels and because measurements of their values in Indian Wells Valley are limited and therefore are considered more uncertain than the other parameters. PEST was applied to optimize the selected parameter values to achieve the best fit of simulated to observed steady-state groundwater levels.

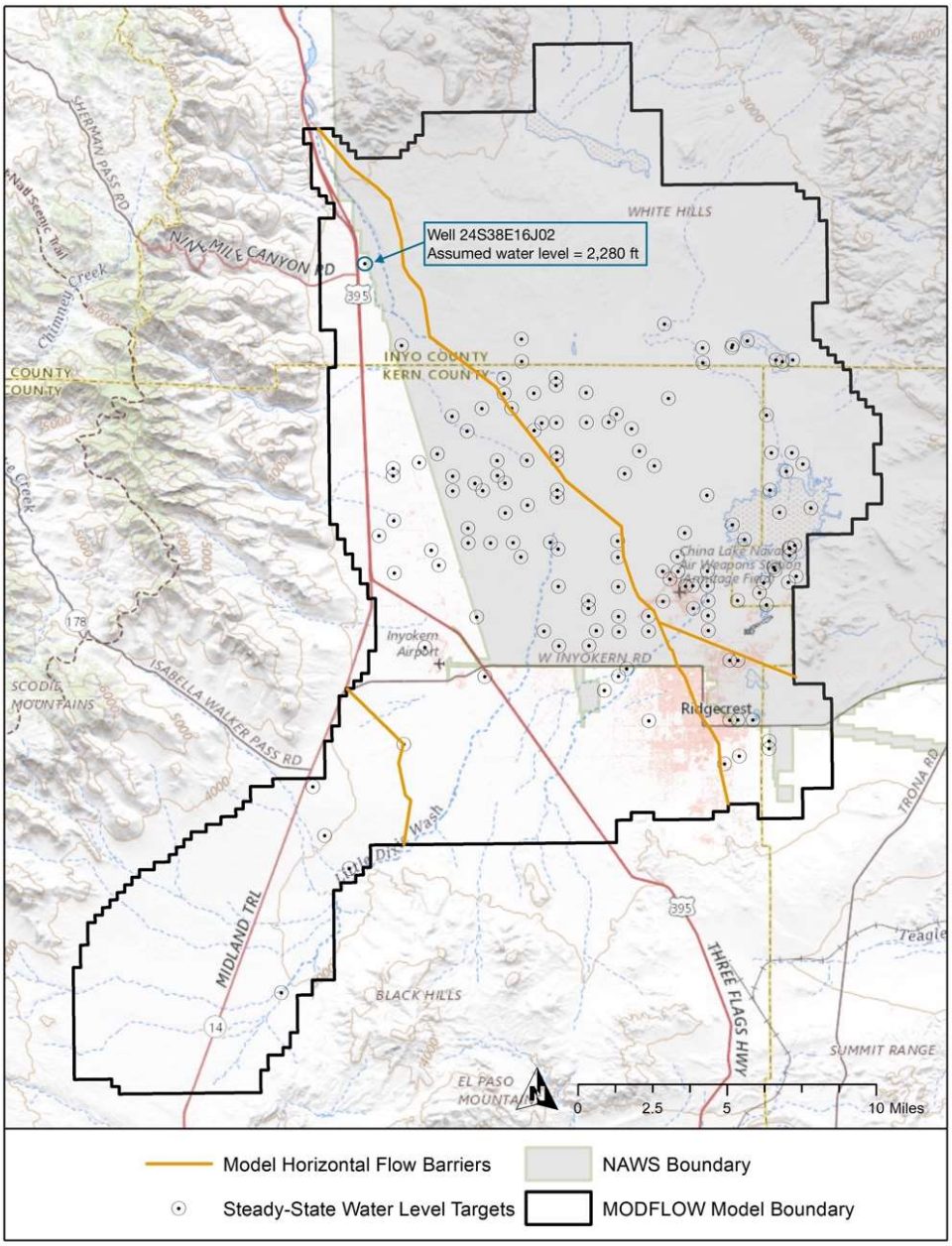

Figure 12. Locations of groundwater level targets for the steady-state pre-development model (from Garner et al. [2017]). One artifical point was included in the northwest (indicated in blue) to constrain simulated water levels to values thought to be representative of that area. There are no pre-development water levels available in the El Paso sub-basin, so mean values of recent stable water levels at the four available wells are used. Refer to Figure 3 for the names of the fault segments.

The vertical anisotropy ratio of hydraulic conductivity (K_z/K_x) is set at 0.3, the value determined during calibration of DRI's groundwater flow model for the Navy (McGraw et al., 2016). This value of anisotropy ratio is assigned throughout the model domain. Hydraulic conductivity is assumed to be laterally heterogeneous within all six model layers. Values of K in Layer 1 were calibrated using 54 pilot point

locations. Eighteen of these pilot points are located at well locations where pumping tests provide estimates of K (Figure 13), the values of which are fixed at these pilot points during calibration. In Layers 2 and 3, K was calibrated using the same 54 pilot point locations; however, no known pumping tests are available at these depths in the basin so calibration could not be guided by direct estimates of K in these layers. Instead, pilot points in these layers were used to guide calibration toward K values that were consistent with the hydrostratigraphic conceptualization of this depth interval. Lithologic logs of deep wells in the western and central portions of the basin (USBR, 1993) indicate discontinuous zones of fine-grained sediments at these depths. Pilot points were not used for Layers 4, 5, and 6. Each of these layers were divided into three horizontal zones of homogeneous K and PEST was used to adjust the K value within each zone. One zone covers the majority of the basin and two smaller zones represent the El Paso sub-basin and an area in the southeast basin surrounding Ridgecrest.

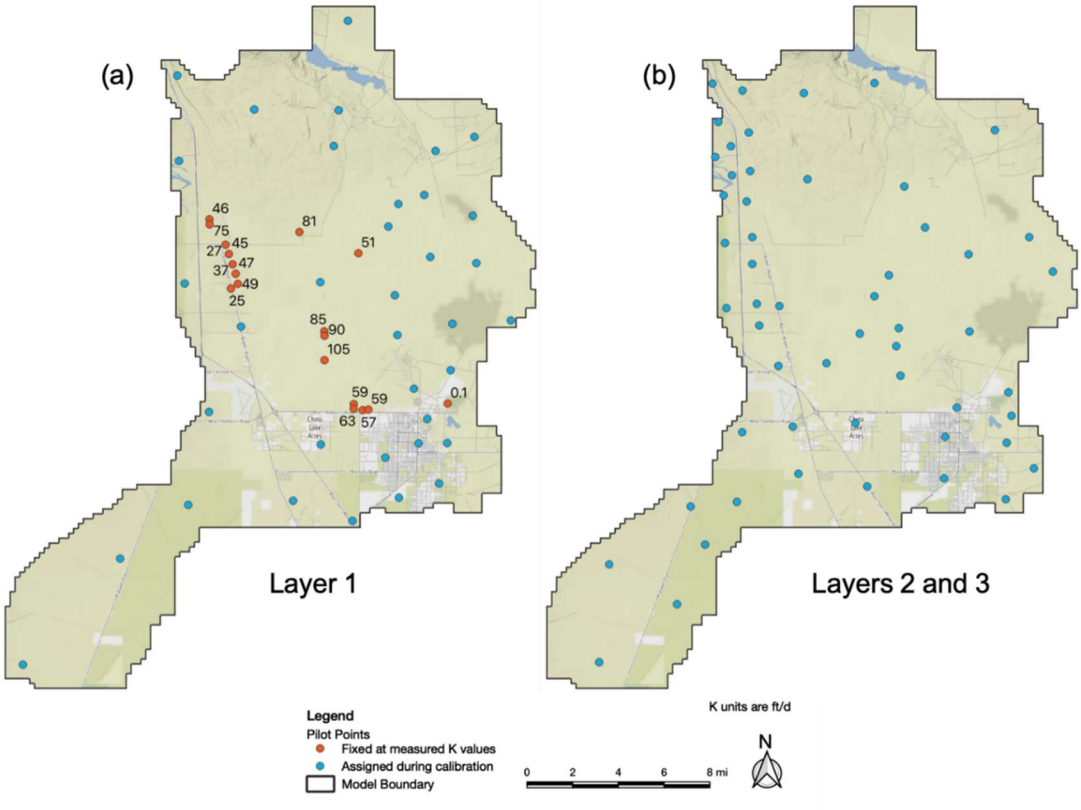

Figure 13. Locations of pilot points in (a) Layer 1 and (b) Layers 2 and 3 that were used for calibration of the steady-state flow model. Pilot points were not used in Layers 3, 4, and 5.

Values of the hydraulic characteristic parameter for the eight fault segments simulated as horizontal flow barriers were also optimized during PEST calibration. The Little Lake fault zone and a connected splay fault are divided into six segments and the El Paso fault was divided into two segments. The fault segments extend vertically through all six model layers and the values of hydraulic characteristic are vertically uniform within each segment.

The ranges in parameter values used for calibration are listed in Table 2. The initial ranges of K were chosen from the values used for the four primary hydrogeologic units by Brown and Caldwell (2009). Lacking site-specific data, initial broad ranges of fault hydraulic characteristic were chosen based on professional experience and judgement. The value of the hydraulic characteristic for the Little Lake Splay fault was chosen as 1×10^{-3} day^{-1} based on model performance and was fixed during calibration.

Table 2. Summary of ranges of parameter values and calibrated values estimated during calibration of the steady-state model.

Model Parameter	Model Element	Parameter Range		Calibrated Value
		Minimum	Maximum	
Hydraulic Conductivity (ft/day)	Layer 1	0.01	41	0.03 to 40
	Layers 2 and 3	0.01	11	0.01 to 10
	Layers 4 to 6 Main Basin	1.00E-10	100	0.51
	Layers 4 to 6 SE Main Basin	0.01	0.1	0.10
	Layers 4 to 6 El Paso	1.00E-10	100	5.00E-04
Hydraulic Characteristic of Horizontal Flow Barriers (day^{-1})	Little Lake North	1.00E-08	1.00E-04	5.54E-05
	Little Lake Central	1.00E-08	100	8.19E-04
	Little Lake South, segment A	1.00E-08	100	1.00E-05
	Little Lake South, segment B	1.00E-10	100	1.00
	El Paso South	1.00E-08	100	2.11E-05
	El Paso North	1.00E-08	100	1.42E-05

The distributions of calibrated K values in each layer are shown in Figure 14 and the values are listed in Table 2. The hydraulic conductivity values range from 0.01 to 41 ft/day in Layer 1 (Figure 14[a]) and 0.01 to 11 ft/day in Layers 2 and 3 (Figure 14[b]. Calibrated hydraulic conductivity values for layers 4, 5, and 6 are 0.5 ft/day in the main basin, 0.1 ft/day in the southeastern main basin, and 5×10^{-4} ft/day in the El Paso sub-basin (Figure 14[c]). The distribution of K is consistent with the generalized hydrostratigraphy in the basin. In the shallow subsurface, high K in the central basin represents unconsolidated coarse-grained younger alluvium, lower K in the China Lake area is associated with fine-grained playa and lacustrine deposits, and lower K in the El Paso sub-basin relates to high hydraulic gradients observed there. Information from lithologic logs of deep wells (USBR, 1993) suggest that discontinuous zones of fine-grained sediment are present at depths represented by model Layers 2 and 3. The lower K associated with this stratigraphy is captured in the calibrated K values in these layers (Figure 14[b] and Figure 15). Higher calibrated K is related to coarse-grained sediments conceptualized at greater depths throughout most of the basin (Figures 14[c] and 15), though lower K values were required in the El Paso sub-basin and the southeastern main basin to best fit water-level observations in these areas. Few deep boreholes are available in these areas to provide the lithologic information that can guide calibration.

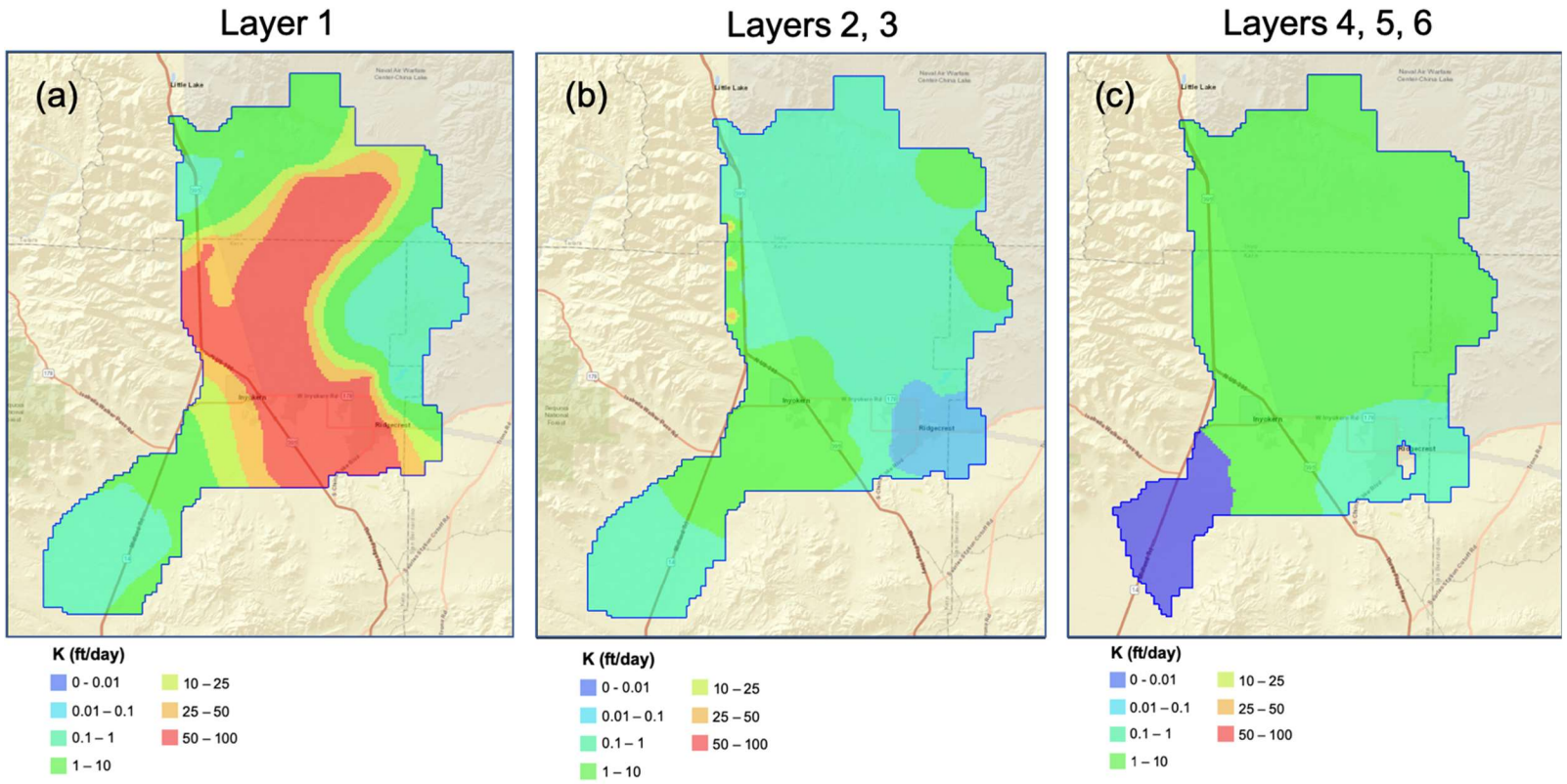

Figure 14. Calibrated hydraulic conductivity in (a) Layer 1, (b) Layers 2 and 3, and (c) Layers 3, 4, and 5 of the steady state model.

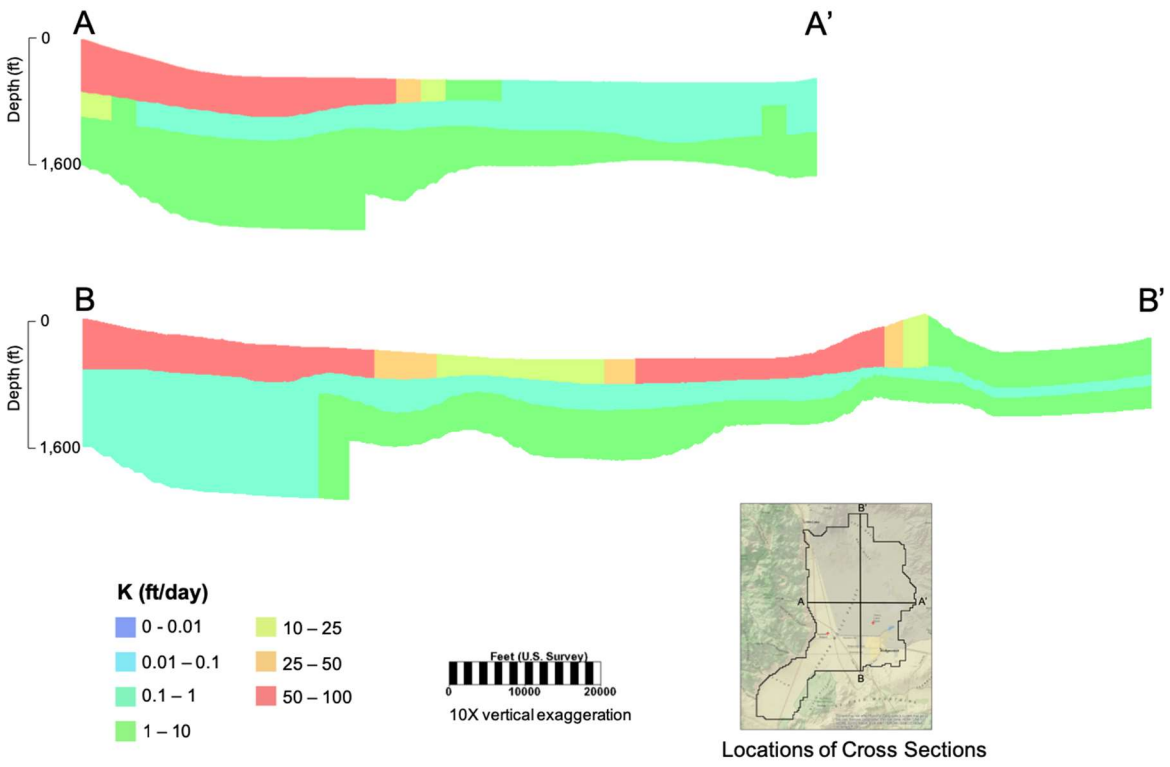

Figure 15. Cross sections showing examples of the distribution of calibrated hydraulic conductivity within the layers of the steady state model.

The results of steady-state calibration show that the model provides a good simulation of observed groundwater levels. The mean absolute error (*MAE*) in water levels was calculated using the equation

$$MAE_{water\ level} = \frac{1}{n}\sum_{w=0}^{n} abs\{h_{sim} - h_{obs}\} \quad (1)$$

where $MAE_{water\ level}$ = mean absolute error in the water level, n = number of water-level measurements, h_{sim} = simulated groundwater level, and h_{obs} = measured groundwater level.

The mean absolute error between simulated and observed water levels is 4.5 ft. The relative error in water levels, which is the MAE divided by the range in observed water levels, is one percent, which is well below the 10-percent threshold that is generally considered an acceptable maximum relative error for use of the model as a tool for water-level predictions. Models with a relative error less than five percent are considered excellent (Anderson et al., 2015). Head residuals of the steady-state model range from -15.3 to +16 feet (Figure 16), with most residuals in the range of -4.5 to +4.5 feet. There is no apparent bias between simulated and observed water levels; water levels are well simulated over the entire range of water-level observations. (Figure 17).

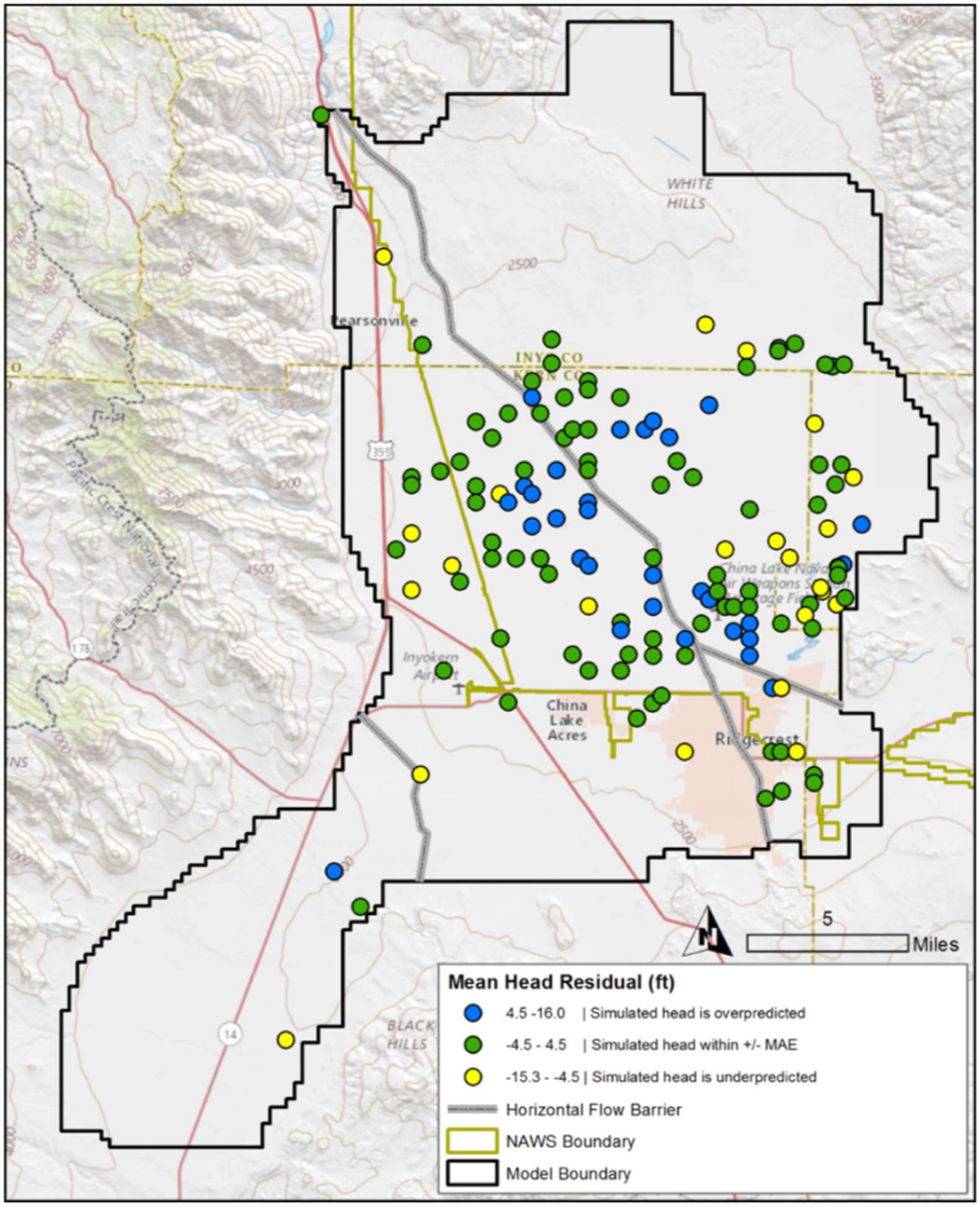

Figure 16. Residuals between simulated and observed groundwater levels for the calibrated steady-state model. Refer to Figure 3 for the names of the fault segments.

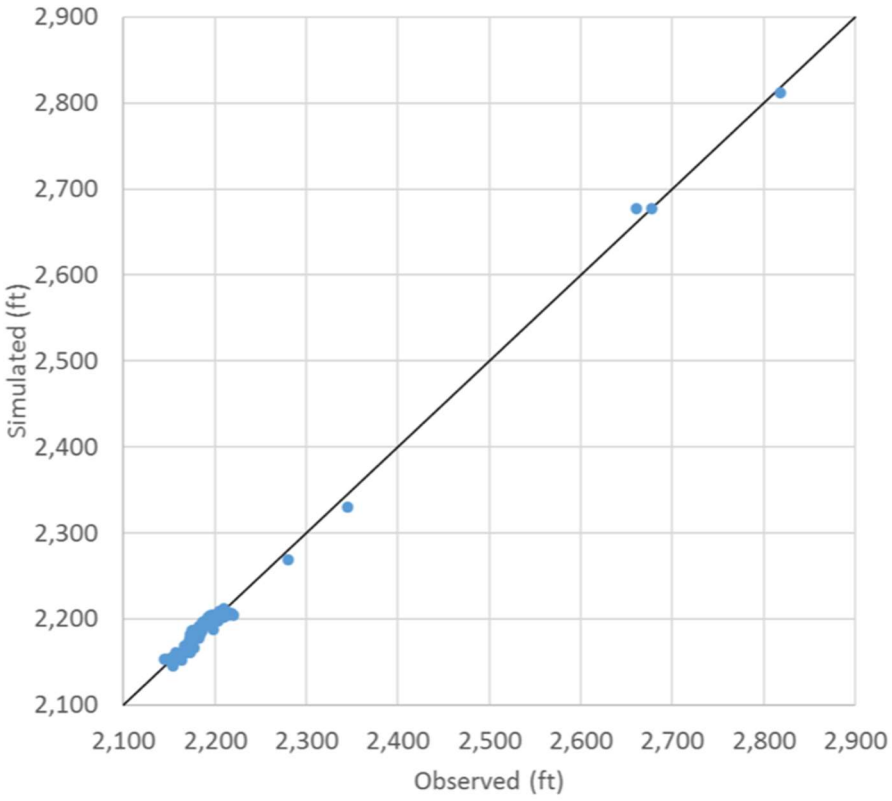

Figure 17. Plot of simulated heads to observed heads in the calibrated steady-state model.

The groundwater budget for the steady state model is tabulated in Table 3. The sole sources of inflow to the model are mountain block recharge and interbasin flow from Rose Valley, at a combined rate of 7,650 AFY. Evapotranspiration is the primary component of outflow (7,510 AFY), with interbasin flow to Salt Wells Valley (140 AFY) providing the remainder.

Table 3. Groundwater budget simulated by the steady-state model.

INFLOW	**(acre-ft/year)**
Recharge and Interbasin Flow	7,650
Coso and Argus Ranges	1,600
Rose Valley	2,400
Sierra Nevada North	2,100
Sierra Nevada South	1,500
El Paso sub-basin	50
Total:	**7,650**

OUTFLOW	**(acre-ft/year)**
Evapotranspiration	7,510
Flow to Salt Wells Valley	140
Total:	**7,650**

Groundwater flow directions prior to development as simulated by the steady state model are shown in Figure 18. Flow paths originate at recharge boundaries and as interbasin flow from Rose Valley and are directed toward areas of evapotranspiration and interbasin flow to Salt Wells Valley. Groundwater flow is parallel to northern segments of the Little Lake Fault where fault conductivity is lower and crosses the fault further south where fault conductivity is higher.

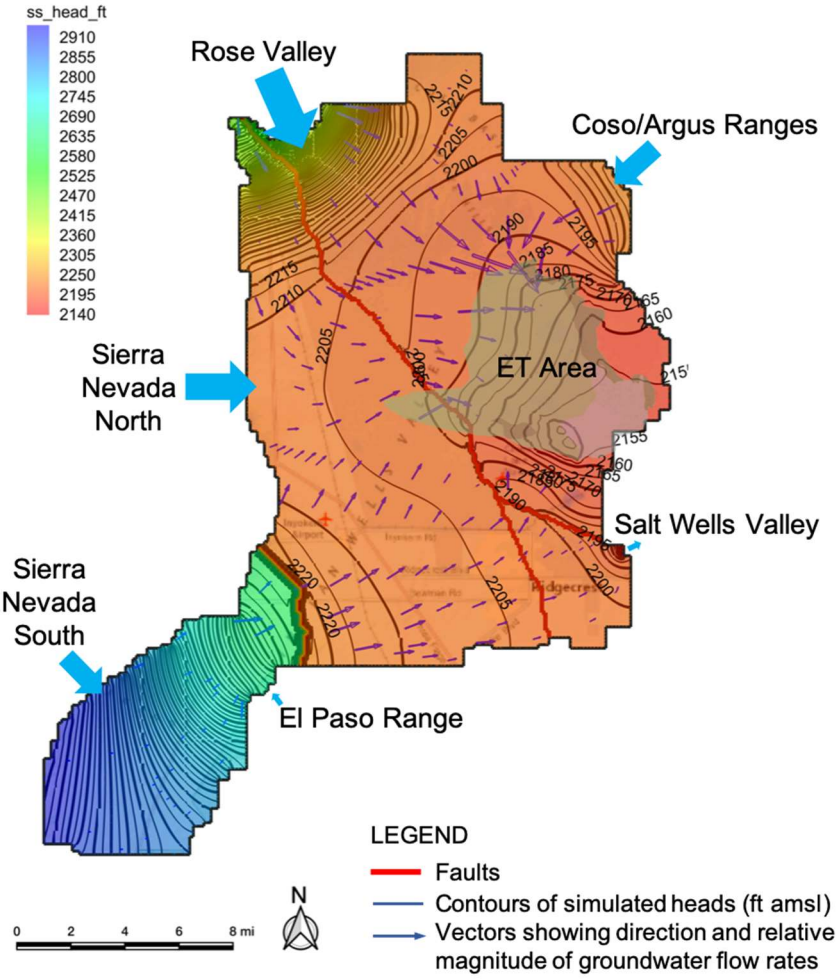

Figure 18. Groundwater flow directions and hydraulic heads simulated on Layer 1 of the pre-development steady-state model. Locations of recharge and interbasin flow boundaries are indicated by large blue arrows. Refer to Figure 3 for the names of the fault segments.

2.5.2 Transient-Historical Model

Groundwater conditions during the period 1921 through 2016 are simulated by the transient-historical flow model, which includes groundwater withdrawals at the 1,191 wells contained in the revised groundwater-pumping database (Garner et al., 2017). Mountain-block recharge rates are constant over this time period. This model is calibrated to water budget terms and historic water-level trends and altitudes observed in 36 wells (Figure 19) by adjusting values of the transient storage parameters

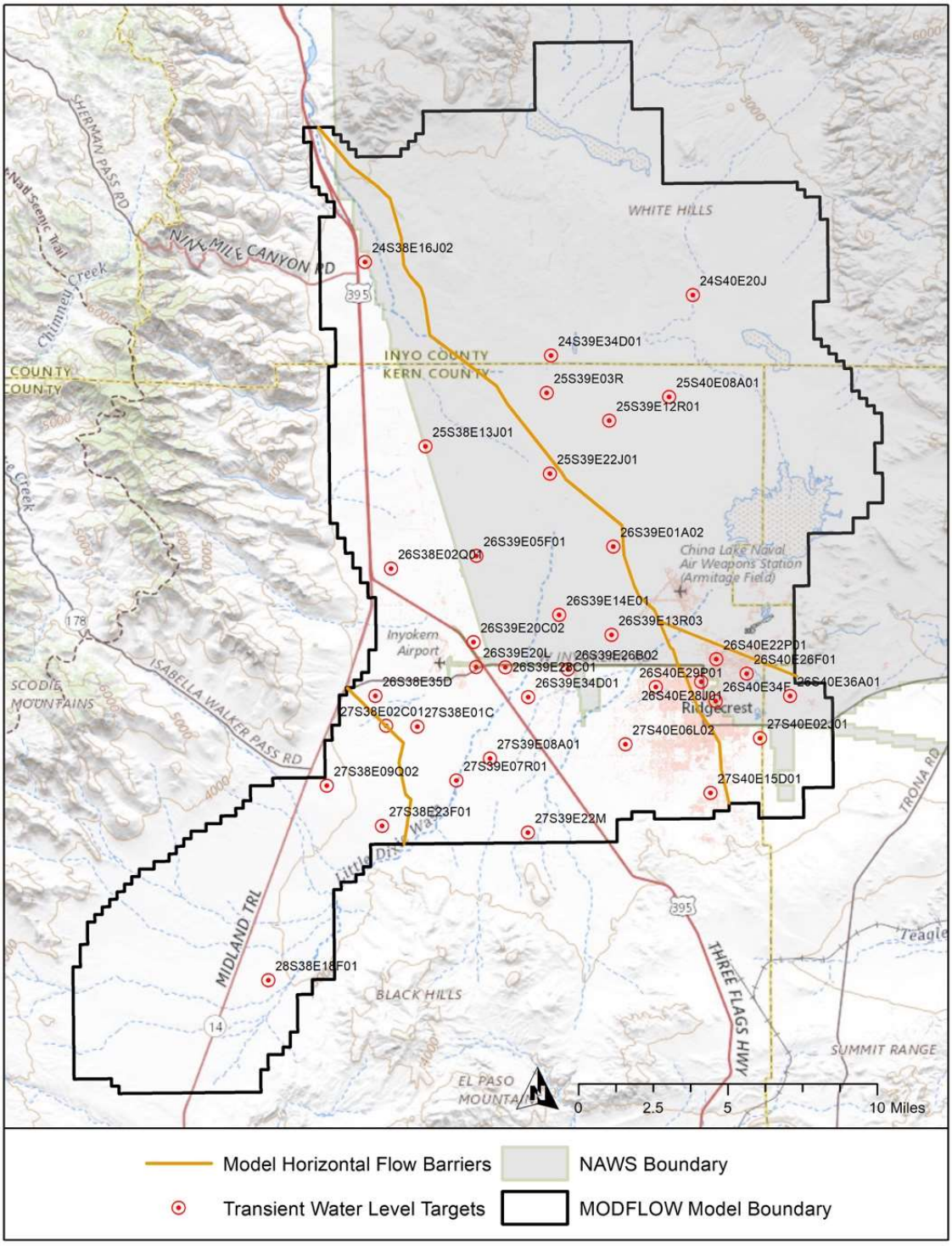

Figure 19. Locations of groundwater level targets used for calibration of the transient-historical flow model. Refer to Figure 3 for the names of the fault segments.

specific storage and specific yield. The values of the hydraulic conductivity and fault hydraulic characteristic parameters determined during calibration of the steady-state model were adopted unchanged in the transient-historical model. Model results were found to be insensitive to specific storage so this parameter was assigned a constant value of 3×10^{-6} ft^{-1} for all confined model layers.

The transient-historical model uses observed rates of water-level drawdown that resulted from groundwater withdrawals as a calibration metric to supplement the MAE of water level altitudes. This approach was used because errors in correctly simulating the rates of drawdown will have a large effect on forecasted water levels and thus is the critical factor for simulating the effect of overdraft conditions. The water-level altitude is generally controlled by hydraulic conductivity and recharge, parameters that were determined in the steady-state model, while drawdown rates are strongly affected by storage parameters. This approach minimizes errors in the calibration that might result from the model attempting to resolve offsets in water level altitudes simulated by the steady-state model.

A robust regression slope-fitting approach was used to remove observation outliers and compute the differences in slope of the simulated and observed water-level trends at the 36 observation locations. Ordinary least squares regression assumes a normal distribution of errors in the observed responses. If the data to be fitted contain erroneous or stress affected measurements, the resulting slope fit will be skewed by the outlier data points. A robust regression fit is better suited to these circumstances because the approach automatically removes outlier observations within the analysis period by assigning a weight to each data point. The weights are iteratively recomputed to exclude data points farther from model predictions.

For each simulated variation in the specific yield parameter, the difference in the slope of the head observations and the simulated head values is computed using the equation

$$MAE_{slope} = \frac{1}{n}\sum_{w=0}^{n} abs\{[\log(abs(S_{sim})) - \log(abs(S_{obs}))]\} \quad (2)$$

where MAE_{slope} = mean absolute error in the drawdown slope, n = number of monitoring wells, S_{sim} = drawdown slope (simulated), and S_{obs} = drawdown slope (observed). It was necessary to take the logarithm of the data to reduce the inherent bias of comparing values that span several orders of magnitude. This *MAE* results from taking the difference in logs and has no units.

An example result from the robust regression slope fitting approach for California state well number (SWN) 26S39E05F01 is shown in Figure 20. Red circles represent observed water levels, blue circles represent simulated water levels, and orange and green circles represent the observed and simulated water levels that were input to the regression model after outlier observations were removed. The observed drawdown slope is -2.35 ft/yr and the simulated slope is -2.56 ft/year corresponding to a slope difference of -0.21 ft/year. Plots of the simulated and measured groundwater level hydrographs over the transient-historical calibration period are provided for all monitoring wells used in the calibration in Appendix A.

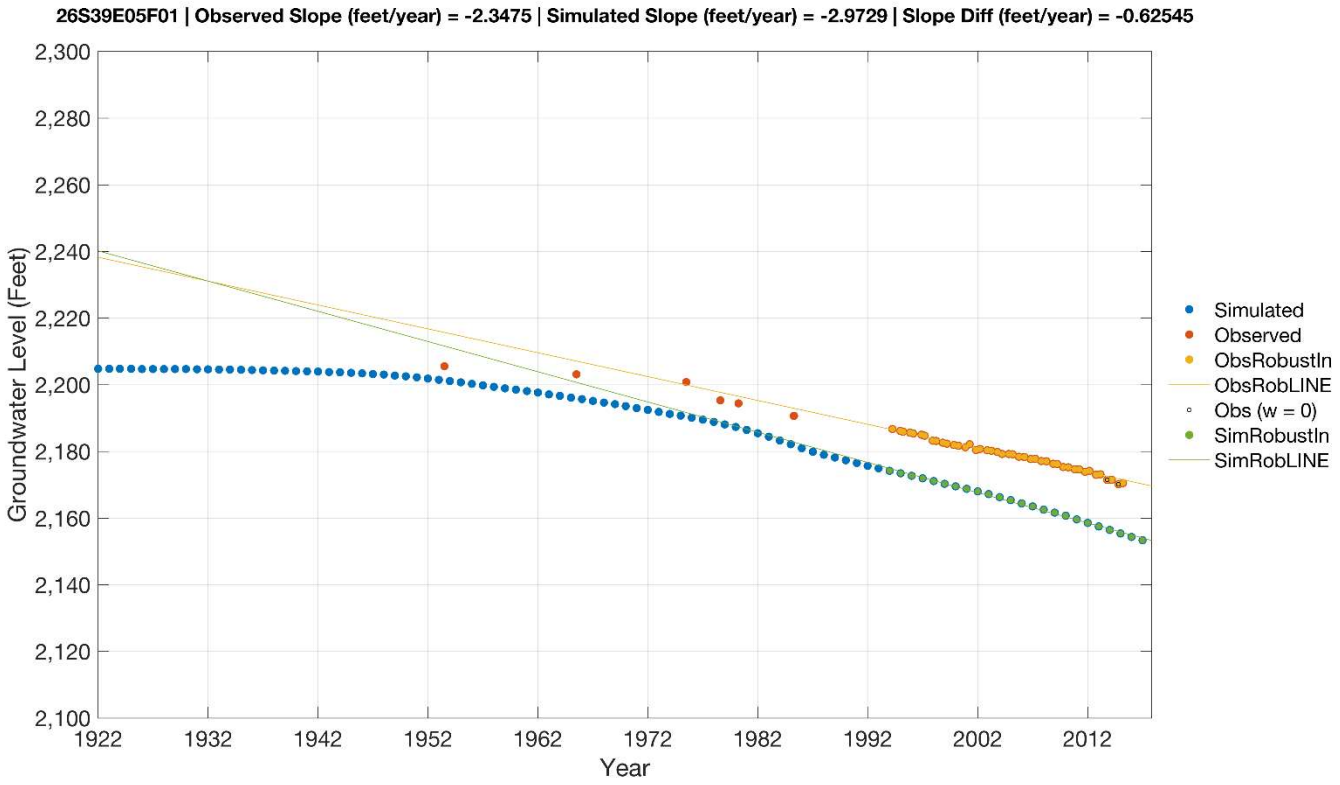

Figure 20. Example of the hydrograph slope-fitting method used for calibration of the transient-historical flow model. Plots for all monitoring wells used for the transient model calibration are provided in Appendix A.

The transient-historical model was manually calibrated using six values of specific yield that together represent a reasonable range for the basin-fill sediments. The calibration metrics that resulted from these runs are shown in Figure 21. The optimal solution using drawdown slope as the metric is obtained for a specific yield value of 0.225, whereas an optimum specific yield of 0.25 results when using MAE of water levels as the metric. Although these values are very close in magnitude, the value of 0.225 was selected because the optimal fit of drawdown slope is critical to effective forecasting of drawdowns for predictive pumping scenarios.

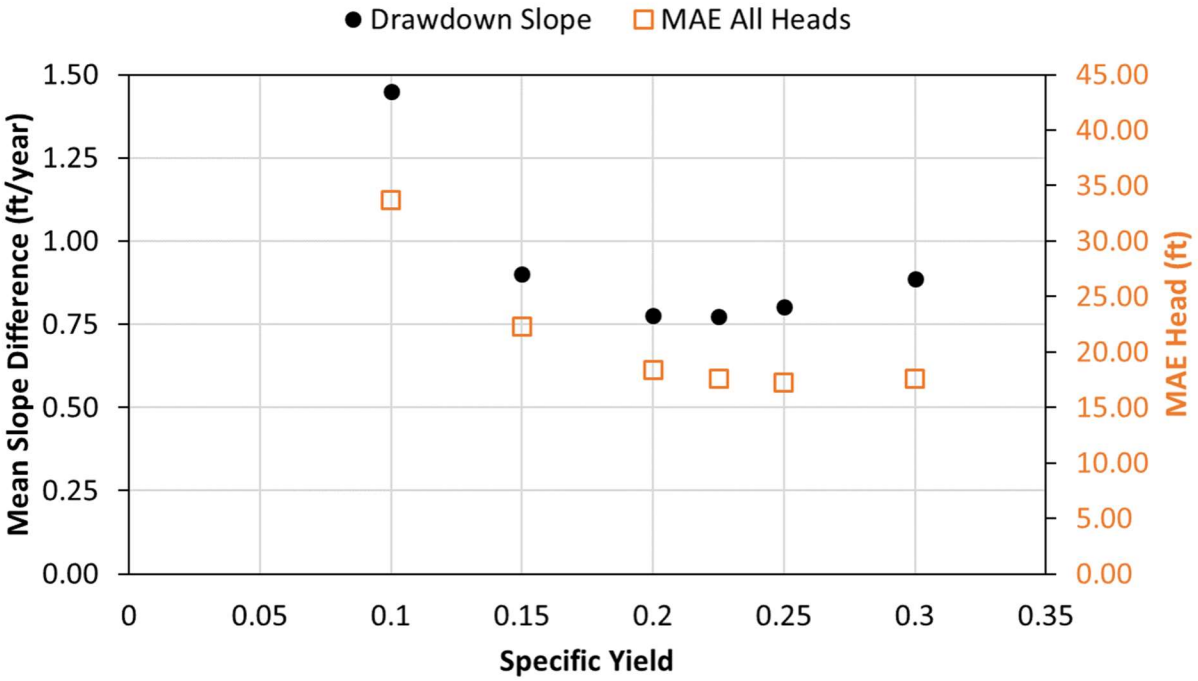

Figure 21. Results of calibration metrics Drawdown Slope and MAE of All Heads used for calibration of the transient-historical flow model.

Although the specific yield value of 0.225 was globally optimal, drawdown slopes were underpredicted in the southern portion of the basin. Manual adjustment resulted in a lower value of 0.08 that improved the fit to observed drawdowns and was found to be consistent with a value of specific yield of 0.04 estimated from the results of an aquifer testing program in the IWVWD southwest well field (Krieger & Stewart, 1996). The horizontal spatial distribution of specific yield throughout the model domain was obtained by kriging, with a value of 0.08 assigned around the IWVWD southwest well field and values of 0.225 used as constraints throughout the rest of the model. The results are shown in Figure 22. All model layers are assigned the same distribution of specific yield.

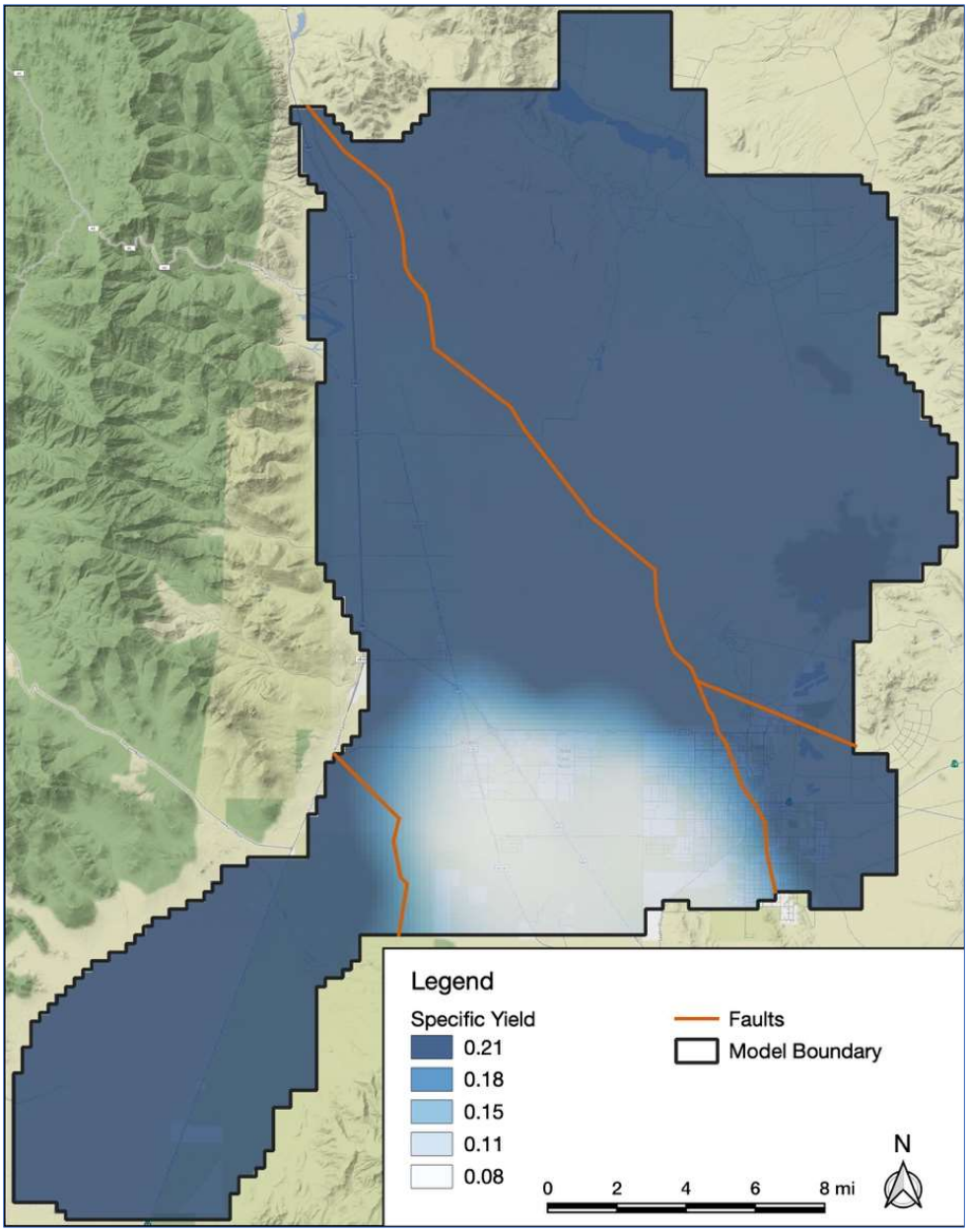

Figure 22. Spatial distribution of specific yield obtained by kriging in the calibrated transient-historical model. All model layers are assigned the same spatial distribution of specific yield. Refer to Figure 3 for the names of the fault segments.

The mean absolute error between simulated and observed water levels in the transient-historical model is 14 ft, which is higher than the value of 4.5 ft in the steady state model, but reasonable considering the challenges faced when using a regional model to fit to transient groundwater conditions measured at a local scale. The relative error in water levels is two percent, which is well below the 10-percent threshold that is generally considered an acceptable maximum relative error for use of the model as a tool for water-level predictions. Models with a relative error less than five percent are considered excellent (Anderson et al., 2015). Head residuals of the transient-historical model range from -128.4 to

+26.4 feet (Figure 23), with most residuals in the range between -14.0 and +14.1 feet. Bias between simulated and observed water levels is greater than in the steady state model; the transient-historical model shows a tendency to slightly underpredict some observed water levels (Figure 24). The underpredicted transient water levels at well 27S38E02C01 are described below. Most underpredicted water levels occur in the area where the northern El Paso joins the main basin, indicating that the hydraulic characteristics of the hydrogeologic system here are not well defined.

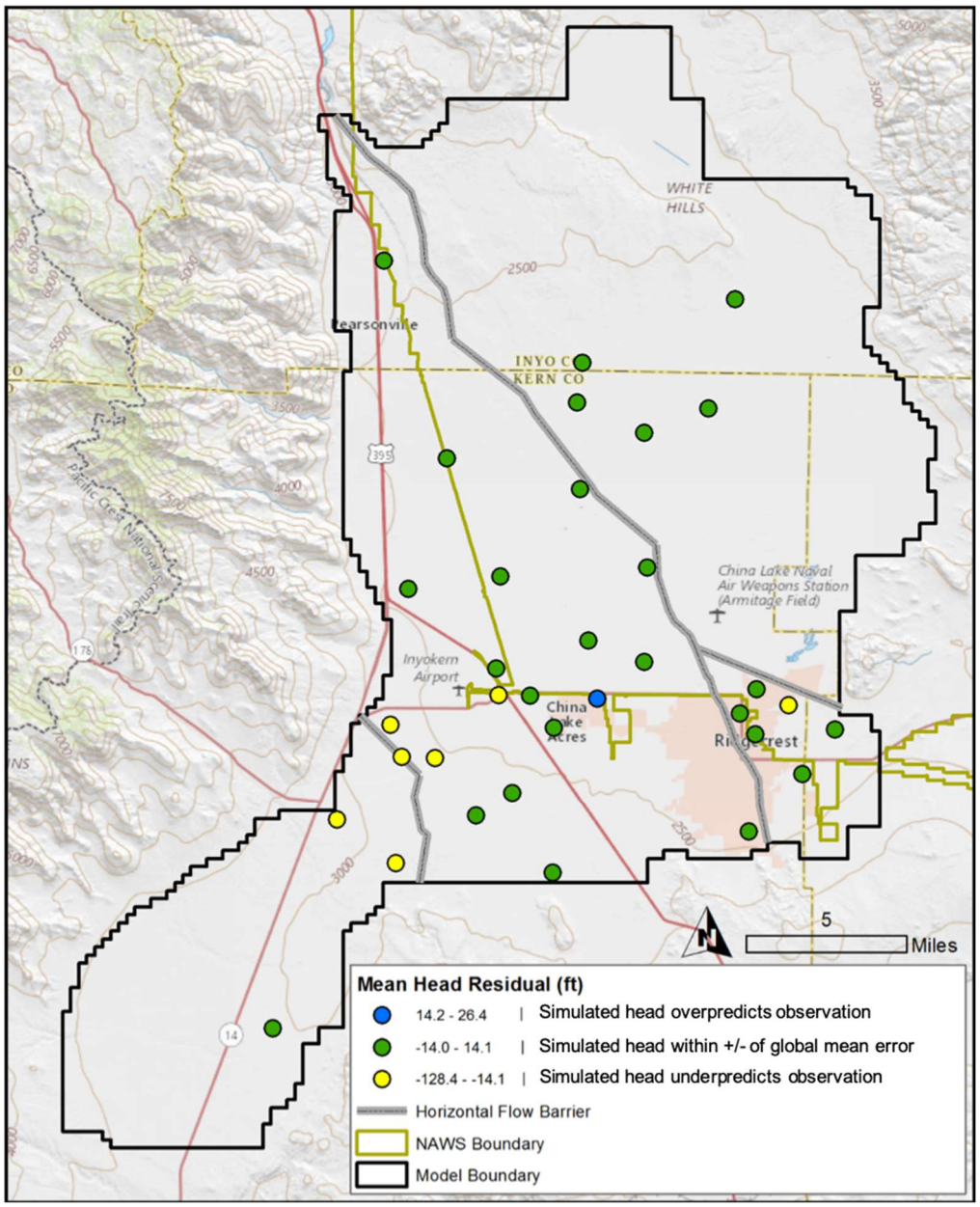

Figure 23. Mean residuals between simulated and observed groundwater levels for the calibrated transient-historical model. Refer to Figure 3 for the names of the fault segments.

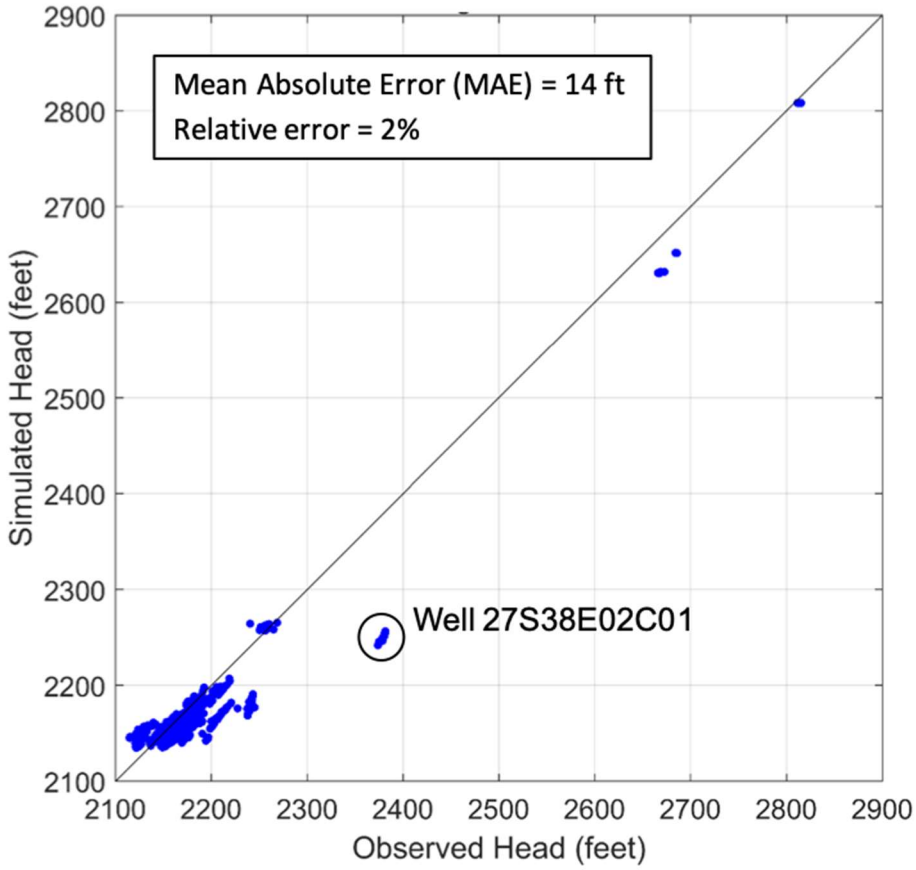

Figure 24. Plot of simulated heads to observed heads in the calibrated transient-historical model. Transient water levels at well 27S38E02C01 are described in the text.

The largest error between simulated and observed water levels occurs at well 27S38E02C01, which is located in a model cell through which also passes the El Paso Fault (Figure 25). The fault is simulated as a barrier to groundwater flow, causing a large decline in water levels as groundwater crosses the fault from southwest to northeast. The well is located in the fault zone, but the hydraulic barrier that represents the fault in the model bounds the model cell on the western and southern sides, meaning that this cell is located on the down-hydraulic-gradient side of the simulated fault barrier where heads are lower. MODFLOW simulates heads in the centroid of each cell, causing the transient heads in this cell to be simulated significantly lower than the observations at well 27S38E02C01. Mean residuals between simulated and observed drawdown slopes in the transient-historical model range from -1.99 ft/yr to +1.8 ft/yr, with most residuals in the 1.55-ft/yr range of -0.77 to +0.78 ft/yr (Figure 26).

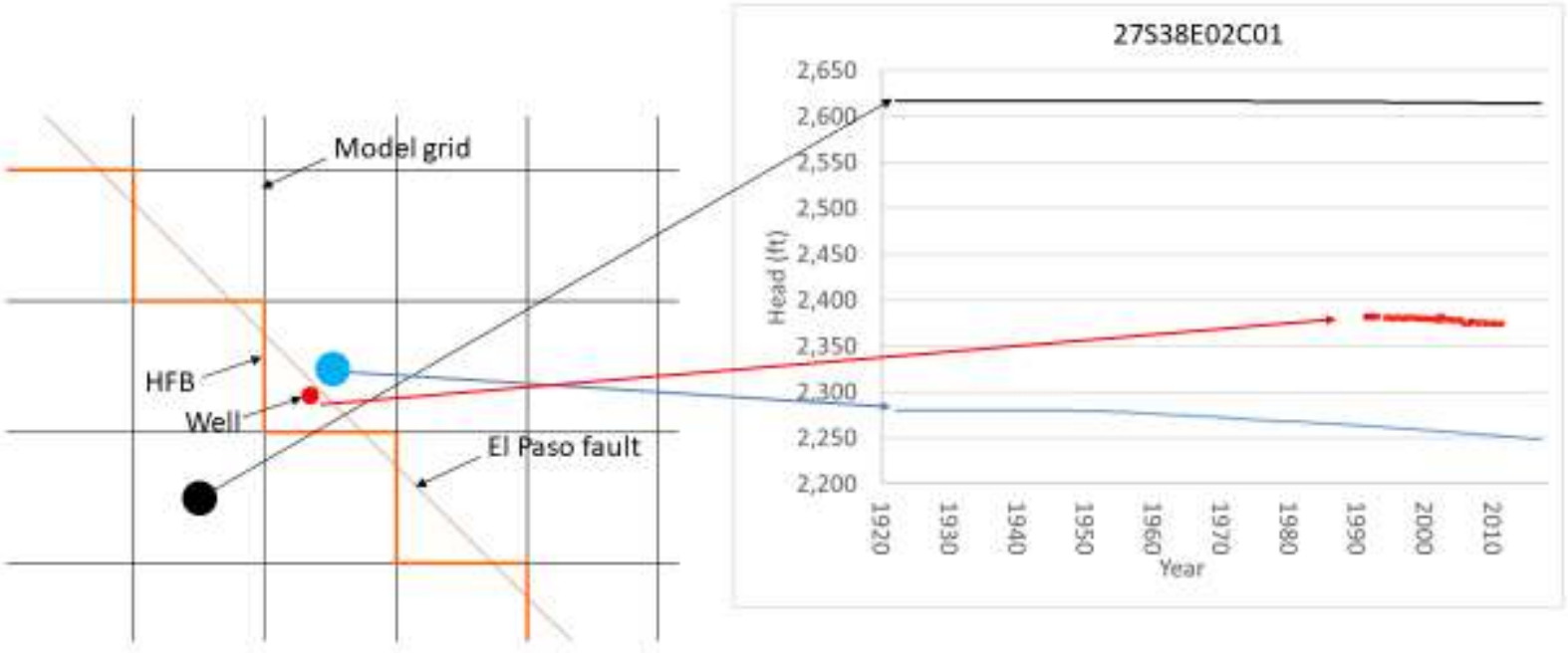

Figure 25. Simulated and observed heads at well 27S38E02C01 near the El Paso fault zone.

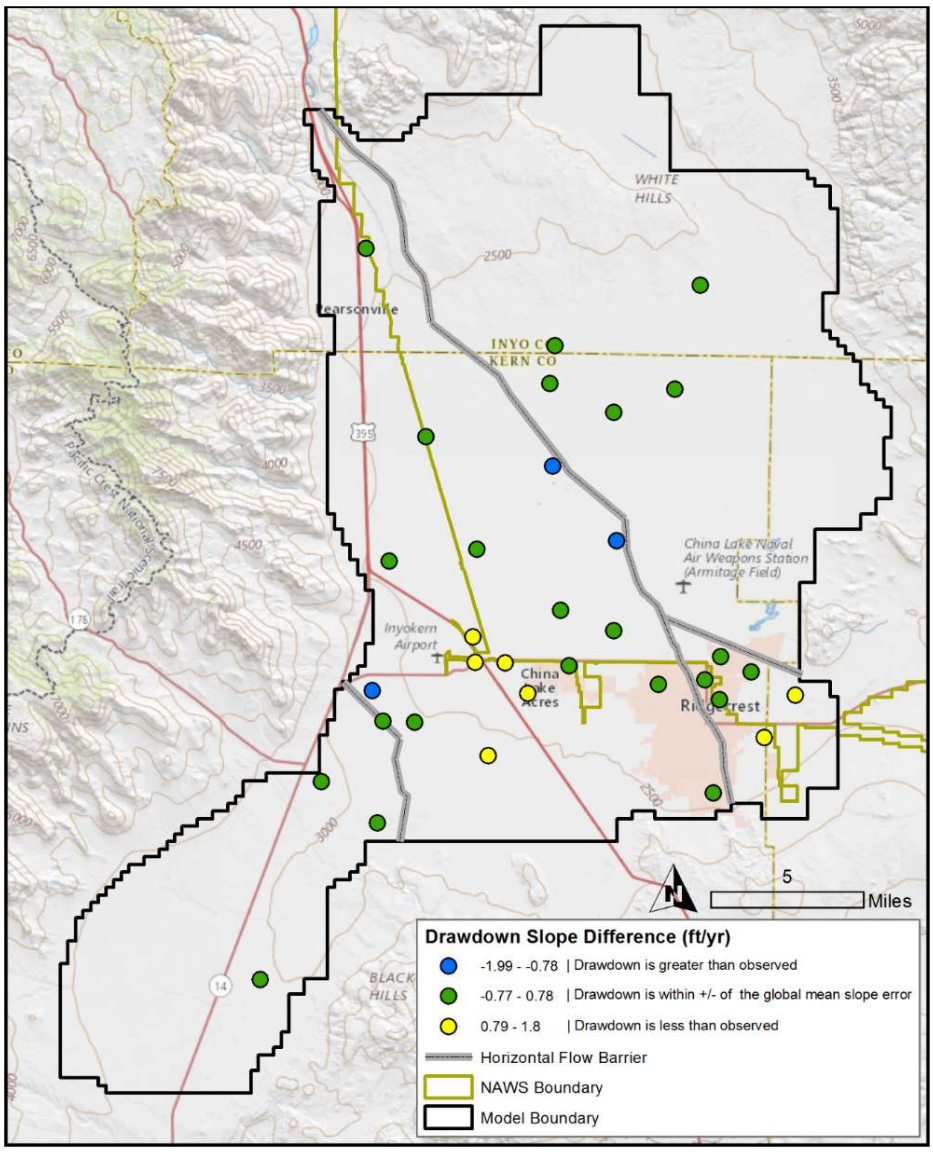

Figure 26. Mean residuals between simulated and observed drawdown slopes in the transient-historical model. Refer to Figure 3 for the names of the fault segments.

Water levels simulated by the transient-historical model in year 2016 are compared to water levels observed in 2016 in Figure 27. Groundwater flow directions and gradients are generally consistent, though local features represented by small numbers of grouped observations are not simulated by the model to the same degree because its larger scale limits accurate simulation of local detail. Note that the effects of the fault barriers are clearly seen in the contours of simulated head. The scarcity of observations points, particularly near faults, prevents the same effects from being revealed in the contours of observed water levels near most of the faults in the basin. Notably, high gradients in groundwater heads observed near the El Paso Fault indicate the barrier effect of this fault (Garner et al., 2017).

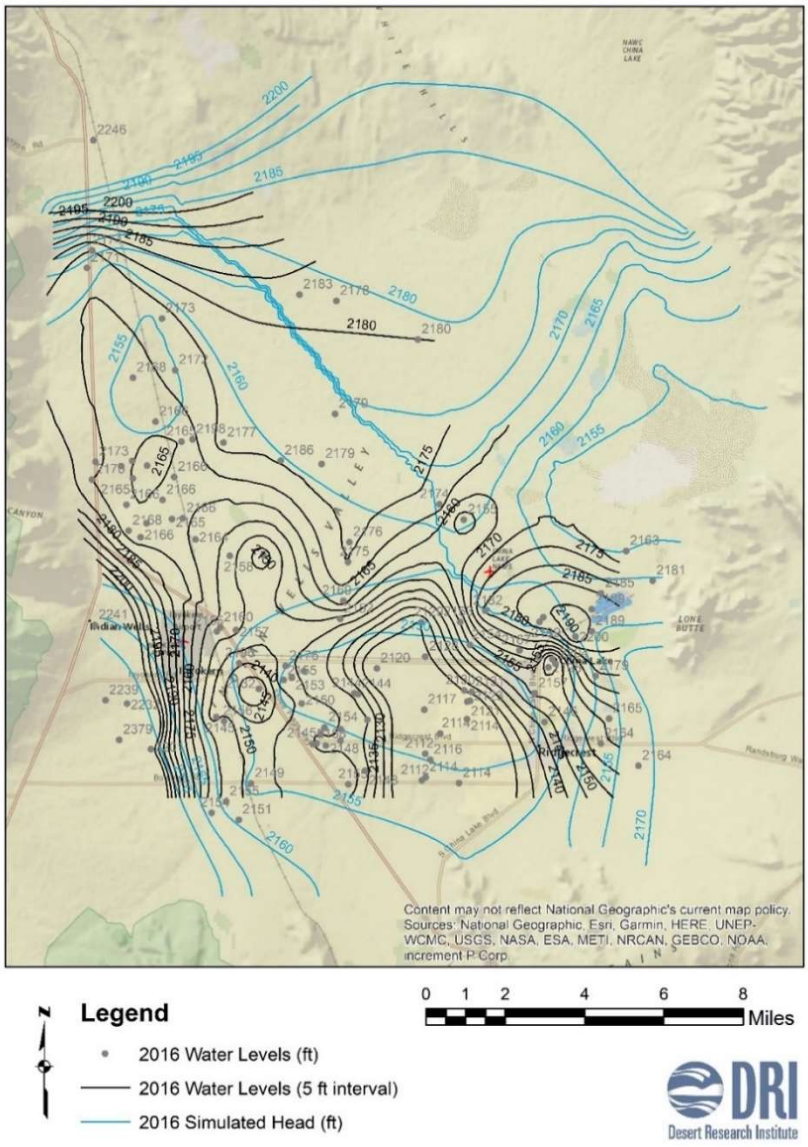

Figure 27. Comparison of water levels simulated by the transient-historical model to observed water levels for the year 2016.

As discussed previously, no direct measurements of ET over a multiple-year period are available in the basin. Instead, estimates of ET rate and ET extinction depth were made for phreatophytes and bare soil in eastern Indian Wells Valley and the model calculated ET based on depth to groundwater. The annual rate of ET computed by the transient-historical model declines from 7,600 AFY in 1922 to 2,852 AFY in 2016 (Figure 28). Also shown on Figure 28 are the ET rates estimated from enhanced vegetation index (EVI) values obtained from Landsat imagery covering the phreatophyte area in eastern Indian Wells Valley and the empirical relationship of Beamer et al. (2013). The plot shows an excellent agreement of the model-simulated ET to the EVI-estimated ET for the period 1997 through 2008. Most importantly, the similar slope of these ET trends indicates that the flow model is correctly simulating the processes that are contributing to the decline in ET observed in the eastern basin.

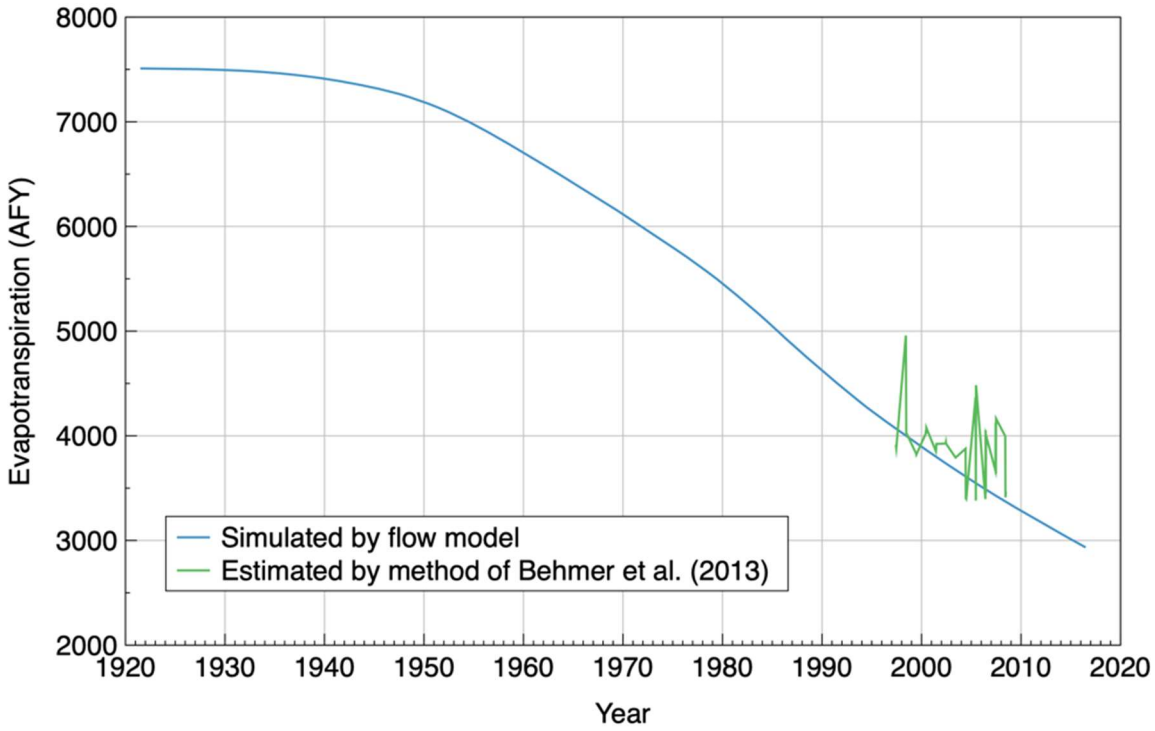

Figure 28. Evapotranspiration (ET) simulated by the transient-historical model plotted against ET estimated by the empirical relationship established by Beamer et al. (2013) between EVI and ET.

The groundwater budget for 2016, the final year simulated by transient-historical model, is tabulated in Table 4. Mountain block recharge is set at the same value of 7,650 AFY as in the steady-state model. However, drawdowns related to groundwater withdrawals during the transient stress period causes the outflow components of evapotranspiration (2,963 AFY) and interbasin flow to Salt Wells Valley (67 AFY) to be reduced from their values in the steady-state model. The area of ET and ET rates are reduced as water levels in the western basin decline below extinction depths. Similarly, hydraulic gradients near the boundary with Salt Wells Valley are reduced by declines in groundwater levels caused by pumping centers near Ridgecrest, which reduces the eastward-directed hydraulic gradient. The largest component of the transient-historical groundwater budget is groundwater pumping at a value of 24,472 AFY in 2016.

Table 4. Groundwater budget simulated by the transient-historical model for the year 2016.

INFLOW	**(acre-ft/year)**
Recharge	7,650
Coso and Argus Ranges	1,600
Rose Valley	2,400
Sierra Nevada North	2,100
Sierra Nevada South	1,500
El Paso sub-basin	50
Total:	**7,650**

OUTFLOW	**(acre-ft/year)**
Pumping (total)	24,473
Agricultural	12,363
Domestic	993
Municipal	7,142
NAWS	1,596
SVM	2,379
Evapotranspiration	2,934
Flow to Salt Wells Valley	74
Total:	**27,481**
CHANGE IN STORAGE	**-19,831**

2.6 Sensitivity Analysis

A sensitivity analysis of the flow model was performed to identify the parameters and boundary conditions that model results are particularly responsive to. For this analysis, a version of the transient-historical flow model was run in forward mode for the years 2018 through 2067. Five model parameters were adjusted in individual model runs using values that were 50 percent and 150 percent of their calibrated values and the effects of these adjustments on simulated heads were evaluated. Values of three of the parameters, specific yield, specific storage, and recharge, are constant throughout the simulation period and model domain or in specific zones within the model domain. The base values of these parameters are the values used in the transient-historical model previously described and their values as used in the sensitivity runs are shown in Table 5. Hydraulic conductivity varies spatially in the model, by cell in Layer 1 and by zones in Layers 2 through 6, so their many values are not included in Table 5. However, this parameter was adjusted in the same way, the base K value in every model cell was adjusted by 50 percent and 150 percent. The annual variation in recharge rate used in the transient-predictive models was also incorporated in this analysis by adjusting each yearly rate by 50 percent and 150 percent. Groundwater withdrawals were set at a constant rate of 24,473 AFY, the rate used in the final year of the transient model.

Table 5. Values of constant parameters used in the sensitivity analysis. Separate sensitivity runs addressed hydraulic conductivity and annual variation in recharge rate. See text for explanation.

Parameter	Parameter Value		
	50%	Base	150%
Constant Recharge Total	3,825	7,650	11,474
Coso and Argus Ranges	800	1,600	2,400
Rose Valley	1,200	2,400	3,600
Sierra Nevada North	1,050	2,100	3,150
Sierra Nevada South	750	1,500	2,250
El Paso sub-basin	25	50	75
Specific Yield	0.1125	0.225	0.3375
Specific Storage	5.00E-07	1.00E-06	1.50E-06

Simulated heads were evaluated at four wells, three in the main basin and one in the El Paso sub-basin (Figure 29). These locations were chosen to represent areas of the model of particular interest for management of groundwater resources, including important municipal and agricultural pumping centers. The effects of the adjusted parameters are shown in Figures 30 through 32. The sensitivity coefficient, defined as the difference between the drawdown for 50 percent and 150 percent of the base values, is calculated for each of the four wells for each parameter and then averaged to provide an overall sensitivity coefficient for each parameter. Model sensitivity is dominated by specific yield, all other parameters have moderate to low effect on simulated heads (Figure 33). The value of specific yield is an important factor for forecasting drawdowns in response to future pumping scenarios, but data supporting the choice of this parameter are limited in the basin. Conducting additional pumping tests with one or more observation wells can reduce the uncertainty in this parameter and provide information of how it varies within the basin-fill aquifers. The uncertainty in hydraulic conductivity can also be reduced through analysis of additional pumping tests.

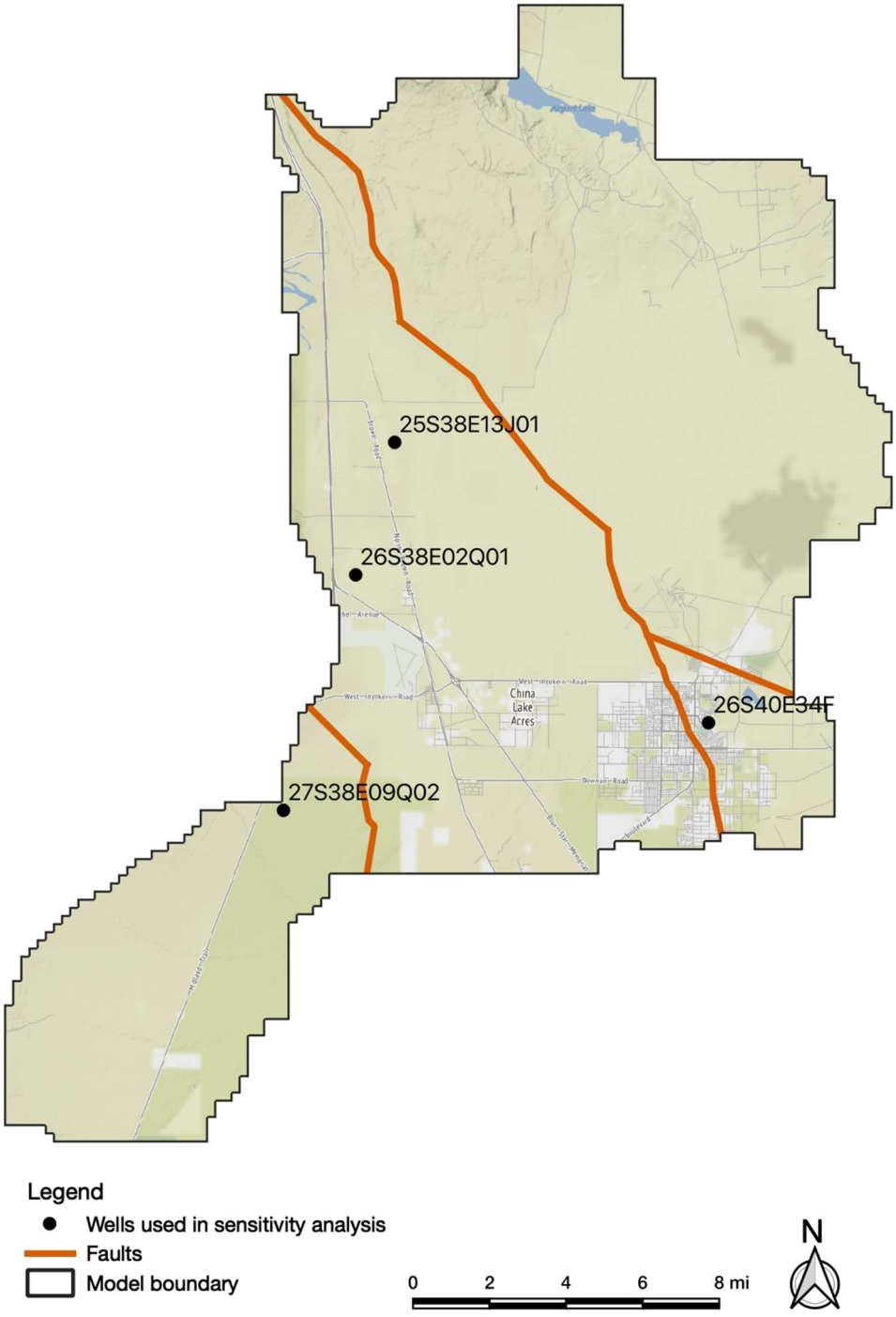

Figure 29. Locations of wells used for water-level observations in the sensitivity analysis. Refer to Figure 3 for the names of the fault segments.

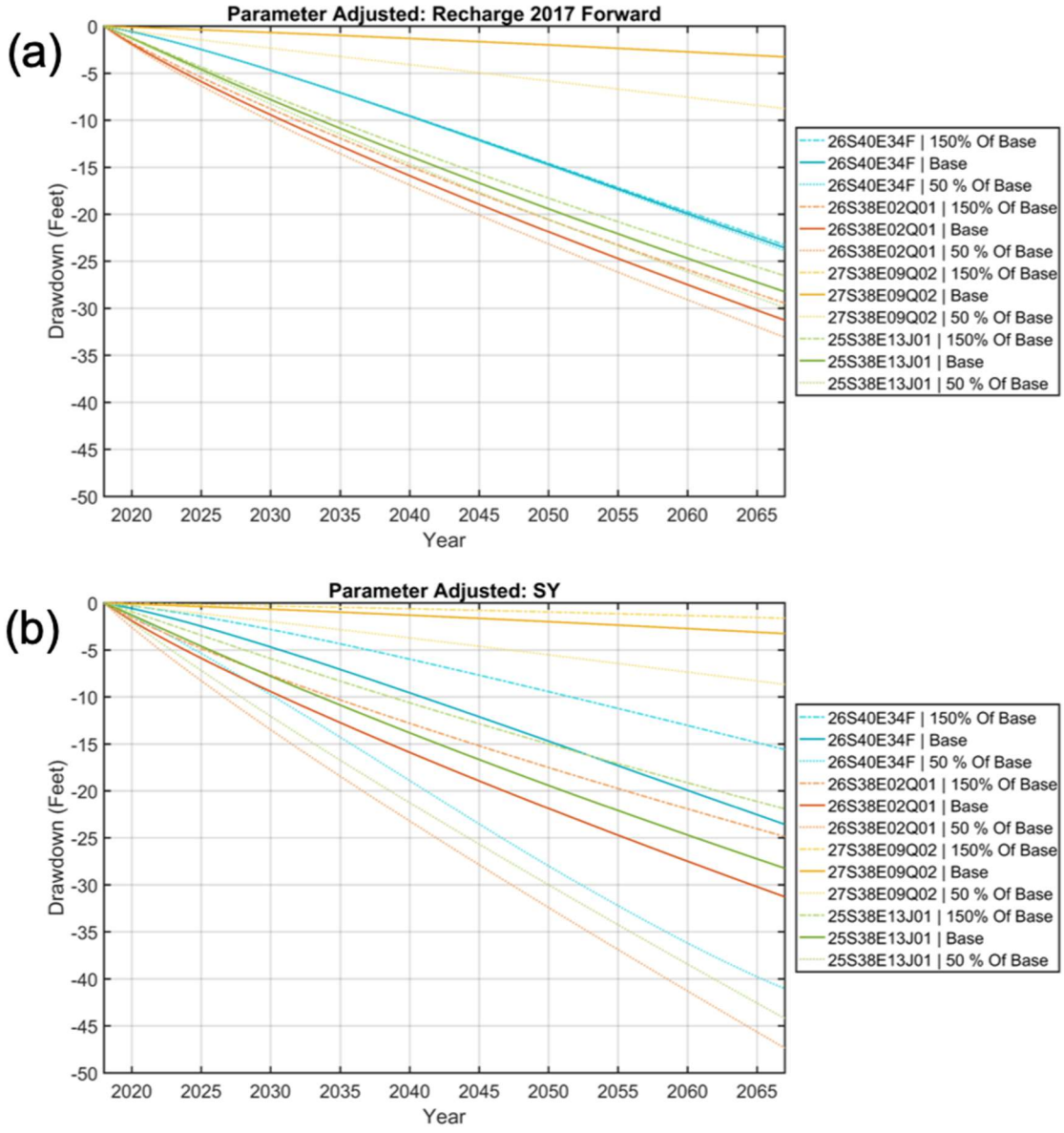

Figure 30. Results of sensitivity analysis for constant recharge rates (a) and specific yield (b). The sensitivity coefficient for each parameter is defined as the difference between the drawdown for 50 percent and 150 percent of the base values.

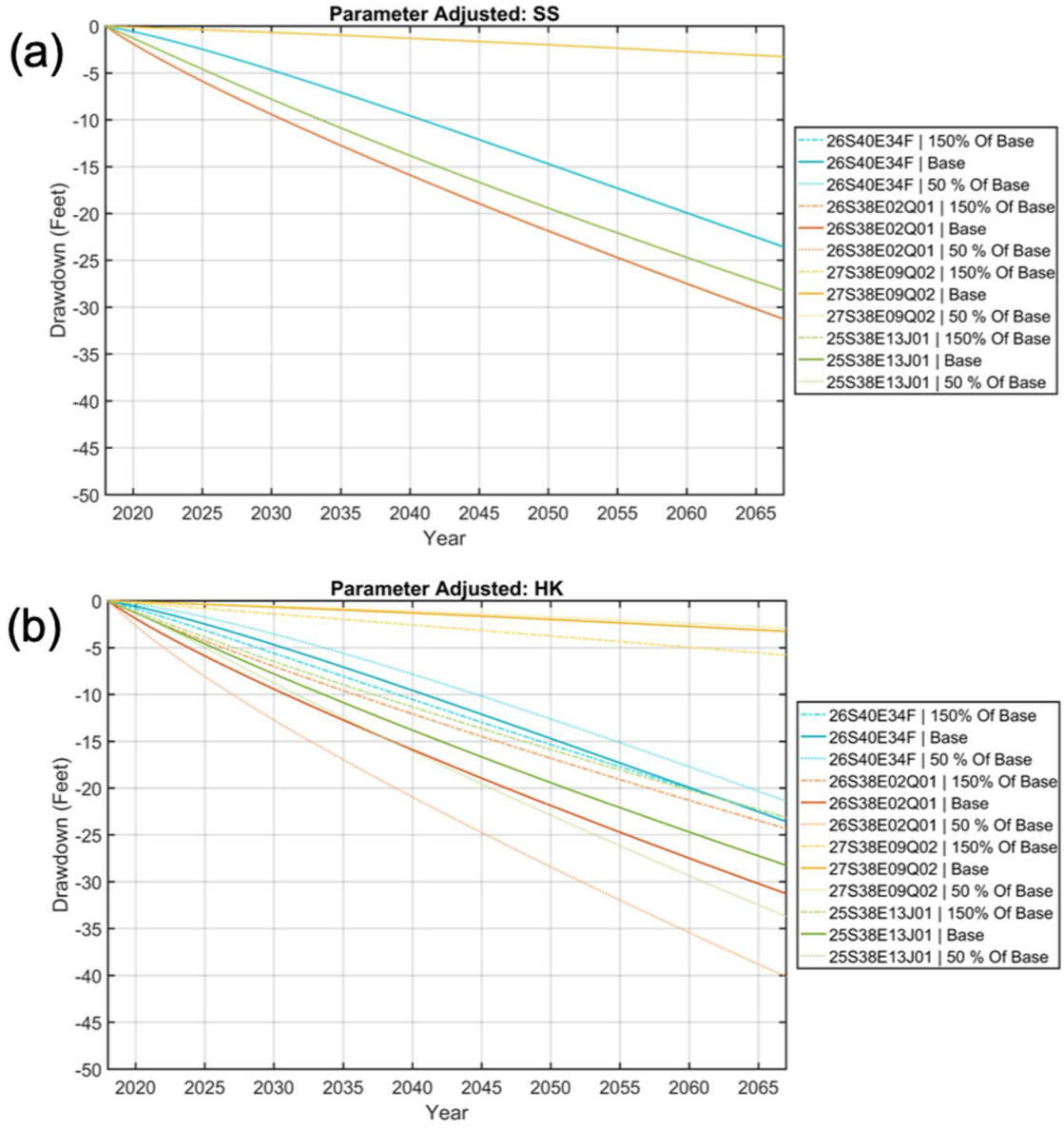

Figure 31. Results of sensitivity analysis for specific storage (a) and hydraulic conductivity (b). The sensitivity coefficient for each parameter is defined as the difference between the drawdown for 50 percent and 150 percent of the base values.

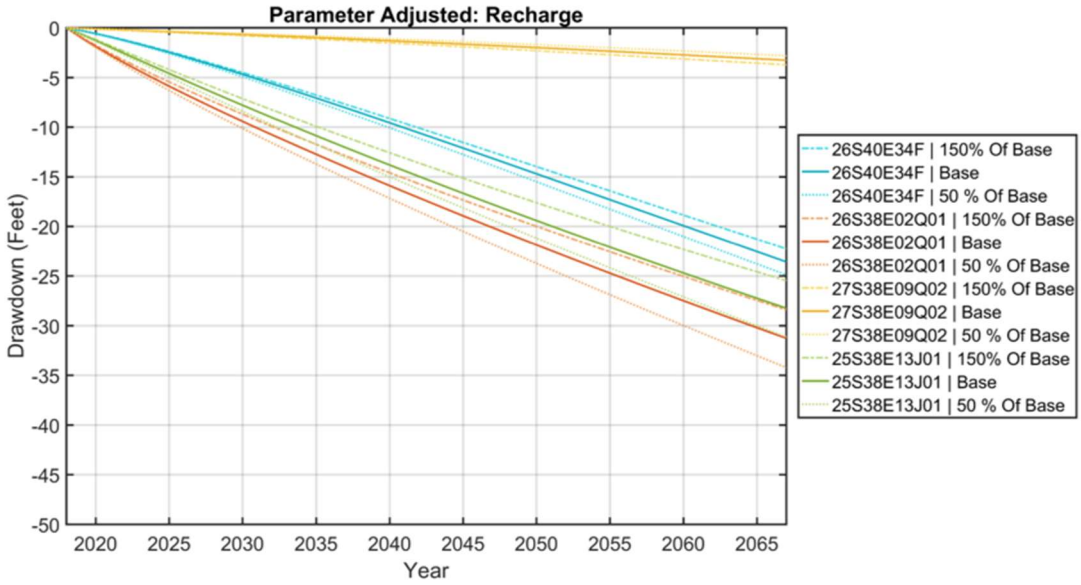

Figure 32. Results of sensitivity analysis for annually variable recharge rate. The sensitivity coefficient for each parameter is defined as the difference between the drawdown for 50 percent and 150 percent of the base values.

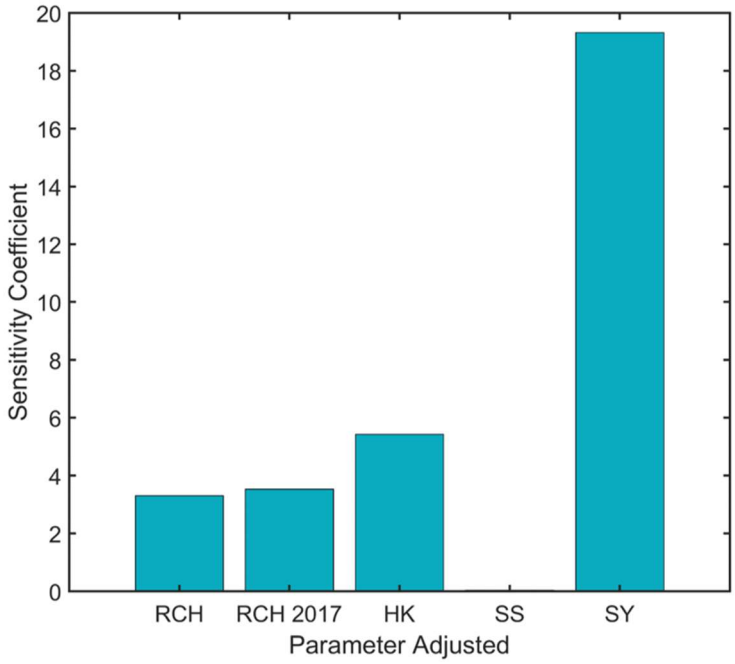

Figure 33. Comparison of the sensitivity coefficients for the five parameters adjusted during the sensitivity analysis.

2.7 Predictive Flow Models

Two predictive flow models were developed from the calibrated transient-historical model to forecast responses of the groundwater flow system to possible future alternative groundwater management scenarios. The baseline flow model simulates a "no action" alternative, where most groundwater withdrawal rates and locations that occurred in 2016 are continued into the future with annual increases to account for modest population growth. The scenario 6.2 flow model simulates the groundwater allocation and management plans described in the Groundwater Sustainability Plan, and includes artificial recharge of imported and recycled water. In both models, a three-year transition period from 2017 through 2019 is used to equilibrate the model to a withdrawal rate of 35,000 AFY that is held constant during the 3-year transition. The predictive model simulations then begin in the year 2020 and extend through 2070 utilizing the annual rates of groundwater withdrawal and artificial recharge shown in Figure 34. Groundwater withdrawals are simulated at the 938 wells included in the pumping allocations for the baseline and 6.2 scenarios, as described in the GSP.

As discussed in Section 2.4.3, natural recharge rates in the predictive models are varied by scaling the constant rate of 7,650 AFY by the annual precipitation amounts observed in and near Indian Wells Valley over a balanced hydrologic period from 1990 through 2014 (Stetson Engineers, 2018). This 26-year period is then repeated to obtain the natural recharge input for the predictive models. Other than this variability in natural recharge and the two scenarios of groundwater withdrawal and artificial recharge, there are no differences between the predictive flow models and the calibrated transient-historical flow model.

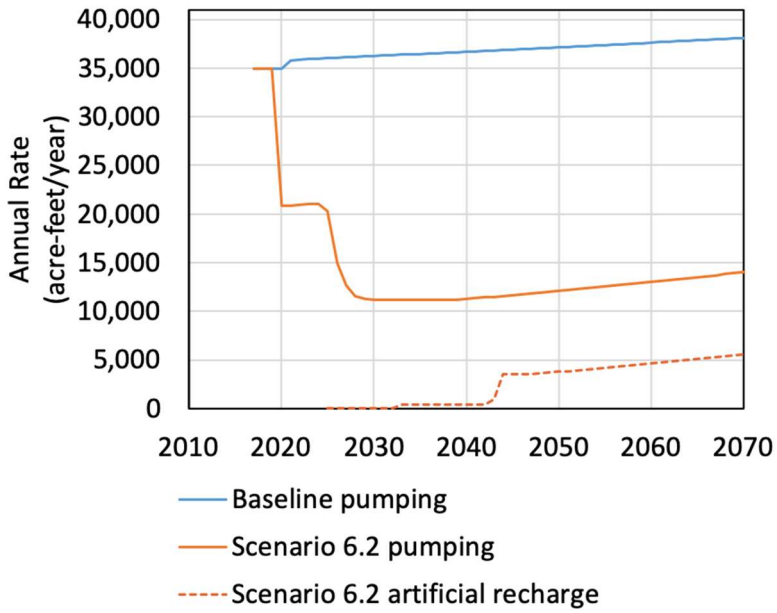

Figure 34. Annual rates of groundwater withdrawal and artificial recharge included in the Baseline and Scenario 6.2 models.

The results forecast by the baseline and scenario 6.2 predictive flow models were presented to the Technical Advisory Committee (TAC). These presentations are included in Appendix 3-H of the Groundwater Management Plan. Included are comparisons of changes in groundwater levels from 2020 through 2070 as maps and hydrographs for selected wells, plots of the change in groundwater storage, plots of evapotranspiration, and the groundwater budgets for the entire basin.

3. Transport Model

3.1 Introduction

Saline groundwater that underlies portions of Indian Wells Valley may reduce water quality in production wells if these poor-quality groundwaters are drawn toward pumping centers. Evidence of increasing salinity in some production wells in the southeastern basin near Ridgecrest has been shown by Berenbrock and Schroeder (1994) and Todd Engineers (2014). Solutes in groundwater within Indian Wells Valley are conceptualized as originating from recharge from surrounding mountain ranges, groundwater flow from surrounding basins, mixing with remnant evaporative brines and geothermal fluids, and concentration by evaporation. Solutes are removed from the groundwater system by discharge to Searles Valley to the southeast. McGraw et al. (2016) summarized numerous studies that together identify areas of generally higher salinity groundwater to the east near China Lake Playa, to the northwest toward Rose Valley, around eastern Ridgecrest, and in several other locations associated with clay horizons or geothermal zones. Evidence of increasing salinity in wells in the Ridgecrest area has been documented by Berenbrock and Schroeder (1994) and Todd Engineers (2014). The Indian Wells Valley transport model was developed to investigate how the distribution of salinity within the groundwater system may be influenced by alternative scenarios for groundwater management.

3.2 Code Selection and Documentation

The MT3D-USGS: Groundwater Solute Transport Simulator for MODFLOW was applied to assess the effects of pumping on groundwater quality over time. The model was constructed using the Groundwater Modeling System (GMS) environment (version 10.2) developed by Aquaveo, LLC. As for the flow model, GMS serves as a database for all of the hydrogeologic information in the model and provides an easy to use graphical pre- and post-processor interface to MODFLOW/MT3D-USGS. Although developed within GMS, the MT3D-USGS input and output files are in standard MODFLOW format and the model can be run without the use of GMS.

3.3 Configuration

The framework of the transport model coincides with the groundwater flow model of Indian Wells Valley, employing the same model domain, grid structure, and layers. MT3D solves the transport equations using the groundwater flow rates and directions simulated by the groundwater flow model. The transport model uses total dissolved solids (TDS) concentrations as a surrogate for groundwater salinity to forecast TDS concentrations from the present to the year 2070 by incorporating the volumetric groundwater flow rates simulated by the flow model for the GSP management scenario. Stress periods of one month are used to be consistent with the transient-predictive flow model. The results are presented as maps showing the spatial distribution of forecasted TDS concentrations for selected times, and maps showing rates of change of TDS concentration for selected times. The concentration units in the model and in the plots are mg/L.

Two transport models were developed using the flow results from the predictive groundwater flow models described in Section 2.7 to forecast movement of solutes in response to possible alternative scenarios for groundwater management. The baseline model simulates a “no action” alternative, where most groundwater withdrawal rates and locations in place in 2016 are continued into the future with annual increases to account for modest population growth. The scenario 6.2 model simulates the groundwater allocation and management plan described in Section 3.5.5 of the GSP, and includes artificial recharge of imported and recycled water. The transport simulations begin in the year 2020 and extend through 2070.

3.4 Initial and Boundary Conditions

A database of wells and groundwater TDS concentrations over time was developed by Stetson Engineers Inc. from TDS measurements compiled from numerous sources, with the majority obtained from the Groundwater Ambient Monitoring and Assessment Program (GAMA) database (California Water Board, 2018), publications by the U.S. Geological Survey (including Moyle, 1963; Berenbrock, 1987, and Berenbrock and Schroeder, 1994), data from Meadowbrook Dairy (E. Teasdale, personal communication, Sept. 11, 2018), and a database by the Kern County Water Agency (2018). The database includes 563 locations and 2,006 TDS values, with data collected over a 70-year period.

The TDS initial condition dataset for the transport model was developed from a subset of the full database. Wells with unknown depth or screened interval were excluded from the initial condition data set. Historical TDS measurements did not provide uniform coverage over time and therefore the most-recent TDS concentration was selected at each well as the initial value (Figure 35). This approach provides an approximation of initial conditions for the basin for forecasts into the future, but does not account for historical variation or trends in TDS concentrations at individual wells. The TDS concentrations of the most recent measurements and their locations are shown in Figure 36.

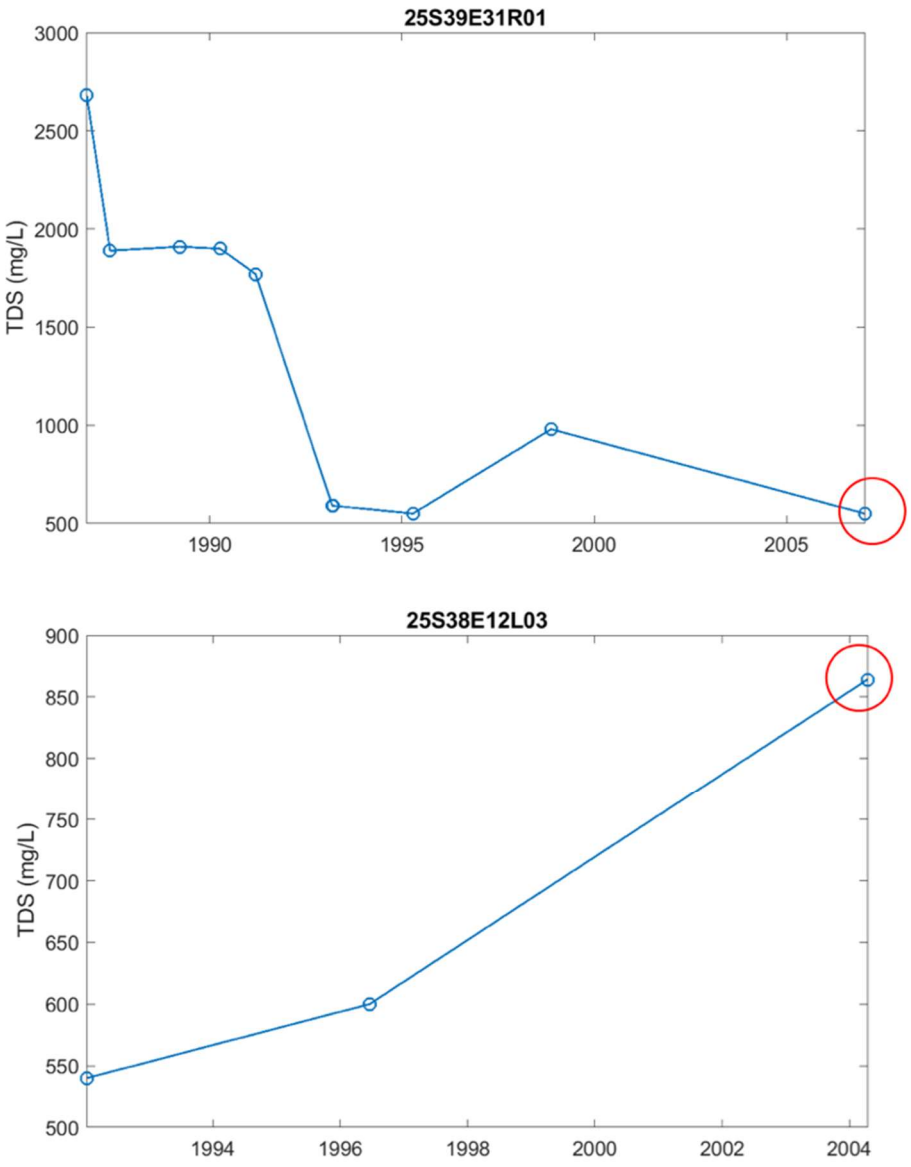

Figure 35. Examples of TDS temporal trends and the selection of the most recent TDS concentration (indicated by red circles) for wells having multiple measurements. Using this approach, the initial TDS data set represents the most recent data for the basin, though historical trends at individual wells are not explicitly included.

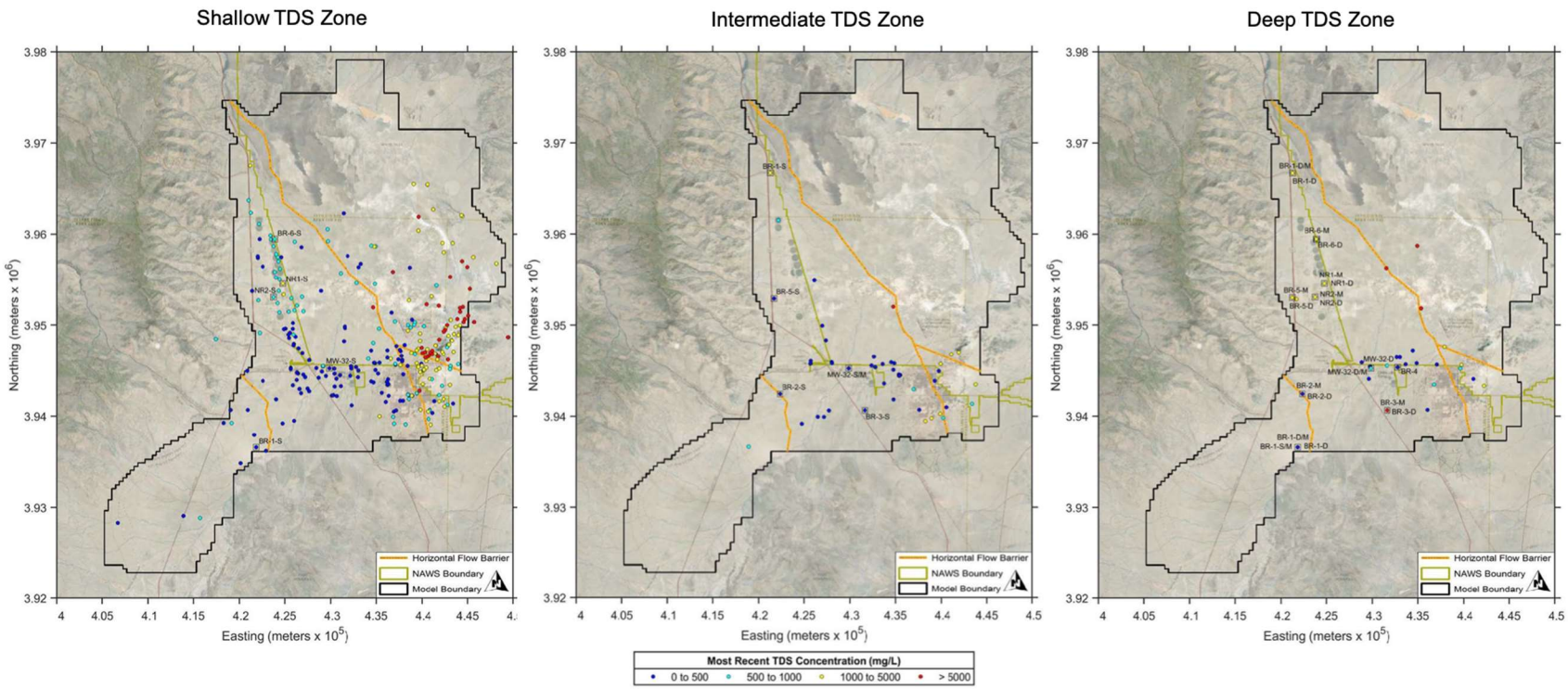

Figure 36. Locations of wells and the most recent TDS concentrations in the three TDS zones used to develop the TDS initial conditions for the transport model. The TDS scale shown applies to all three TDS Zones. Refer to Figure 3 for the names of the fault segments.

Because of sparse horizontal and vertical data coverage, particularly for model layers 2 through 6, it wasn't possible to interpolate the measurements to each model layer independently, so the measurements were assigned to one of three vertical zones (Shallow, Intermediate, and Deep). The Shallow TDS zone includes measurements within the depth range of flow model layer 1, where most measurements are located. TDS measurements are limited below layer 1, so the lower portion of the model was divided into two TDS zones. The Intermediate TDS zone corresponds to flow model layers 2 and 3, and the Deep TDS zone includes measurements within the depth ranges of flow model layers 4, 5, and 6. Each well was assigned to one of the zones based on the centroid of the depth of its screened interval. In the case of the fourteen wells that have multiple screens within a single TDS zone, the arithmetic mean of their measured concentrations was computed and used as the initial condition in that zone (Figure 37). The mean TDS values were not weighted by the relative flow rates contributed by screens at multiple depths because flow-rate data were generally unavailable. An example cross section through the model showing the configuration of the three TDS zones is shown in Figure 38. The locations of wells where the means of multiple TDS concentrations were calculated for a single zone are shown in Figure 39. The refined database is comprised of 391 well locations.

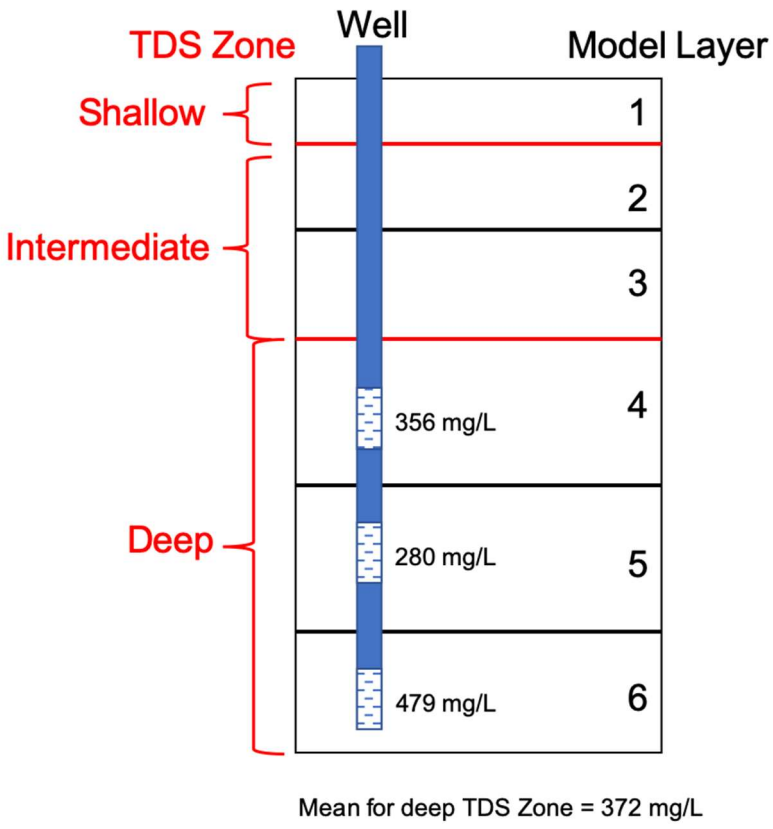

Figure 37. Example of calculation of mean TDS values at wells having multiple measurements in a single TDS zone.

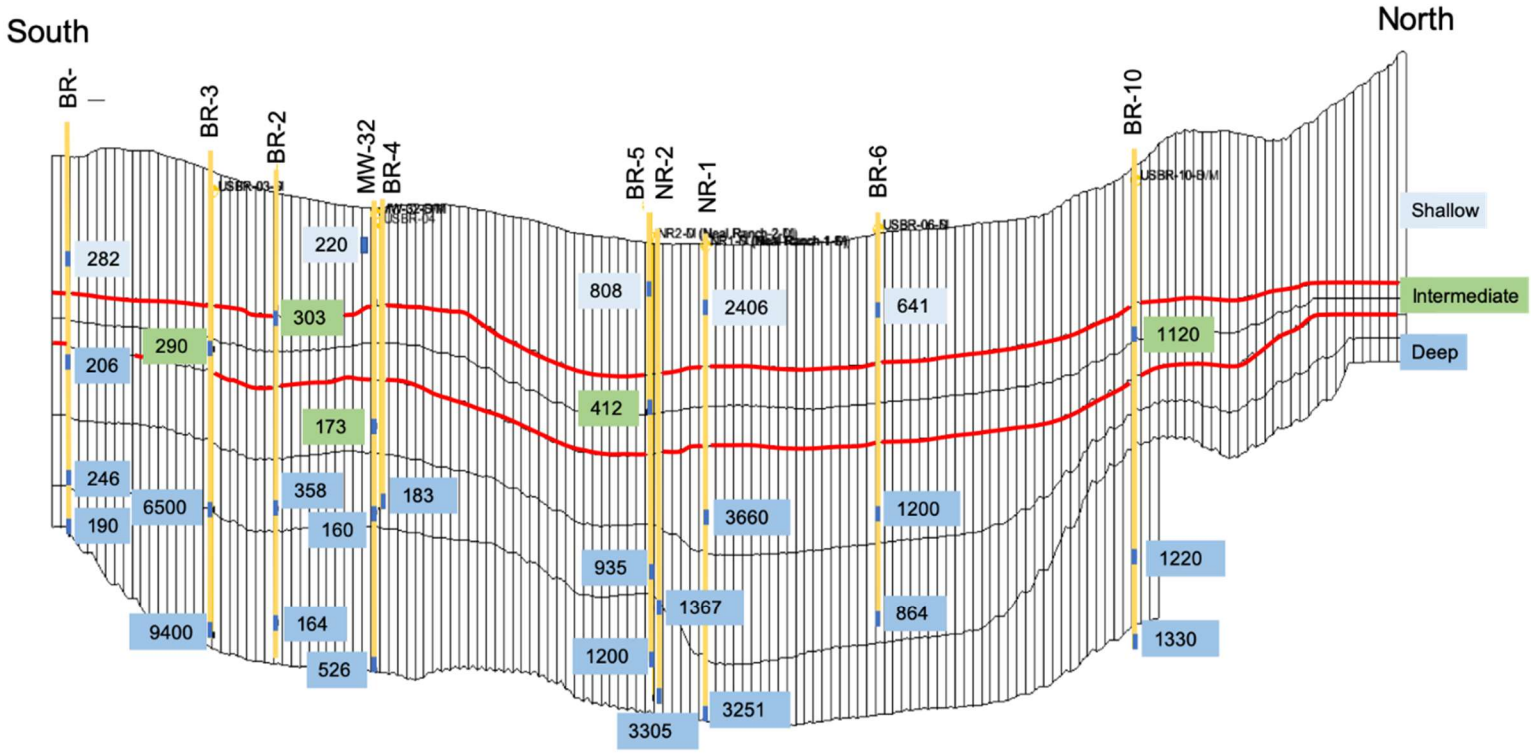

Figure 38. An example North-South cross section through the transport model illustrating the relationship between of the Shallow, Intermediate, and Deep TDS zones (separated by red lines) to the six computational layers in the flow model. TDS measurements at selected well locations are shown to illustrate the averaging of multiple values within a zone. Measured TDS concentrations were interpolated to the transport model grid cells based on the TDS zone in which they fall.

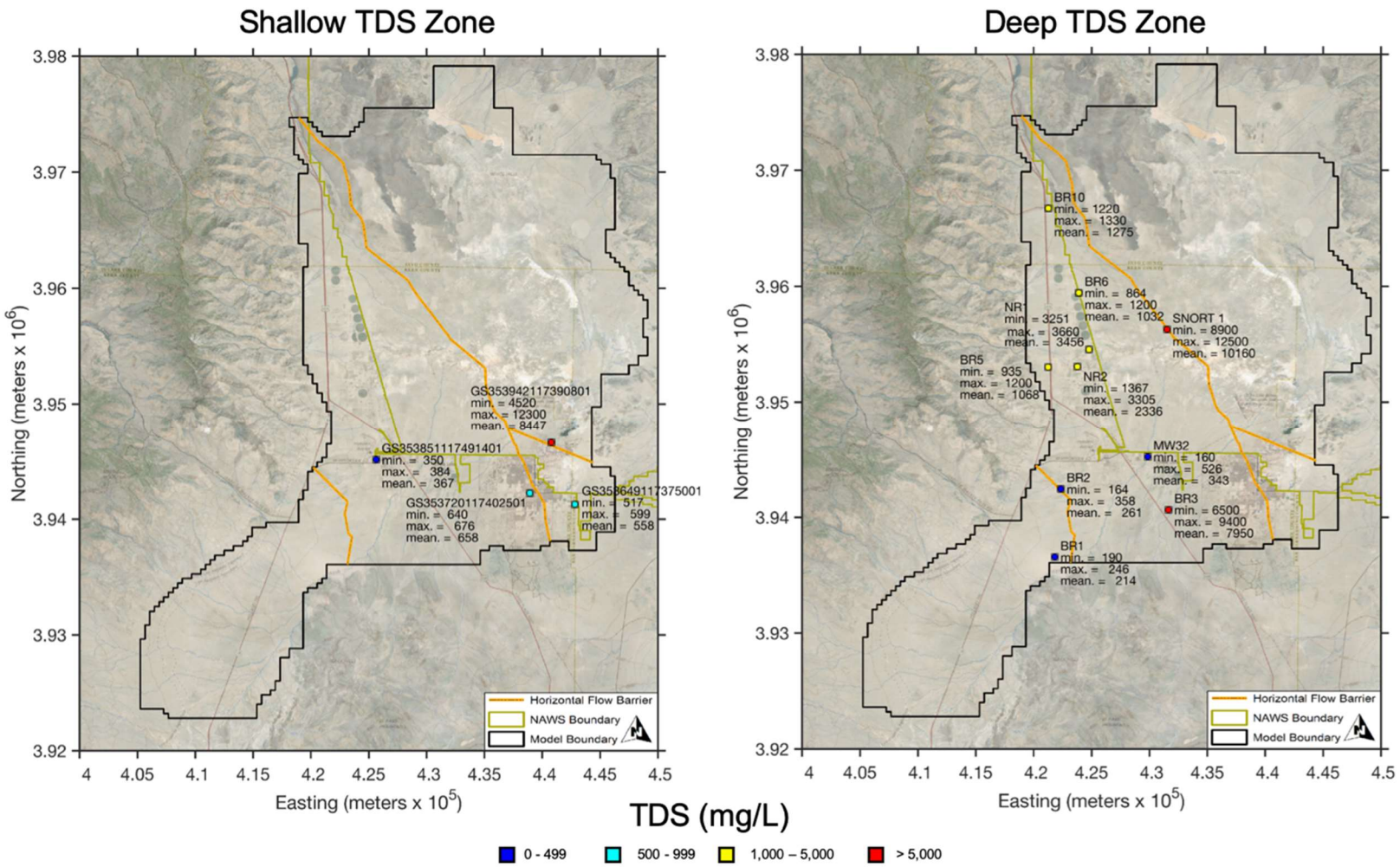

Figure 39. Locations of wells having multiple screens and TDS measurements in the Shallow and Deep TDS zones. There are no wells of this type in the Intermediate TDS zone. Refer to Figure 3 for the names of the fault segments.

Initial TDS conditions for the transport model were developed by spatial interpolation of the TDS values in the refined database within the shallow, intermediate and deep TDS zones. Each active model grid cell was assigned an initial TDS value based on the zone-layer relationship defined above. Kriging was used to interpolate the point data using a semivariogram structure with no nugget, a range of 1.1 km, and a variance of 1.9×10^7 $(mg/L)^2$ to fit the experimental variogram. Kriging interpolation was performed on the $\log_{10}$ of the TDS concentration values because of the large range in values. The interpolated TDS maps for the three TDS zones are shown in Figure 40. In areas where no TDS measurements exist, control points were established to fully populate the model domain (open squares in Figure 40) and ensure that the interpolated TDS distributions were consistent with conceptualized TDS distributions. These points were assigned a value of 1,500 mg/L in the northern basin and a value of 450 mg/L in the El Paso sub-basin. In both cases, the values were selected to be consistent with TDS measurements in nearby areas of the basin. The spatial distribution of interpolated TDS is generally consistent with the salinity patterns identified by previous studies (e.g. Berenbrock and Schroeder, 1994; Morgan, 2010). For example, TDS in the northwest and east-central portions of the basin is higher in the intermediate zone than in the shallow zone, corresponding to the finer-grained material at these depths in these areas. TDS is also higher in the area of China Lake playa, where groundwater concentrations of some major ions increase because of geochemical reactions with lacustrine deposits (Berenbrock and Schroeder, 1994).

Groundwater recharge carries dissolved solutes into the groundwater system (Figure 41). The TDS concentration of recharge along the western edge of the model was assumed to be 67 mg/L in the previous Navy model (McGraw et al., 2016), based on measurements in “recharge areas of the high Sierra Nevada” reported by Güler and Thyne (2004). However, those locations are associated with springs above 6,500 ft elevation. A value of 356 mg/L represents samples from the Sierra Nevada and other mountain ranges at elevations mostly below 6,500 ft. Citing Maxey (1968), Güler and Thyne (2004) point out that these lower elevation areas provide the majority of recharge to basin-fill aquifers. This led to the choice of 350 mg/L during initial transport model development. Following an update to the TDS database by Stetson Engineers in January 2019, the TDS concentration for the southern Sierra Nevada boundary was revised to 450 mg/L to reflect TDS measurements in the range of 447 to 630 mg/L in wells in southern El Paso sub-basin.

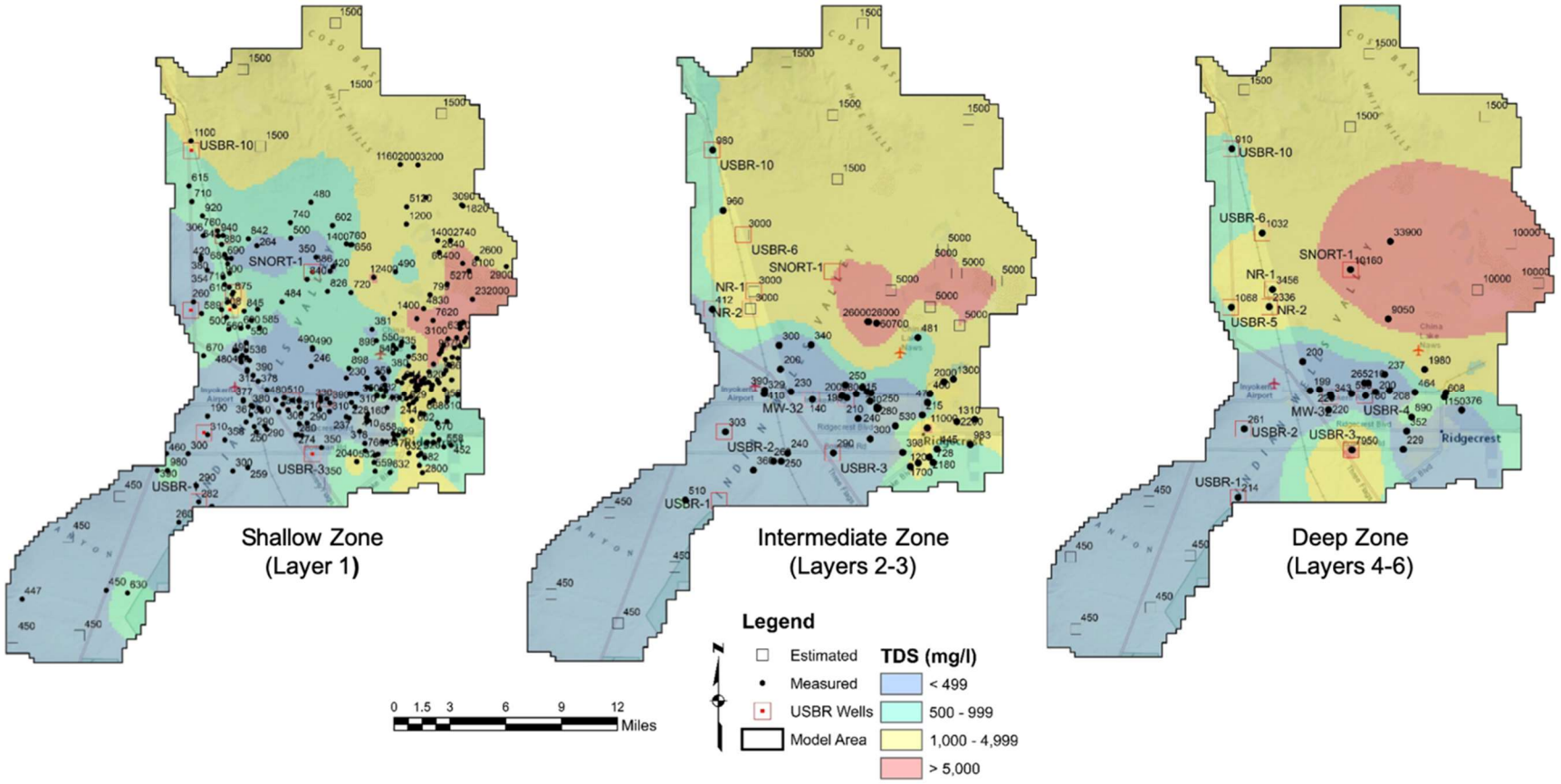

Figure 40. Spatial distributions of TDS concentration in the three TDS zones that are used for initial conditions in the transport model. Hollow squares are control points used to improve interpolation. These points were assigned a value of 1,500 mg/L in the north northern basin and a value of 450 mg/L in the El Paso sub-basin.

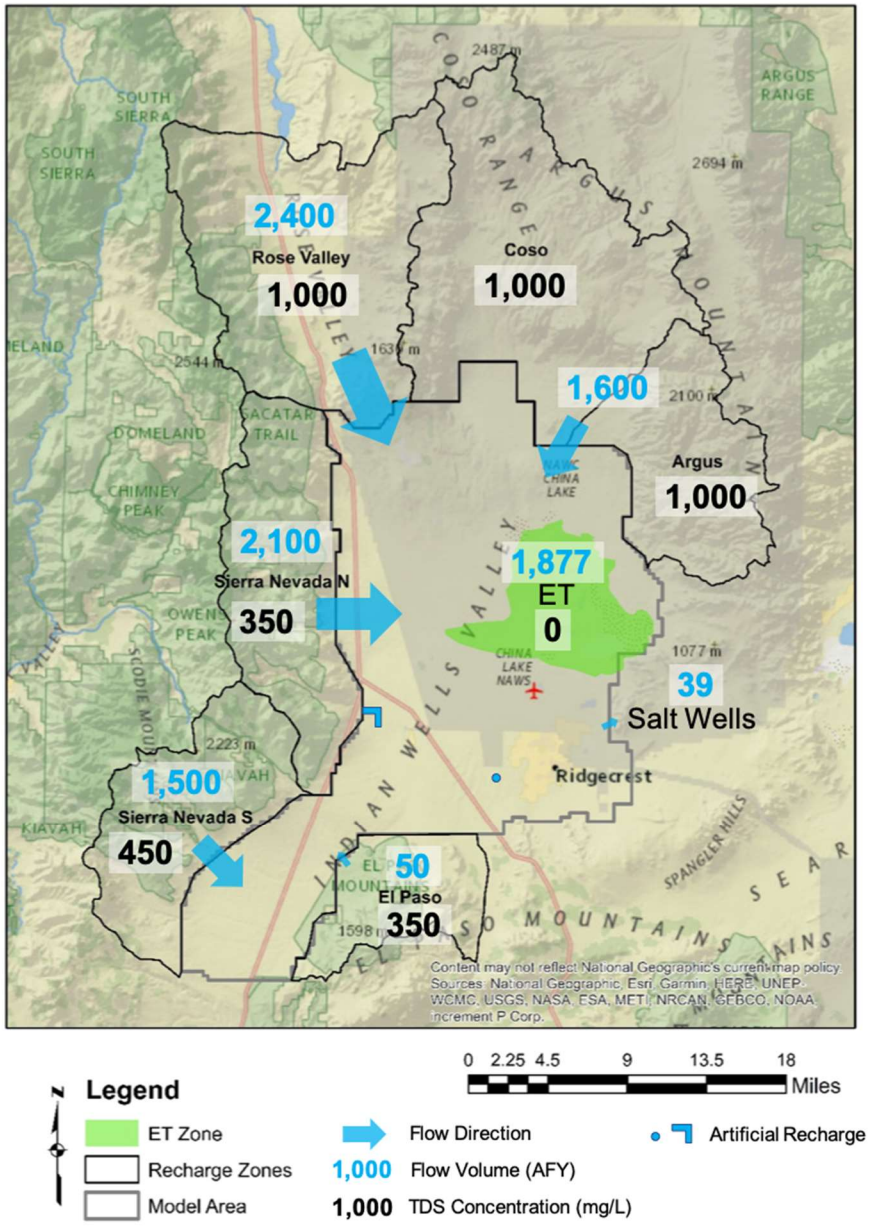

Figure 41. TDS concentrations assigned to groundwater recharge areas in the transport model. The TDS of the artificial recharge is 280 mg/L for imported water (western location) and 250 mg/L for recycled water (eastern location).

In addition to the natural sources of TDS described above, the scenario 6.2 transport model includes TDS sources in the form of artificial recharge of imported and recycled water (Figure 41). Imported water having a TDS concentration of 280 mg/L is recharged via an infiltration basin located west of the Inyokern Airport. Because site-specific infiltration data were not available, the model applies this recharge directly to the saturated zone and thus evaporation and potential subsequent concentration of TDS in the recharge water are not simulated. Recycled water having a TDS concentration of 250 mg/L is recharged directly to the saturated zone via an injection well west of Ridgecrest.

The values of TDS transport parameters are based on those used in DRI's groundwater transport model for the Navy (McGraw et al., 2016). The value of longitudinal dispersivity was chosen to be consistent with the large size of the model domain and the potential for movement of saline groundwater over substantial distances. The mean advective transport distance in model layer 1 during the 50-year simulation period is 365 m, which corresponds to a longitudinal dispersivity value of 100 m based on the relationship between the scale of field observations and values of longitudinal dispersivity presented by Gelhar et al. (1992). Horizontal transverse dispersivity was set at 10 m as defined by the typical ratio of 0.1 to longitudinal dispersivity (Dullien, 1992), and vertical transverse dispersivity was set at 1 m. Effective porosity was set at 0.225, which is the specific yield value used in the flow models and is a value typical for unconsolidated basin fill materials (Stephens et al., 1998). The value of the diffusion coefficient is set to zero and there are no geochemical reactions or sorption effects included in the transport model.

The transport model utilizes the standard finite difference (SFD) method with upstream weighting solution scheme employed in the MT3D-USGS code for solving the advection term of the transport equation. Although several solution schemes are available in MT3D-USGS, the SFD method was chosen for its efficiency. This method is considered reasonably accurate for transport models having a Peclet number less than four (Zheng and Wang, 1999). The Peclet number, P_e, is defined as

$$P_e = \frac{|v|\Delta x}{D} \tag{3}$$

where $|v|$ is the mean seepage velocity (LT^{-1}), Δx is the grid spacing (L), and D is the dispersion coefficient (L^2T^{-1}). D is the product of longitudinal dispersivity and mean seepage velocity. For the IWV predictive flow model for Scenario 6.2, Δx is 250 m, D is 100 m, and $|v|$ in model layer 1 is 0.023 m/d in 2020 and 0.017 m/d in 2070. Using the mean of these values of seepage velocity gives a Peclet number of 2.5, indicating that the SFD method is appropriate for this model.

3.5 Calibration

A quantitative calibration of the transport model was not performed because the initial TDS distribution integrates available measurements that span many decades, thus a single historic simulation period could not be developed for calibration. Instead, a qualitative calibration compared the forecasts of TDS trends simulated by the baseline transport model (described in Section 3.6) to general historic trends and spatial distributions represented by the conceptual model of groundwater salinity. Nine wells in the TDS database were selected for the comparison. These wells are among the nineteen wells used to evaluate TDS trends by Todd Engineers (2014). Though they did not identify the wells that were used, the nine wells listed in Table 6 correspond to the locations of the wells plotted in Figure 7 of Todd Engineers (2014). Historical trends were calculated from the available data using linear regression. Assuming that historical trends in TDS concentrations and groundwater withdrawals continue 50 years into the future, the baseline transport model forecasts show reasonable agreement to changes in TDS concentrations (Figure 42).

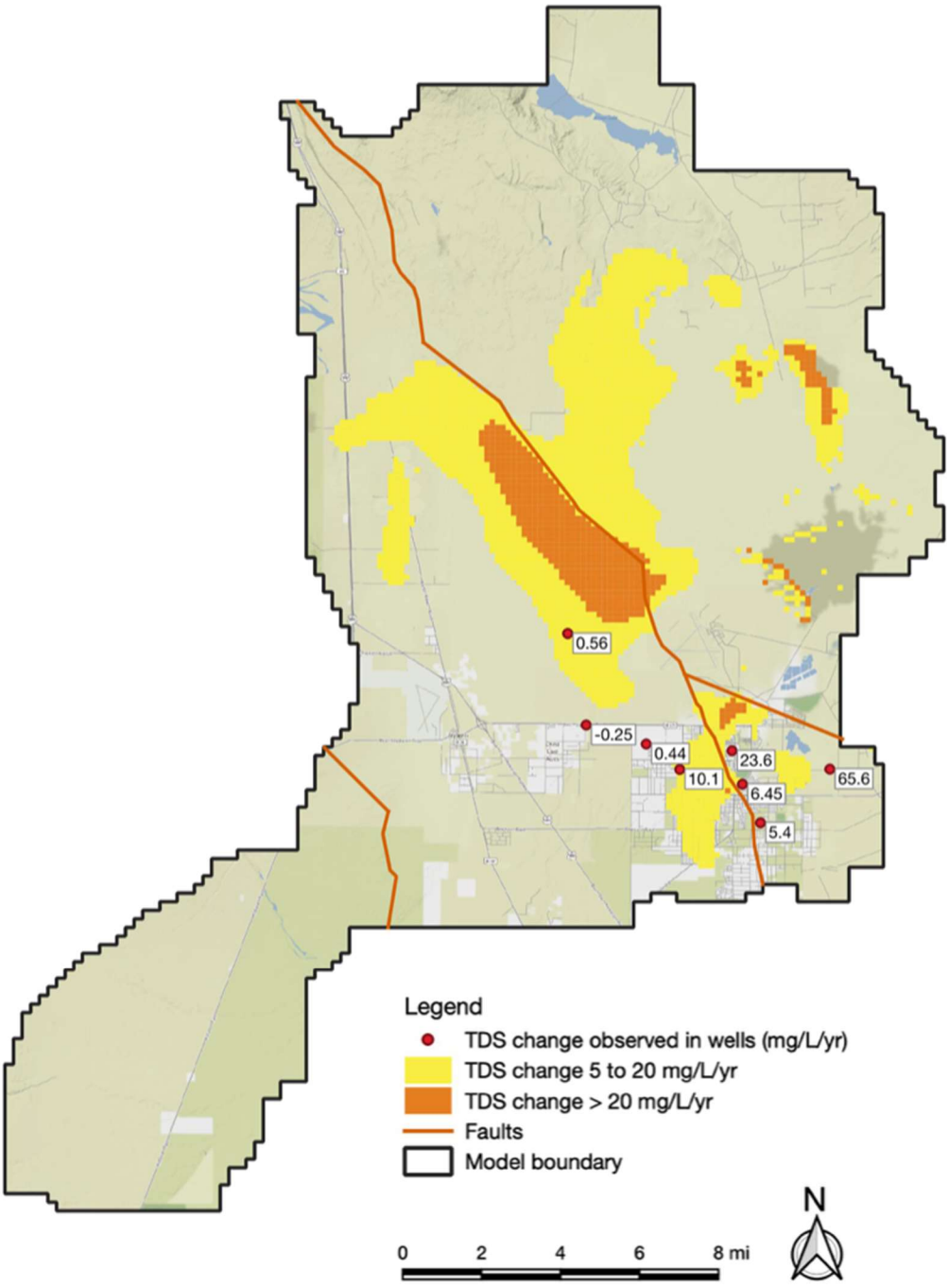

Figure 42. Comparison of annual rate of change in TDS (mg/L/yr) forecasted for the years 2020 to 2070 in the Shallow TDS Zone to historical annual rates of change observed in wells. Refer to Figure 3 for the names of the fault segments.

Table 6. Wells used for comparison of observed to simulated TDS concentration trends.

Well Name	TDS Slope (mg/L/yr)	Depth (ft)
26S/39E-11E01	6.18	250
26S/40E-36A01	65.6	270
26S/39E-10N01	0.56	--
26S/40E-28J01	23.6	--
RC HGTS WELL #7	5.40	304
26S/40E-34N01	6.45	232
IWVWD Well 17	-0.25	1030
26S/39E-24Q01	0.44	345
IWVWD Well 13	10.1	720

3.6 Transport Results

Changes in TDS concentrations forecast by the baseline and scenario 6.2 transport models were presented to the TAC. These presentations are included as Attachment B to this Appendix. The results are also summarized in Section 3.5.3 of the GSP report.

Simulated TDS concentrations in year 2070 in the shallow TDS zone for the baseline and scenario 6.2 models show similar spatial distributions to each other and to the year 2020 (Figure 43) despite 50 years of groundwater withdrawals at very different rates. This result is primarily a function of very low groundwater velocities in the basin that prevent large-scale TDS transport by advection. The largest TDS differences occur in the west-central portion of the basin where high-volume groundwater withdrawals are focused in the baseline at a rate of 38,063 AFY, but are significantly reduced to a rate of 14,011 AFA in scenario 6.2.

The largest area of TDS change is in the shallow TDS zone where most groundwater pumping takes place and where evapotranspiration increases salinity through concentration. These areas are shown in yellow for both models in Figure 44 and generally correspond to the region of highest hydraulic conductivity in model layer 1 as shown in Figure 14. The higher conductivity allows greater groundwater velocities relative to other areas in response to the high pumping rates in the central-west portion of the basin, drawing groundwater of higher salinity in the direction of the pumping centers. The area of largest TDS change is larger in the baseline model because the pumping rates are substantially higher than in scenario 6.2, which drives increased movement of salinity. In deeper zones, even low velocity groundwater movement can cause high rates of TDS change owing to the much higher salinity. Overall, however, simulated TDS concentrations change very little over the predictive time period.

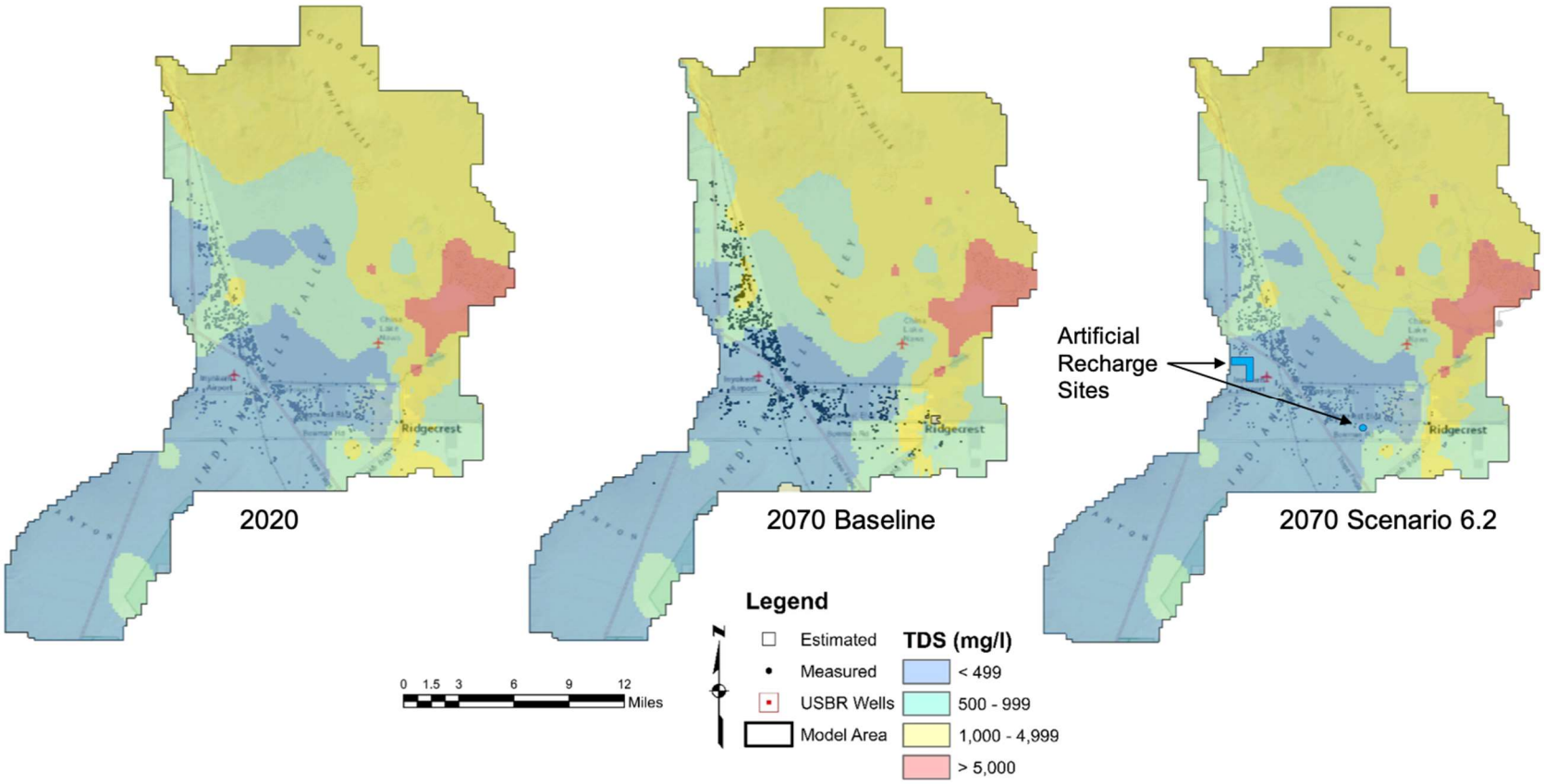

Figure 43. Comparison of the spatial distributions of simulated TDS concentration in the shallow TDS zone in the year 2020 (left), and the year 2070 for the baseline model (center) and the scenario 6.2 model (right).

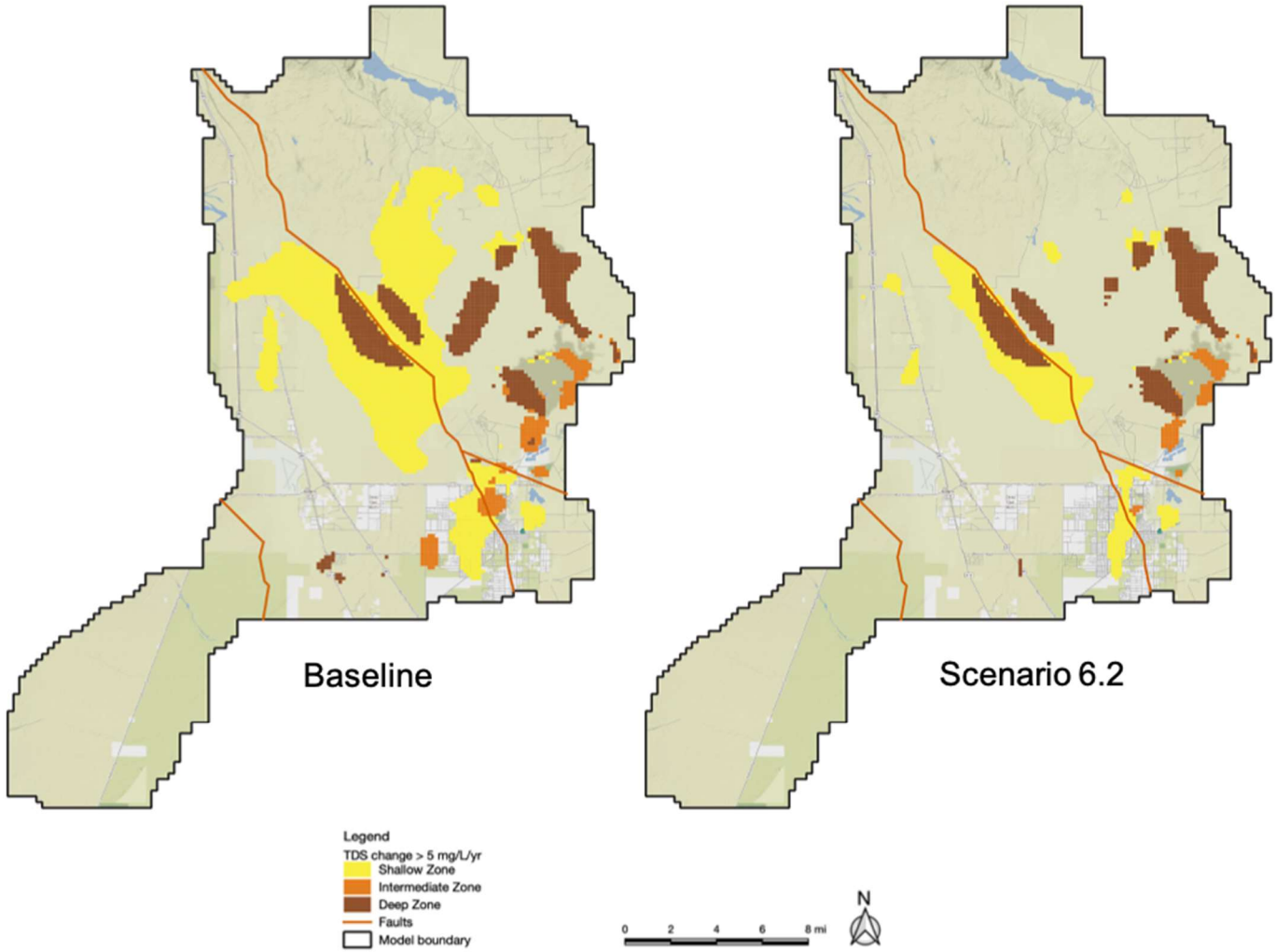

Figure 44. Areas where the forecasted annual rate of change in TDS concentration exceeds 5 mg/L/yr for the years 2020 to 2070 for the baseline model (left) and scenario 6.2 model (right). The areas for all three TDS Zones are superimposed. Refer to Figure 3 for the names of the fault segments.

4. Model Limitations

Though the Indian Wells Valley GSP model has been shown to be a reasonable representation of the conceptualization of the groundwater flow system and honors available local data, the model has limitations, including:

1. Evapotranspiration is not directly measured in the basin, and currently can only be quantified as a component of the simulated groundwater volumetric balance. In any case, the simulated ET is well characterized and shows good agreement with the results of the EVI approach.
2. The model is currently not designed to simulate the physical processes of artificial recharge from infiltration basins, instead the imported water was added directly to the saturated zone. The infiltration process can be incorporated in the model using field measurements of infiltration, soil properties, and climate data.
3. The transport model was designed to investigate how the distribution of salinity within the groundwater system may be influenced by alternative scenarios for groundwater management. Owing to limitations in the TDS dataset and the overall scale of the model, the transport model was not designed for use as a predictor of TDS concentrations at the local scale.

References

Anderson, M. P., Woessner, W. W., and Hunt R. J., 2015. Applied Groundwater Modeling, Second Edition: Simulation of Flow and Advective Transport, Elsevier, New York, 564p.

Bullard, T. F., Bacon, S. N., Adams, K. D., and Decker, D. L., 2019. Geomorphic map of China Lake basin below 700 m elevation in Support of Cultural Resource Management at Naval Air Weapons Station China Lake, prepared by Desert Research Institute for Naval Air Warfare Center Weapons Division, China Lake, California.

Lancaster, N. L., Bacon, S. N., Bullard, T. F., Baker, S. E. and Decker, D. L., 2019. Eolian Hazard Assessment for the SNORT Facility, prepared by Desert Research Institute for Naval Air Warfare Center Weapons Division, China Lake, California.

Banta, E. R., 2000. MODFLOW-2000, The U.S. Geological Survey Modular Ground- Water Model—Documentation of Packages for Simulating Evapotranspiration with a Segmented Function (ETS1) and Drains with Return Flow (DRT1). U.S. Geological Survey Open-File Report 00-466.

Beamer, J. P., Huntington, J. L., Morton, C. G., and Pohll, G. M., 2013. Estimating Annual Groundwater Evapotranspiration from Phreatophytes in the Great Basin Using LANDSAT and Flux Tower Measurements. *Journal of the American Water Resources Association*, 49(3):518-533.

Bean, R.T., 1989. Hydrogeologic Conditions in Indian Wells Valley and Vicinity, Prepared for California Department of Water Resources, 56p.

Berenbrock, C., 1987, Ground-water data for Indian Wells Valley, Kern, Inyo, and San Bernardino Counties, California, 1977-84. U.S. Geological Survey Open-File Report 86-315, 56 p.

Berenbrock, C. and Martin, P., 1991. The Ground-Water Flow System in Indian Wells Valley, Kern, Inyo, and San Bernardino Counties, California. U.S. Geological Survey Water-Resources Investigations Report 89-4191.

Berenbrock, C., and Schroeder, R. A., 1994. Ground-Water Flow and Quality, and Geochemical Processes, in Indian Wells Valley, Kern, Inyo, and San Bernardino Counties, California, 1987-88. U.S. Geological Survey, Water-Resources Investigations Report 93-4003.

Brown and Caldwell, 2009. Indian Wells Valley Basin Groundwater Model and Hydrogeologic Study, Final report. Prepared for Indian Wells Valley Water District, Ridgecrest, California.

Bullard, T. F., Bacon, S. N., Adams, K. D., and Decker, D. L., 2015. Phase II: Geomorphic Map of the China lake Basin below 700 m in Support of cultural Resource Management at NAWS China Lake. Report prepared by Desert Research Institute for Naval Air Warfare Center, Weapons Division, NAWS China Lake, CA, March 2015. DRI Division of Hydrologic Sciences, NESEP Publication No. 50011, 58 p. + 2 appendices and map.

California Water Boards, Groundwater Ambient Monitoring and Assessment Program (GAMA). https://geotracker.waterboards.ca.gov/gama/gamamap/public/ accessed November 2018.

Danskin, W.R., 1998. Evaluation of the hydrologic system and selected water-management alternatives in the Owens Valley, California, U.S. Geological Survey Water Supply Paper 2370-H.

Doherty, J. E. and Hunt, R. J., 2010. Approaches to highly parameterized inversion---A guide to using PEST for groundwater-model calibration. U.S. Geological Survey Scientific Investigations Report 2010-5169.

Dullien, F.A.L., 1992. Porous Media: Fluid Transport and Pore Structure, Academic, San Diego.

Gelhar, L. W., Welty, C., and Rehfeldt, K. R., 1992. A critical review of data on field-scale dispersion in aquifers. *Water Resources Research*, 28(7):1955-1974, doi:/10.1029/92WR00607.

Garner, C., Bacon, S., Pohll, G., and Chapman, J., 2017. Indian Wells Valley Groundwater Model Update. Desert Research Institute Technical Memorandum.

Güler, C. and Thyne, G. D., 2004. Hydrologic and geologic factors controlling surface and groundwater chemistry in Indian Wells-Owens Valley area, southeastern California, USA. *Journal of Hydrology*, 285(1):177--198, doi:/10.1016/j.jhydrol.2003.08.019.

Harbaugh, A. W., 2005. MODFLOW-2005: the U.S. Geological Survey modular ground-water model--the ground-water flow process. U.S. Geological Survey Techniques and Methods 6-A16.

Kern County Water Agency, Base WQ spreadsheet. Received by Stetson Engineers Dec. 17, 2018 from Michelle Anderson.

Krieger & Stewart, 2011. 2010 Urban Water Management Plan. Ridgecrest, California. Prepared for Indian Wells Valley Water District, Ridgecrest, California.

Maxey, G. B., 1968. Hydrogeology of Desert Basins. *Ground Water*, 6(5):10-22, doi:/10.1111/j.1745-6584.1968.tb01660.x.

McGraw, D., Carroll, R., Pohll, G., Chapman, J., Bacon, S., and Jasoni, R., 2016. Groundwater Resource Sustainability: Modeling Evaluation for the Naval Air Weapons Station, China Lake. California. prepared by Desert Research Institute for the Naval Air Warfare Center Weapons Division, Final Evaluation Report NAWCWD TP 8811.

Menke, J., Reyes, E., Glass, A., Johnson, D., and Reyes, J., 2013. 2013 California Vegetation Map in Support of the Desert Renewable Energy Conservation Plan. Final Report. Prepared for the California Department of Fish and Wildlife Renewable Energy Program and the California Energy Commission. Aerial Information Systems, Inc., Redlands, CA.

Moyle, W.R., Jr., 1963. Data on water wells in Indian Wells Valley area, Inyo, Kern, and San Bernardino Counties, California. California Department of Water Resources Bulletin 91-9, 243 p.

Niswonger, R. G., Sorab, P., and Motomu, I., 2011. MODFLOW-NWT, A Newton formulation for MODFLOW-2005. U.S. Geological Survey Techniques and Methods 6-A37, 44 p.

Stephens, D.B, K. Hsu, M.A. Prieksat, M.D. Ankeny, N. Blandford, T.L. Roth, J.A. Kelsey, and J.R. Whitworth, 1998. A comparison of estimated and calculated effective porosity, Hydrogeology Journal, 6, pp. 156-165.

Stetson Engineers, 2018. Notes on Determination of Balanced Hydrologic Period and Model Recharge Distribution. Memo to Greg Pohll, Desert Research Institute, December 12, 2018.

Thyne, G.D., Gillespe, J.M., and Ostdick, J.R., 1999. Evidence for interbasin flow through bedrock in the southeastern Sierra Nevada. Geological Society of America Bull. 111 (11): pp. 1600-1616.

Todd Engineers, 2014. Indian Wells Valley Resource Opportunity Plan - Water Availability and Conservation Report, prepared for Kern County Planning & Community Development Department.

TriEcoTt, Joint Venture, 2012. Technical Justification for Beneficial Use Changes for Groundwater in Salt Wells Valley and Shallow Groundwater in Eastern Indian Wells Valley. Prepared for Department of the Navy, Naval Facilities Engineering Command Southwest, San Diego, California.

U.S. Bureau of Reclamation, 1993. Indian Wells Valley Groundwater Project: USBR Technical Report Volumes I and II.

Zheng, C. and Wang, P. P., 1999. MT3DMS: a modular three-dimensional multispecies transport model for simulation of advection, dispersion, and chemical reactions of contaminants in groundwater systems: documentation and user's guide. Prepared for U.S. Army Corps of Engineers, Strategic Environmental Research and Development Program Contract Report SERDP-99-1.

Attachment A. Plots of Simulated and Measured Groundwater Level Hydrographs for Calibration of the Transient-Historical Model

The MATLAB robust regression slope-fitting function *robustfit* was used to automatically identify and remove observation outliers and compute the regression slopes for observed and simulated water level trends at the 36 observation locations in the transient-historical model. Observations from the years 1994 through 2016 were chosen for this analysis because sufficient data were available during this period in all wells except well 25S40E08A01. Manual screening was performed prior to the regression analysis to remove observations earlier than 1994 (except well 25S40E08A01) and observations that were clearly related to pumping activities in nearby wells (post-2012 in well 26S39E20L and Fall 1996 through Spring 2003 in well 26S39E13R03).

The title of each plot in this appendix provides the California State Well Number and gives the slopes of the regression lines for the observed and simulated water levels and the difference between these slopes.

Red circles represent all observed water levels (Observed).
Orange circles represent observed water levels used in the regression model after outliers were manually removed (ObsRobustIn).
Small black unfilled circles represent observed water levels that were automatically removed during computation of the regression (Obs [w = 0]).
Orange line is the fitted regression line for the observed water levels (ObsRobustLINE).

Blue circles represent water levels simulated by the transient-historical model (Simulated).
Green circles represent simulated water levels used in the regression model (SimRobustIn).
Small black filled circles represent simulated water levels that were automatically removed during computation of the regression (Sim [w = 0]).
Green line is the fitted regression line for the simulated water levels (SimRobLINE).

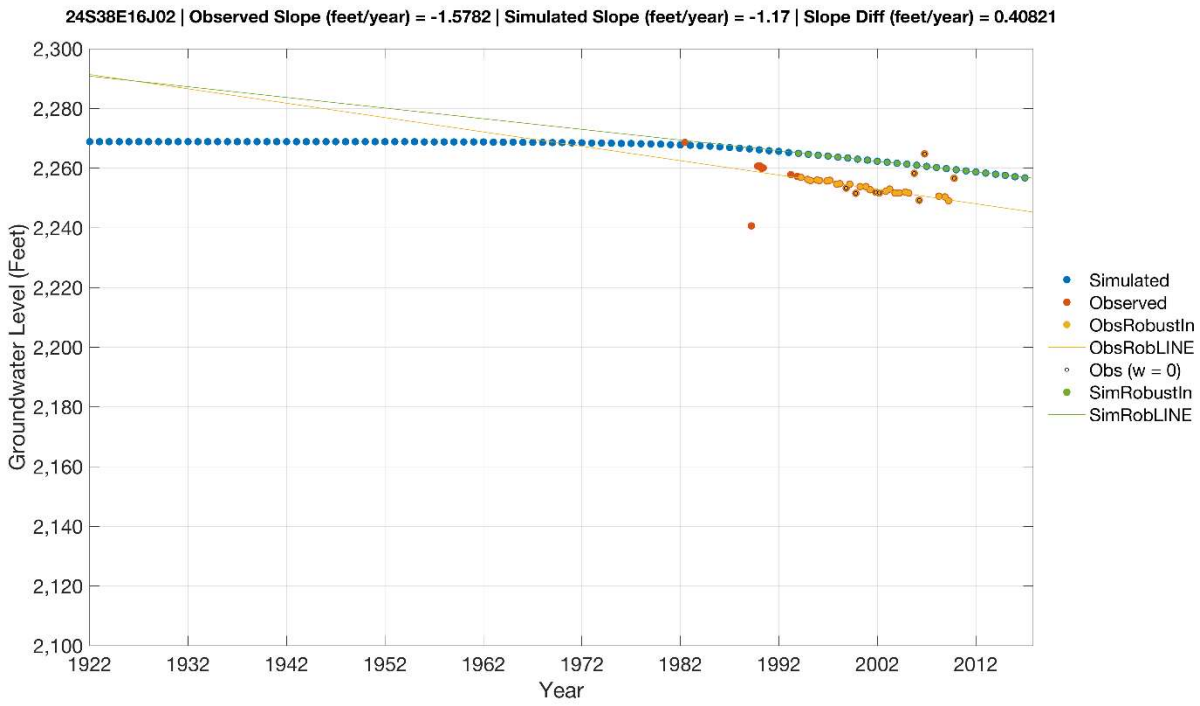

Figure A-1

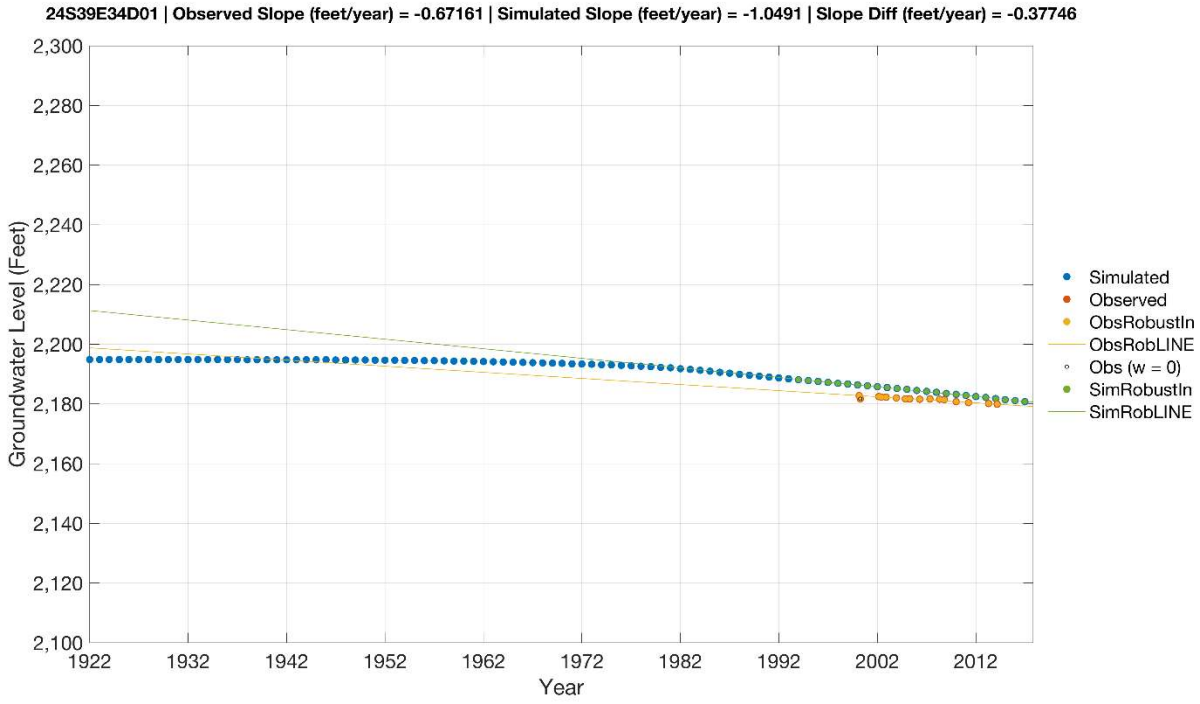

Figure A-2

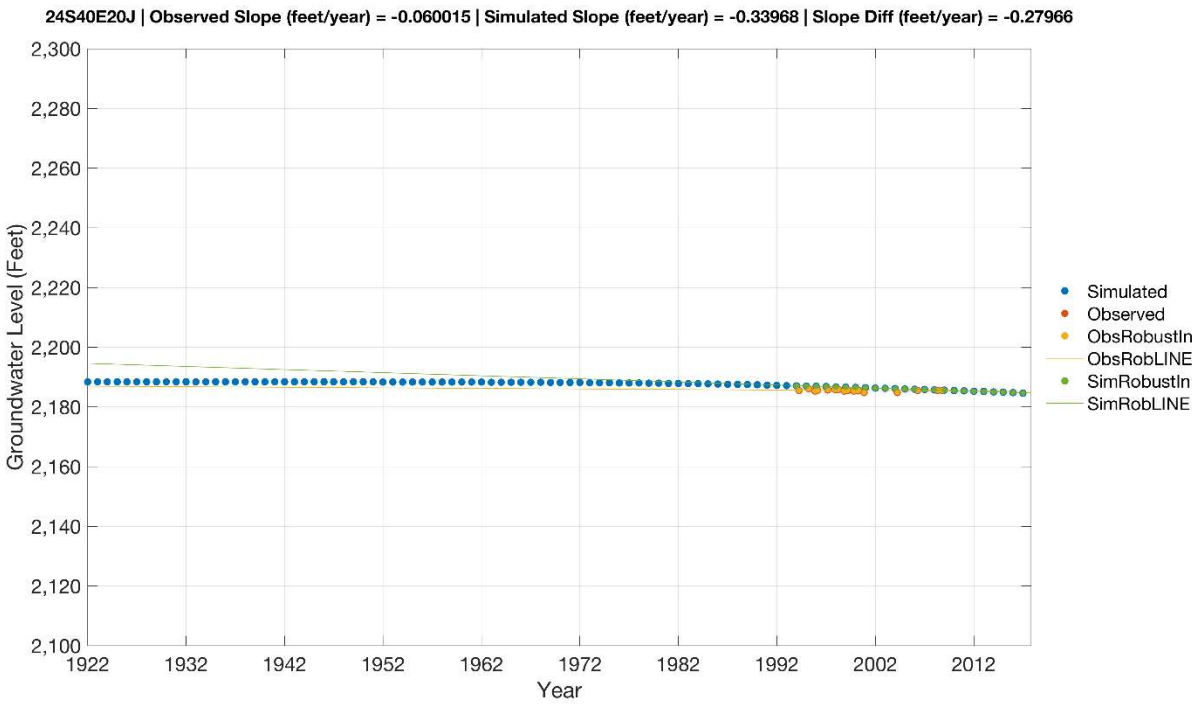

Figure A-3

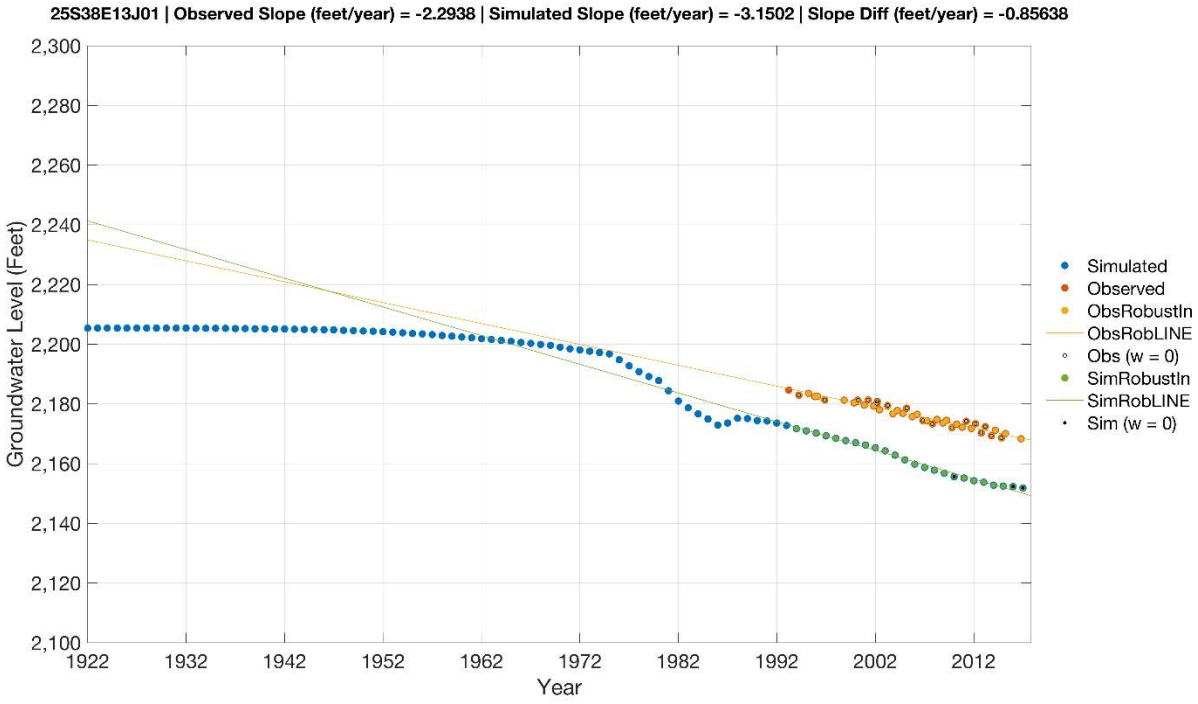

Figure A-4

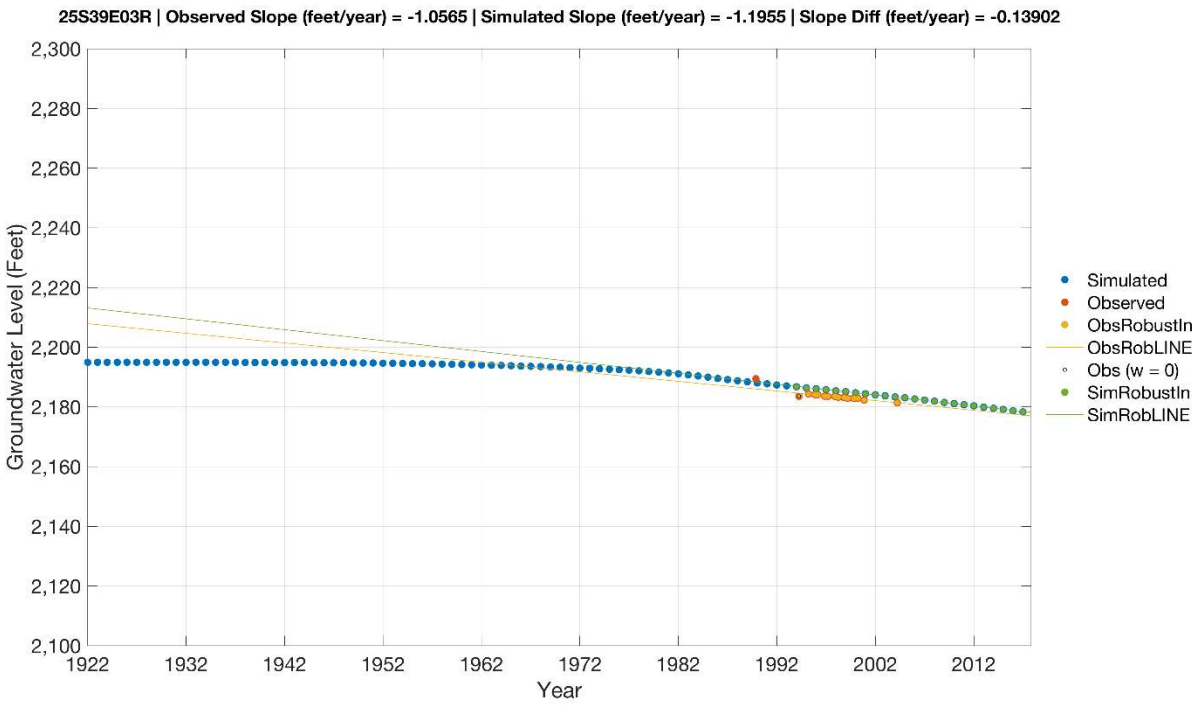

Figure A-5

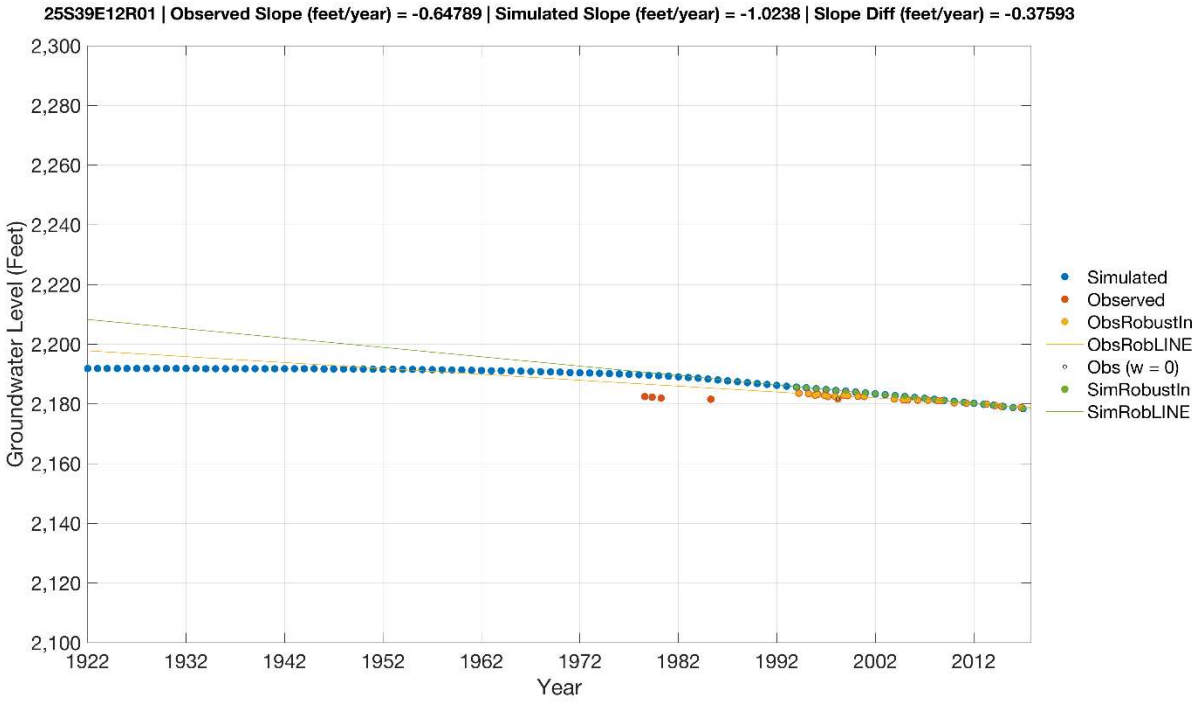

Figure A-6

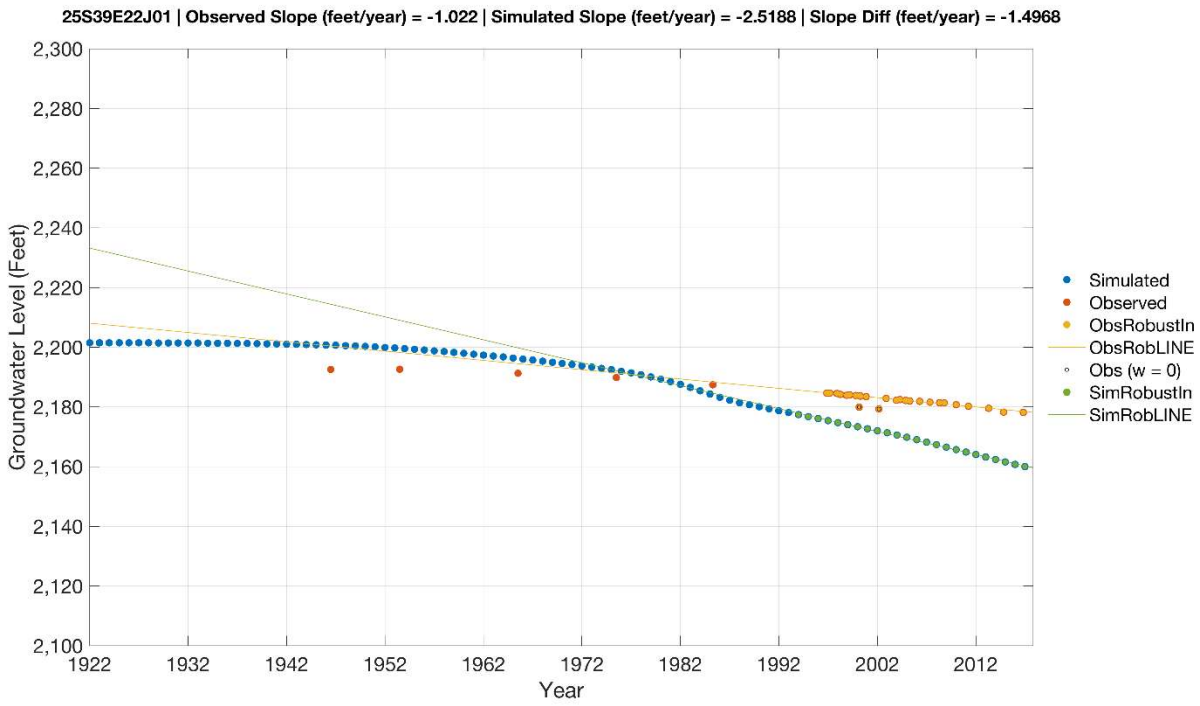

Figure A-7

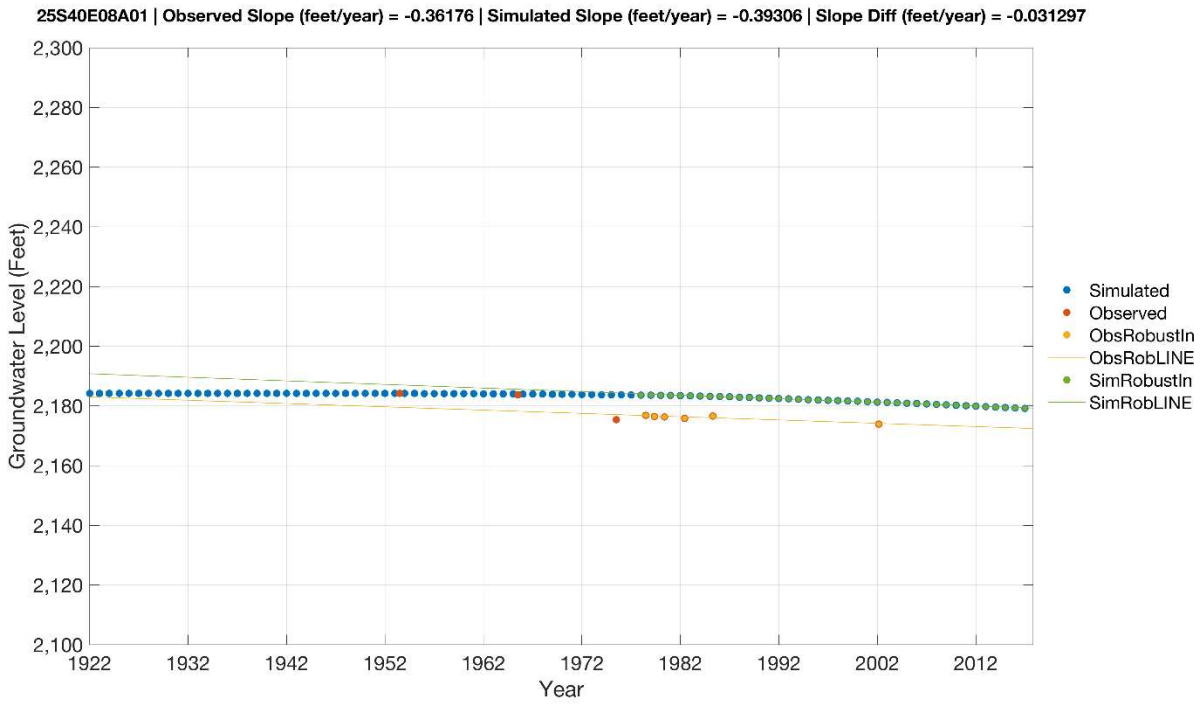

Figure A-8

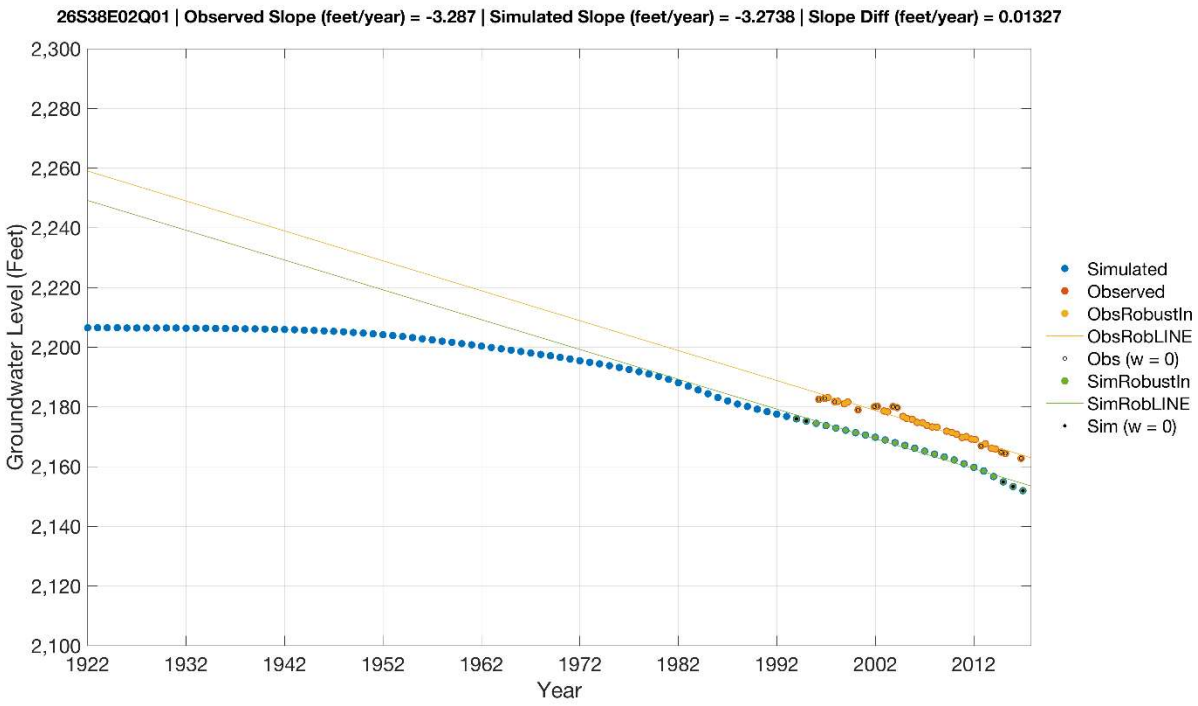

Figure A-9

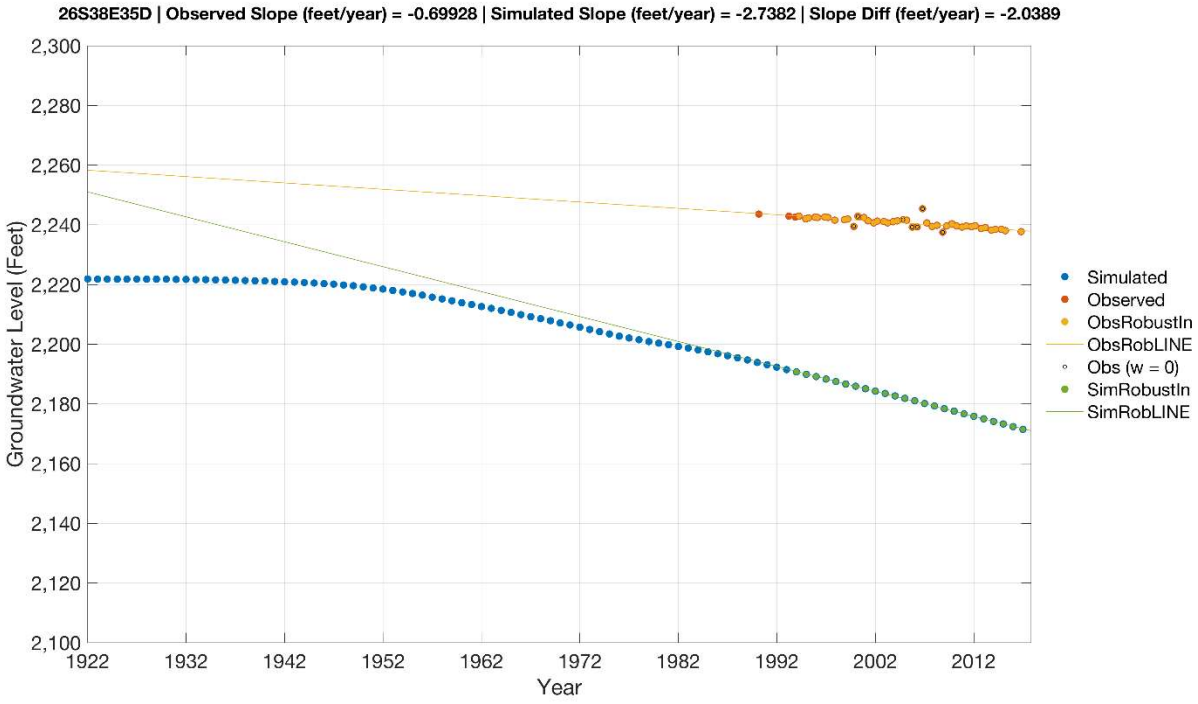

Figure A-10

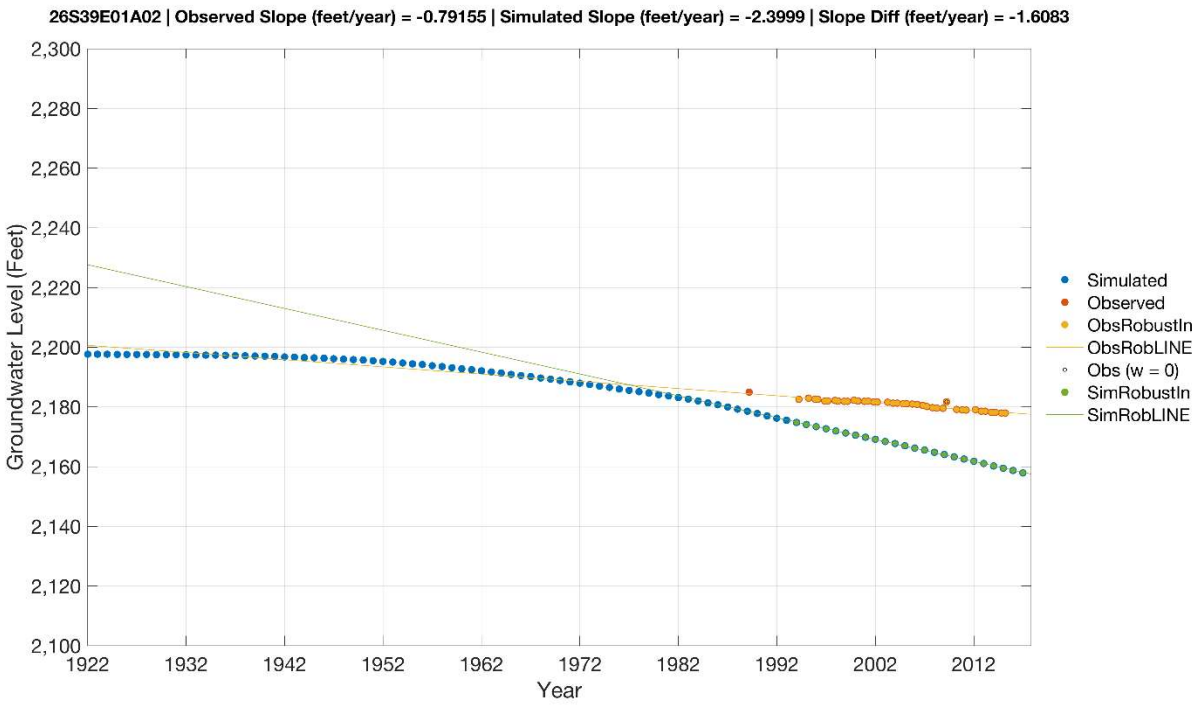

Figure A-11

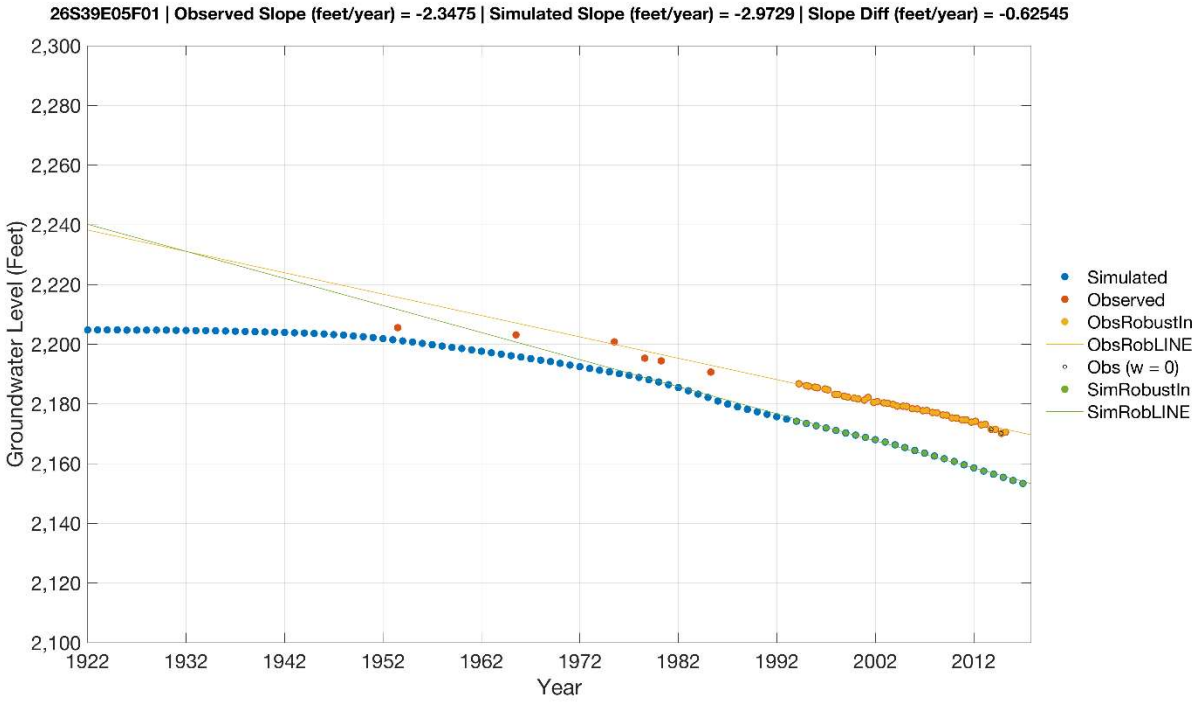

Figure A-12

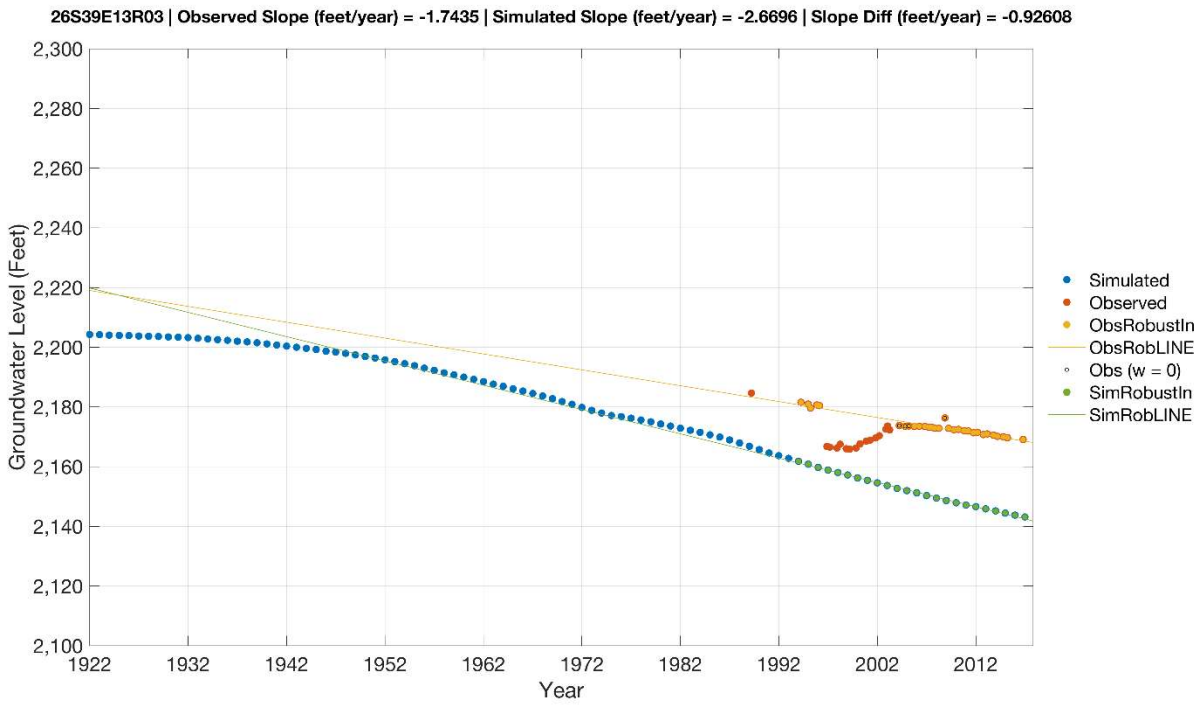

Figure A-13

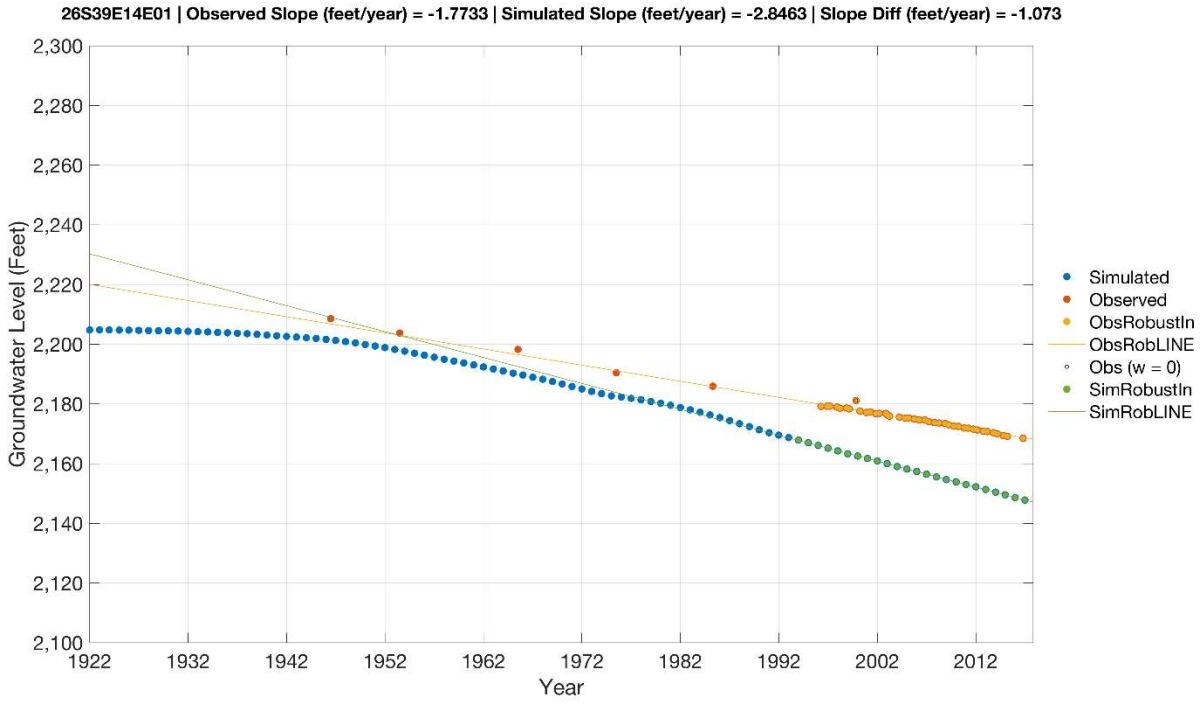

Figure A-14

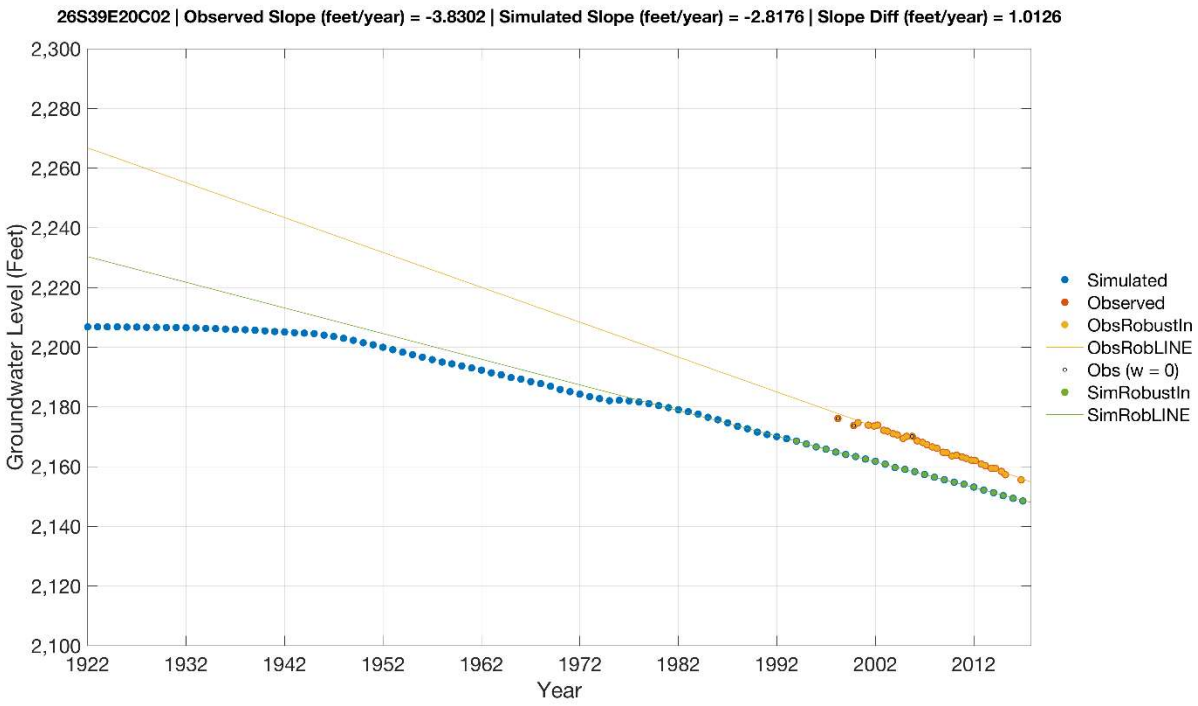

Figure A-15

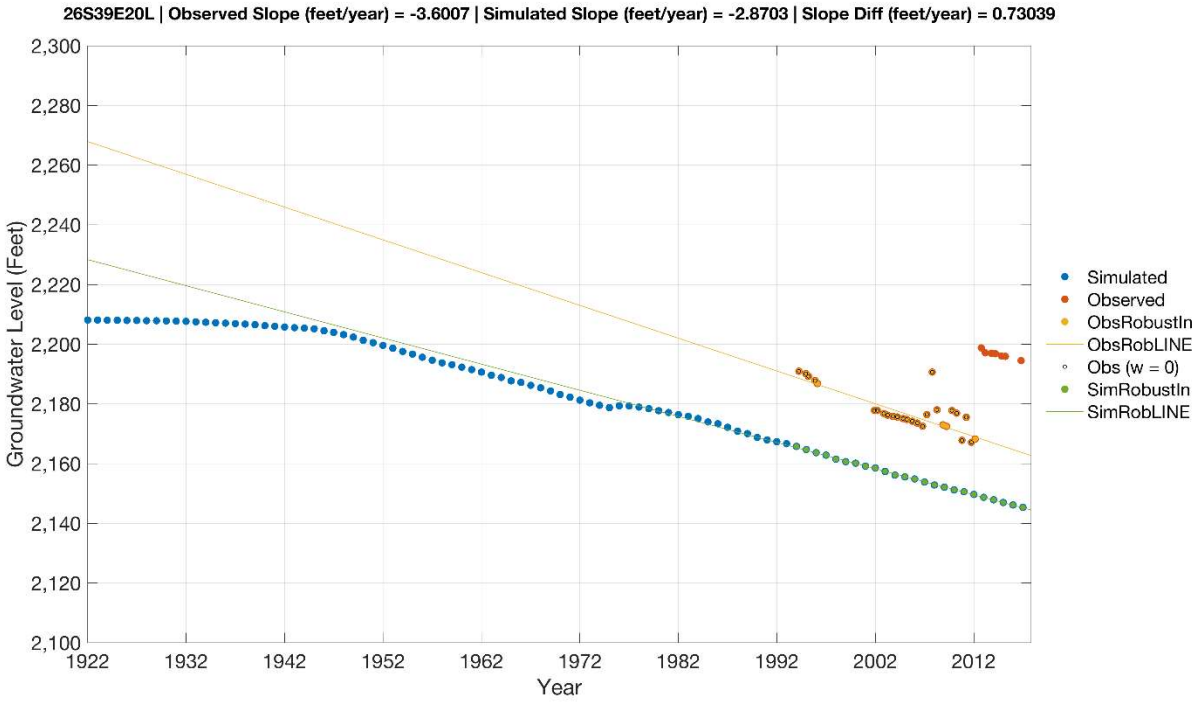

Figure A-16

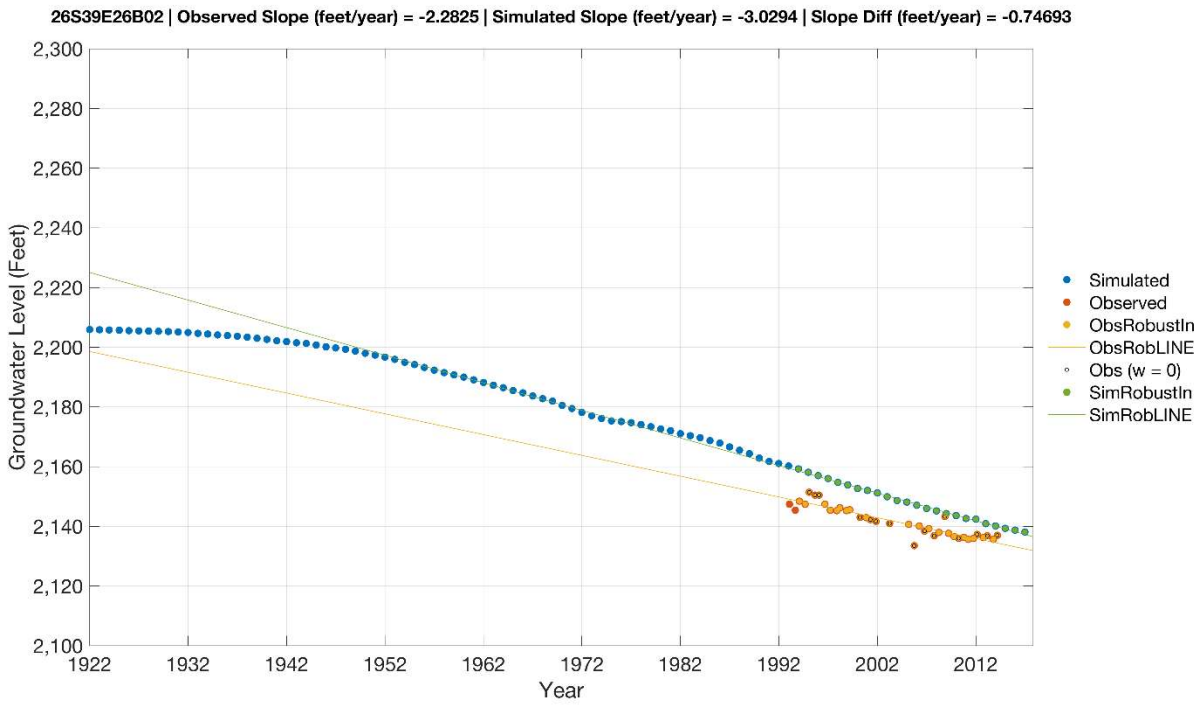

Figure A-17

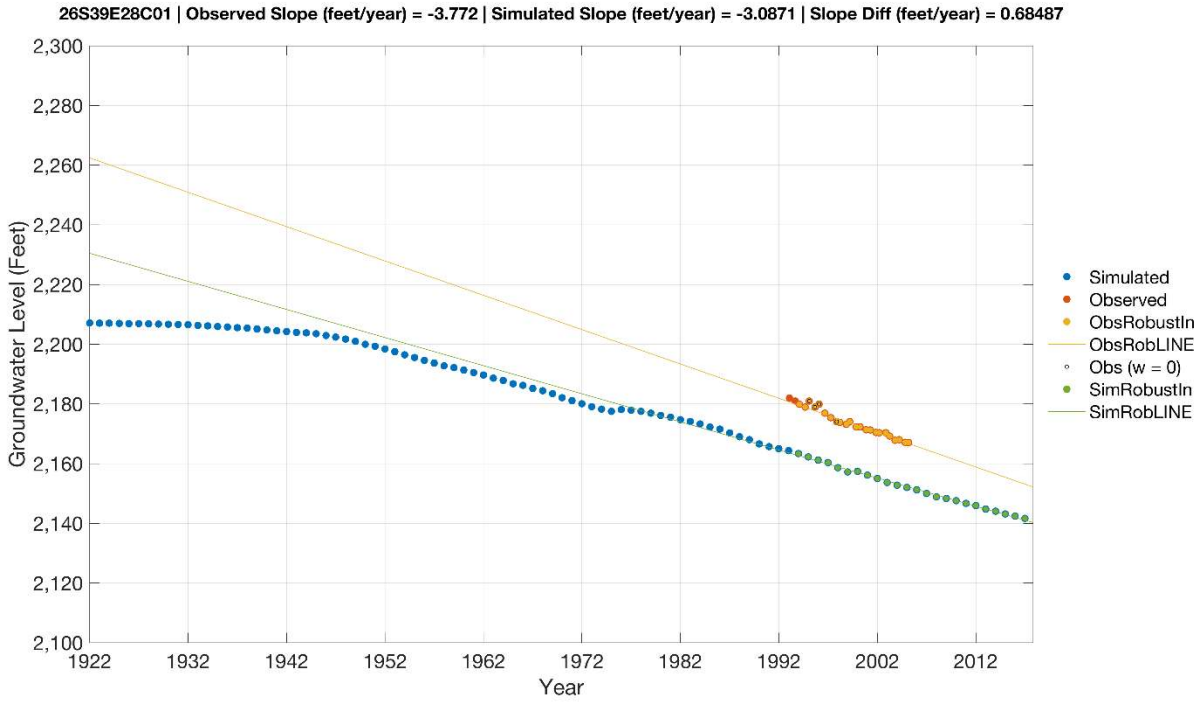

Figure A-18

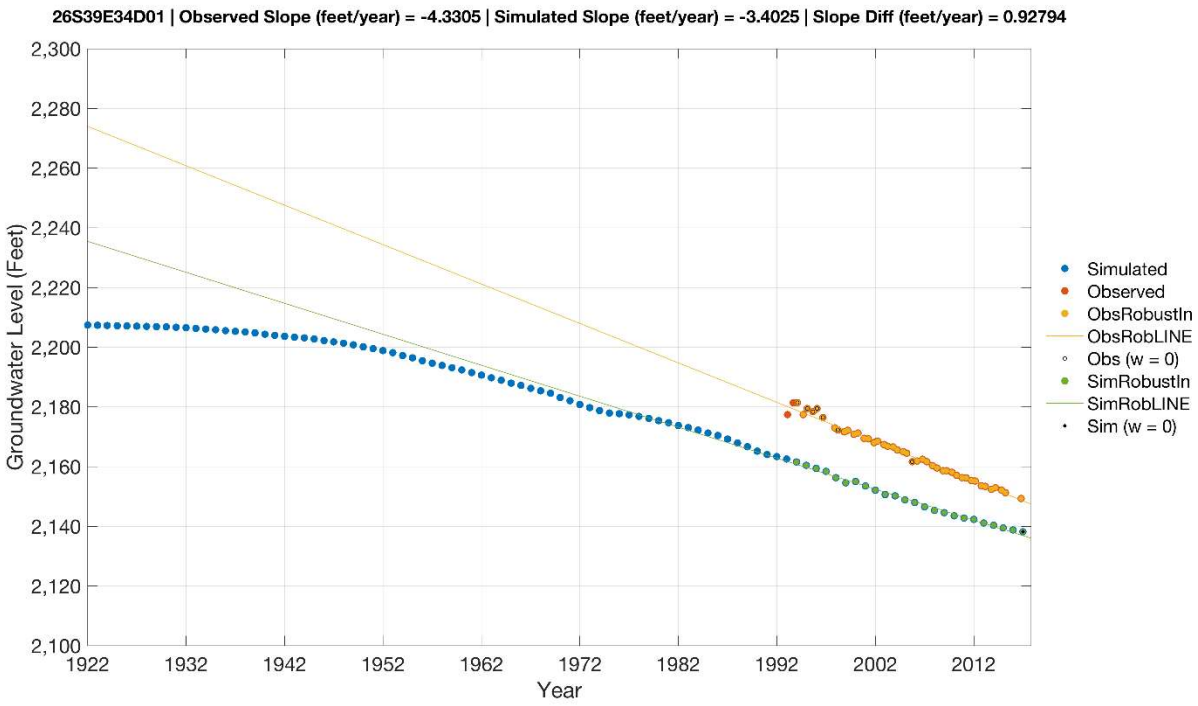

Figure A-19

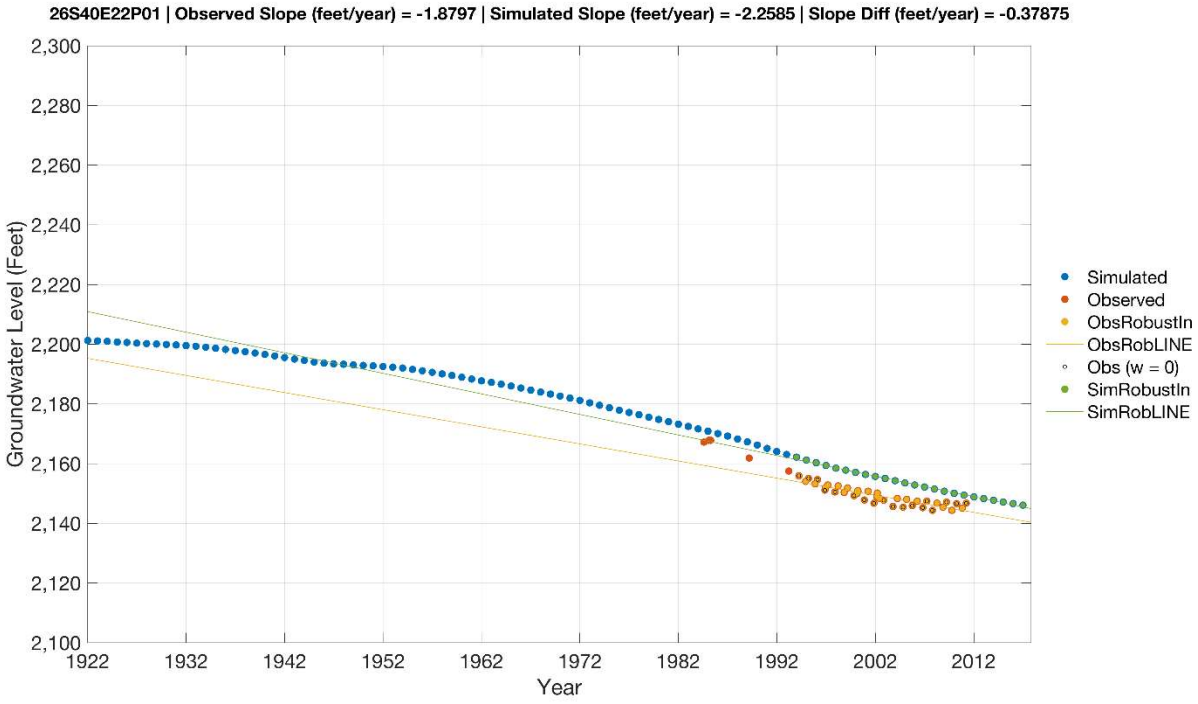

Figure A-20

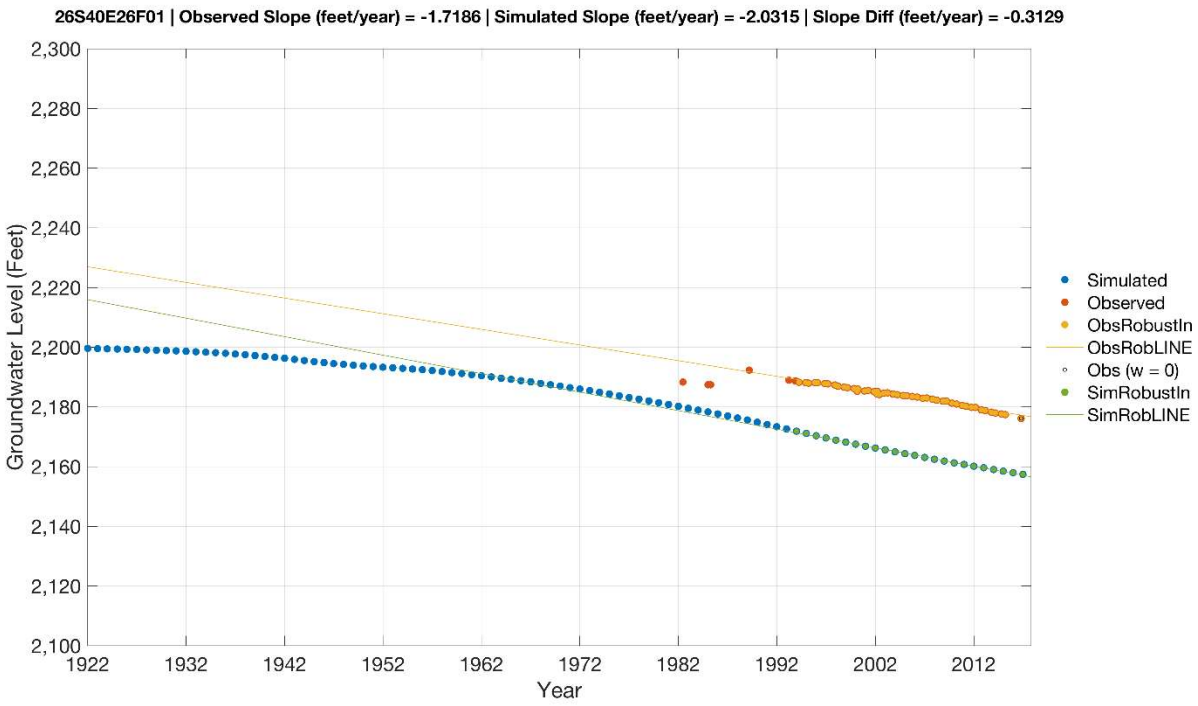

Figure A-21

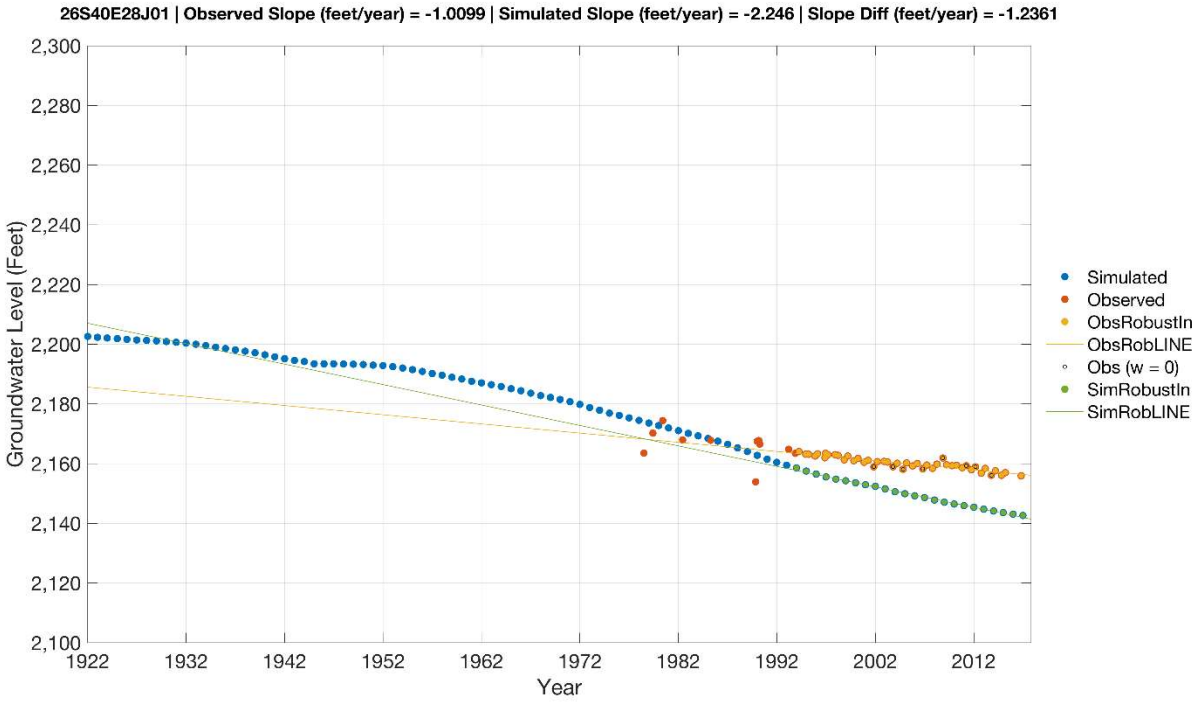

Figure A-22

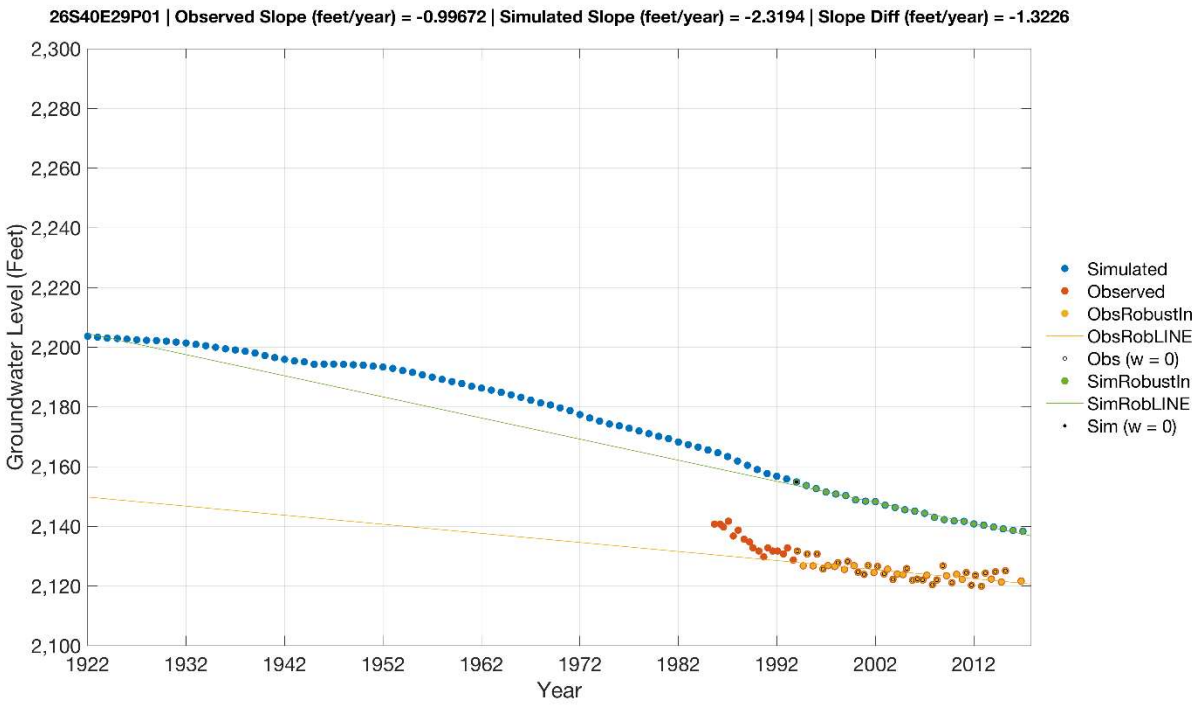

Figure A-23

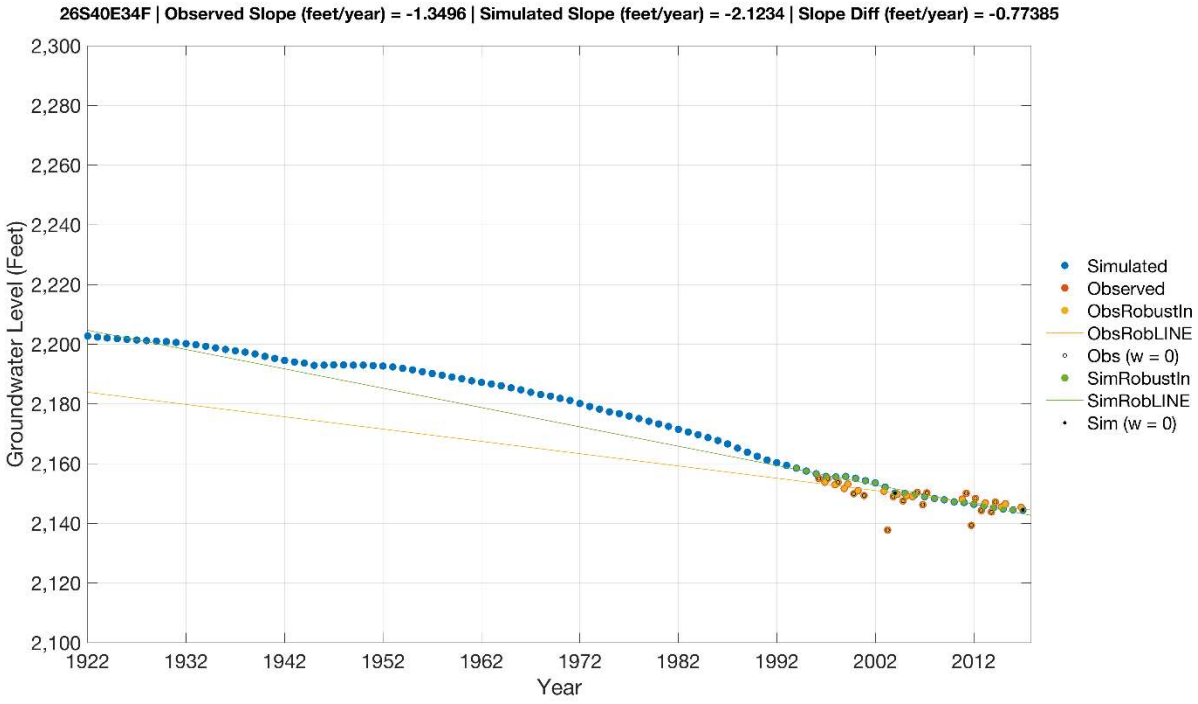

Figure A-24

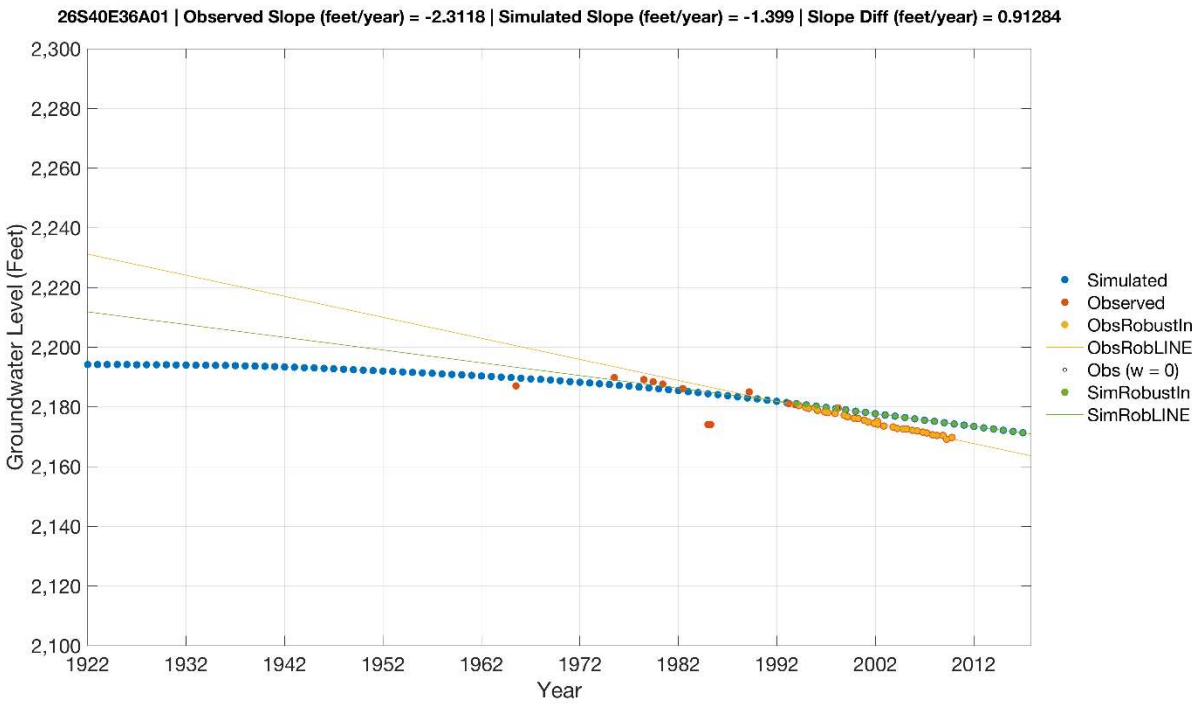

Figure A-25

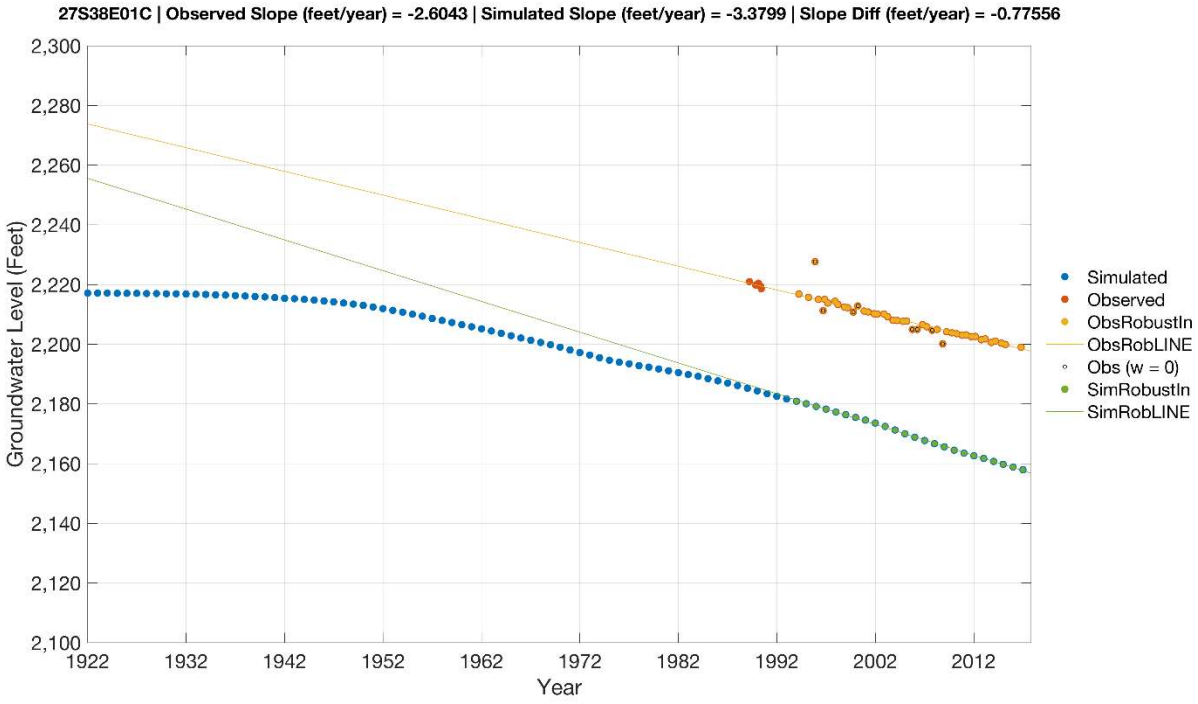

Figure A-26

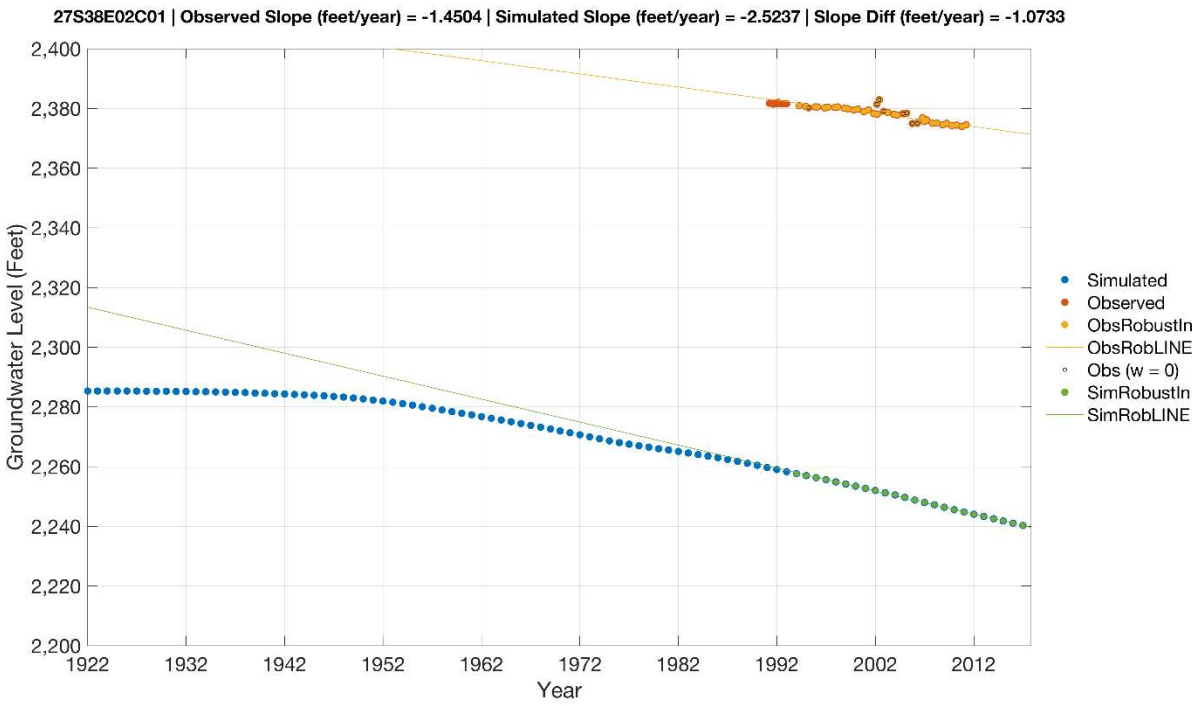

Figure A-27

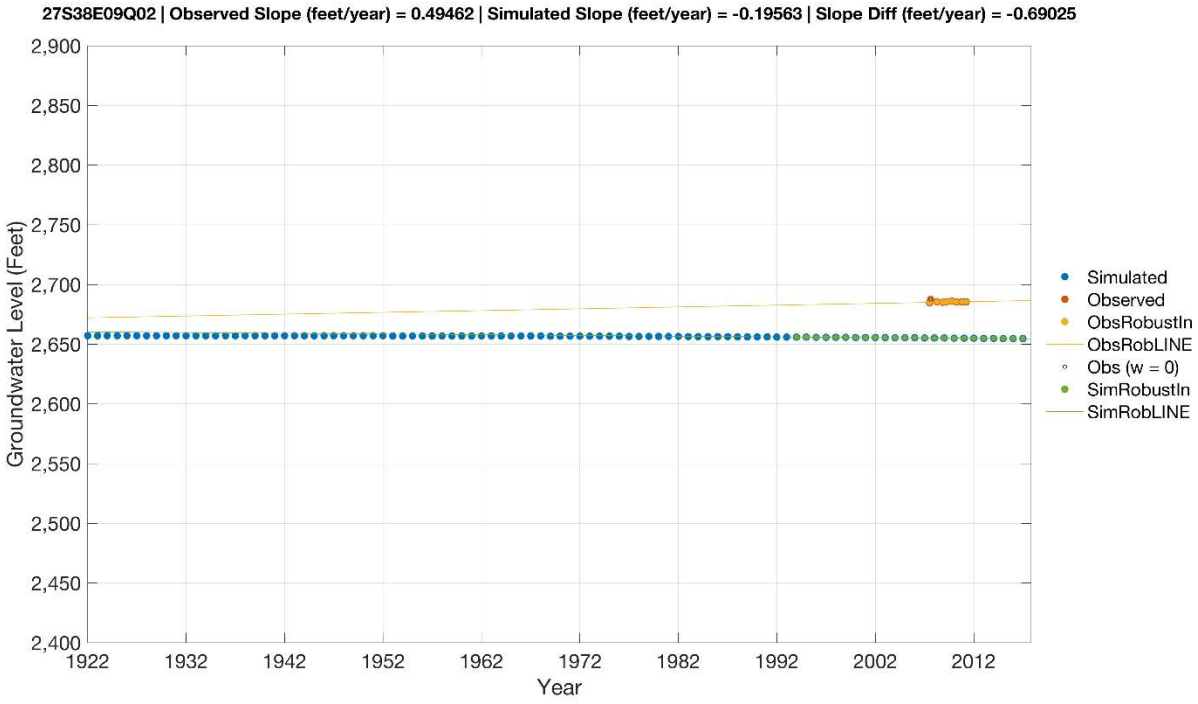

Figure A-28

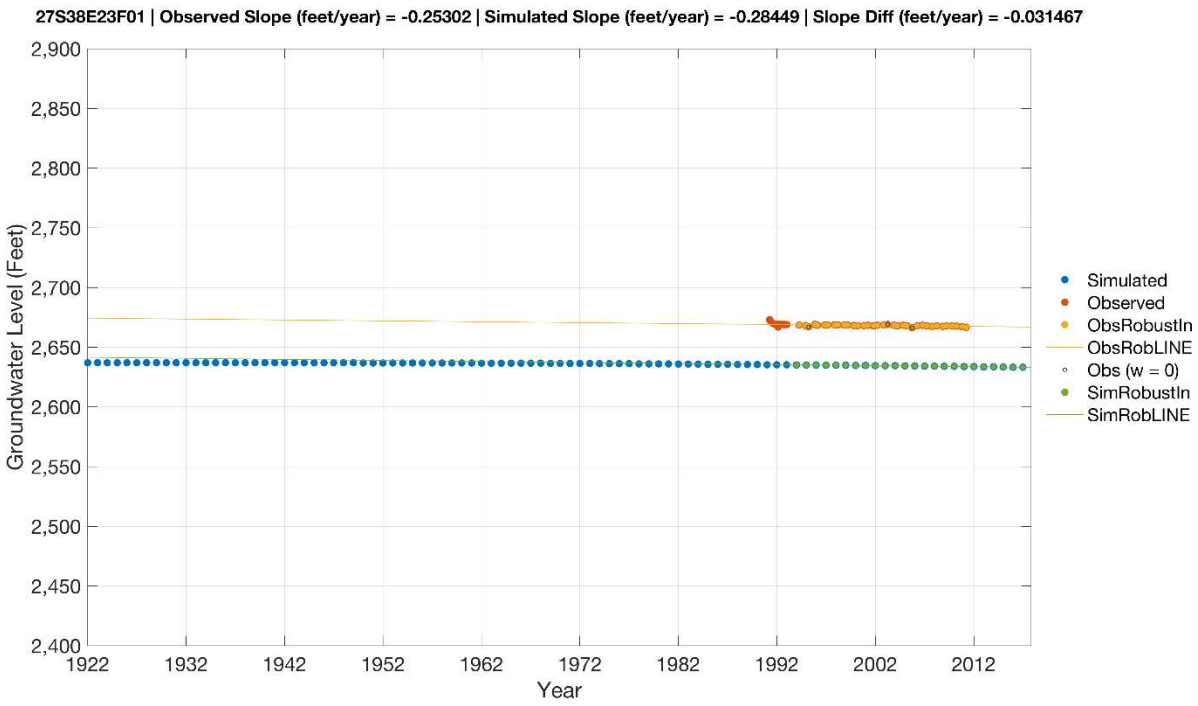

Figure A-29

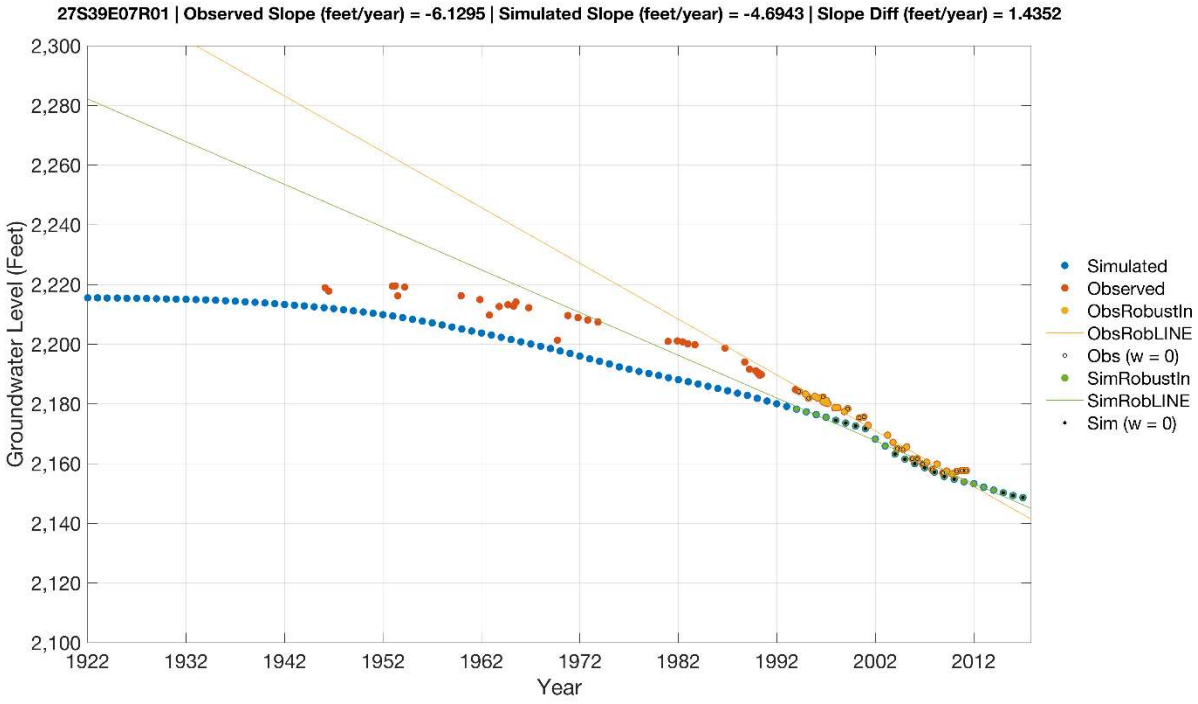

Figure A-30

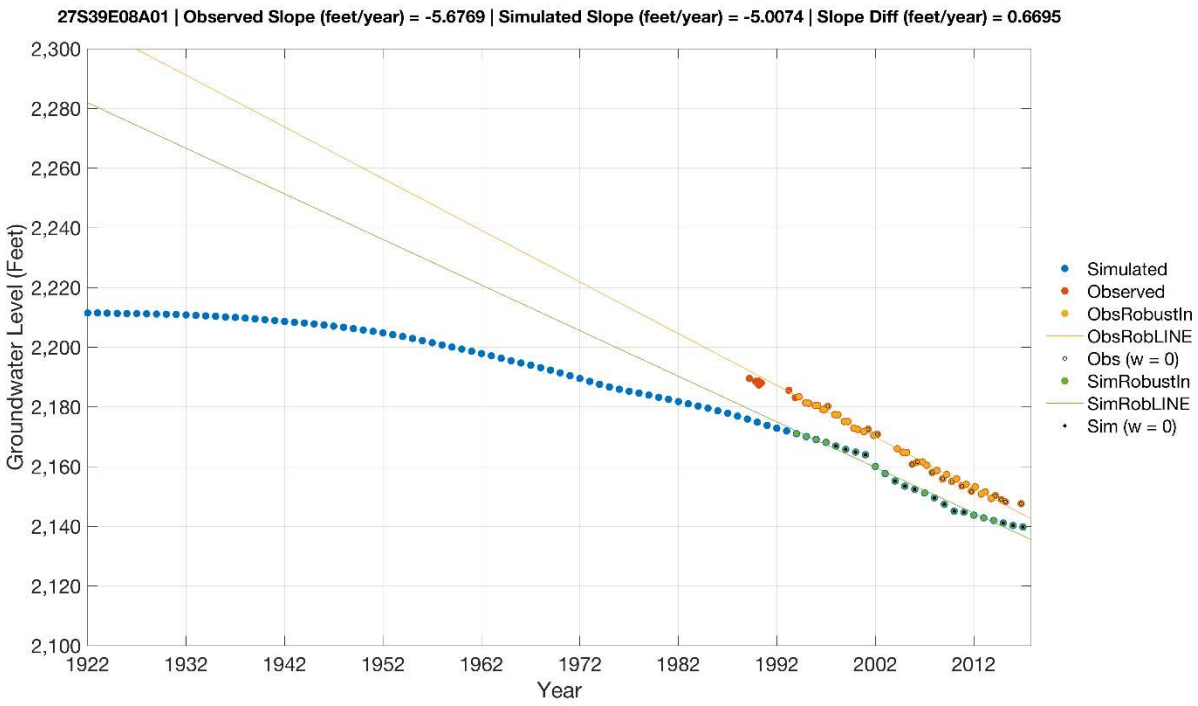

Figure A-31

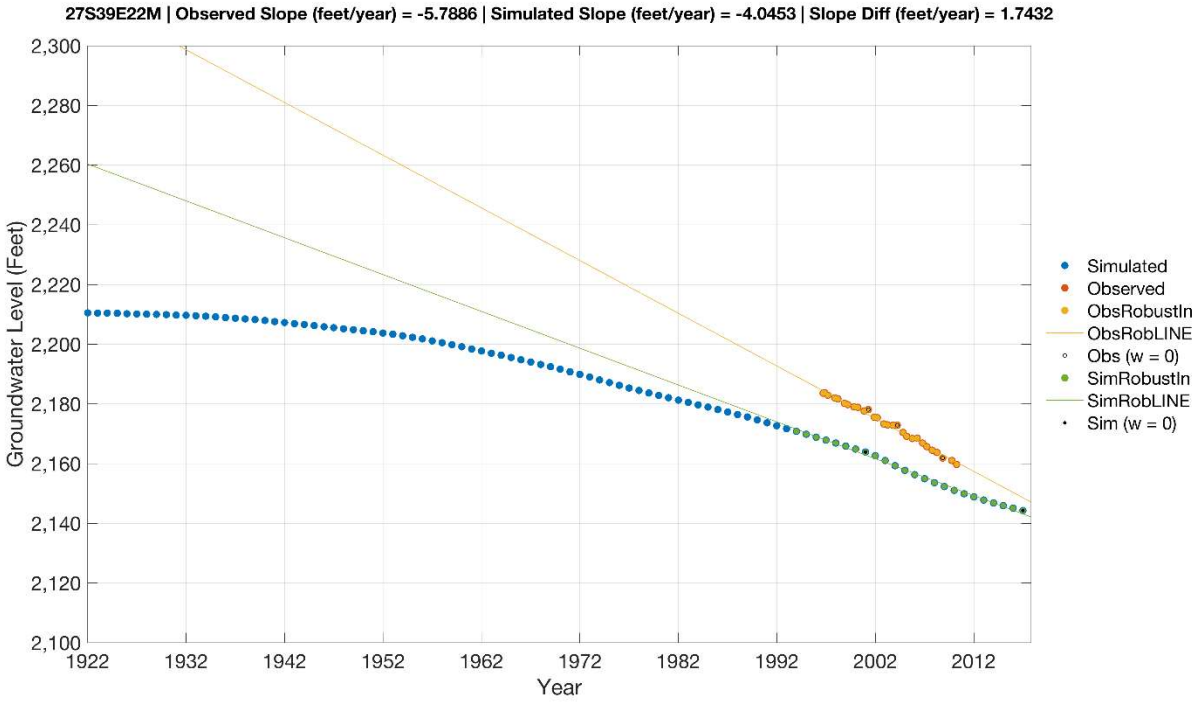

Figure A-32

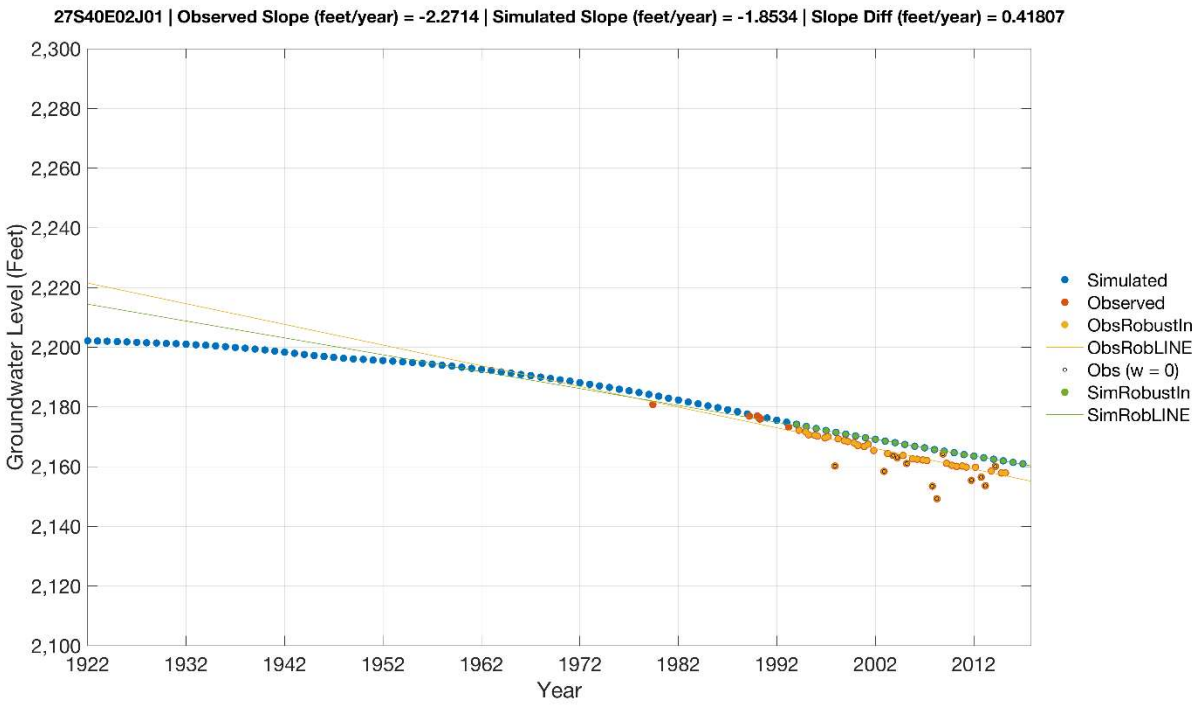

Figure A-33

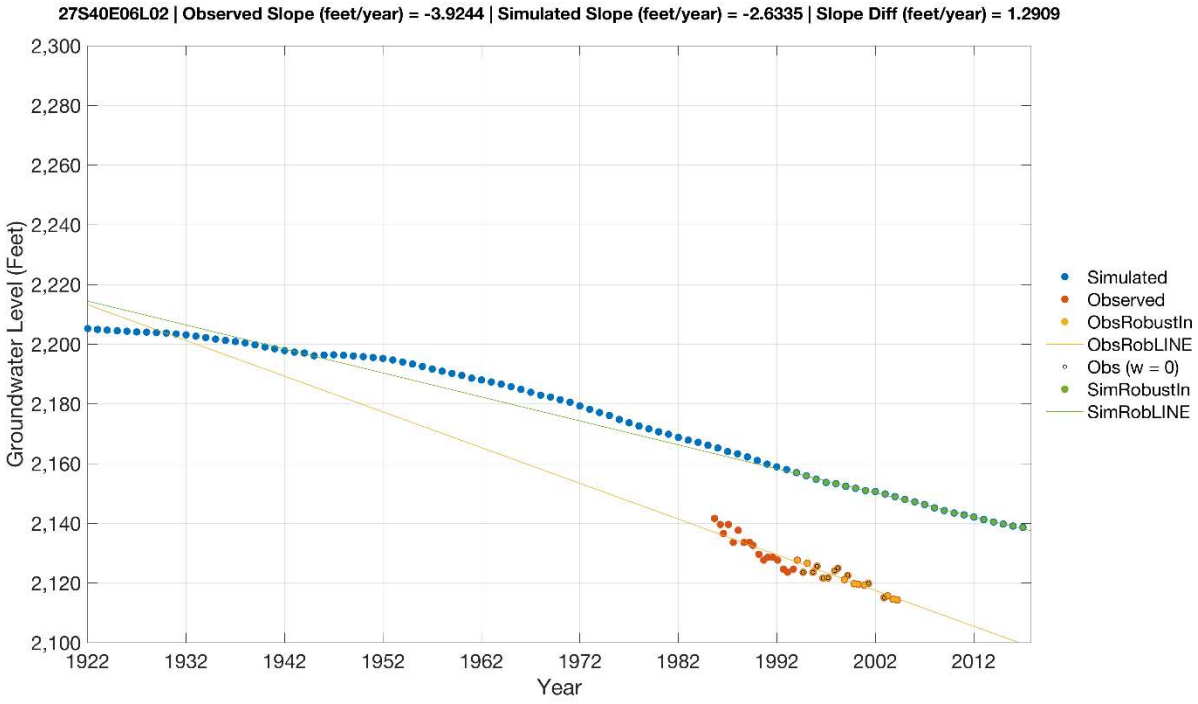

Figure A-34

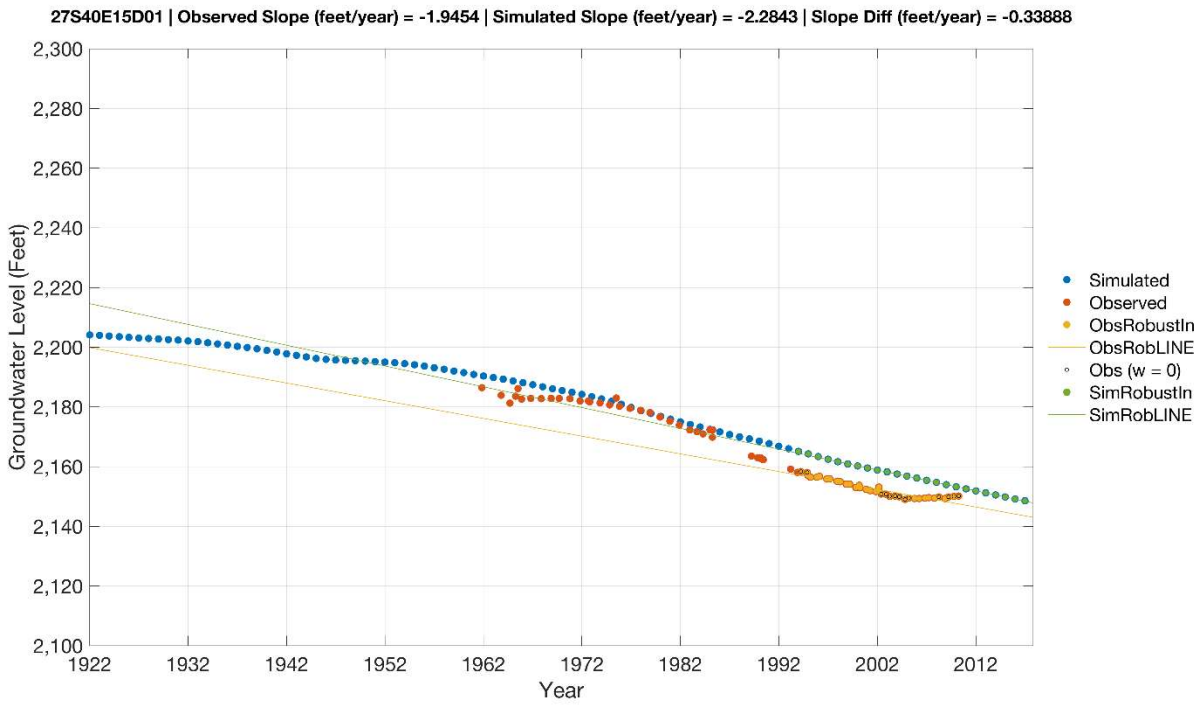

Figure A-35

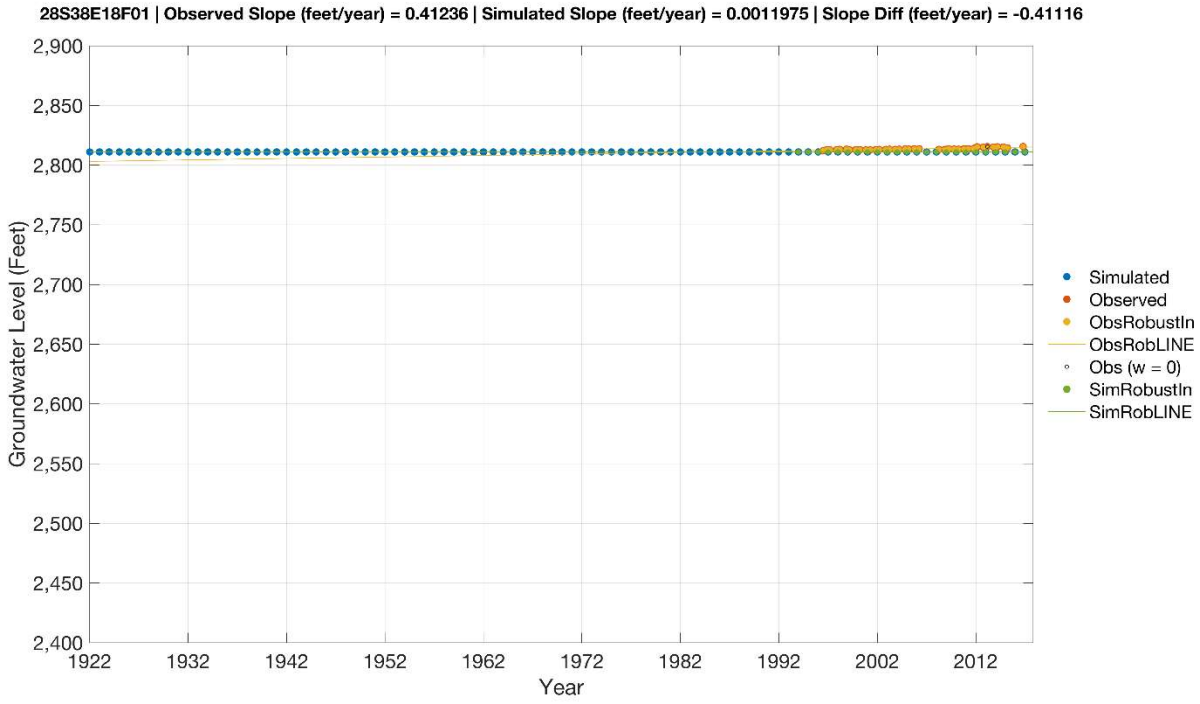

Figure A-36

Indian Wells Valley
Baseline Groundwater Model Results

January 3, 2019

- Model assumptions
- Model results
  - Drawdown
  - Hydrographs by model analysis zone
  - Water budget

Model Assumptions

- Simulation period: 2017 – 2070
- Monthly time steps
- Water level initial condition from historical model
- Variable recharge
- Baseline pumping

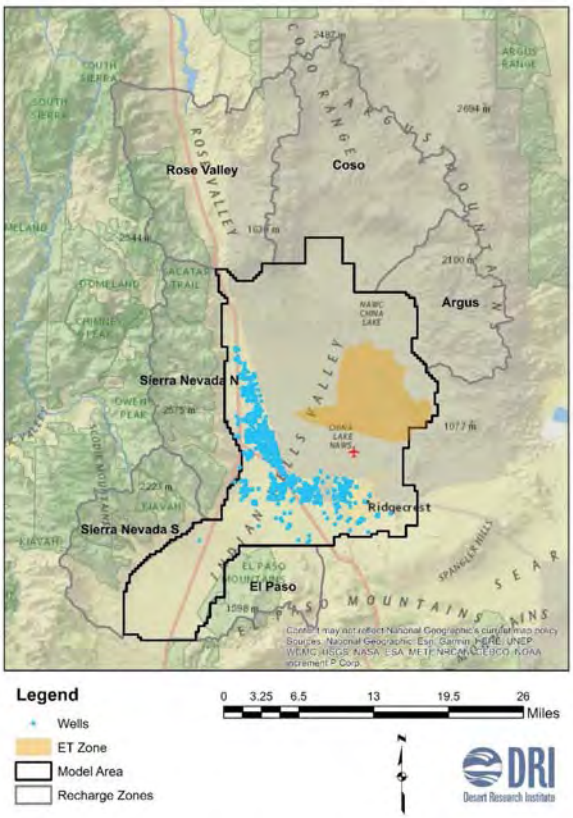

Recharge

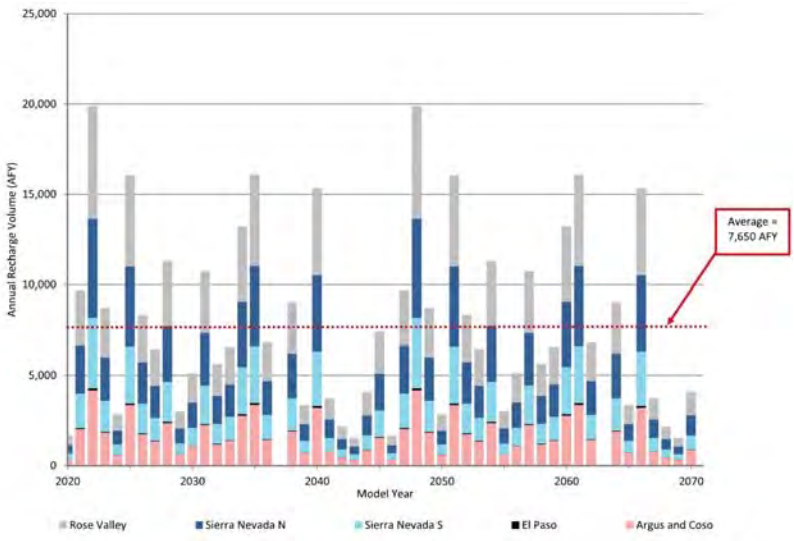

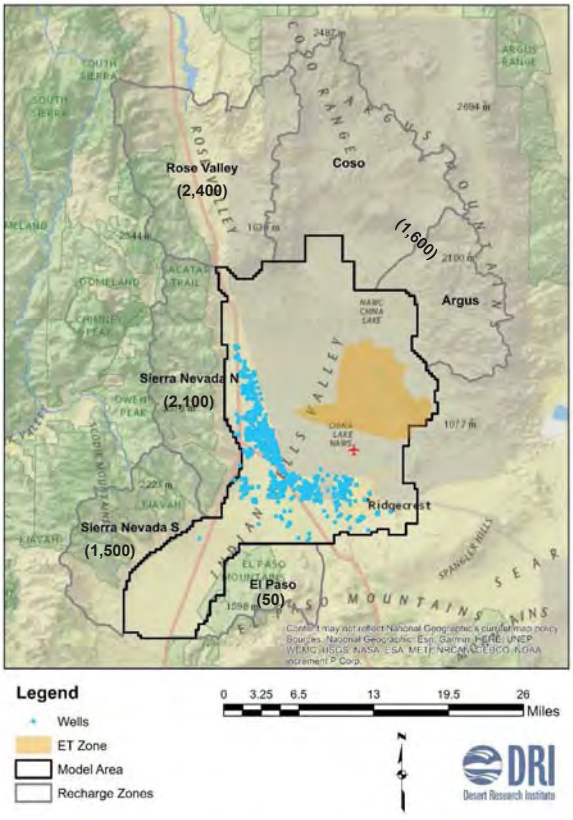

Simulated Pumping

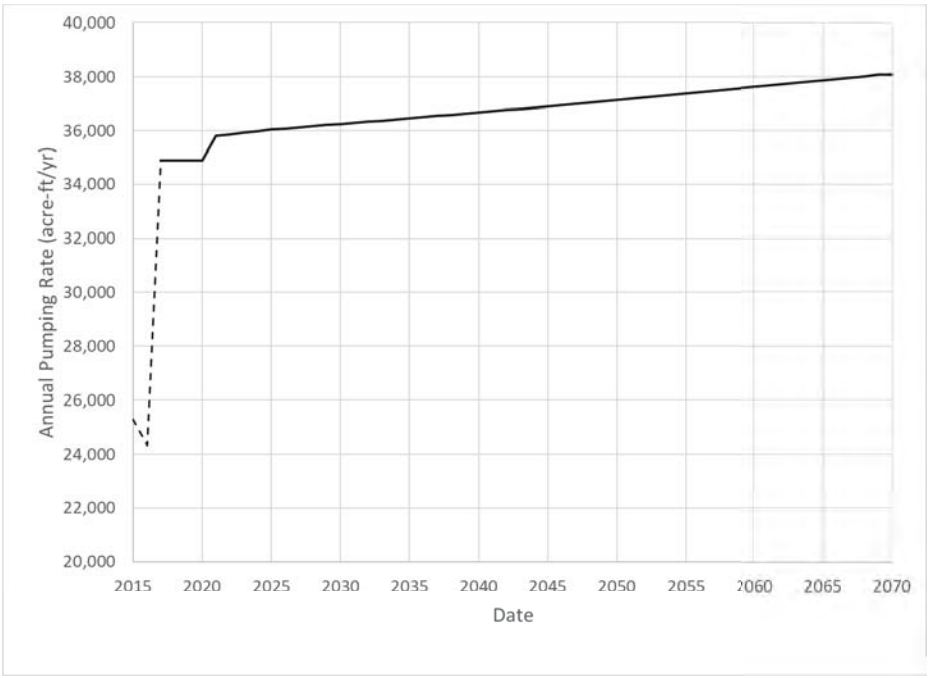

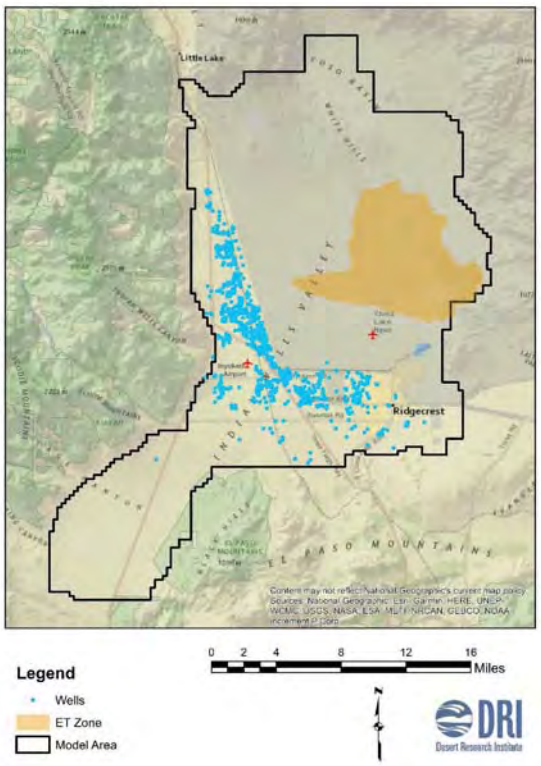

Simulated Pumping

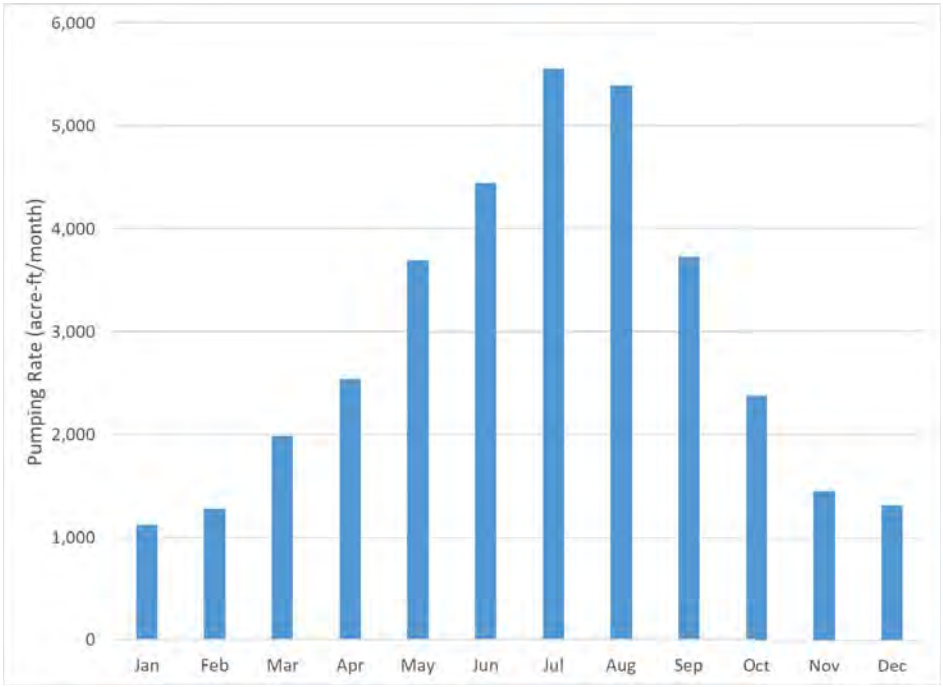

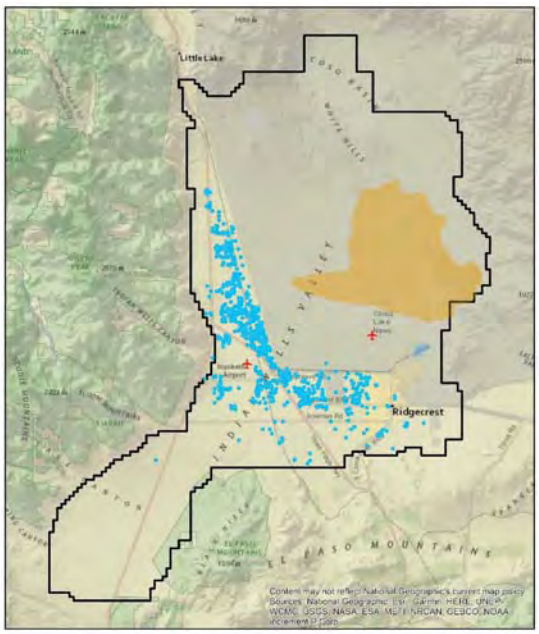

2020-2070 Average Water Budget

INPUTS

	(acre-ft/year)
Recharge	7,650
Storage	30,880
Total:	38,530

OUTPUTS

	(acre-ft/year)
Pumping	36,880
ET	1,610
Flow to Salt Wells Valley	40
Total:	38,530

Drawdown Results

- Drawdown from 2020 to 2070

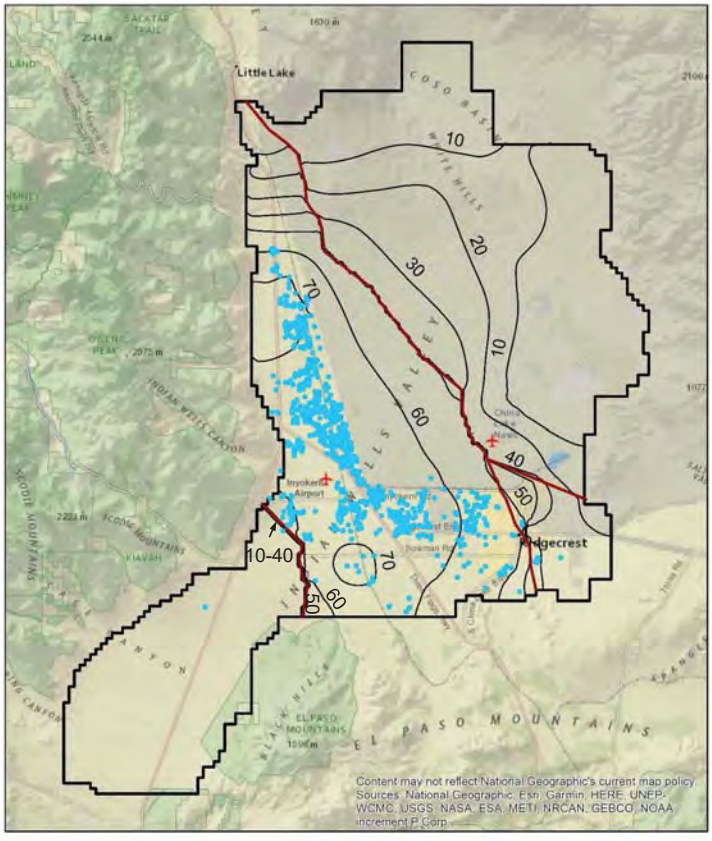

Legend
- Wells
- Geologic Faults
- Drawdown (2020-2070) ft
- Model Area

0 1.5 3 6 9 12 Miles

N

DRI Desert Research Institute

Simulated Water Levels by Model Analysis Zones

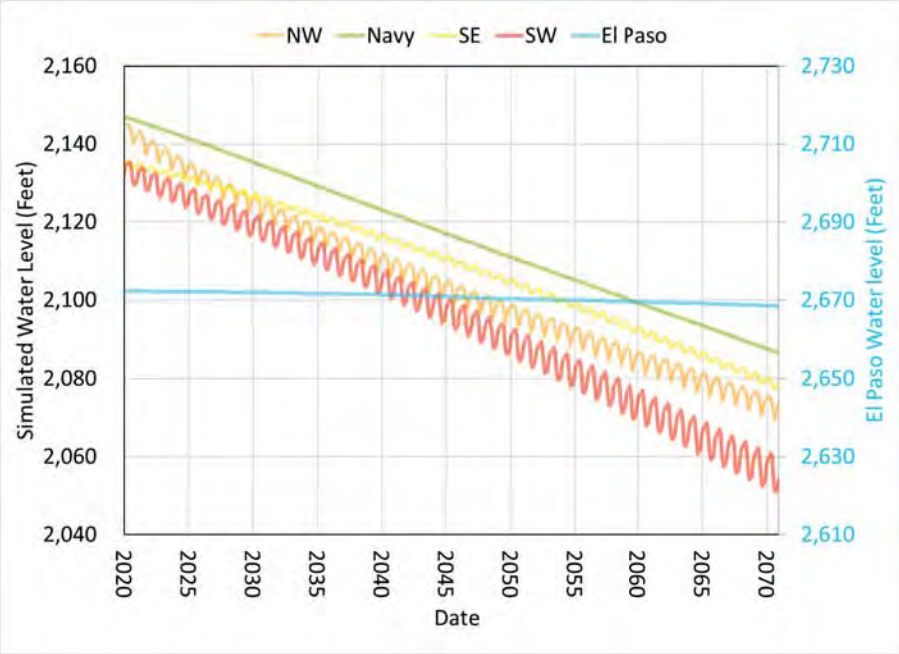

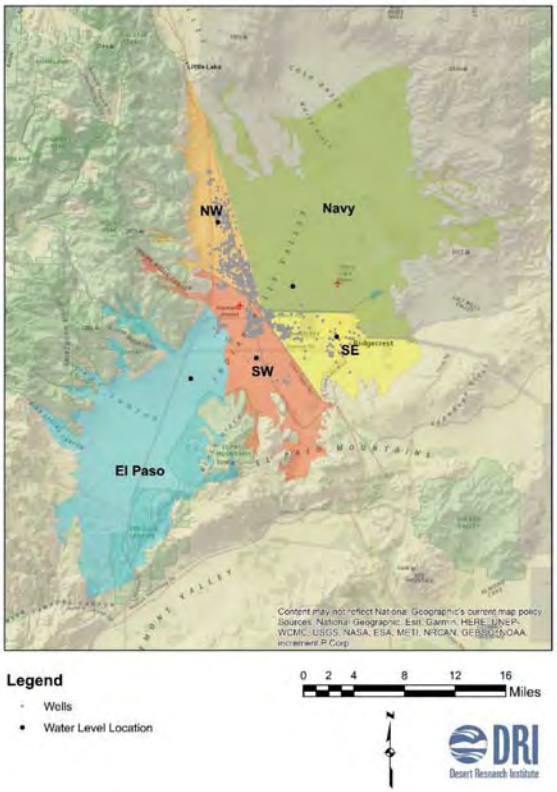

Change in Groundwater Storage

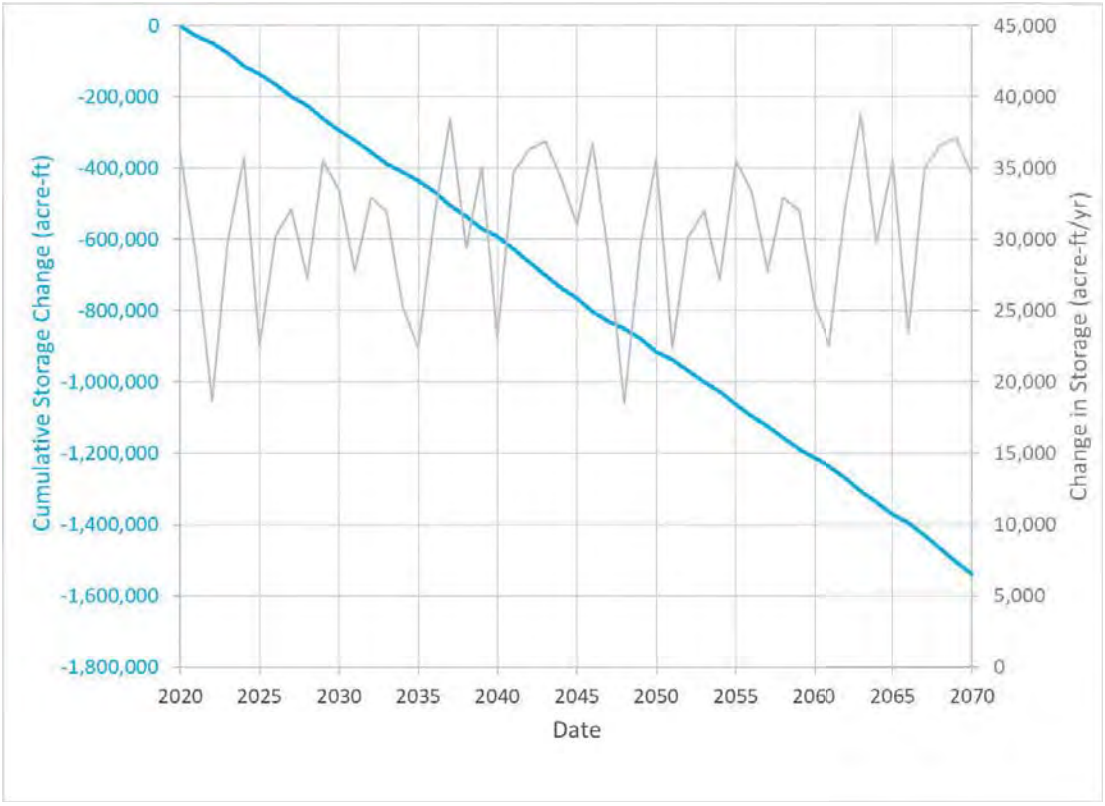

Simulated Outputs (Wells)

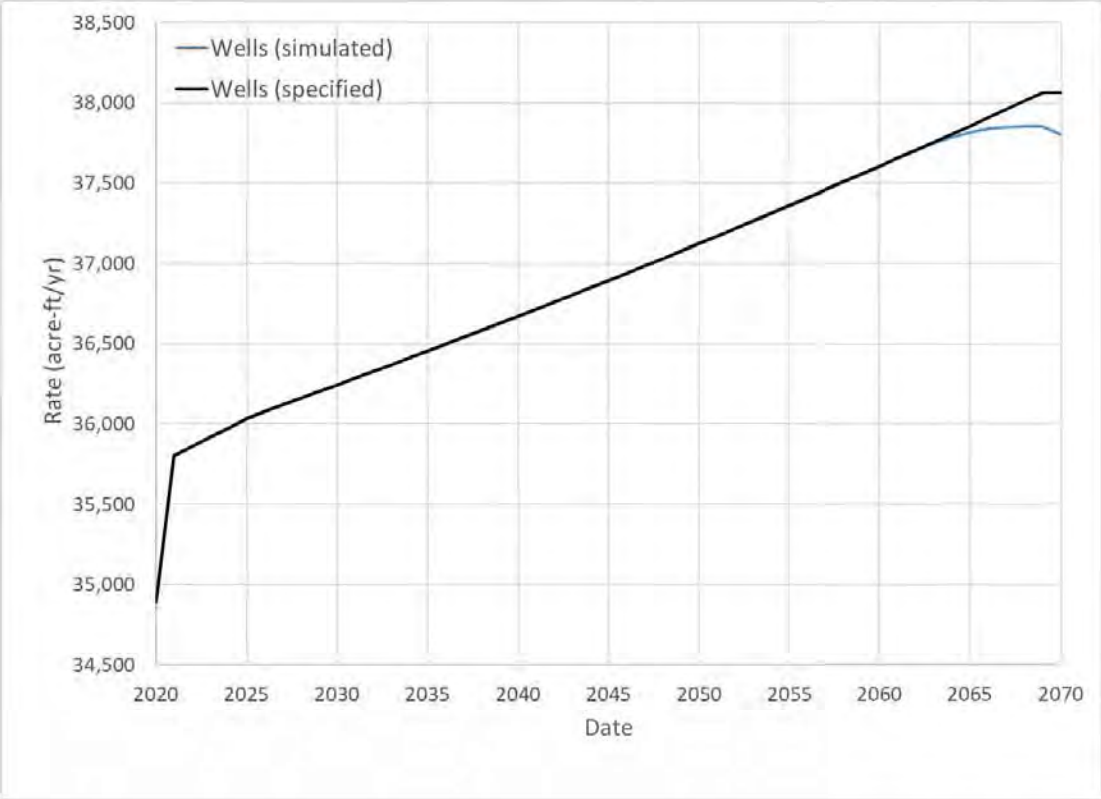

Simulated ET & Flow to Salt Wells

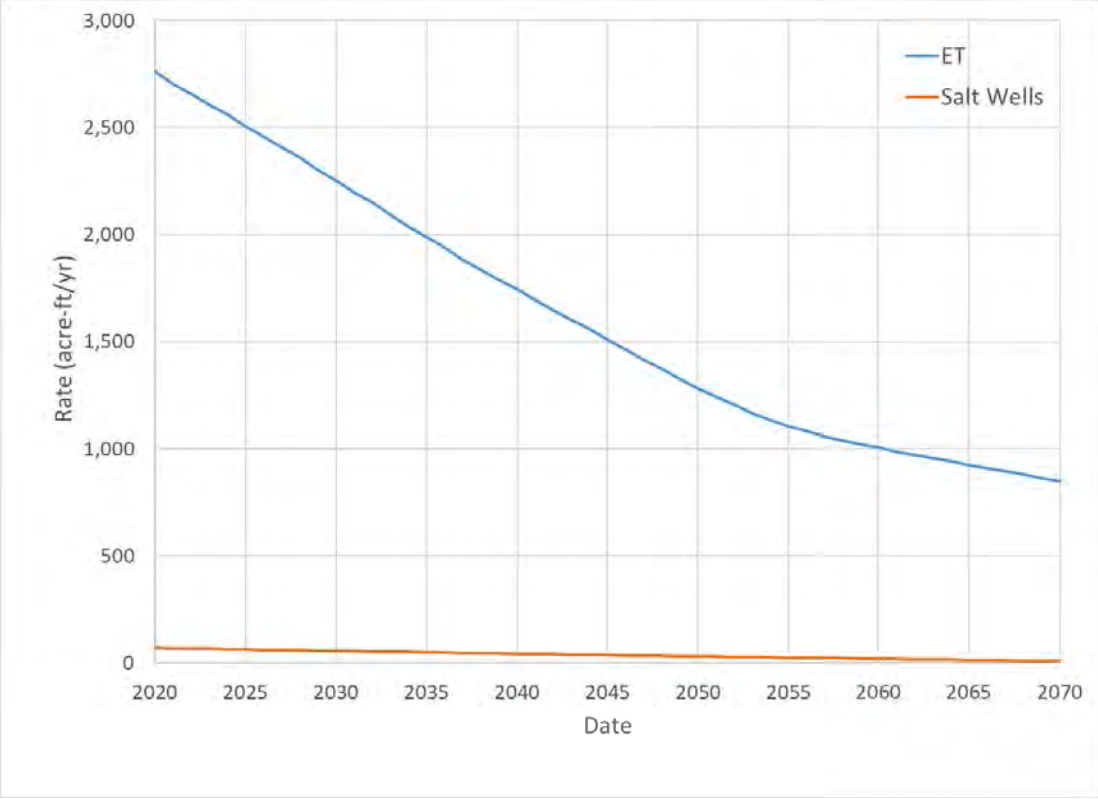

Questions

https://clminternship.org

ET Changes (2020 to 2070)

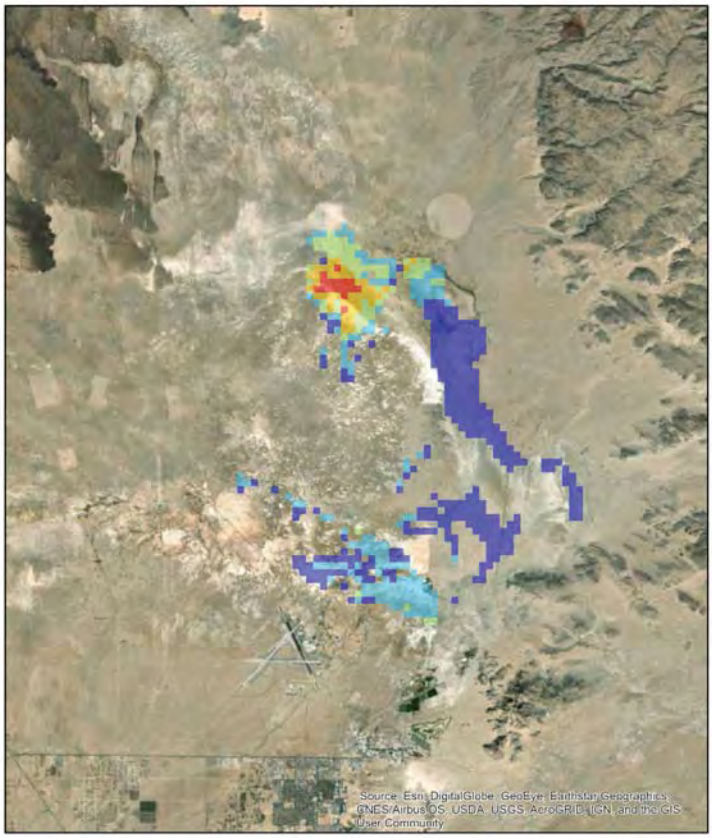

Scenario 6 Summary

1

Scenario 6 Development

- Results of Scenarios 3, 4, and 5 presented to the Board in May and June
  - Emphasis on minimizing loss of groundwater in storage
  - Scenario 4 identified as a potentially viably acceptable solution
- IWVGA Attorney's meeting on July 12
  - Discussion of basin water demands, groundwater in storage, use of storage, and GSP implementation
  - Agreement to proceed with a new modeling scenario (Scenario 6)
    - Modified version of Scenario 4 (Water Buyout) with "blocks" of allowed non-domestic pumping
- Draft summary of concepts for Scenario 6 was developed in coordination with the Attorneys
  - Final model inputs provided to DRI after finalizing the summary of concepts with the Attorneys
- Discussion of Scenario 6 results and goals with DRI
  - Second iteration of Scenario 6 (6.2) developed to further evaluate imported water requirement

2

Scenario 6 Objectives

- Create an allocation and management plan based on 2010-2014 pumping history and the highest beneficial uses of groundwater
- Maintain a similar cumulative loss of groundwater in storage as in Scenario 4 (Water Buyout) by replicating the total pumping volume used in Scenario 4
- Provide pumping "blocks" to non-domestic pumpers approximately equivalent to total non-domestic pumping in Scenario 4
  - More practical and feasible than the "ramp-down" in Scenario 4
- Optimize pumping locations to minimize future large drawdowns

3

Recap - Model Scenario 4 (Water Buyout)

- Start of Management Action – January 2022
  - Current pumping maintained in 2020 and 2021
- 2022: Total pumping going forward consists only of allocated rights (Federal and State rights).
  - Pumping includes reduced quantities of unprotected pumping (subject to ramp-down), plus protected pumping (not subject to ramp-down).
  - Pumpers who did not pump in each of the allocation years (2010-2014) identified during Scenario 4 preparation (Simmons, Blubaugh), were given zero allocation.
- 2023 through 2027: Unprotected allocations reduced by equal increments each year to reach Total Pumping of ~12,000 AFY in 2027
- 2025: Recycled water available to help reduce overdraft
- 2028 through 2070: Total Annual Pumping of ~12,000 AFY
- 2035 through 2070: Imported water supply available for basin recharge to operate sustainably

4

Summary of Model Scenario 6 (Modified Water Buyout)

- Discontinue all pumping that was **not continuous** from 2010-2014 (i.e. post-SGMA pumpers)
  - McGee, Blubaugh, Simmons Ranch
    - Status as post-SGMA pumpers to be verified as a post-GSP action
- Pumpers with continuous pumping from 2010 – 2014 categorized into one of two groups:

Domestic Group	Non-Domestic Group
Kern County	Meadowbrook
City of Ridgecrest	Mojave
IWVWD	SVM (industrial)
Inyokern CSD	Other small ag. (Quist, Sierra Shadows, Amberglow, Terese, Hickle, Bellino)
SVM (Trona only)	
Mutuals and domestic/private wells	
Navy	

5

Summary of Model Scenario 6 (Modified Water Buyout) (cont.)

Domestic group

- Starting in February 2020, allocation equal to lowest annual pumping from 2010-2014
  - Does not result in decreases in current pumping, except for a minor decrease for City of Ridgecrest
- Modeled pumping for 2020-2070 is equal to allocation, except the IWVWD
  - IWVWD pumping in 2020 equal to 6,507 AFY (based on 2017 actual pumping)
  - Assumed growth rate of 1% per year for IWVWD demands
  - IWVWD pumping above allocation due to growth will be offset by purchasing additional imported water
  - City stops pumping when recycled water becomes available

6

Summary of Model Scenario 6 (Modified Water Buyout) (cont.)

- Domestic group allocations
  - Navy 2,041 AFY
  - Kern County 18 AFY
  - IWVWD 7,319 AFY
  - Private/domestic wells 800 AFY
  - Mutuals 300 AFY
  - Inyokern CSD 108 AFY
  - City of Ridgecrest 339 AFY
  - SVM (Trona) 225 AFY

  11,150 AFY

- Domestic group modeled 2020 pumping
  - Navy 2,041 AFY
  - Kern County 18 AFY
  - IWVWD 6,507 AFY
  - Private/domestic wells 800 AFY
  - Mutuals 300 AFY
  - Inyokern CSD 108 AFY
  - City of Ridgecrest 339 AFY
  - SVM (Trona) 225 AFY

  10,338 AFY

Summary of Model Scenario 6 (Modified Water Buyout) (cont.)

Non-domestic group

- Pumpers have no allocations but are allowed to pump up to an assigned portion of a non-domestic pool/block volume.
- Total non-domestic pool/block volume: **63,836 AF**
  - Approximately equal to total non-domestic pumping in Scenario 4 over 8 years (2 years of current pumping and 6 years of "ramp-down" pumping)
- Agricultural pumpers: assigned portion of the pool volume is distributed proportionate to existing information on irrigated acres from 2010-2014
  - Acreage per the March 2014 Farm Group letter
- SVM (industrial): assigned portion of the pool volume is distributed proportionate to SVM's lowest pumping in 2010-2014 compared to the total of the lowest pumping by each non-domestic producer in 2010-2014
- All pumping from the non-domestic pool is required to cease by **2040**
  - For modeling purposes, non-domestic group pumpers continue to pump at current levels over a "cliff" period until their assigned portions of the pool volume are depleted
  - Assigned portion of the pool volume may be used variably until 2040, but total pumping shall not exceed assigned portion.

Summary of Model Scenario 6 (Modified Water Buyout) (cont.)

Name	Irrigated Acreage (acres)	Portion of Pool Volume (AF)	Estimated "Cliff" Period (months)
Meadowbrook	890	31,832	60
Mojave*	120	4,292	8
Quist	140	5,007	92
Sierra Shadows	168	6,009	94
Amberglow	12	429	83
Terese	80	2,861	111
Hickle	17	608	86
Bellino	13	465	112
SVM (industrial)**	-	12,333	62
Total	**1,440**	**63,836**	-

*Irrigated acres consists only of 120 acres of alfalfa converted to pistachio
**Does not reflect recent information provided by SVM on pumping before establishment of China Lake NAWS

9

Summary of Model Scenario 6 (Modified Water Buyout) (cont.)

- Lease Market
  - Possible sellers
    - Meadowbrook
    - IWVWD (after accounting for annual growth)
    - City of Ridgecrest (demands assumed to be replaced with recycled water in 2025)
  - Possible buyers
    - Mojave
    - SVM (industrial)
    - Small Ag
  - SVM would purchase lease water or recycled water for its industrial demands until imported water becomes available in 2035.
- Some IWVWD and SVM pumping relocated towards Brown Road to optimize pumping.
- Imported water assumed to be available for basin recharge starting in 2035 to offset pumping above sustainable yield and offset increased pumping demands due to projected growth (IWVWD).
  - Included in Scenarios 6.1 and 6.2
- 2,500 AFY of additional imported water would be required for recharge to offset ongoing losses of groundwater in storage due to evapotranspiration.
  - **Only included in Scenario 6.1**

10

Management Scenario 6.2 - Pumping and Recharge Scenarios

Pumping

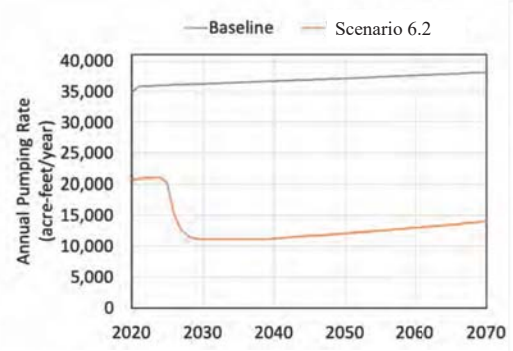

Recharge

Includes natural and artificial recharge

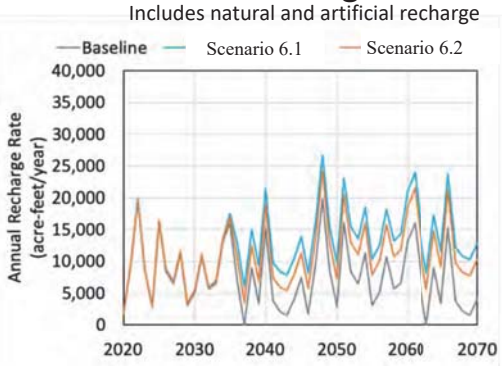

Net Pumping

Pumping minus artificial recharge

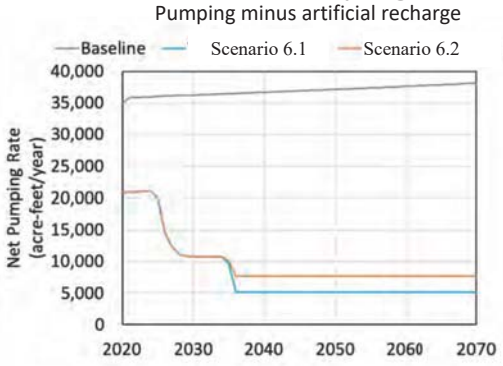

DRAFT – Subject to change

Water Level Change (2020-2070)

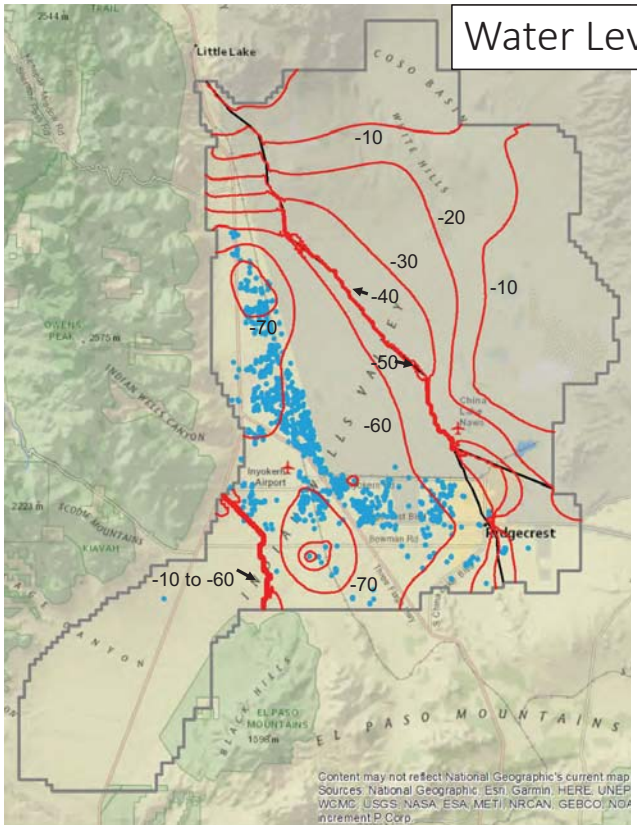

Rising
Neutral
Falling

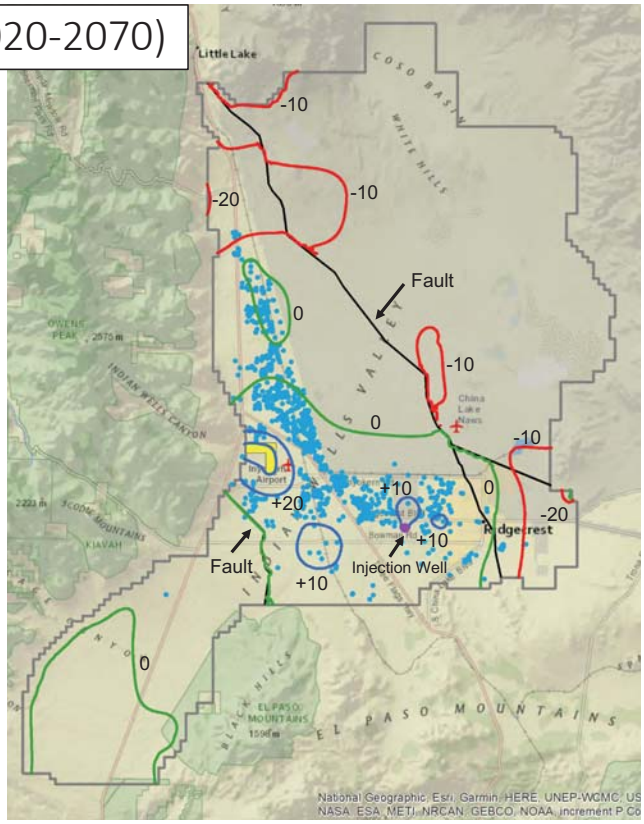

DRAFT – Subject to change

Baseline

DRAFT – Subject to change

Scenario 6.2

Units: feet

Water Level Change 2020-2040

Management Scenario 6.2

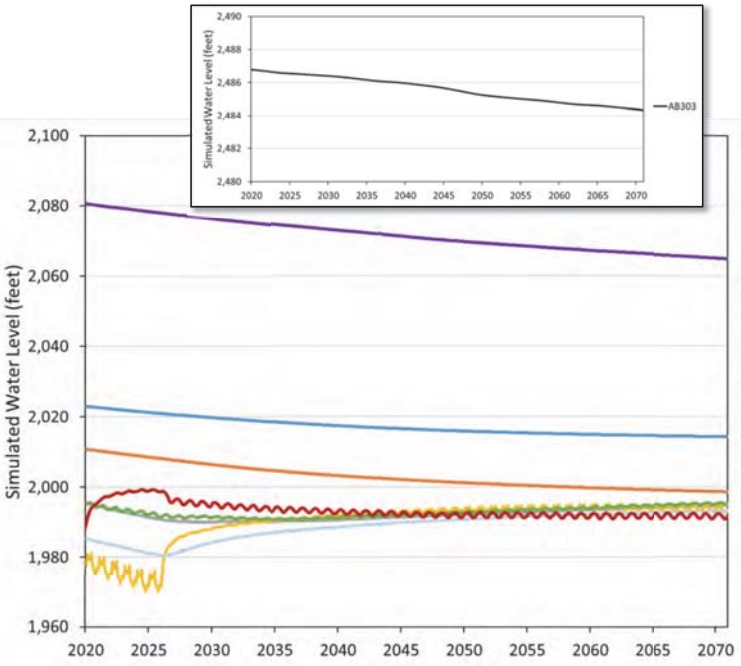

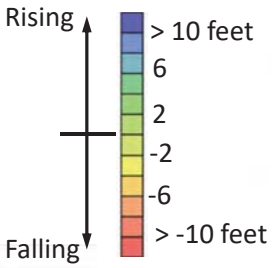

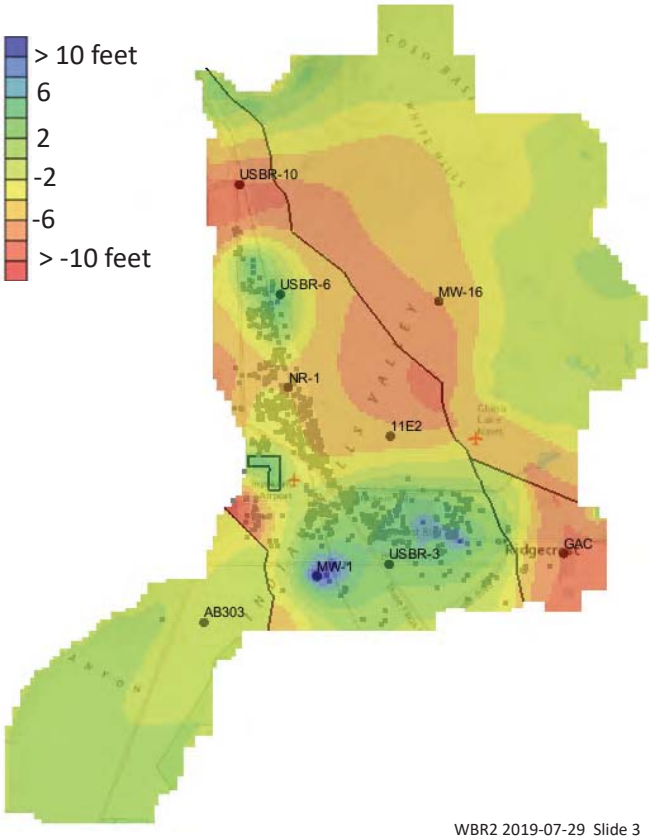

DRAFT – Subject to change

Water Level Change 2040-2070

Management Scenario 6.2

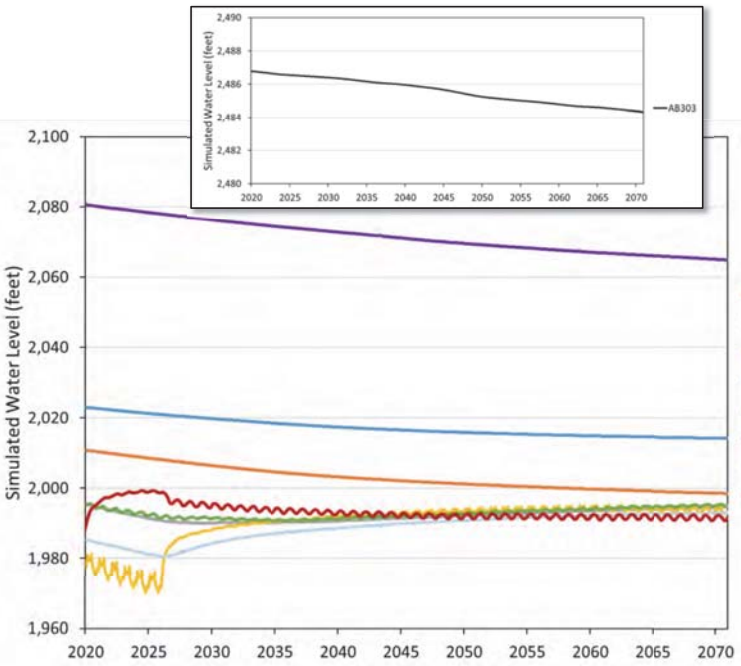

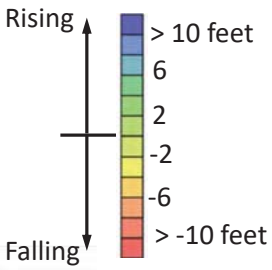

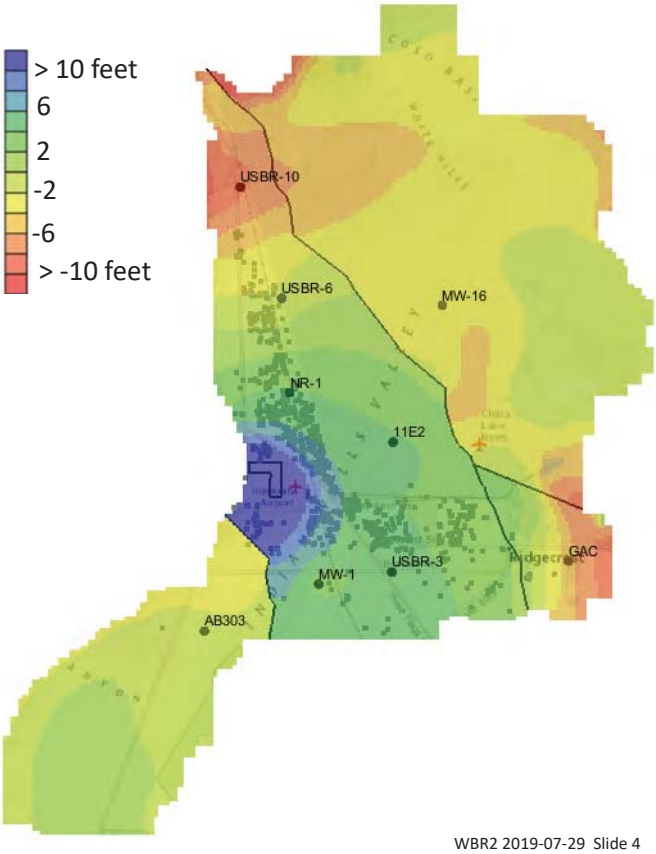

DRAFT – Subject to change

Water Level Change 2020-2070

Management Scenario 6.2

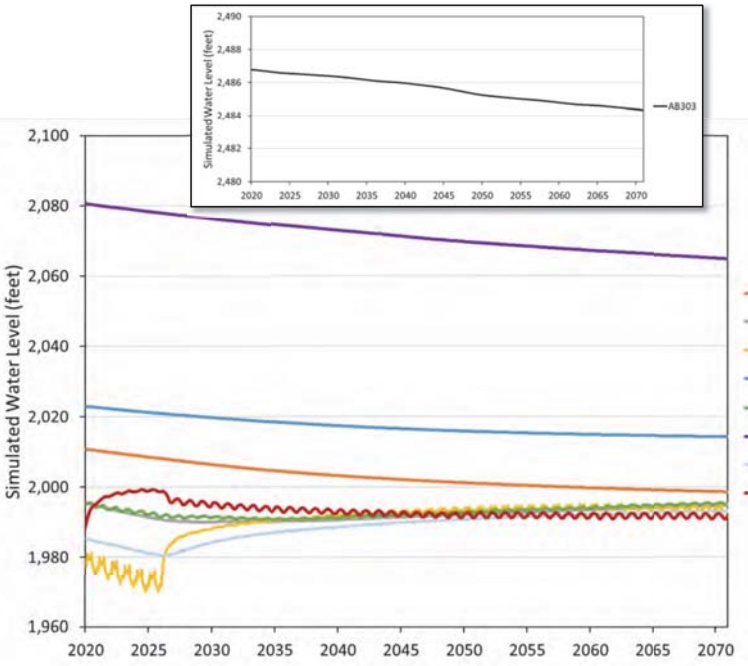

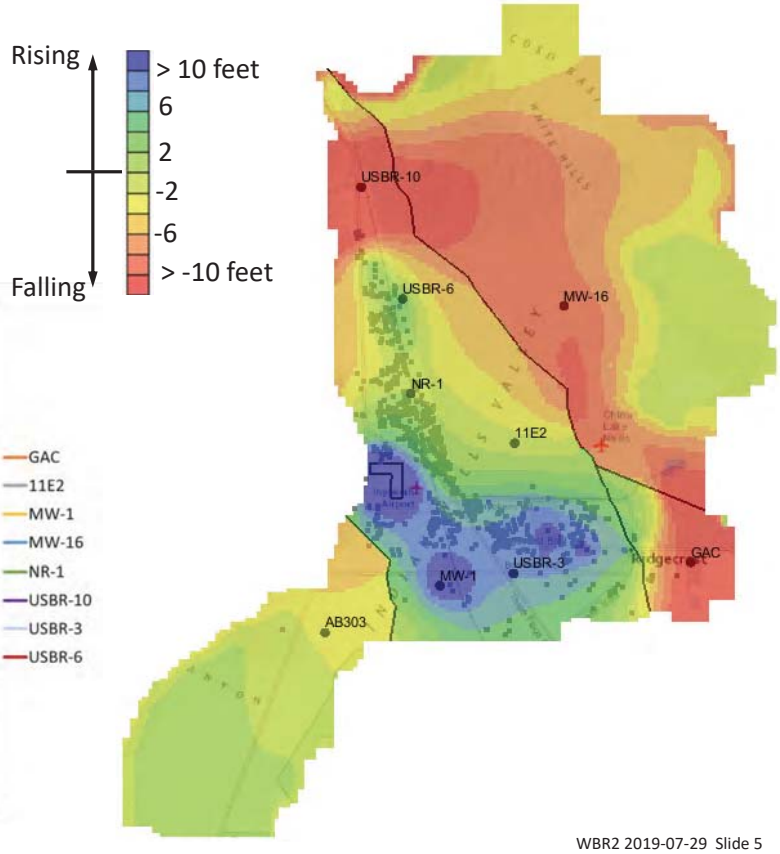

Basin Groundwater Budgets for 2020 through 2070

Annual Average (acre-feet/year)

	Baseline	Water Buyout	Scenario 6.1	Scenario 6.2
INFLOW				
Recharge	7,650	10,959	12,707	10,990
TOTAL	7,650	10,959	12,707	10,990
OUTFLOW				
Pumping	36,880	13,176	13,260	13,260
Evapotranspiration	1,610	1,944	1,885	1,877
Flow to Salt Wells Valley	40	38	39	39
TOTAL	38,530	15,158	15,184	15,176
CHANGE IN GW STORAGE	-30,880	-4,199	-2,477	-4,186

Cumulative (acre-feet)

	Baseline	Water Buyout	Scenario 6.1	Scenario 6.2
INFLOW				
Recharge	390,405	558,906	648,042	560,507
TOTAL	390,405	558,906	648,042	560,507
OUTFLOW				
Pumping	1,880,898	671,973	676,270	676,270
Evapotranspiration	82,347	99,128	96,141	95,722
Flow to Salt Wells Valley	1,893	1,931	1,991	1,990
TOTAL	1,965,139	773,033	774,402	773,982
CHANGE IN GW STORAGE	-1,574,734	-214,127	-126,360	-213,475

Change in Basin Groundwater Storage

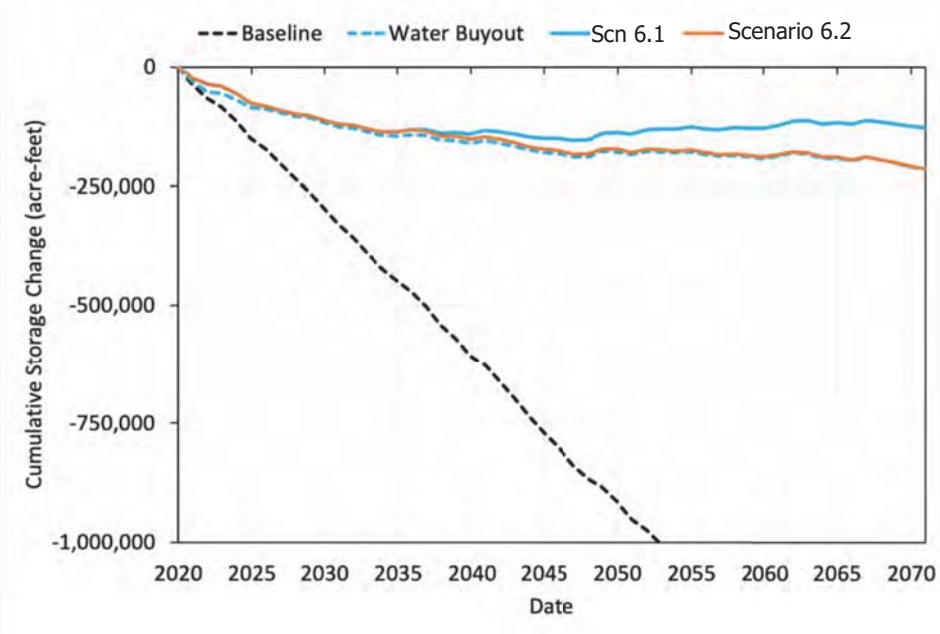

Evapotranspiration

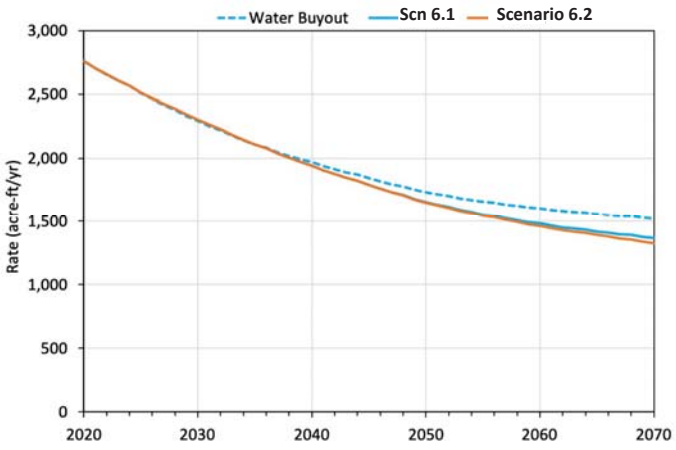

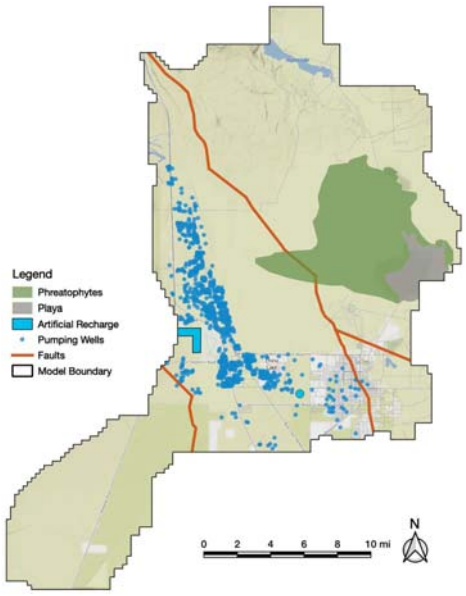

Management Scenario 6.2 - Pumping and Recharge Scenarios

Pumping

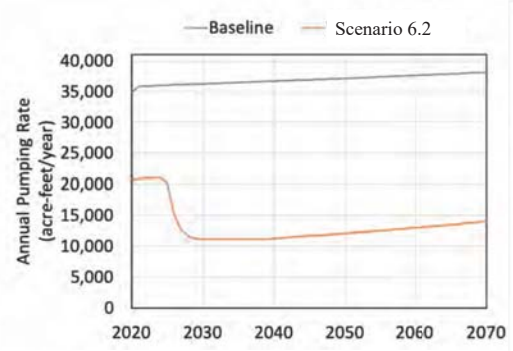

Recharge

Includes natural and artificial recharge

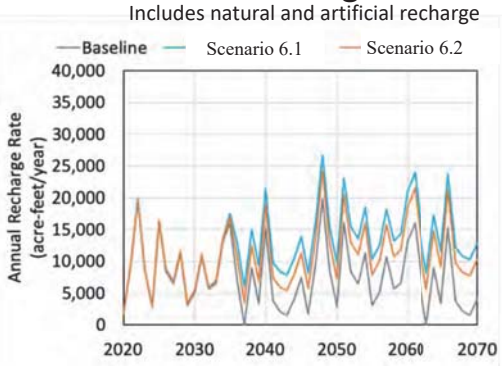

Net Pumping

Pumping minus artificial recharge

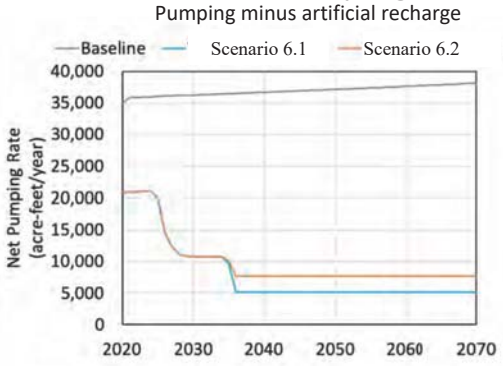

DRAFT – Subject to change

Water Level Change (2020-2070)

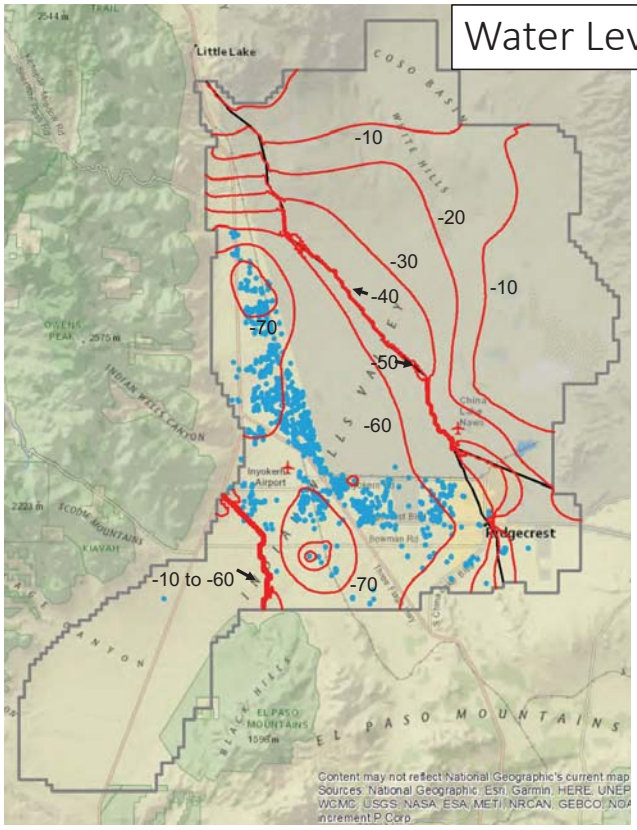

Rising
Neutral
Falling

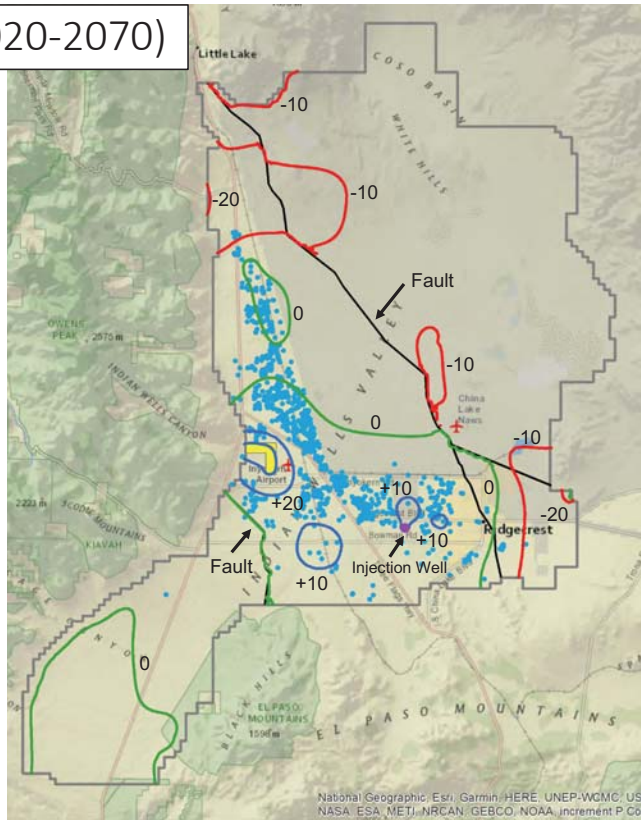

DRAFT – Subject to change

Baseline

DRAFT – Subject to change

Scenario 6.2

Units: feet

Water Level Change 2020-2040

Management Scenario 6.2

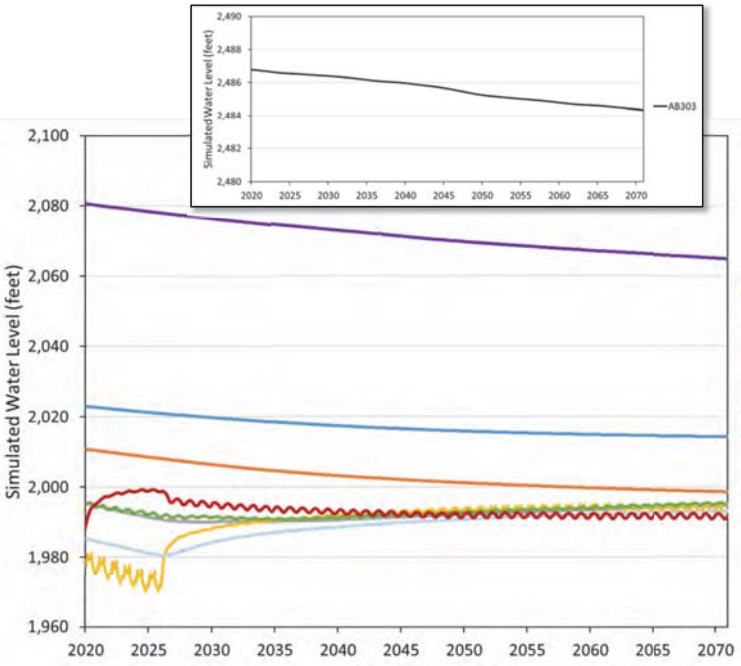

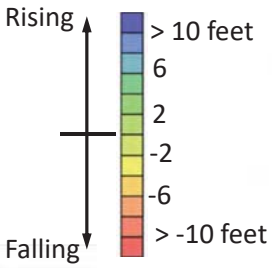

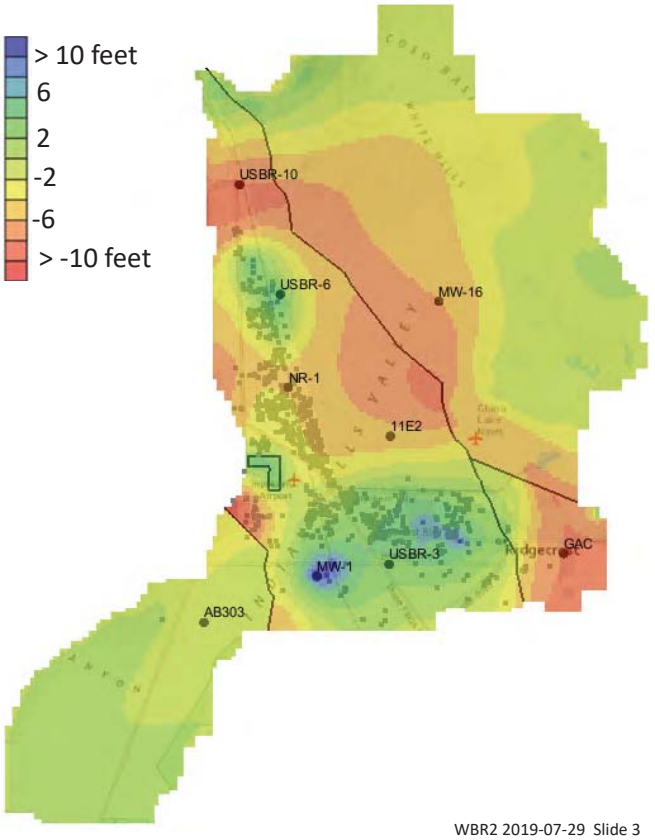

DRAFT – Subject to change

Water Level Change 2040-2070

Management Scenario 6.2

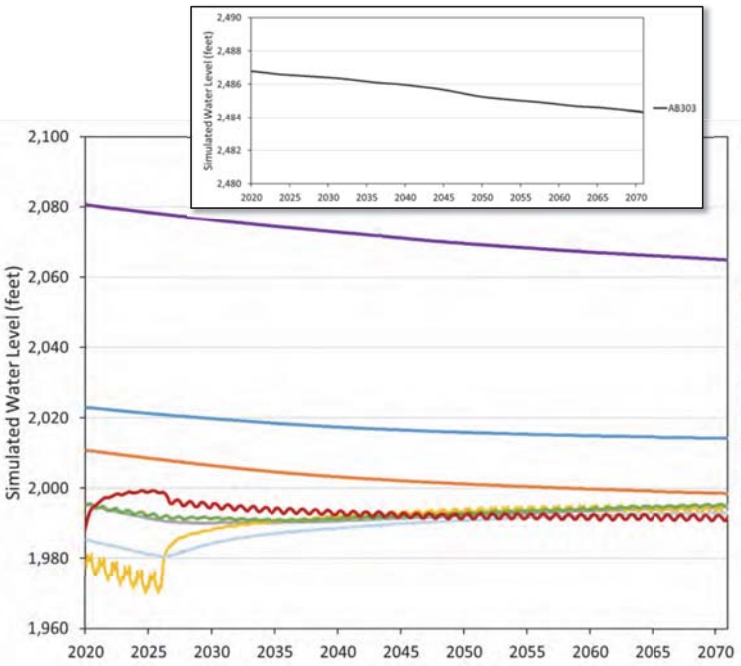

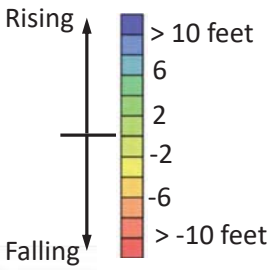

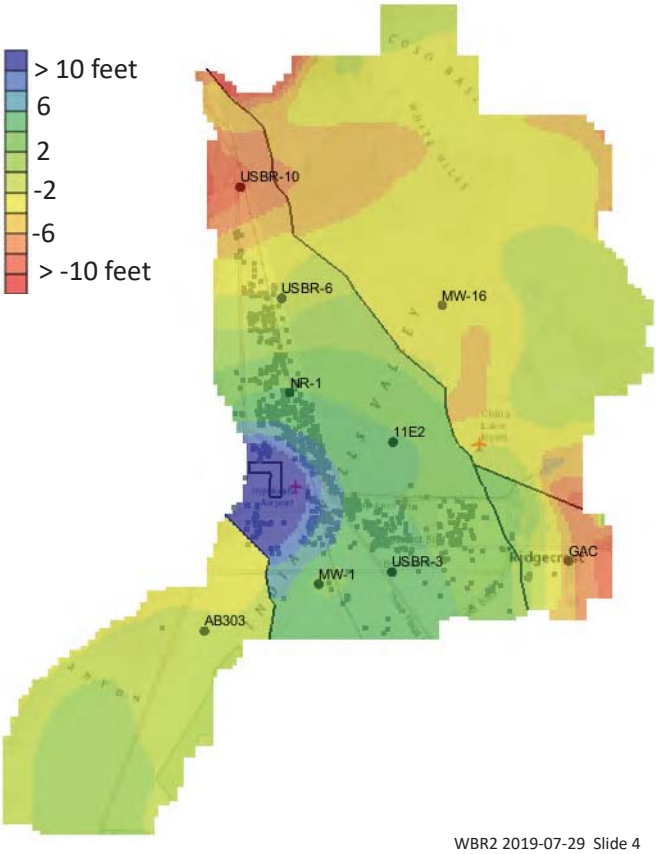

DRAFT – Subject to change

Water Level Change 2020-2070

Management Scenario 6.2

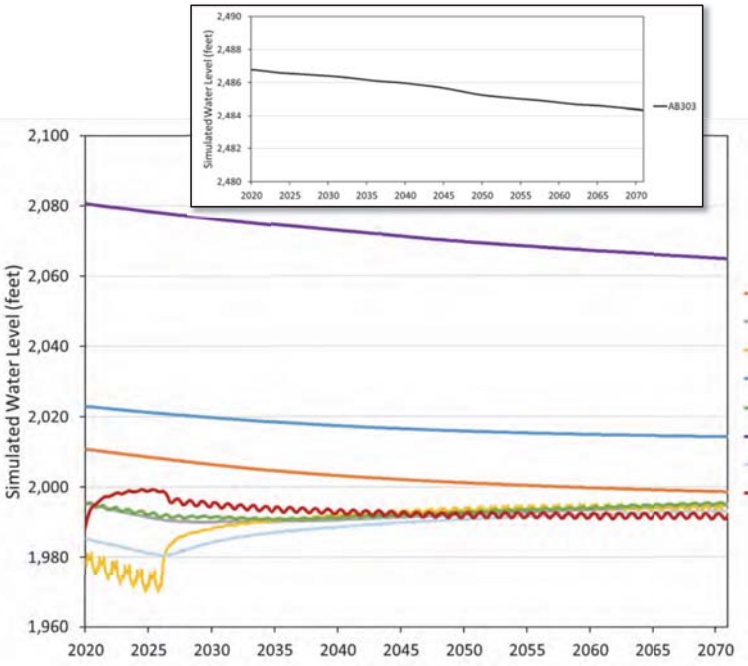

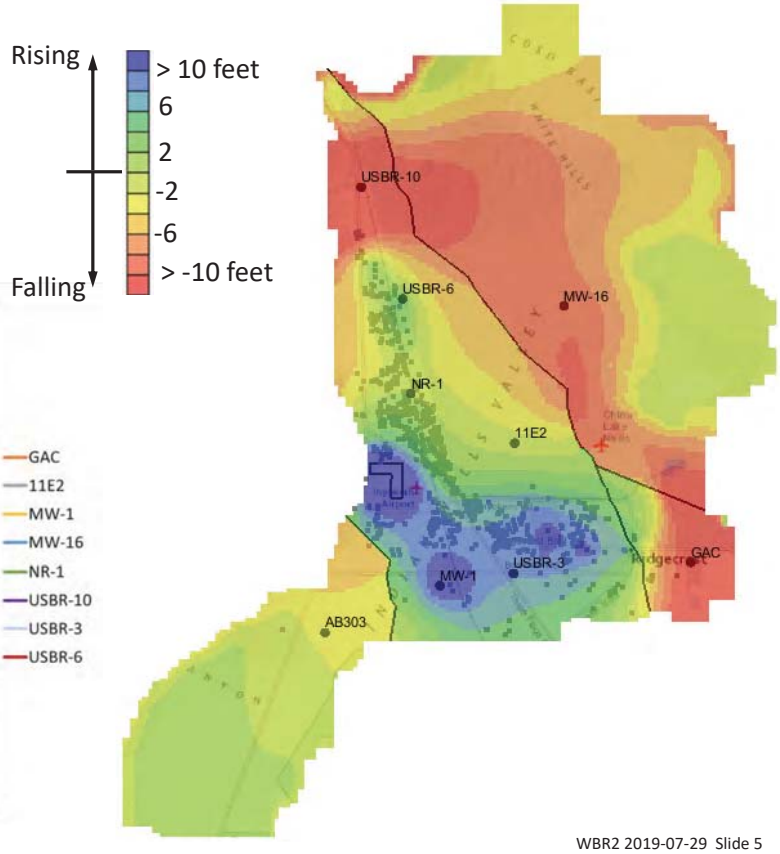

Basin Groundwater Budgets for 2020 through 2070

Annual Average (acre-feet/year)

	Baseline	Water Buyout	Scenario 6.1	Scenario 6.2
INFLOW				
Recharge	7,650	10,959	12,707	10,990
TOTAL	7,650	10,959	12,707	10,990
OUTFLOW				
Pumping	36,880	13,176	13,260	13,260
Evapotranspiration	1,610	1,944	1,885	1,877
Flow to Salt Wells Valley	40	38	39	39
TOTAL	38,530	15,158	15,184	15,176
CHANGE IN GW STORAGE	-30,880	-4,199	-2,477	-4,186

Cumulative (acre-feet)

	Baseline	Water Buyout	Scenario 6.1	Scenario 6.2
INFLOW				
Recharge	390,405	558,906	648,042	560,507
TOTAL	390,405	558,906	648,042	560,507
OUTFLOW				
Pumping	1,880,898	671,973	676,270	676,270
Evapotranspiration	82,347	99,128	96,141	95,722
Flow to Salt Wells Valley	1,893	1,931	1,991	1,990
TOTAL	1,965,139	773,033	774,402	773,982
CHANGE IN GW STORAGE	-1,574,734	-214,127	-126,360	-213,475

Change in Basin Groundwater Storage

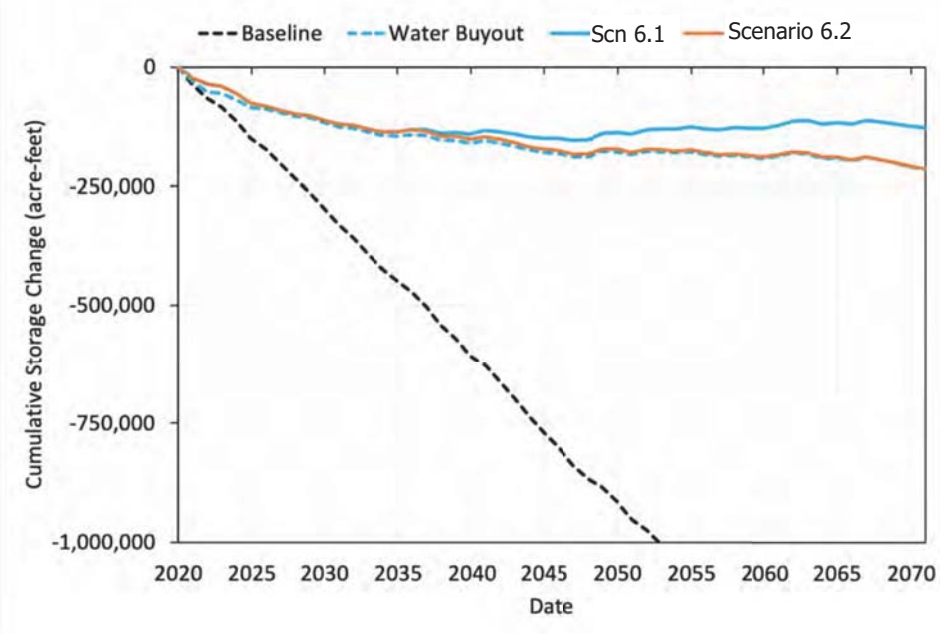

Evapotranspiration

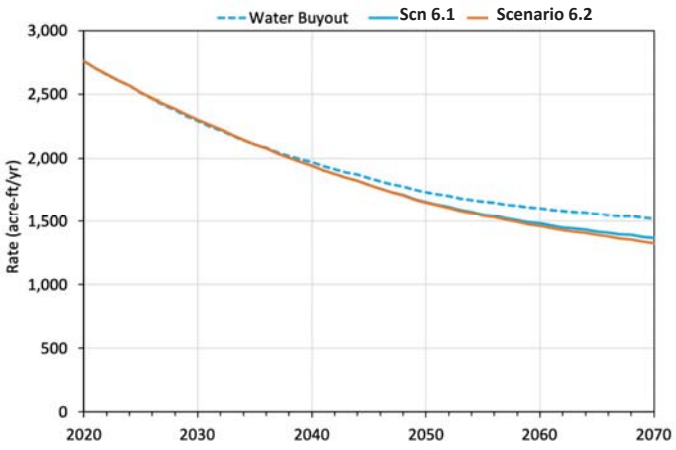

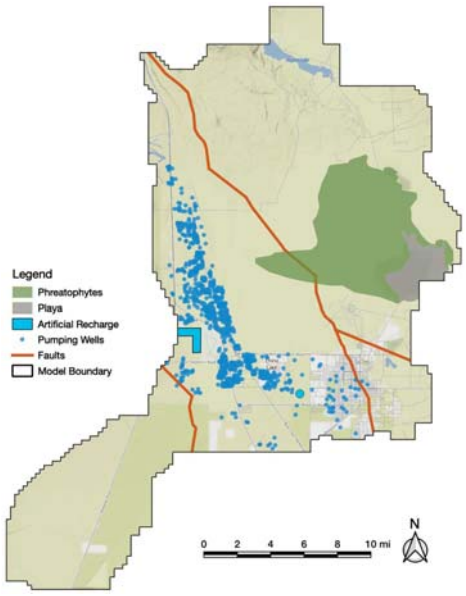

Indian Wells Valley
Draft TDS Transport Model
Baseline Pumping Conditions

February 7, 2019

Conceptual Model

- Sources:
  - Solutes in recharge
  - Dissolution of minerals in basin
  - Mixing with saltier groundwater
    - Remnant evaporative brines
    - Geothermal fluids
- Concentration by evaporation

- Sinks:
  - Solutes in discharge to Searles valley
  - Precipitation of minerals

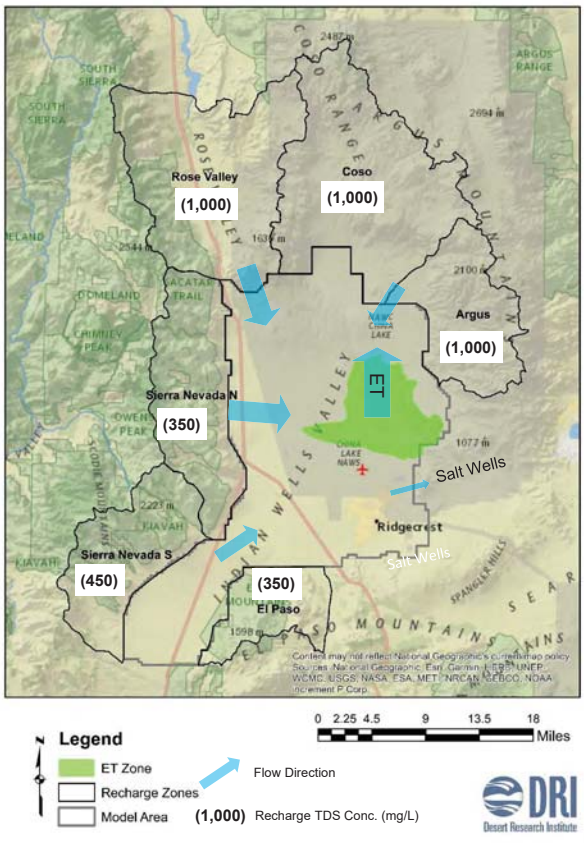

TDS Model Process

- Step #1 – Compile and QA Dataset
  - Dataset from Stetson – quality checked back to original published sources. Includes data compiled in BWG database, GAMA, and from AB303 (2003). Stetson identified 548 wells and 1,993 TDS values.
  - DRI used TDS data for 402 wells (wells missing depths were excluded). The most recent TDS measurement is used, if multiple dates are available.

TDS Model Process

- Step #2 – Select most recent TDS value for single well

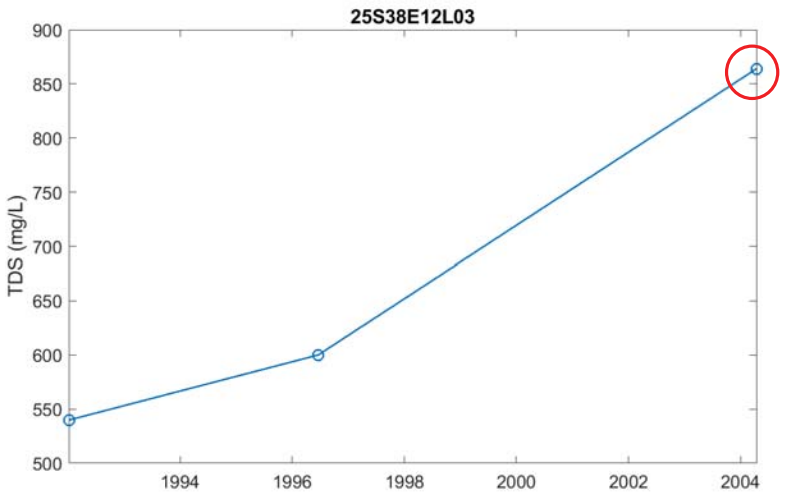

TDS Model Process

- <u>Step #3 – Partition domain into three layers</u>
  - Shallow (model layer 1)
  - Intermediate (model layers 2-3)
  - Deep (model layers 4-6)
  - Not enough TDS data to interpolate to six layers independently
- <u>Step #4 – Average TDS values</u>
  - Average TDS values if multiple values fall into single layer

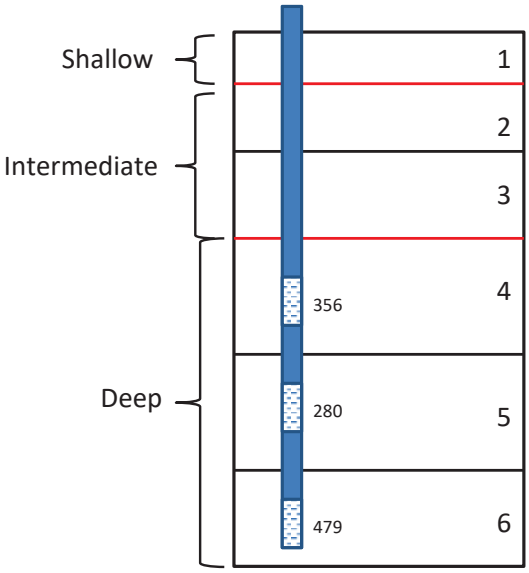

Average for deep layer = 372

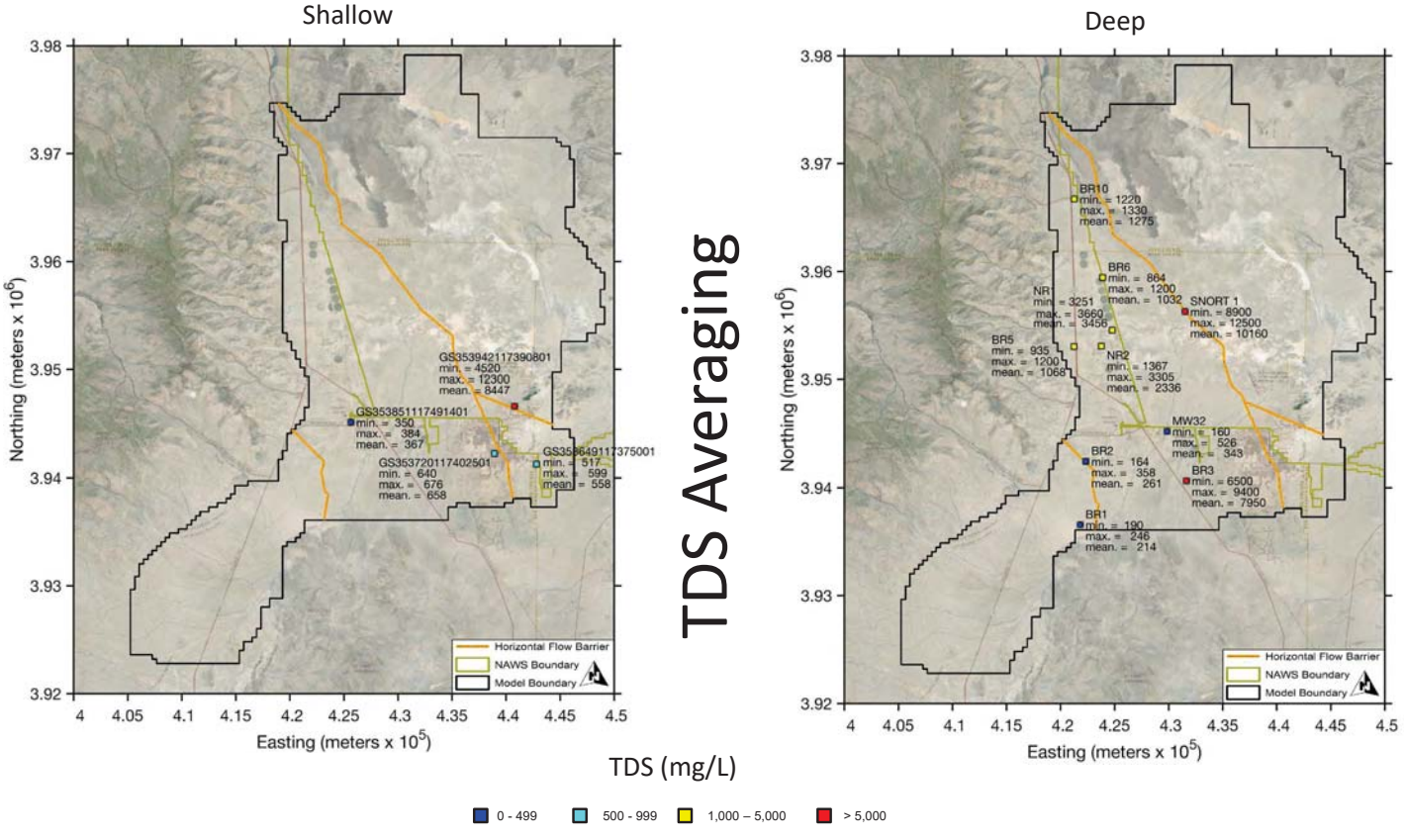

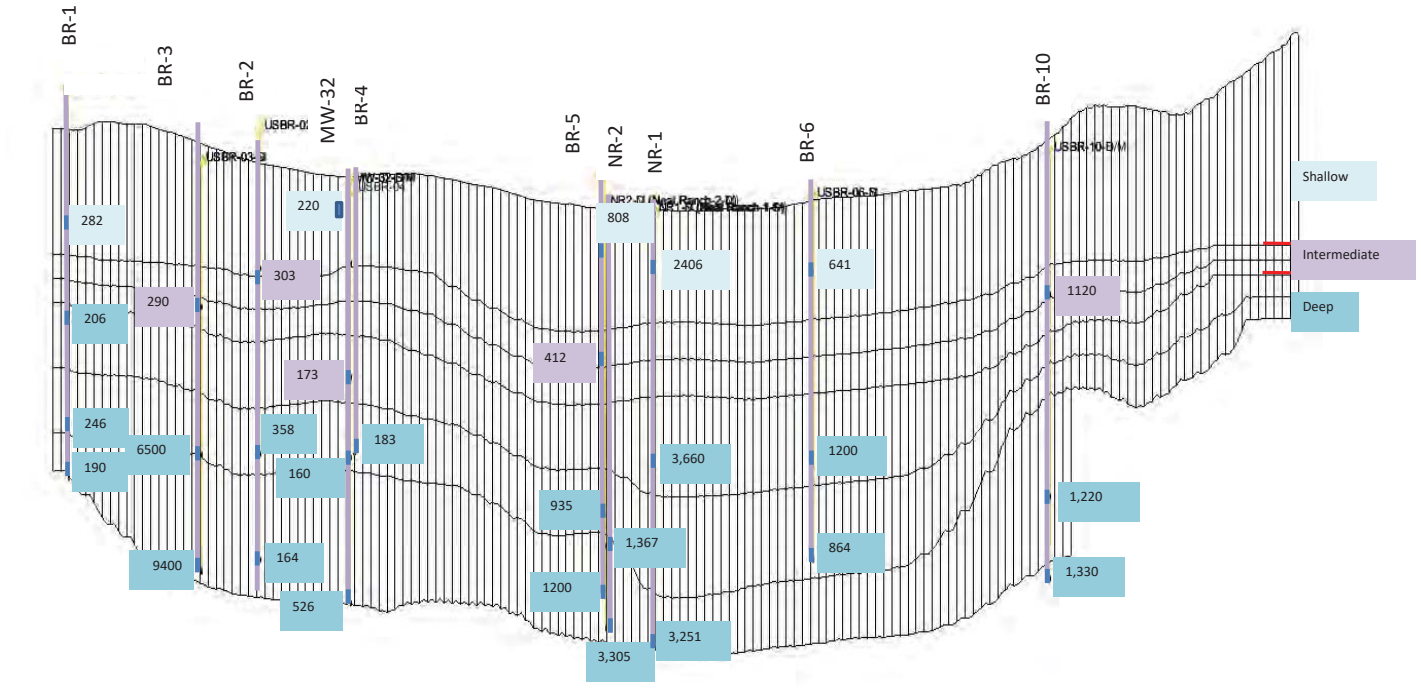

South

North

Note: Shallow BR-5 & BR-10 are in intermediate layer

TDS Model Process

- Step #5 – Add estimated TDS points

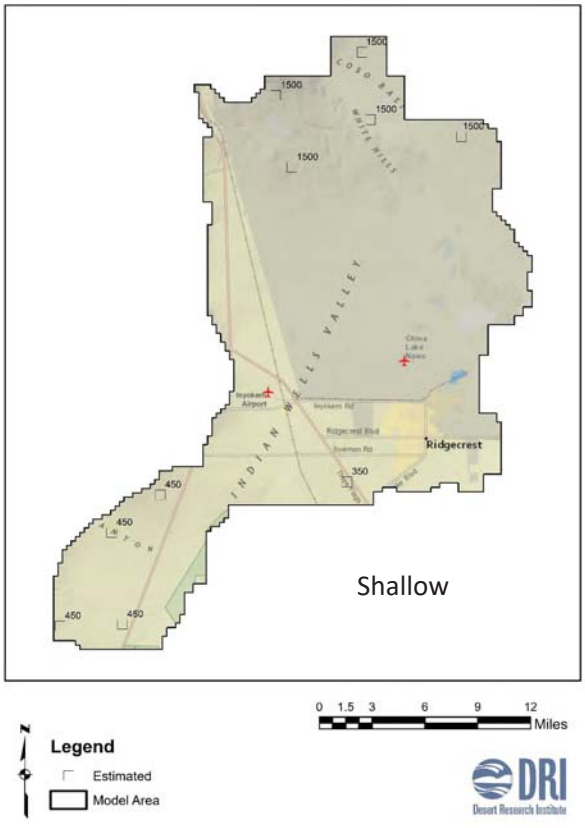

TDS Model Process

- Step #6 – Combine measured and estimated datasets
- Step #7 – Interpolate combined dataset
  - Repeat for shallow, intermediate, and deep layers
  - Interpolated values represent continuous values
- Step #8 – Setup initial conditions for transport model and run using baseline flow model (~35k pumping)

TDS Initial Condition

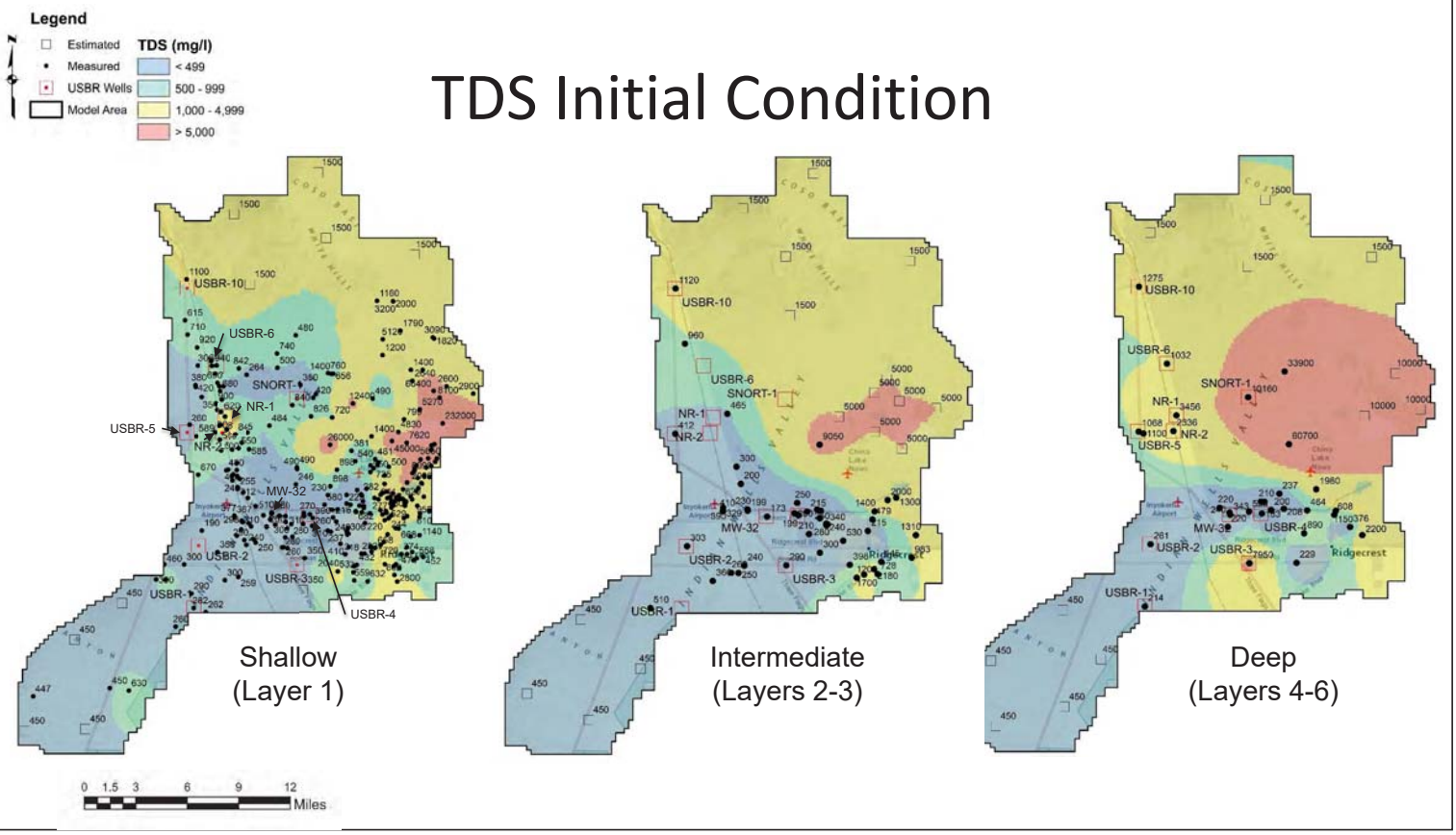

Simulated TDS Concentration - Shallow

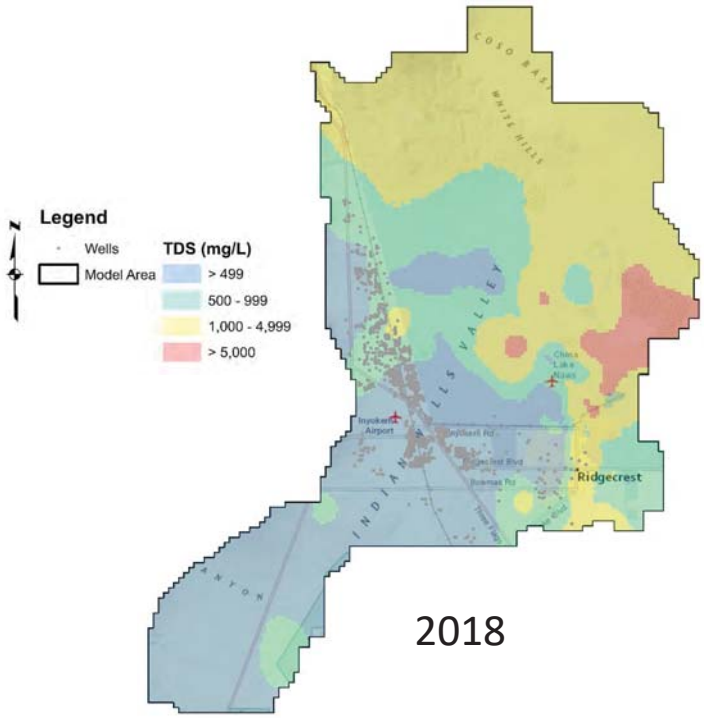

2018

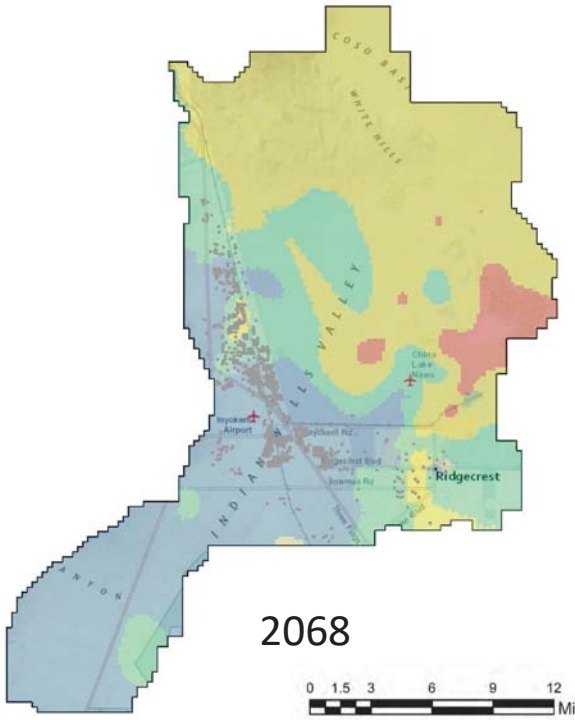

2068

0 1.5 3 6 9 12 Miles

Simulated TDS Concentration - Intermediate

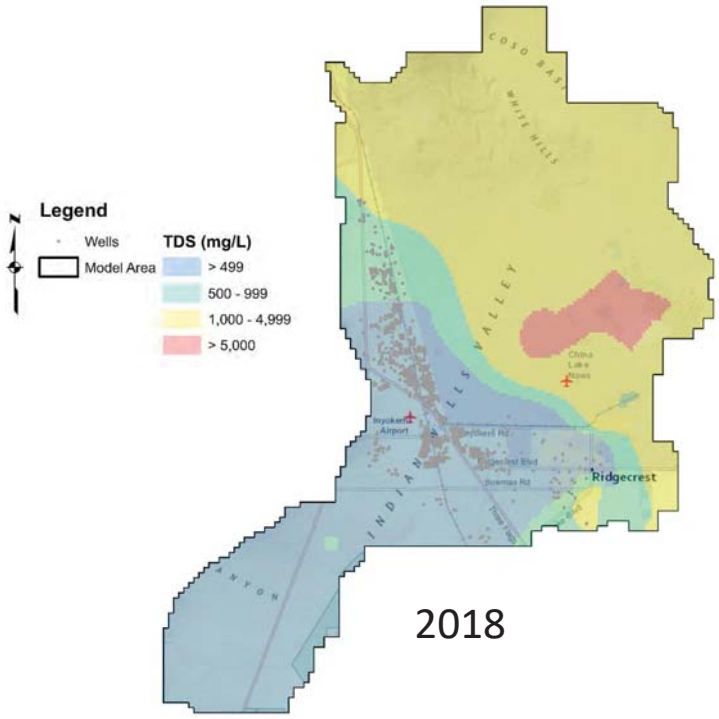

2018

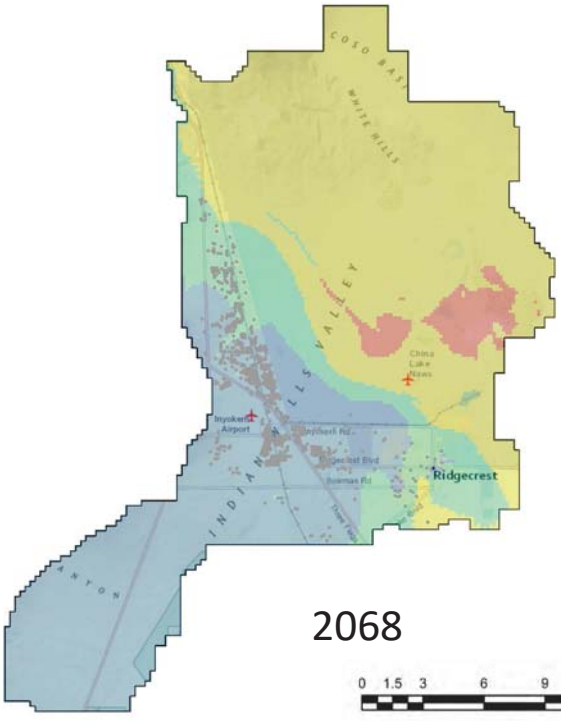

2068

0 1.5 3 6 9 12 Miles

Simulated TDS Concentration - Deep

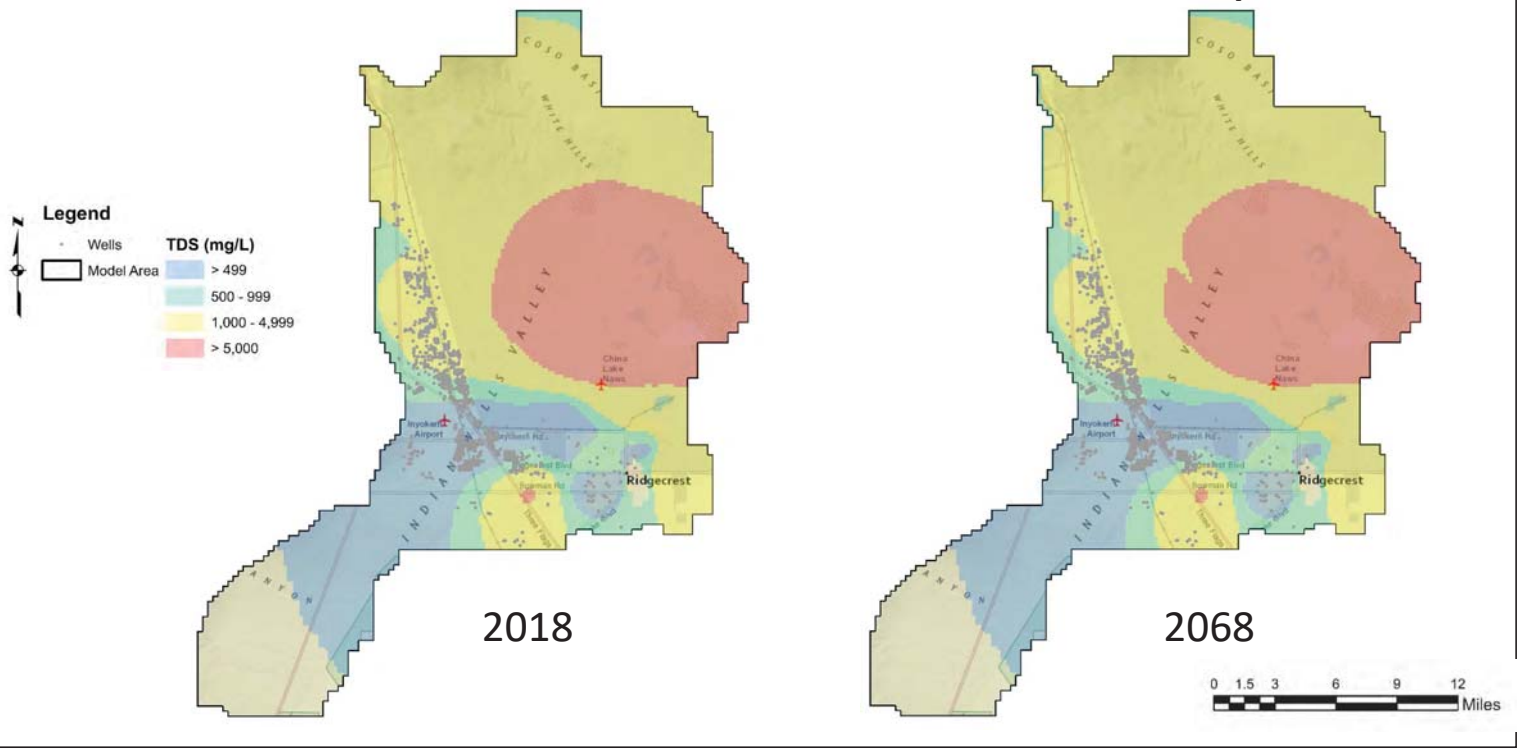

Simulated TDS Trends

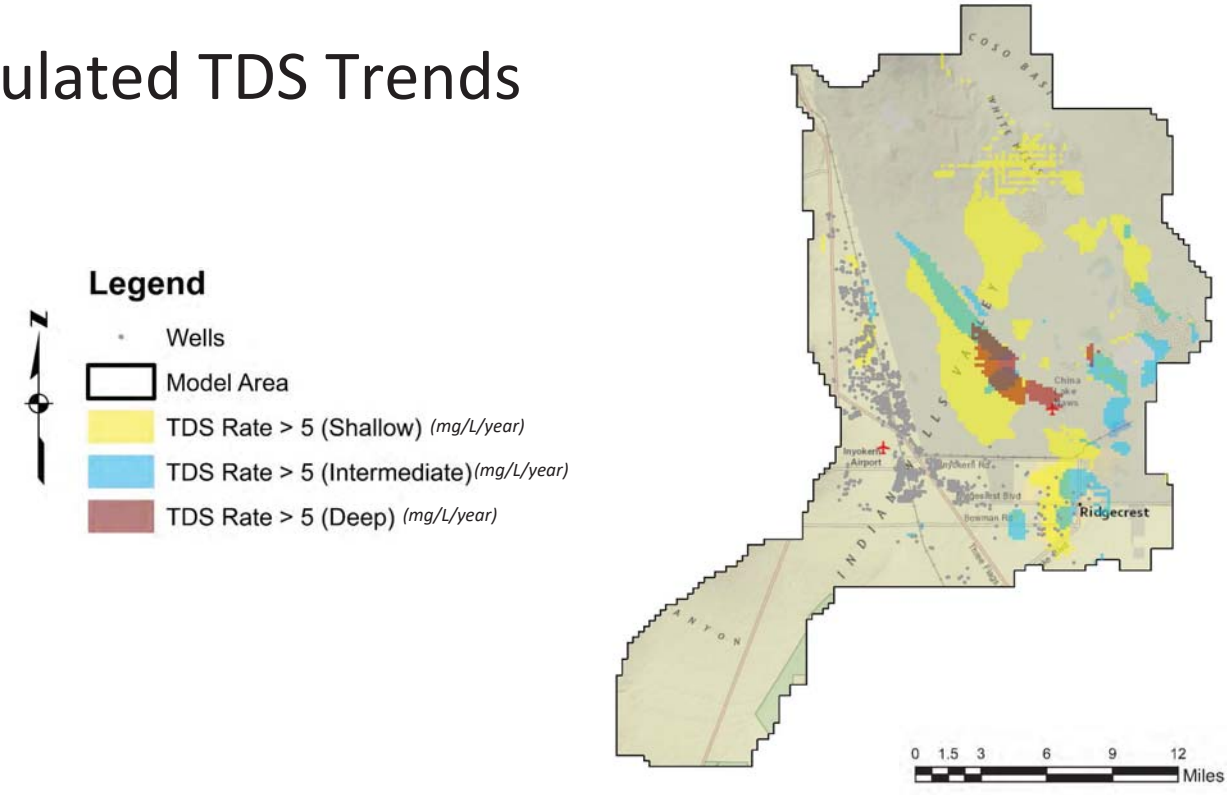

Questions
https://clminternship.org

Results from Groundwater Flow and TDS Transport Model Scenario 6.2

Comparison with Baseline

Pumping and Recharge Scenarios

Pumping

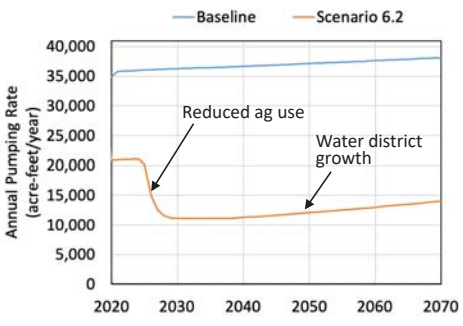

Artificial Recharge

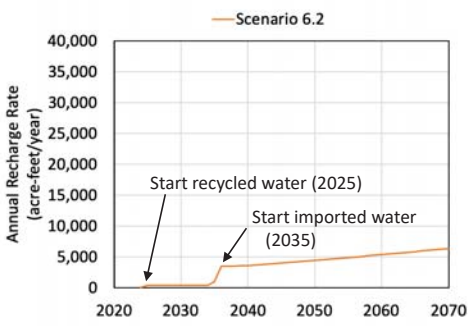

Net Pumping

Pumping minus artificial recharge

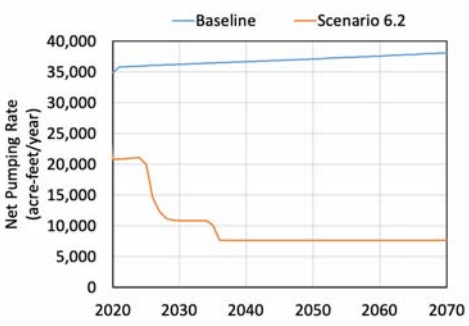

Groundwater Flow Prior to Development

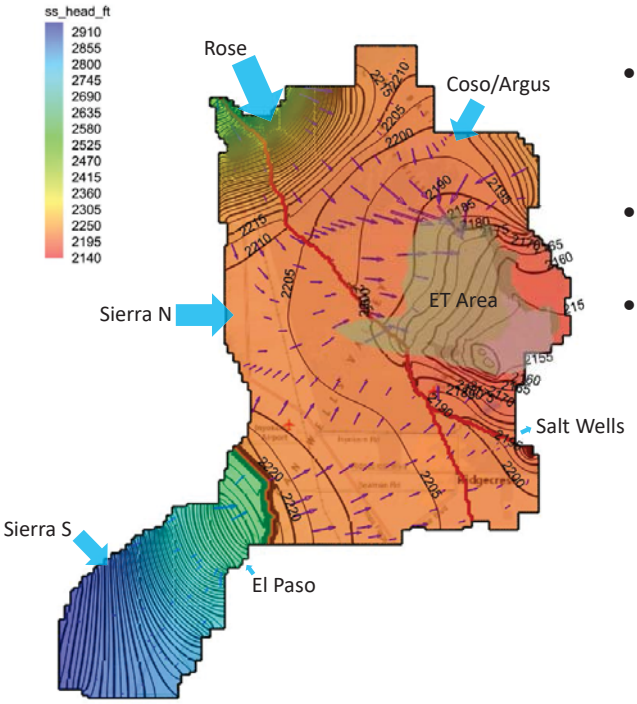

- Groundwater flow simulated from recharge areas to discharge at playa (ET) and toward Salt Wells Valley
- Flow parallel to northern Little Lake Fault where fault conductivity is lower
- Flow crosses Little Lake Fault where fault conductivity is higher

LEGEND
- Faults
- Contours of simulated heads (ft amsl)
- Vectors showing direction and relative magnitude of groundwater flow rates

Map shows results for Layer 1 of the steady-state model

Pumping Effects on Groundwater Flow Directions

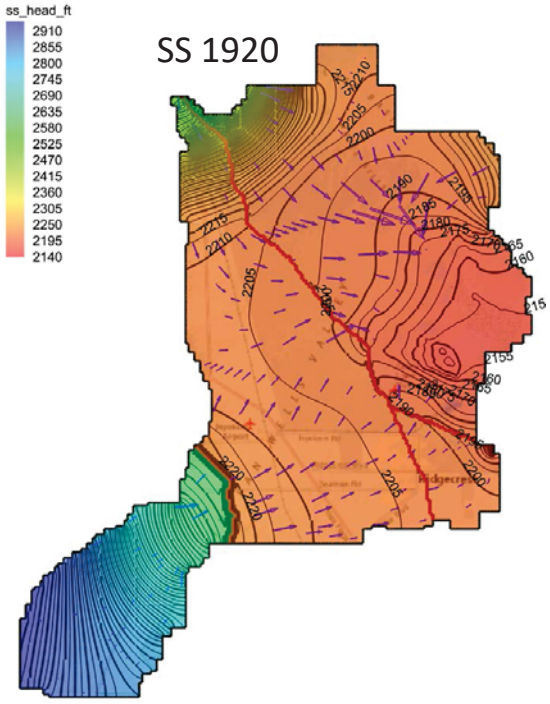

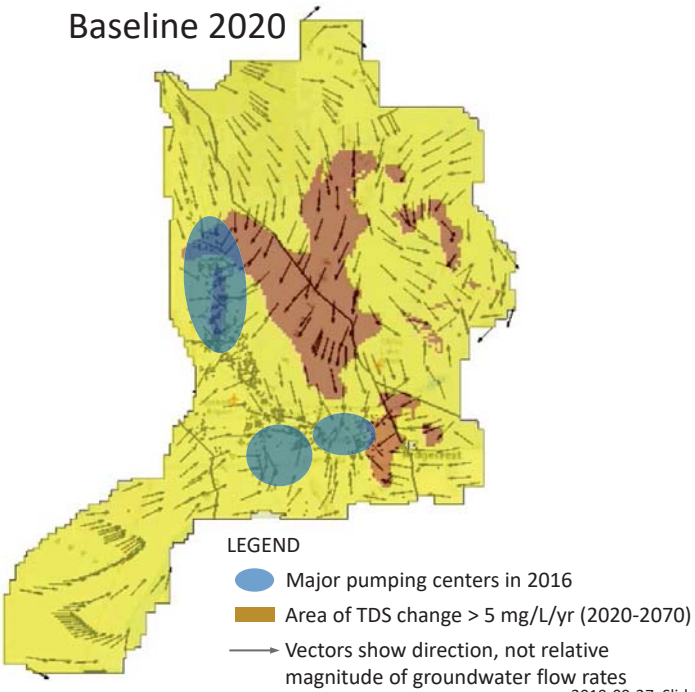

Groundwater Flow Directions in 2030

Baseline

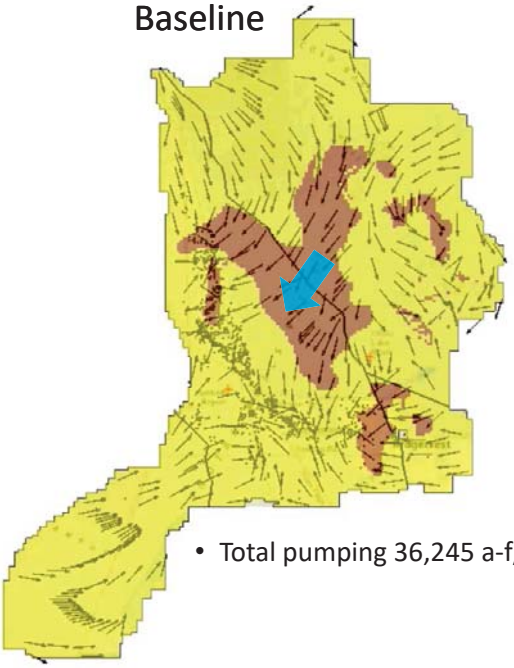

- Total pumping 36,245 a-f/yr

Scenario 6.2

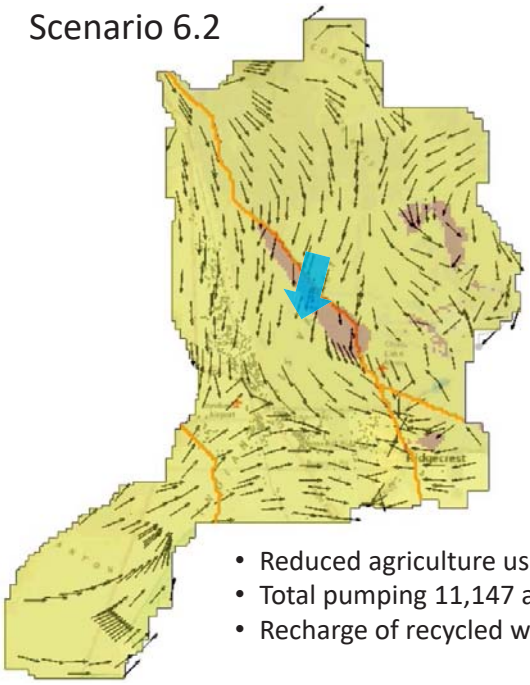

- Reduced agriculture use
- Total pumping 11,147 a-f/yr
- Recharge of recycled water starts 2025

Groundwater Flow Directions in 2050

Baseline

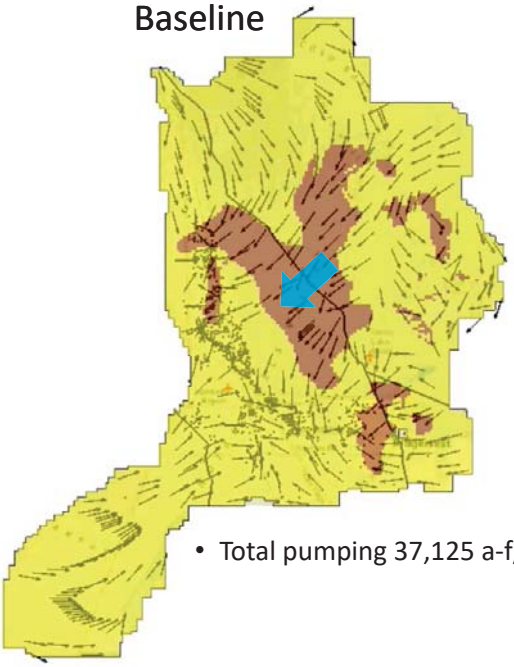

- Total pumping 37,125 a-f/yr

Scenario 6.2

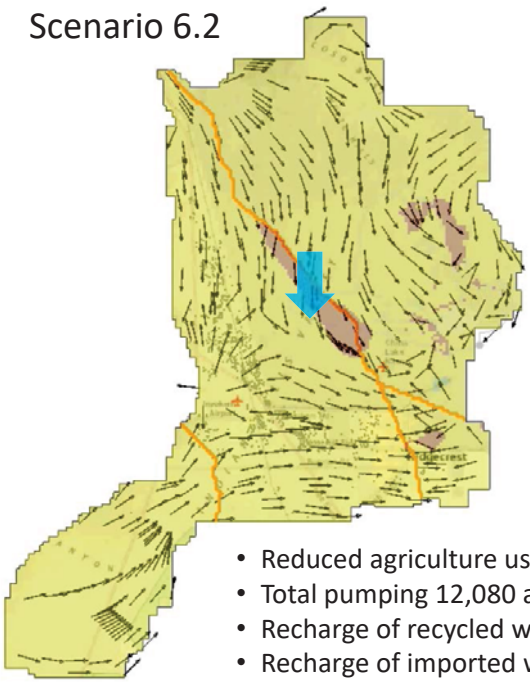

- Reduced agriculture use
- Total pumping 12,080 a-f/yr
- Recharge of recycled water starts 2025
- Recharge of imported water starts 2035

Groundwater Flow Directions in 2070

Baseline

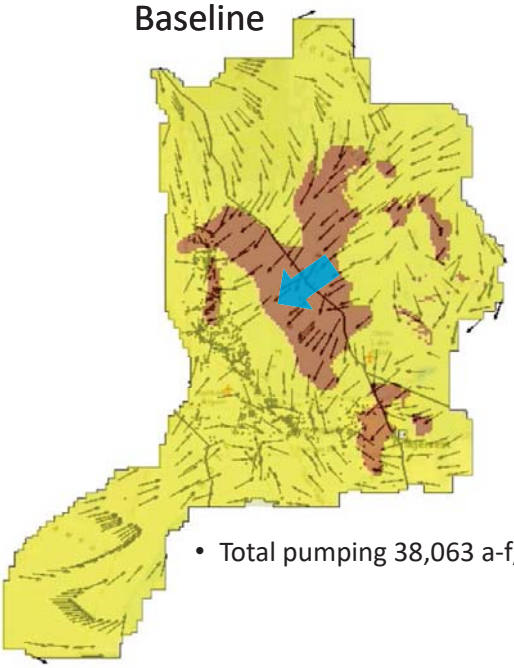

- Total pumping 38,063 a-f/yr

Scenario 6.2

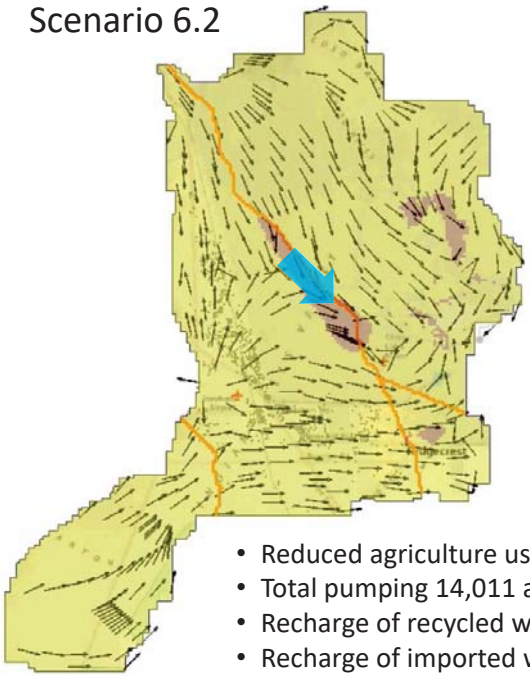

- Reduced agriculture use
- Total pumping 14,011 a-f/yr
- Recharge of recycled water starts 2025
- Recharge of imported water starts 2035

Groundwater Level Changes 2020 - 2070

Baseline

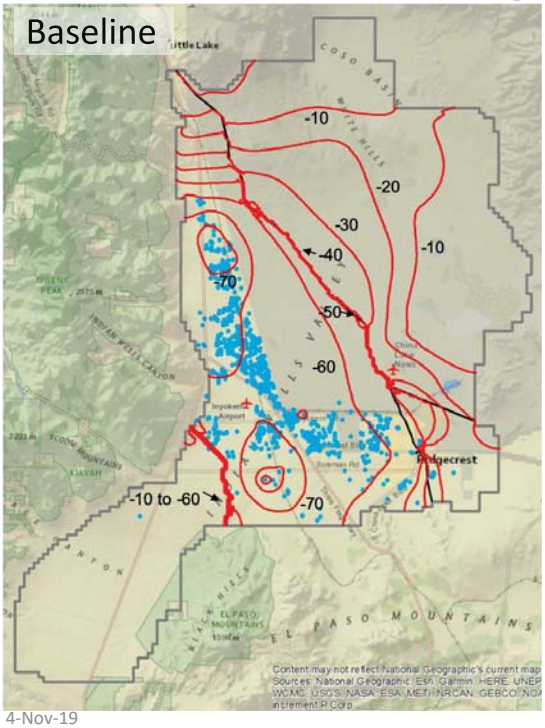

Rising
No change
Falling

Scenario 6.2

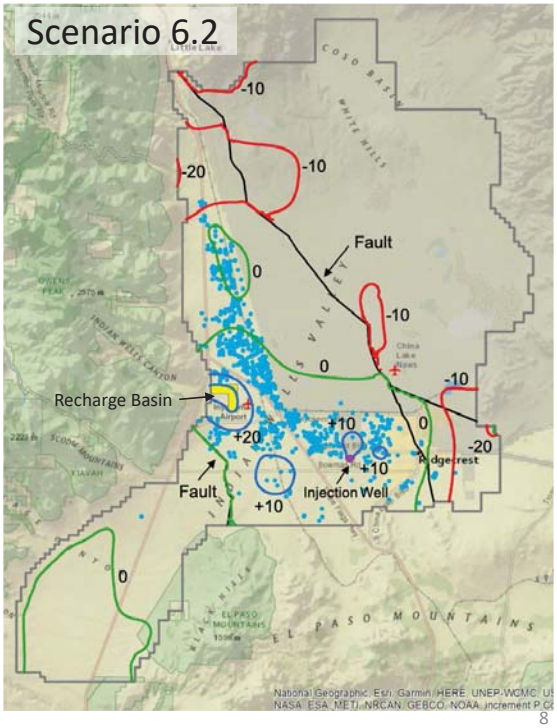

Groundwater Level Changes 2020 - 2070

Baseline

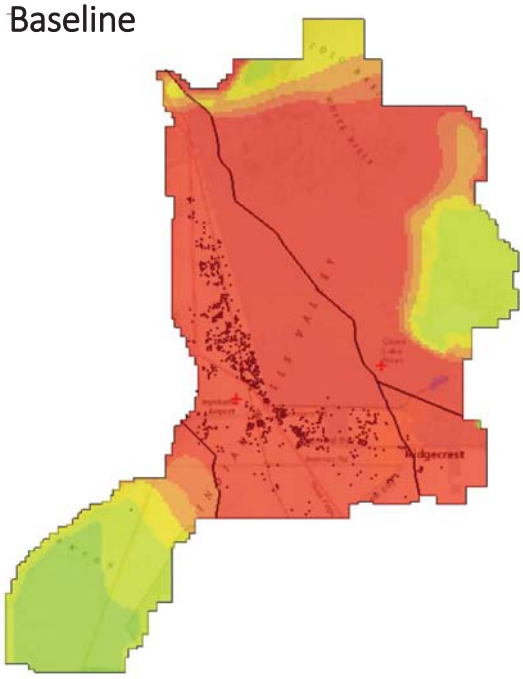

Scenario 6.2

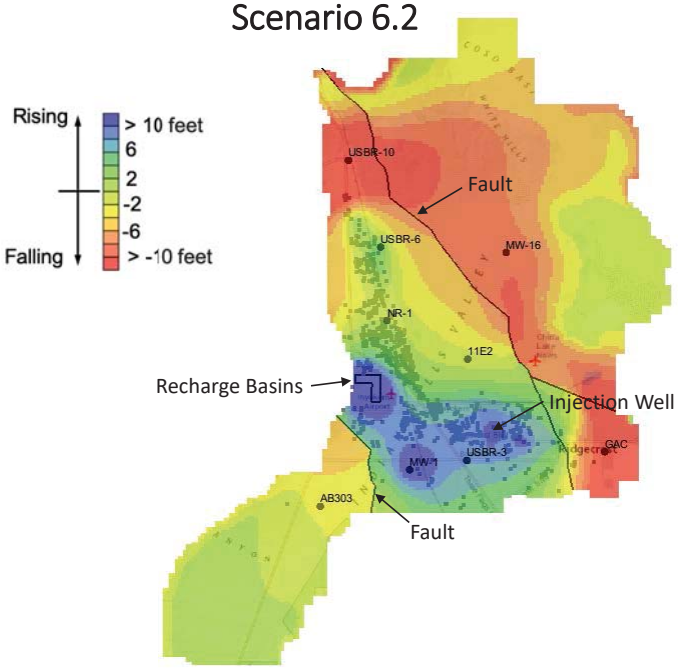

Results from TDS Transport Model Scenario 6.2

Comparison with Baseline

TDS Transport Models

TDS Sources
- Natural recharge
- Artificial recharge (Scenario 6.2)
  Imported: 280 mg/L
  Recycled: 250 mg/L
- Mixing with higher-TDS GW
- Concentration by evaporation

TDS Sinks
- Extraction wells
- Discharge to Salt Wells Valley

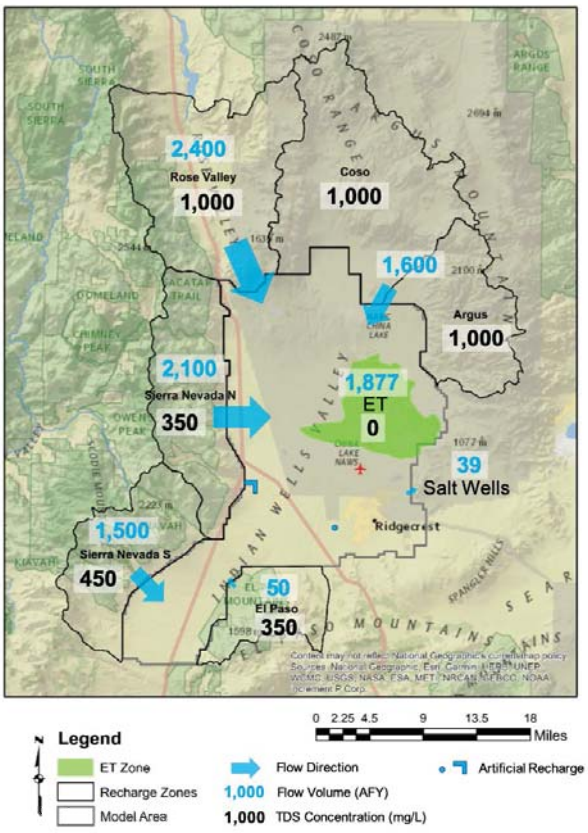

Initial Conditions for TDS Concentration

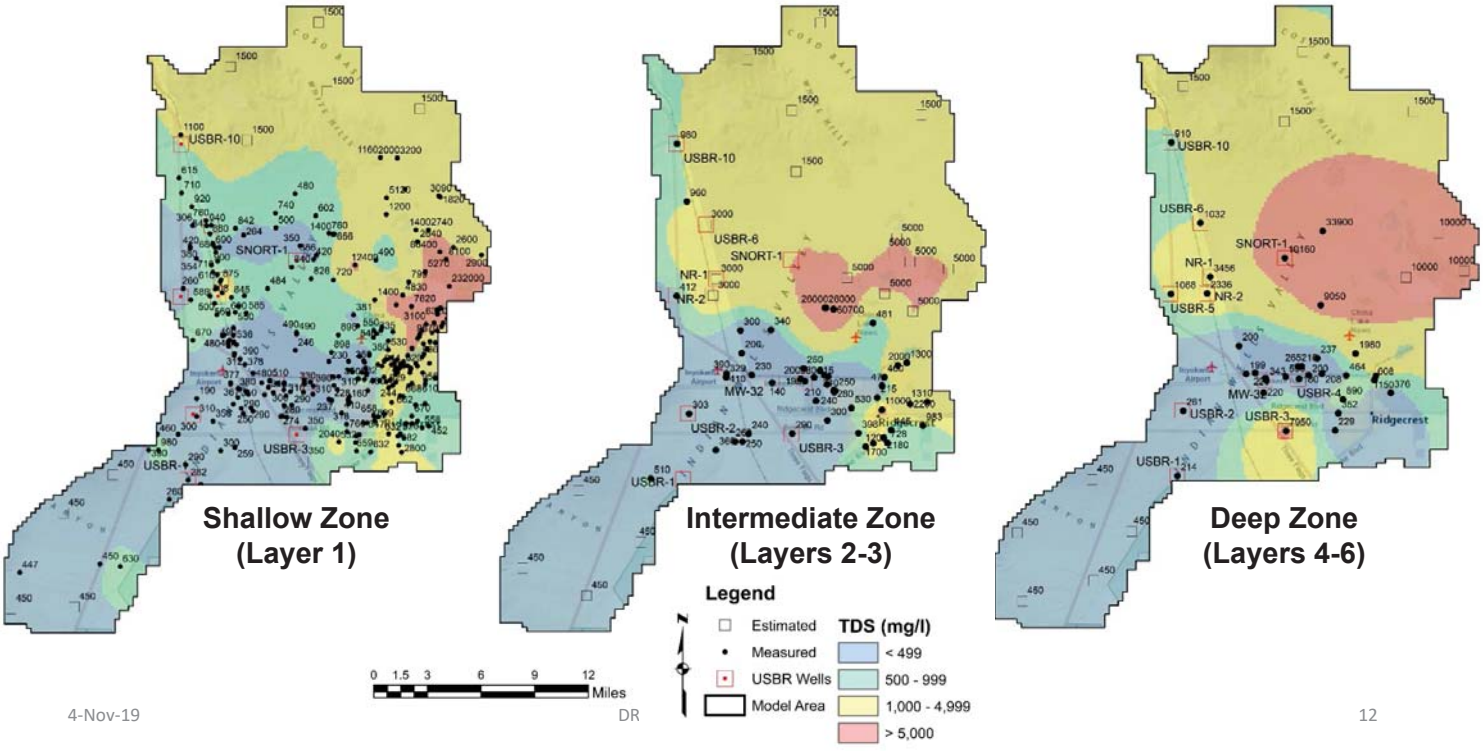

TDS Concentrations in 2030 in the Shallow Zone

Baseline

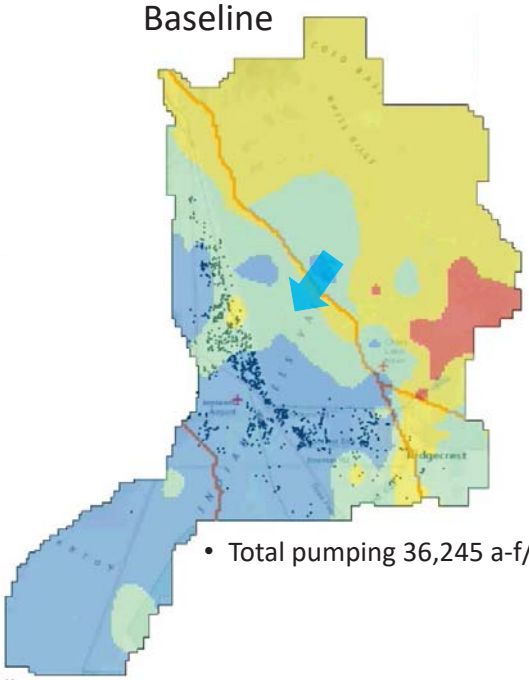

- Total pumping 36,245 a-f/yr

Scenario 6.2

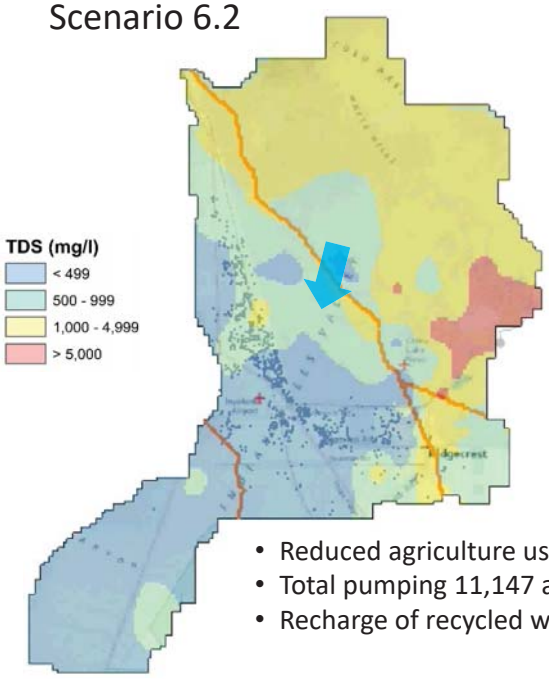

- Reduced agriculture use
- Total pumping 11,147 a-f/yr
- Recharge of recycled water starts 2025

TDS Concentrations in 2050 in the Shallow Zone

Baseline

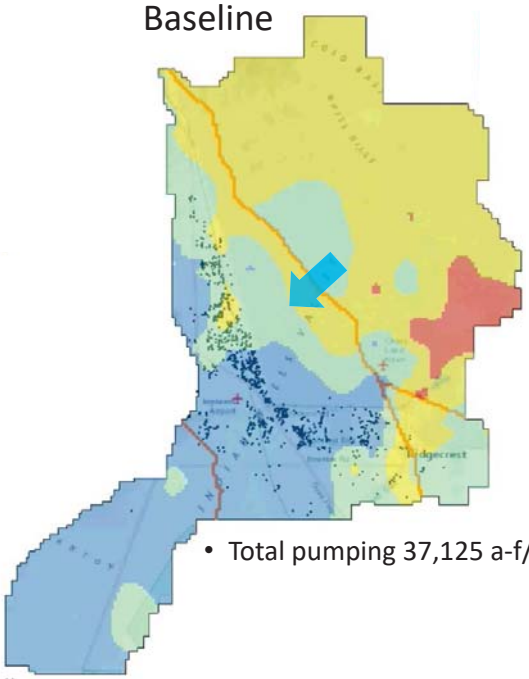

- Total pumping 37,125 a-f/yr

Scenario 6.2

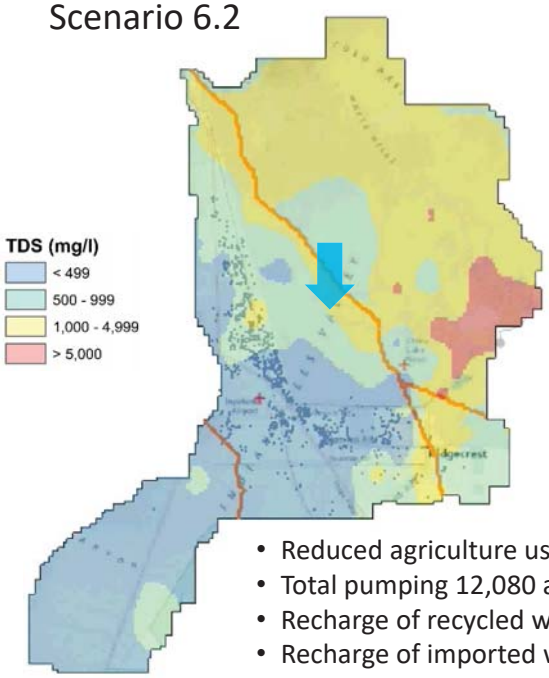

- Reduced agriculture use
- Total pumping 12,080 a-f/yr
- Recharge of recycled water starts 2025
- Recharge of imported water starts 2035

TDS Concentrations in 2070 in the Shallow Zone

Baseline

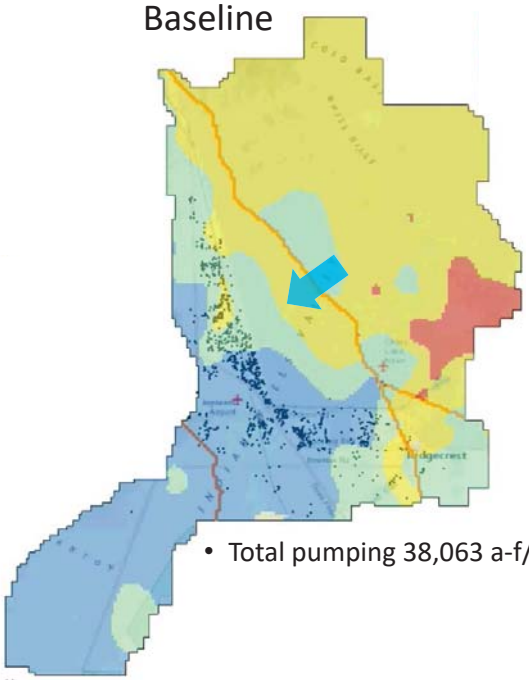

- Total pumping 38,063 a-f/yr

Scenario 6.2

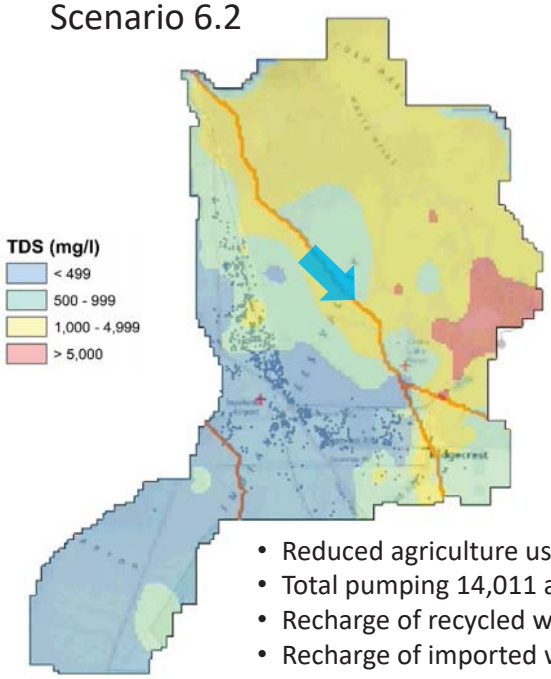

- Reduced agriculture use
- Total pumping 14,011 a-f/yr
- Recharge of recycled water starts 2025
- Recharge of imported water starts 2035

TDS Concentration Trends 2020 through 2070 – All Zones

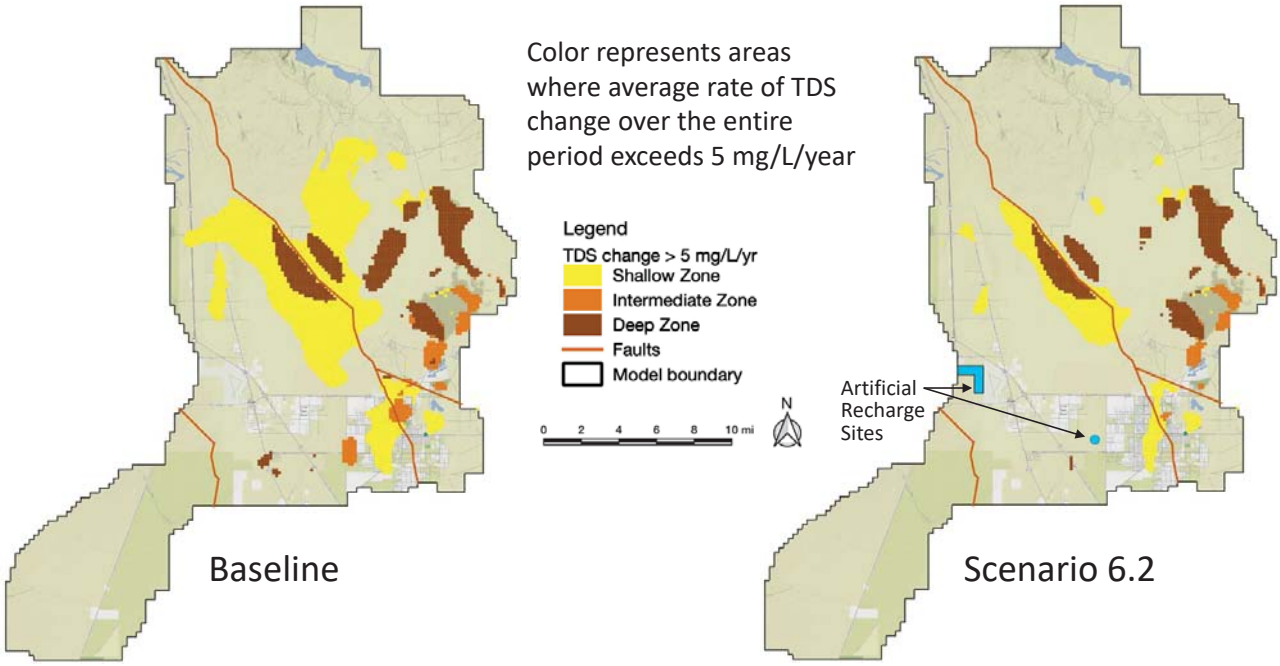

APPENDIX 4-A

NAVY LETTER ON ENCROACHMENT CONCERN

(Page Intentionally Left Blank)

DEPARTMENT OF THE NAVY
NAVAL AIR WEAPONS STATION
1 ADMINISTRATION CIRCLE
CHINA LAKE CA 93555-6100

IN REPLY REFER TO
1000
Ser N00/034
20 Feb 19

Board of Directors
Indian Wells Valley Ground Water Authority (IWVGWA)
Ridgecrest, California 93555

Dear Members of the Board:

Subj: GROUNDWATER RESOURCES

1. This letter serves to formally communicate that Commander Navy Region Southwest (CNRSW), in consultation with U.S. Navy commands located within the Indian Wells Valley, deems groundwater resources as the number one encroachment concern/issue which has the potential to impact missions enabled on and around Naval Air Weapons Station China Lake (NAWSCL). Water sustainability is critical to NAWSCL's mission accomplishment.

2. The Navy's human capital and its ability to recruit and retain talented personnel is integral to these critical national defense missions. We must emphasize the importance of Navy civilian and military personnel's continued access to economically viable potable water as critical to the IWVGWA's implementation of the Sustainable Groundwater Management Act (SGMA).

3. The Navy has leaned forward for decades, reducing water consumption on the installation by 54 percent since 2007, funding the Desert Research Institute modeling effort that the IWVGWA is now utilizing, and voluntarily providing reports of its groundwater extractions to assist the basin in understanding the Navy's current water use. NAWSCL engages in these initiatives as a matter of comity and as a good neighbor, rather than state law and local ordinance mandates. The purpose of this cooperative posture is to help the IWVGWA with comprehensive planning efforts to achieve groundwater sustainability as directed by the SGMA.

4. NAWSCL relies entirely upon groundwater as its sole source of potable water. In implementing SGMA, the Department of Water Resources (DWR) classified the Indian Wells Valley (IWV) groundwater basin as "Critically Over Drafted" in January 2016. Therefore, an imbalance between pumping and recharge associated with the basin creates growing concern, despite the efforts and cooperation of community stakeholders.

5. NAWSCL has engaged in consistent, proactive, and cooperative advocacy since the standup of the IWVGWA via a Joints Powers Agreement, with formal recognition as Ex-Officio non-voting Liaison on the IWVGA Board, active participation on the Technical Advisory Committee, Public Advisory Committee, SKYTEM, and other data gathering efforts to supplement the modeling effort. In addition, NAWSCL has committed, per my letter to you dated February 12, 2019, to submitting proposed projects for higher headquarters' consideration as applicable under FY19 NDAA. NAWSCL has a vested interest in participating in the SGMA effort with

IWVGWA as lead and responsible for developing a plan for the groundwater basin to achieve a sustainable yield in 20 years.

6. The Navy appreciates that IWVGWA recognizes the unique position of NAWSCL's Federal Reserve Water Rights (FRWR) dating back in time to when the base was established in 1943. The SGMA statute itself recognizes that FRWRs shall be respected in full, and in the case of any conflict, federal law will prevail. CA Water Code Section 10720.3(d). IWVGWA has also recognized the fact that there is no waiver of sovereign immunity subjecting the Navy to GW regulation, pumping limitations, or fee assessment. Despite these unique federal legal limitations, NAWSCL intends to continue to be a good neighbor and work cooperatively with the IWVGWA.

7. In summary, we appreciate the magnitude of the task ahead for the IWVGWA.

P. M. DALE
Captain, USN
Commanding Officer

APPENDIX 4-B

REGIONAL WATER QUALITY CONTROL BOARD WATER QUALITY OBJECTIVES

(Page Intentionally Left Blank)

Chapter 3
WATER QUALITY OBJECTIVES

The Porter-Cologne Water Quality Control Act defines "water quality objectives" as the allowable "limits or levels of water quality constituents or characteristics that are established for the reasonable protection of beneficial uses of water or the prevention of nuisance within a specific area." Thus, water quality objectives are intended to protect the public health and welfare, and to maintain or enhance water quality in relation to the existing and/or potential beneficial uses of the water. The objectives, when compared to future water quality data, will also provide the basis for detecting any future trend toward degradation or enhancement of basin waters.

The water quality objectives in this Basin Plan supersede and replace those contained in:

The 1975 *Water Quality Control Plan for the North Lahontan Basin,* as amended through 1990, and

The 1975 *Water Quality Control Plan for the South Lahontan Basin,* as amended through 1990, and

The 1980 *Lake Tahoe Basin Water Quality Plan*, as amended through 1989.

Water quality objectives apply to "waters of the State" and "waters of the United States." Some of the waters of the Lahontan Region are interstate waters, flowing into either Nevada or Oregon. The Lahontan Regional Board has a responsibility to ensure that waters leaving the state meet the water quality standards of the receiving state (see the discussion of "Interstate Issues" in the Introduction to Chapter 4).

Water Quality Standards

The federal Clean Water Act defines "water quality standards" to include both "designated uses" (i.e., beneficial uses) and "water quality criteria" (i.e., water quality objectives). Thus, the beneficial uses designated in Chapter Two of this Basin Plan and the water quality objectives of this Chapter are this Region's water quality standards for purposes of the Clean Water Act.

In addition to state water quality objectives, federal water quality criteria for certain toxic "priority pollutants" promulgated by the U.S. Environmental Protection Agency under the California Toxics Rule (40 CFR 131.38) and National Toxics Rule (40 CFR 131.36) apply to surface waters of the United States within the Lahontan Region. Most federal water quality criteria are recommended, science-based thresholds for the protection of aquatic life or human health that can be used by states to set enforceable limits. The criteria in the California Toxics Rule and National Toxics Rule are enforceable and are incorporated in the State Water Board's *Policy for Implementation of Toxics Standards for Inland Surface Waters, Enclosed Bays, and Estuaries of California (2005)*.

Water Quality Objectives and Effluent Limits

It is important to recognize the distinction between ambient water quality objectives and "effluent limitations" or "discharge standards," which are conditions in state and federal waste discharge permits. Effluent limitations are established in permits both to protect water for beneficial uses within the area of the discharge, and to meet or achieve water quality objectives.

Methodology For Establishing Water Quality Objectives

Water quality objectives are numerical or narrative. Narrative and numerical water quality objectives define the upper concentration or other limits that the Regional Board considers protective of beneficial uses.

The general methodology used in establishing water quality objectives involves, first, designating beneficial water uses; and second, selecting and quantifying the water quality parameters necessary to protect the most vulnerable (sensitive) beneficial uses. Because of the limited human impact on many waters of the Region, and because site-specific information is limited for many waters in the Region, many water quality objectives were established at levels better than that necessary to protect the most vulnerable beneficial use. As additional information is obtained on the quality of the Region's waters and/or the beneficial uses of those waters, certain water quality objectives and/or beneficial uses may be updated based on the new information.

In establishing water quality objectives, factors in addition to designated beneficial uses are considered. These factors include environmental and economic considerations specific to each hydrologic unit, the need to develop and use

recycled water, as well as the level of water quality that could be achieved through coordinated control of all factors that affect water quality in an area. Controllable water quality factors are those actions, conditions, or circumstances resulting from human activities that may influence the quality of the waters of the State, and that may be reasonably controlled.

Water quality objectives can be reviewed and, if appropriate, revised by the Lahontan Regional Board. Revised water quality objectives would then be adopted as part of this Basin Plan by amendment. Opportunities for formal public review of water quality objectives will be available at a minimum of once every three years following the adoption of this Basin Plan to determine the need for further review and revision.

As a component of the State's continuing planning process, data may be collected and numerical water quality objectives may be developed for additional water bodies and/or constituents where sufficient information is presently not available for the establishment of such objectives. If appropriate, these objectives may be adopted by the Regional Board and amended to this Basin Plan. Since 1997, scientific peer review has been required for changes in regulations, including water quality objectives that require scientific justification.

Establishment of Numerical Objectives for Specific Water Bodies

Where available data were sufficient to define existing ambient levels of constituents, these levels were used in developing the numerical objectives for specific water bodies. By utilizing annual mean, 90th percentile values and flow-weighted values, the objectives are intended to be realistic within the variable conditions imposed by nature. This approach provides an opportunity to detect changes in water quality as a function of time through comparison of annual means, while still accommodating variations in the measured constituents.

Prohibited Discharges

Discharges that cause violation of any narrative or numerical water quality objective are prohibited. (See also Section 4.1, “Waste Discharge Prohibitions.”)

After application of reasonable control measures, ambient water quality shall conform to the narrative and numerical water quality objectives included in this Basin Plan. When other factors result in the degradation of water quality beyond the limits established by these water quality objectives, controllable human activities shall not cause further degradation of water quality in either surface or ground waters.

Compliance with Water Quality Objectives

The purpose of text, in italics, following certain water quality objectives is to provide specific direction on compliance with the objective. General direction on compliance with objectives is described in the last section of this Chapter. It is not feasible to cover all circumstances and conditions that could be created by all discharges. Therefore, it is within the discretion of the Regional Board to establish other, or additional, direction on compliance with objectives of this Basin Plan. The purpose of the italic text is to provide direction only, and **not** to specify method of compliance.

Antidegradation Policy

On October 28, 1968, the State Water Resources Control Board adopted Resolution No. 68-16, “Statement of Policy with Respect to Maintaining High Quality of Waters in California,” establishing an antidegradation policy for the protection of water quality. This policy requires continued maintenance of existing high quality waters. Whenever the existing quality of water is better that the quality of water established in this Basin Plan as objectives (both narrative and numerical), such existing quality shall be maintained unless appropriate findings are made under the policy. The U.S. Environmental Protection Agency, Region IX, has also issued detailed guidelines for implementation of federal antidegradation regulations for surface waters (40 CFR 131.12). For more information, see the discussion on “General Direction Regarding Compliance With Objectives” at the end of this Chapter.

As required by the federal Clean Water Act and implementing regulations, no permanent or long-term degradation is allowed in water designated as an Outstanding National Resource Water (ONRW). Lake Tahoe and Mono Lake have been designated as ONRWs; other waters in the Region may be designated as ONRWs in the future. Section 114 of the federal Clean Water Act also indicates the need to “preserve the fragile ecology of Lake Tahoe.”

Water Quality Objectives for Surface Waters

Water quality objectives for surface waters are divided into the three categories of:

1. **Water Quality Objectives That Apply to All Surface Waters.**

   Listed alphabetically below, these narrative and numerical water quality objectives apply to a**ll** surface waters (including wetlands) within the Lahontan Region:

   Ammonia
   Bacteria, Coliform
   Biostimulatory Substances
   Chemical Constituents
   Chlorine, Total Residual
   Color
   Dissolved Oxygen
   Floating Materials
   Oil and Grease
   Non-degradation of Aquatic Communities and Populations
   pH
   Radioactivity
   Sediment
   Settleable Materials
   Suspended Materials
   Taste and Odor
   Temperature
   Toxicity
   Turbidity

2. **Water Quality Objectives For Certain Water Bodies**

   Some narrative and numerical water quality objectives are directed toward protection of surface waters (including wetlands) in specific areas. To the extent of overlap, these site-specific water quality objectives supersede the "Water Quality Objectives That Apply to All Surface Waters" described above. The areas for which site-specific objectives have been adopted are listed below in order of hydrologic units (HUs) and hydrologic areas (HAs) within the Lahontan Region, in a north to south direction:

HU/HA	Figure	Table
Surprise Valley HU	3-1	3-7
Eagle Drainage HA	3-2	3-8
Susanville HU	3-3	3-9
Little Truckee River HU	3-4	3-10
Truckee River HU	3-5	3-11
Lake Tahoe HU	3-6	3-12
Fallen Leaf Lake	3-6	3-13
West Fork Carson River HU	3-7	3-14
East Fork Carson River HU	3-7	3-14
West Walker River HU	3-8	3-15
East Walker River HU	3-8	3-15
Mono HU	3-9	3-16
Owens HU	3-10	3-17
Pine Creek, Inyo Co.	3-11	3-18
Antelope HU	3-12	3-19
Mojave HU	3-13	3-20
San Bernardino Mtns. Area	3-14	3-21

3. **Water Quality Objectives for Fisheries Management Activities Using the Fish Toxicant Rotenone**

   Rotenone is a fish toxicant presently used by the California Department of Fish and Wildlife (DFW) and the United States Fish and Wildlife Service (USFWS) for fishery management purposes. (See detailed discussions later in this Chapter and in Chapter 4.) Additional water quality objectives pertinent to rotenone treatments are: Color, Chemical Constituents, and Toxicity.

Water Quality Objectives That Apply to All Surface Waters

Ammonia

The neutral, un-ionized ammonia species (NH_3) is highly toxic to freshwater fish. The fraction of toxic $NH_3$to total ammonia species ($NH_4^+ + NH_3$) is a function of temperature and pH. Tables 3-1 to 3-4 were derived from USEPA ammonia criteria for freshwater. Ammonia concentrations shall not exceed the values listed for the corresponding conditions in these tables. For temperature and pH values not explicitly in these tables, the most conservative value neighboring the actual value may be used or criteria can be calculated from numerical formulas developed by the USEPA. For one-hour ($1h\text{-}NH_3$) and four-day ($4d\text{-}NH_3$) unionized ammonia criteria, the following equations apply:

$1h\text{-}NH_3 = 0.52 \div (FT \times FPH \times 2)$

$4d\text{-}NH_3 = 0.80 \div (FT \times FPH \times RATIO)$

where:

$FT = 10^{[0.03(20-TCAP)]}$
for: $TCAP \leq T \leq 30$

$FT = 10^{[0.03(20-T)]}$
for: $0 \leq T \leq TCAP$

$FPH = (1+10^{(7.4-pH)}) \div 1.25$
for: $6.5 \leq pH \leq 8.0$

FPH = 1
for: 8.0≤pH≤9.0

RATIO = 20.25 x $(10^{(7.7-pH)})$ ÷ $(1+10^{(7.4-pH)})$
for: 6.5≤pH≤7.7

RATIO = 13.5
for: 7.7≤pH≤9.0

and:

T = temperature in °C

TCAP = temperature cap in °C

For 1h-NH_3, TCAP is 20°C with salmonids present and 25°C with salmonids absent. For 4d-NH_3, TCAP is 15°C with salmonids present and 20 C with salmonids absent.

For interpolation of total ammonia ($NH_4^+ + NH_3$) criteria, the following equations can be used:

n_{1h} = 1h-NH_3 ÷ f, or n_{4d} = 4d-NH_3 ÷ f

where:

n_{1h} is the one-hour criteria for total ammonia species ($NH_4^+ + NH_3$)

n_{4d} is the four-day criteria for total ammonia species ($NH_4^+ + NH_3$)

f = 1 ÷ $(10^{(pKa-pH)}+1)$

pKa = 0.0901821 + [2729.92 ÷ (T+273.15)]

and:

pKa is the negative log of the equilibrium constant for the $NH_4^+ \rightleftharpoons NH_3 + H^+$ reaction

f is the fraction of unionized ammonia to total ammonia species: [NH_3 ÷ ($NH_4^+ + NH_3$)]

Values outside of the ranges 0-30°C or pH 6.5-9.0 cannot be extrapolated from these relationships. Site-specific objectives must be developed for these conditions. A microcomputer spreadsheet to calculate ammonia criteria was developed by Regional Board staff. An example of output from this program is given in Table 3-5. Contact the Regional Board if a copy is desired.

Bacteria, Coliform

Waters shall not contain concentrations of coliform organisms attributable to anthropogenic sources, including human and livestock wastes.

The fecal coliform concentration during any 30-day period shall not exceed a log mean of 20/100 ml, nor shall more than 10 percent of all samples collected during any 30-day period exceed 40/100 ml. *The log mean shall ideally be based on a minimum of not less* than *five samples collected as evenly spaced as practicable during any 30-day period. However, a log mean concentration exceeding 20/100 ml for any 30-day period shall indicate violation of this objective even if fewer than five samples were collected.*

Biostimulatory Substances

Waters shall not contain biostimulatory substances in concentrations that promote aquatic growths to the extent that such growths cause nuisance or adversely affect the water for beneficial uses.

Chemical Constituents

Waters designated as MUN shall not contain concentrations of chemical constituents in excess of the maximum contaminant level (MCL) or secondary maximum contaminant level (SMCL) based upon drinking water standards specified in the following provisions of Title 22 of the California Code of Regulations, which are incorporated by reference into this plan: Table 64431-A of Section 64431 (Inorganic Chemicals), Table 64431-B of Section 64431 (Fluoride), Table 64444-A of Section 64444 (Organic Chemicals), Table 64449-A of Section 64449 (Secondary Maximum Contaminant Levels-Consumer Acceptance Limits), and Table 64449-B of Section 64449 (Secondary Maximum Contaminant Levels-Ranges). This incorporation-by-reference is prospective including future changes to the incorporated provisions as the changes take effect.

Waters designated as AGR shall not contain concentrations of chemical constituents in amounts that adversely affect the water for beneficial uses (i.e., agricultural purposes).

Waters shall not contain concentrations of chemical constituents in amounts that adversely affect the water for beneficial uses.

Chlorine, Total Residual

For the protection of aquatic life, total chlorine residual shall not exceed either a median value of 0.002 mg/L or a maximum value of 0.003 mg/L. Median values shall be based on daily measurements taken within any six-month period.

Color

Waters shall be free of coloration that causes nuisance or adversely affects the water for beneficial uses.

Dissolved Oxygen

The dissolved oxygen concentration, as percent saturation, shall not be depressed by more than 10 percent, nor shall the minimum dissolved oxygen

concentration be less than 80 percent of saturation.

For waters with the beneficial uses of COLD, COLD with SPWN, WARM, and WARM with SPWN, the minimum dissolved oxygen concentration shall not be less than that specified in Table 3-6.

Floating Materials

Waters shall not contain floating material, including solids, liquids, foams, and scum, in concentrations that cause nuisance or adversely affect the water for beneficial uses.

For natural high quality waters, the concentrations of floating material shall not be altered to the extent that such alterations are discernable at the 10 percent significance level.

Oil and Grease

Waters shall not contain oils, greases, waxes or other materials in concentrations that result in a visible film or coating on the surface of the water or on objects in the water, that cause nuisance, or that otherwise adversely affect the water for beneficial uses.

For natural high quality waters, the concentration of oils, greases, or other film or coat generating substances shall not be altered.

Nondegradation of Aquatic Communities and Populations

All wetlands shall be free from substances attributable to wastewater or other discharges that produce adverse physiological responses in humans, animals, or plants; or that lead to the presence of undesirable or nuisance aquatic life.

All wetlands shall be free from activities that would substantially impair the biological community as it naturally occurs due to physical, chemical and hydrologic processes.

pH

In fresh waters with designated beneficial uses of COLD or WARM, changes in normal ambient pH levels shall not exceed 0.5 pH units. For all other waters of the Region, the pH shall not be depressed below 6.5 nor raised above 8.5.

The Regional Board recognizes that some waters of the Region may have natural pH levels outside of the 6.5 to 8.5 range. Compliance with the pH objective for these waters will be determined on a case-by-case basis.

Radioactivity

Radionuclides shall not be present in concentrations that are deleterious to human, plant, animal, or aquatic life or that result in the accumulation of radionuclides in the food web to an extent that presents a hazard to human, plant, animal, or aquatic life.

Waters designated as MUN shall not contain concentrations of radionuclides in excess of the limits specified in Table 4 of Section 64443 (Radioactivity) of Title 22 of the California Code of Regulations, which is incorporated by reference into this plan. This incorporation-by-reference is prospective including future changes to the incorporated provisions as the changes take effect.

Sediment

The suspended sediment load and suspended sediment discharge rate of surface waters shall not be altered in such a manner as to cause nuisance or adversely affect the water for beneficial uses.

Settleable Materials

Waters shall not contain substances in concentrations that result in deposition of material that causes nuisance or that adversely affects the water for beneficial uses. For natural high quality waters, the concentration of settleable materials shall not be raised by more than 0.1 milliliter per liter.

Suspended Materials

Waters shall not contain suspended materials in concentrations that cause nuisance or that adversely affects the water for beneficial uses.

For natural high quality waters, the concentration of total suspended materials shall not be altered to the extent that such alterations are discernible at the 10 percent significance level.

Taste and Odor

Waters shall not contain taste or odor-producing substances in concentrations that impart undesirable tastes or odors to fish or other edible products of aquatic origin, that cause nuisance, or that adversely affect the water for beneficial uses. For naturally high quality waters, the taste and odor shall not be altered.

Temperature

The natural receiving water temperature of all waters shall not be altered unless it can be demonstrated to the satisfaction of the Regional

Board that such an alteration in temperature does not adversely affect the water for beneficial uses.

For waters designated WARM, water temperature shall not be altered by more than five degrees Fahrenheit (5°F) above or below the natural temperature. For waters designated COLD, the temperature shall not be altered.

Temperature objectives for COLD interstate waters and WARM interstate waters are as specified in the "Water Quality Control Plan for Control of Temperature in The Coastal and Interstate Waters and Enclosed Bays and Estuaries of California" including any revisions. This plan is summarized in Chapter 6 (Plans and Policies), and included in Appendix B.

Toxicity

All waters shall be maintained free of toxic substances in concentrations that are toxic to, or that produce detrimental physiological responses in human, plant, animal, or aquatic life. *Compliance with this objective will be determined by use of indicator organisms, analyses of species diversity, population density, growth anomalies, bioassays of appropriate duration and/or other appropriate methods as specified by the Regional Board.*

The survival of aquatic life in surface waters subjected to a waste discharge, or other controllable water quality factors, shall not be less than that for the same water body in areas unaffected by the waste discharge, or when necessary, for other control water that is consistent with the requirements for "experimental water" as defined in *Standard Methods for the Examination of Water and Wastewater* (American Public Health Association, et al. 2012, or subsequent editions).

Turbidity

Waters shall be free of changes in turbidity that cause nuisance or adversely affect the water for beneficial uses. Increases in turbidity shall not exceed natural levels by more than 10 percent.

Water Quality Objectives For Certain Water Bodies

The narrative and numerical water quality objectives that follow in this section are directed toward protection of surface waters (including wetlands) in certain hydrologic units (HUs), watersheds, or water bodies within the Lahontan Region. These surface waters are listed by hydrologic unit, in a north to south direction. Specific numerical criteria are organized in a tabular format. Maps (figures) are included to illustrate the locations of surface waters listed in the tables. Figures and tables are located at the end of the Chapter.

Surprise Valley Hydrologic Unit

(See Figure 3-1 and Table 3-7 for water quality objectives for the Surprise Valley HU.)

***Susanville* Hydrologic Un**it

(Figures 3-2 and 3-3, Tables 3-8 and 3-9)
Unless otherwise specified, the following additional water quality objectives apply to all surface waters of the ***Eagle Drainage Hydrologic Area*** (Figure 3-2):

Algal Growth Potential: The mean monthly mean of algal growth potential shall not be altered to the extent that such alterations are discernible at the 10 percent significance level.

Bacteria, Fecal Coliform

The fecal coliform concentration based on a minimum of not less than five samples for any 30-day period, shall not exceed a log mean of 20/100 ml, nor shall more than 10 percent of total samples during any 30-day period exceed 75/100 ml.

Biostimulatory Substances: The concentrations of biostimulatory substances shall not be altered in an amount that could produce an increase in aquatic biomass to the extent that such increases in aquatic biomass are discernible at the 10 percent significance level.

Chlorophyll-a: For the following Eagle Lake stations listed below and mapped in Figure 3-2, the chlorophyll-a levels, as measured in micrograms per liter on a mean of monthly mean basis, shall not exceed the following values:

Station	Chlorophyll-a
Middle Basin 4A	5.2
South Basin 11	4.5

Also, chlorophyll-a levels in Eagle Lake shall not be increased to the extent that such alterations are discernible at the 10 percent significance level.

Dissolved Oxygen: In all waters of Eagle Lake except for the hypolimnion, the dissolved oxygen concentration shall not be depressed by more than 10 percent, below 80 percent saturation, or below 7.0 mg/L at any time, whichever is more restrictive.

pH: In the hypolimnion of Eagle Lake, the pH shall not be depressed below 7.6 at any time. For all

other Eagle Lake waters, changes in normal ambient pH shall not exceed 0.1 units.

Plankton Counts: For the Eagle Lake stations listed below and mapped in Figure 3-2, total phytoplankton abundance as calculated per milliliter on a mean of monthly means basis shall not exceed the following values:

Station	Plankton Count (number per mL)
Middle Basin 4A	7,400
South Basin 11	4,600

Also, for the waters of Eagle Lake, the phytoplankton abundance shall not be increased to the extent that such alterations are discernible at the 10 percent significance level.

Species Composition: Species composition of the aquatic biota shall not be altered to the extent that such alterations are discernible at the 10 percent significance level.

Taste and Odor: The taste and odor shall not be altered.

Transparency: Transparency of Eagle Lake waters as measured by a secchi disk on a mean of monthly mean basis shall not fall below the following values for each of the three index stations mapped in Figure 3-2:

Station	Secchi Disk Transparency
North Basin 6B	3.1 meters
Middle Basin 4A	2.3 meters
South Basin 11	4.4 meters

Also, the secchi disk transparency of Eagle Lake waters shall not be decreased to the extent that such alterations are discernible at the 10 percent significance level.

The following additional water quality objectives apply to ***Honey Lake*** (Figure 3-3):

The average value at any given time (based on at least 3 samples from 3 different locations) shall not exceed:

Arsenic (in mg/L)
= 37,113 x (lake volume in acre-feet)$^{-0.98418}$

Boron (in mg/L)
= 836,820 x (lake volume in acre-feet)$^{-0.98133}$

Molybdenum (in mg/L)
= 16,667 x (lake volume in acre-feet)$^{-0.97658}$

The pH (based on the average of values from at least 3 samples from 3 different locations) shall not at any time be depressed below 8.0 nor raised above 10.0.

Little Truckee River Hydrologic Unit

(Figure 3-4, Table 3-10)
The following additional water quality objectives apply to all surface waters of the Little Truckee River Hydrologic Unit:

Algal Growth Potential: The mean monthly algal growth potential shall not be altered to the extent that such alterations are discernible at the 10 percent significance level.

Biostimulatory Substances: The concentration of biostimulatory substances shall not be altered in an amount that could produce an increase in aquatic biomass to the extent that such increases are discernible at the 10 percent significance level.

Color: The color shall not exceed an eight (8) Platinum Cobalt Unit mean of monthly means [approximately equivalent to the State of Nevada standard of a twelve (12) Platinum Cobalt Unit sample mean].

Dissolved Oxygen: The dissolved oxygen concentration shall not be depressed by more than 10 percent, below 80 percent saturation, or below 7.0 mg/L at any time, whichever is more restrictive.

pH: Changes in normal ambient pH levels shall not exceed 0.5 unit.

Species Composition: The species composition of aquatic organisms shall not be altered to the extent that such alterations are discernible at the 10 percent significance level.

Taste and Odor: The taste and odor shall not be altered.

Turbidity: The turbidity shall not be raised above 3 Nephelometric Turbidity Units (NTU) mean of monthly means. (This objective is approximately equal to the State of Nevada standard of 5 NTU sample mean.)

Truckee River Hydrologic Unit

(Figure 3-5, Table 3-11)
Unless otherwise specified, the following additional water quality objectives apply to all surface waters of the Truckee River Hydrologic Unit:

Algal Growth Potential: The mean monthly algal growth potential shall not be altered to the extent that such alterations are discernible at the 10

percent significance level. This objective does not apply to Martis Creek; however, nuisance or pollution levels of algal growth potential shall not be discernible at these stations.

Biostimulatory Substances: The concentration of biostimulatory substances shall not be altered in an amount that could produce an increase in aquatic biomass to the extent that such increases are discernible at the 10 percent significance level. This objective does not apply to Martis Creek or the Truckee River stations downstream of Martis Creek; however, no nuisance or pollution levels of algal biomass shall be discernible at these stations at any time.

Color: The color shall not exceed an eight (8) Platinum Cobalt Unit mean of monthly means (approximately equivalent to the State of Nevada standard of a twelve (12) Platinum Cobalt Unit sample mean).

Dissolved Oxygen: The dissolved oxygen concentrations shall not be depressed by more than 10 percent, below 80 percent saturation, or below 7.0 mg/L at any time, whichever is more restrictive.

pH: Changes in normal ambient pH levels shall not exceed 0.5 unit.

Species Composition: The species composition of aquatic organisms shall not be altered to the extent that such alterations are discernible at the 10 percent significance level. This objective does not apply to Martis Creek or the Truckee River stations downstream of Martis Creek; however, alterations in species composition that result in a nuisance or pollution shall not be discernible at these stations at any time.

Taste and Odor: The taste and odor shall not be altered.

Turbidity: The turbidity shall not be raised above 3 Nephelometric Turbidity Units (NTU) mean of monthly means. (This objective is approximately equal to the State of Nevada standard of 5 NTU sample mean.)

Lake Tahoe Hydrologic Unit

(Figure 3-6, Tables 3-12 and 3-13)

Unless otherwise specified, the following additional water quality objectives apply to all waters of the Lake Tahoe Hydrologic Unit:

Algal Growth Potential: For Lake Tahoe, the mean algal growth potential at any point in the Lake shall not be greater than twice the mean annual algal growth potential at the limnetic reference station. *The limnetic reference station is located in the north central portion of Lake Tahoe. It is shown on maps in annual reports of the Lake Tahoe Interagency Monitoring Program. Exact coordinates can be obtained from the U.C. Davis Tahoe Research Group.*

Biological Indicators: For Lake Tahoe, algal productivity and the biomass of phytoplankton, zooplankton, and periphyton shall not be increased beyond the levels recorded in 1967-71, based on statistical comparison of seasonal and annual means. *The "1967-71 levels" are reported in the annual summary reports of the "California-Nevada-Federal Joint Water Quality Investigation of Lake Tahoe" published by the California Department of Water Resources.*

Clarity: For Lake Tahoe, the vertical extinction coefficient shall be less than 0.08 per meter when measured below the first meter. When water is too shallow to determine a reliable extinction coefficient, the turbidity shall not exceed 3 Nephelometric Turbidity Units (NTU). In addition, turbidity shall not exceed 1 NTU in shallow waters not directly influenced by stream discharges. *The Regional Board will determine when water is too shallow to determine a reliable vertical extinction coefficient based upon its review of standard limnological methods and on advice from the U.C. Davis Tahoe Research Group.*

Conductivity, Electrical: In Lake Tahoe, the mean annual electrical conductivity shall not exceed 95 µmhos/cm at 25°C at any location in the Lake.

pH: In Lake Tahoe, the pH shall not be depressed below 7.0 nor raised above 8.4.

Plankton Counts: For Lake Tahoe, the mean seasonal concentration of plankton organisms shall not be greater than 100 per ml and the maximum concentration shall not be greater than 500 per ml at any point in the Lake.

Suspended Sediment: Suspended sediment concentrations in streams tributary to Lake Tahoe shall not exceed a 90th percentile value of 60 mg/L. (This objective is equivalent to the Tahoe Regional Planning Agency's regional "environmental threshold carrying capacity" standard for suspended sediment in tributaries.) *The Regional Board will consider revision of this objective in the future if it proves not to be protective of beneficial uses or if review of*

monitoring data indicates that other numbers would be more appropriate for some or all streams tributary to Lake Tahoe.

Transparency: For Lake Tahoe, the annual average deep water transparency as measured by the Secchi disk shall not be decreased below 29.7 meters, the levels recorded in 1967-71 by the University of California, Davis.

Turbidity: see "Clarity" above

West Fork Carson River Hydrologic Unit

(Figure 3-7, Table 3-14)
The following additional water quality objectives apply to all surface waters of the West Fork Carson River Hydrologic Unit:

Algal Growth Potential: The mean of monthly mean of algal growth potential shall not be altered to the extent that such alterations are discernible at the 10 percent significance level.

Biostimulatory Substances: The concentrations of biostimulatory substances shall not be altered in an amount that could produce an increase in aquatic biomass to the extent that such increases in aquatic biomass are discernible at the 10 percent significance level.

Color: The color shall not exceed the 13 Platinum Cobalt Unit mean of monthly means (approximately equal to the State of Nevada standard of 13 Platinum Cobalt Unit sample mean).

Dissolved Oxygen: The dissolved oxygen concentration shall not be depressed by more than 10 percent, below 80 percent saturation or below 7.0 mg/L at any time, whichever is more restrictive.

pH: Changes in normal ambient pH levels shall not exceed 0.5 unit.

Sodium Adsorption Ratio (SAR): Water quality objectives for SAR are set to protect the irrigated agriculture component of the Agricultural Supply (AGR) beneficial use. SAR is calculated using the following equation, where Na = sodium ion concentration, Ca= calcium ion concentration, and Mg = magnesium ion concentration.

$$SAR = \frac{Na}{\sqrt{\frac{Ca + Mg}{2}}}$$

Concentrations of all chemical constituents in the equation above are expressed in milliequivalents per liter. As a ratio, SAR has no units.

The following water quality objective for SAR, as an annual average, applies to surface waters of the West Fork Carson River HU. Except as noted below, SAR objectives apply to the entire water body and its tributary surface waters in California.

Water Body SAR (Annual Average)

West Fork Carson River **1**

The Lahontan Regional Board recognizes that SAR may be higher than the value above in certain surface waters of the West Fork Carson River watershed due to natural sources of sodium, including geothermal sources. Where higher SAR values occur only as a result of natural sources, the affected water bodies or water body segments will not be considered to be in violation of the applicable SAR objective.

Species Composition: Species composition of the aquatic biota shall not be altered to the extent that such alterations are discernible at the 10 percent significance level.

Taste and Odor: The taste and odor shall not be altered.

Turbidity: The turbidity shall not be raised above a mean of monthly means value of 2 NTU. (This objective is approximately equal to the State of Nevada standard of 2 NTU annual mean.)

East Fork Carson River Hydrologic Unit

(Figure 3-7, Table 3-14)

The following additional water quality objective applies to all surface waters of the East Fork Carson River Hydrologic Unit

Sodium Adsorption Ratio (SAR): Water quality objectives for SAR are set to protect the irrigated agriculture component of the Agricultural Supply (AGR) beneficial use.

SAR is calculated using the following equation, where Na = sodium ion concentration, Ca= calcium ion concentration, and Mg = magnesium ion concentration.

$$SAR = \frac{Na}{\sqrt{\frac{Ca + Mg}{2}}}$$

Concentrations of all chemical constituents in the equation above are expressed in milliequivalents per liter. As a ratio, SAR has no units.

The following water quality objective for SAR, as an annual average, applies to surface waters of

the East Fork Carson River HU. Except as noted below, SAR objectives apply to the entire water body and its tributary surface waters in California.

Water Body SAR (Annual Average)

East Fork Carson River **2**

Bryant Creek **1**

The Lahontan Regional Board recognizes that SAR may be higher than the value above in certain surface waters of the East Fork Carson River watershed due to natural sources of sodium, including geothermal sources. Where higher SAR values occur only as a result of natural sources, the affected water bodies or water body segments will not be considered to be in violation of the applicable SAR objective.

(Figure 3-7, Table 3-14)
The following additional water quality objectives apply to all surface waters of the ***Indian Creek watershed***:

Algal Growth Potential: The mean of monthly mean of algal growth potential shall not be altered to the extent that such alterations are discernible at the 10 percent significance level.

Biostimulatory Substances: The concentrations of biostimulatory substances shall not be altered in an amount that could produce an increase in aquatic biomass to the extent that such increases in aquatic biomass are discernible at the 10 percent significance level.

Color: The color shall not exceed the 13 Platinum Cobalt Unit mean of monthly means (approximately equal to the State of Nevada standard of 13 Platinum Cobalt Unit sample mean).

Dissolved Oxygen: The dissolved oxygen concentration shall not be depressed by more than 10 percent, below 80 percent saturation, or below 7.0 mg/L at any time, whichever is more restrictive.

pH: Changes in normal ambient pH levels shall not exceed 0.5 unit.

Species Composition: Species composition shall not be altered to the extent that such alterations are discernible at the 10 percent significance level.

Taste and Odor: The taste and odor shall not be altered.

West Walker River Hydrologic Unit

(See Figure 3-8 and Table 3-15 for water quality objectives for the West Walker River HU.)

The following additional water quality objective applies to all surface waters of the West Walker River Hydrologic Unit

Sodium Adsorption Ratio (SAR): Water quality objectives for SAR are set to protect the irrigated agriculture component of the Agricultural Supply (AGR) beneficial use. SAR is calculated using the following equation, where Na = sodium ion concentration, Ca= calcium ion concentration, and Mg = magnesium ion concentration.

$$SAR = \frac{Na}{\sqrt{\frac{Ca + Mg}{2}}}$$

Concentrations of all chemical constituents in the equation above are expressed in milliequivalents per liter. As a ratio, SAR has no units.

The following water quality objectives for SAR, as an annual average, apply to surface waters of the West Walker River HU. Except as noted below, SAR objectives apply to the entire water body and its tributary surface waters in California.

Water Body SAR (Annual Average)

West Walker River **2**

Topaz Lake **2**

The Lahontan Regional Board recognizes that SAR may be higher than the value above in certain surface waters of the West Walker River watershed due to natural sources of sodium, including geothermal sources. Where higher SAR values occur only as a result of natural sources, the affected water bodies or water body segments will not be considered to be in violation of the applicable SAR objective.

East Walker River Hydrologic Unit

(See Figure 3-8 and Table 3-15 for water quality objectives for the East Walker River HU.)

The following additional water quality objective applies to all surface waters of the East Walker River Hydrologic Unit

Sodium Adsorption Ratio (SAR): Water quality objectives for SAR are set to protect the irrigated agriculture component of the Agricultural Supply (AGR) beneficial use. SAR is calculated using the following equation, where Na = sodium ion concentration, Ca= calcium ion concentration, and Mg = magnesium ion concentration.

$$SAR = \frac{Na}{\sqrt{\frac{Ca + Mg}{2}}}$$

Concentrations of all chemical constituents in the equation above are expressed in milliequivalents per liter. As a ratio, SAR has no units.

The following water quality objective for SAR, as an annual average, applies to surface waters of the West Walker River HU. Except as noted below, SAR objectives apply to the entire water body and its tributary surface waters in California.

Water Body SAR (Annual Average)
East Walker River **2**

The Lahontan Regional Board recognizes that SAR may be higher than the value above in certainsurface waters of the East Walker River watershed due to natural sources of sodium, including geothermal sources. Where higher SAR values occur only as a result of natural sources, the affected water bodies or water body segments will not be considered to be in violation of the applicable SAR objective.

Mono Hydrologic Unit

(See Figure 3-9 and Table 3-16 for water quality objectives for the Mono HU.)

Owens River Hydrologic Unit

(Figures 3-10 and 3-11, Tables 3-17 and 3-18)

The following additional water quality objectives apply to all surface waters of the ***Pine Creek watershed*** (Figure 3-11):

Ammonia, Un-ionized: The discharge of wastes shall not cause concentrations of un-ionized ammonia (NH_3^o) to exceed 0.01 mg/L (as NH_3^o) in receiving waters.

Settleable Material: The concentration of settleable material shall not be raised by more than 0.2 milliliter per liter (maximum), and by no more than an average of 0.1 milliliter per liter during any 30-day period.

Antelope Hydrologic Unit

(Figures 3-12 and 3-12a, Tables 3-19, 3-19a, and 3-19b.)

The following additional water quality objectives apply to Amargosa Creek downstream of the Los Angeles County Sanitation District No. 14 discharge point, and to the Piute Ponds and associated wetlands. The regionwide ammonia objective applies to all other surface waters of the Antelope Hydrologic Unit. (Note: the regionwide ammonia objective is derived from the USEPA's 1985 freshwater ammonia criteria, and emphasizes un-ionized ammonia. The objective below is derived from the USEPA's 1999 freshwater criteria for total ammonia.)

Ammonia, Total

The acute (1hour) ammonia toxicity limits are dependent on pH, and the chronic (30-day) limits are dependent on pH and temperature. Concentrations of total ammonia in lower Amargosa Creek and the Piute Ponds and wetlands, expressed "as Nitrogen" or "as N," shall not exceed the acute and chronic limits listed for the corresponding temperature and pH conditions in Tables 3-19a and 3-19b more often than once every three years, on the average**.** In addition, the highest four-day average concentration of total ammonia within the 30-day period shall not exceed 2.5 times the chronic toxicity limit.

The values in Table 3-19a are the USEPA's 1999 freshwater acute ammonia criteria for waters with salmonids (salmon and trout) absent and fish early life stages present. The values in Table 3-19b are the chronic ammonia criteria for waters with fish early life stages present. Salmonids are not present in lower Amargosa Creek and the Piute Ponds and wetlands. Early life stages of several warmwater fish species are present.

For temperature and pH values not explicitly in Table 3-19a and Table 3-19b, the most conservative ammonia value neighboring the actual value may be used, or the acute and chronic ammonia limits for waters with salmonids absent and chronic ammonia limits for waters with fish early life stages present can be calculated from the following formulas from the USEPA's 1999 freshwater ammonia criteria document. In these equations, T = temperature in ◦ C, and pH (the measure of acidity or alkalinity) is expressed in standard units.

Acute Toxicity. The formula for the acute toxicity limit (1-hour average) for total ammonia nitrogen (in mg N/L), for waters with salmonids absent, is:

$$\boldsymbol{Acute\ Limit} = \frac{\mathbf{0.411}}{\mathbf{1 + 10^{7.204 - pH}}} + \frac{\mathbf{58.4}}{\mathbf{1 + 10^{pH - 7.204}}}$$

Chronic Toxicity. The formula for the chronic toxicity limit (30-day average) for total ammonia nitrogen (in mg N/L), for waters with fish early life stages present is:

$$\textit{Chronic Limit} = \left(\frac{0.0577}{1+10^{7.688-pH}}+\frac{2.487}{1+10^{pH-7.688}}\right) * MIN(2.85, 1.45 * 10^{0.028*(25-T)})$$

In the equation above, "MIN" means that the calculation should use either 2.85 or the number resulting from the second expression, whichever is lower.

Temperature and pH measurements. If receiving water samples are obtained over a period of time during which pH and/or temperature is not constant, the pH, temperature, and the concentration of total ammonia in each sample should be determined. For each sample, the toxicity limit should be determined at the pH and temperature of the sample, and then the concentration of total ammonia nitrogen in the sample should be divided by the limit to determine a quotient. The acute or chronic toxicity objective is attained if the mean of the quotients is less than 1 over the duration of the averaging period.

Mojave Hydrologic Unit

(See Figures 3-13 and 3-14, and Tables 3-20 and 3-21, for water quality objectives for the Mojave HU.)

Water Quality Objectives for Fisheries Management Activities Using the Fish Toxicant Rotenone

Rotenone is a fish toxicant presently used by the California Department of Fish and Wildlife (DFW) and the United States Fish and Wildlife Service (USFWS) for fishery management purposes. (See Chapter 4 for a more complete discussion of this topic.)

The application of rotenone and the detoxification agent potassium permanganate can cause several water quality objectives to be temporarily exceeded, both inside and outside of project boundaries. (Project boundaries are defined as encompassing the treatment area, the detoxification area, and the area downstream of the detoxification station up to a thirty-minute travel time.)

The Basin Plan (see Chapter 4) contains prohibitions against discharges of waste that result in violation of narrative or numeric water quality objectives. Conditional exemptions to these prohibitions may be granted by the Regional Board or its Executive Officer, if so delegated, for rotenone applications by the DFW or USFWS, provided that such projects comply with the conditions described below and with the criteria described in Chapter 4 under the section entitled "Exemption Criteria for Fisheries Management." The following project-specific water quality objectives of receiving water limitations also apply to fisheries management projects using rotenone during and immediately following treatment.

Color

The characteristic purple discoloration resulting from the discharge of potassium permanganate shall not be discernible more than two miles downstream of project boundaries at any time. Twenty-four (24) hours after shutdown of the detoxification operation, no color alteration(s) resulting from the discharge of potassium permanganate shall be discernible within or downstream of project boundaries.

Chemical Constituents

Chemical residues resulting from rotenone treatment must not exceed the following limitations:

1. The concentration of naphthalene outside of project boundaries shall not exceed 25 µg/liter (ppb) at any time.

2. The concentration of rotenone, rotenolone, trichloroethylene (TCE), xylene, or acetone (or potential trace contaminants such as benzene or ethylbenzene) outside of project boundaries shall not exceed the detection levels for these respective compounds at any time. "Detection level" is defined as the minimum level that can be reasonably detected using state-of-the-art equipment and methodology.

3. After a two-week period has elapsed from the date that rotenone application was completed, no chemical residues resulting from the treatment shall be present at detectable levels within or downstream of project boundaries.

4. No chemical residues resulting from rotenone treatments shall exceed detection levels in ground water at any time.

Toxicity

Chemical residues resulting from rotenone treatment must not exceed the limitations listed above for chemical constituents.

Water Quality Objectives for Ground Water

(See also section 4.6, "Ground Water Protection and Management")

Water quality objectives for ground waters are divided into the two categories of:

1. **Water Quality Objectives That Apply to All Ground Waters.** Listed alphabetically below, these narrative and numerical water quality objectives apply to **all** ground waters within the Lahontan Region:

   Bacteria, Coliform
   Chemical Constituents
   Radioactivity
   Taste and Odor

2. **Water Quality Objectives For Specific Ground Water Basins.** Certain numerical and narrative water quality objectives are directed toward protection of specific ground water basins. These ground water basins are listed below by ground water basin name within the Lahontan Region, in a north to south direction:

   Honey Lake Valley
   Truckee River and Little Truckee River HUs
   Carson Valley
   Mojave River Valley

Water Quality Objectives That Apply to All Ground Waters

Bacteria, Coliform

In ground waters designated as MUN, the median concentration of coliform organisms over any seven-day period shall be less than 1.1/100 milliliters.

Chemical Constituents

Ground waters designated as MUN shall not contain concentrations of chemical constituents in excess of the maximum contaminant level (MCL) or secondary maximum contaminant level (SMCL) based upon drinking water standards specified in the following provisions of Title 22 of the California Code of Regulations, which are incorporated by reference into this plan: Table 64431-A of Section 64431 (Inorganic Chemicals), Table 64431-B of Section 64431 (Fluoride), Table 64444-A of Section 64444 (Organic Chemicals), Table 64449-A of Section 64449 (Secondary Maximum Contaminant Levels-Consumer Acceptance Limits), and Table 64449-B of Section 64449 (Secondary Maximum Contaminant Levels-Ranges). This incorporation-by-reference is prospective including future changes to the incorporated provisions as the changes take effect.

Waters designated as AGR shall not contain concentrations of chemical constituents in amounts that adversely affect the water for beneficial uses (i.e., agricultural purposes).

Ground waters shall not contain concentrations of chemical constituents that adversely affect the water for beneficial uses.

Radioactivity

Ground waters designated as MUN shall not contain concentrations of radionuclides in excess of the limits specified in Table 4 of Section 64443 (Radioactivity) of Title 22 of the California Code of Regulations, which is incorporated by reference into this plan. This incorporation-by-reference is prospective including future changes to the incorporated provisions as the changes take effect.

Taste and Odor

Ground waters shall not contain taste or odor-producing substances in concentrations that cause nuisance or that adversely affect beneficial uses. For ground waters designated as MUN, at a minimum, concentrations shall not exceed adopted secondary maximum contaminant levels specified in Table 64449-A of Section 64449 (Secondary Maximum Contaminant Levels-Consumer Acceptance Limits), and Table 64449-B of Section 64449 (Secondary Maximum Contaminant Levels-Ranges) of Title 22 of the California Code of Regulations, which is incorporated by reference into this plan. This incorporation-by-reference is prospective including future changes to the incorporated provisions as the changes take effect.

Water Quality Objectives For Certain Ground Water Basins

Honey Lake Valley Basin

For ground waters under the **Eagle Drainage Hydrologic Area** (Figure 3-2), the taste and odor shall not be altered.

Truckee River and Little Truckee River HUs

For ground waters under the **Little Truckee River Hydrologic Unit** (Figure 3-4), the taste and odor shall not be altered.

For ground waters under the **Truckee River Hydrologic Unit** (Figure 3-5), the taste and odor shall not be altered.

Carson Valley Basin

For ground waters under the **Indian Creek Watershed** (Figure 3-7), the taste and odor shall not be altered.

For ground waters under the **West Fork Carson River Hydrologic Unit** (Figure 3-7), the taste and odor shall not be altered.

Mojave River Valley Basin

For certain ground waters under the Mojave Hydrologic Unit, see water quality objectives for total dissolved solids and nitrate in Table 3-20 and on Figure 3-13.

General Direction Regarding Compliance With Objectives

This section includes general direction on determining compliance with the narrative and numerical objectives described in this Chapter. (Specific direction on compliance with certain objectives is included, in italics, following the text of the objective.) It is not feasible to cover all circumstances and conditions that could be created by all discharges. Therefore, it is within the discretion of the Regional Board to establish other, or additional, direction on compliance with objectives of this Plan. Where more than one objective is applicable, the **stricter objective shall apply**. (The only exception is where a regionwide objective has been superseded by the adoption of a site-specific objective by the Regional Board.) Where objectives are not specifically designated, downstream objectives apply to upstream tributaries.

Antidegradation Policy

To implement State Board Resolution No. 68-16, the "Statement of Policy with Respect to Maintaining High Quality Waters in California," the Regional Board follows guidance such as that in the USEPA's 1993 *Water Quality Standards Handbook* and the State Board's October 7, 1987 legal memorandum titled "Federal Antidegradation Policy" (Attwater 1987). The State Board has interpreted the Resolution No. 68-16 to incorporate the federal antidegradation policy in order to ensure consistency with federal Clean Water Act requirements (see State Board Order No. WQ 86-17, pages 16-24). For detailed information on the federal antidegradation policy, see USEPA Region IX's *Guidance on Implementing the Antidegradation Provisions of 40 CFR 131.12* and USEPA's *Questions and Answers on Antidegradation*. The Regional Board's procedures for implementation of State and federal antidegradation policies are summarized below. It is important to note that the federal policy applies only to surface waters, while the State policy applies to both surface and ground waters.

Under the State Antidegradation Policy, whenever the existing quality of water is better than that needed to protect all existing and probable future beneficial uses, the existing high quality shall be maintained until or unless it has been demonstrated to the State that any change in water quality will be consistent with the maximum benefit of the people of the State, and will not unreasonably affect present and probable future beneficial uses of such water. Therefore, unless these conditions are met, background water quality concentrations (the concentrations of substances in natural waters that are unaffected by waste management practices or contamination incidents) are appropriate water quality goals to be maintained. If it is determined that some degradation is in the best interest of the people of California, some increase in pollutant level may be appropriate. However, in no case may such increases cause adverse impacts to existing or probable future beneficial uses of waters of the State.

Where the federal antidegradation policy applies, it does not absolutely prohibit any changes in water quality. The policy requires that any reductions in water quality be consistent with the three-part test established by the policy, as described below.

Part One-Instream Uses
[40 CFR § 131.12(a)(1)]

The first part of the test establishes that "existing instream water uses and the level of water quality necessary to protect the existing uses shall be maintained and protected." Reductions in water quality should not be permitted if the change in water quality would seriously harm any species found in the water (other than an aberrational species). Waters of this type are generally referred to as "Tier I" waters.

Part Two-Public Interest Balancing
[40 CFR § 131.12(a)(2)]

The second part of the test applies where water quality is higher than necessary to protect existing instream beneficial uses. This part of the test allows reductions in water quality if the state finds "that allowing lower water quality is necessary to accommodate important economic or social development in the area in which the waters are located" **and** existing beneficial uses are protected. Waters of this type are generally referred to as "Tier II" waters.

Part Three-Outstanding National Resource Waters (ONRWs) [40 CFR § 131.12(a)(3)]

The third part of the test established by the federal policy requires that the water quality of the waters that constitute an outstanding national resource be maintained and protected. No permanent or long-term reduction in water quality is allowable in areas given special protection as Outstanding National Resource Waters (48 Fed. Reg. 51402). Waters that potentially could qualify for ONRW designation are generally classified as "Tier III" waters.

Examples of such waters include, but are not limited to, waters of National and State Parks and wildlife refuges, waters of exceptional recreational or ecological significance, and state and federally designated wild and scenic rivers. To date, the only California waters designated as ONRWs are Lake Tahoe and Mono Lake. However, other California waters would certainly qualify.

ONRWs may be designated as part of adoption or amendment of water quality control plans. It is important to note that even if no formal designation has been made, lowering of water quality should not be allowed for waters that, because of their exceptional recreational and/or ecological significance, should be given the special protection assigned to ONRWs.

Narrative and Numerical Objectives

The sections below provide additional direction on determining compliance with the narrative and numerical objectives of this Basin Plan.

Pollution and/or Nuisance

In determining compliance with narrative objectives that include the terms "pollution" and or "nuisance," the Regional Board considers the following definitions from the Porter-Cologne Water Quality Control Act.

Pollution -- an alteration of the waters of the State by waste to the degree that unreasonably affects either of the following:

- such waters for beneficial uses.
- facilities that serve these beneficial uses.

"Pollution" may include "contamination." Contamination means an impairment of the quality of the waters of the State by waste to a degree that creates a hazard to the public health through poisoning or through the spread of disease. Contamination includes any equivalent effect resulting from the disposal of waste, whether or not waters of the State are affected.

Nuisance -- Anything that meets all of the following requirements:

- Is injurious to health, or is indecent or offensive to the senses, or an obstruction to the free use of property, so as to interfere with the comfortable enjoyment of life or property.
- Affects at the same time an entire community or neighborhood, or any considerable number of persons, although the extent of the annoyance or damage inflicted upon individuals may be unequal.
- Occurs during or as a result of the treatment or disposal of wastes.

References to Taste and Odor, Human Health and Toxicity (also see "acute toxicity" and "chronic toxicity," below)

In determining compliance with objectives including references to Taste and Odor, Human Health or Toxicity, the Regional Board will consider as evidence relevant and scientifically valid water quality goals from sources such as drinking water standards from the California Department of Public Health (State "Action Levels"), the National Interim Drinking Water Standards, Proposition 65 Lawful Levels, National Ambient Water Quality Criteria, the National Academy of Sciences' Suggested No-Adverse-Response Levels (SNARLs), USEPA's Health and Water Quality Advisories, USEPA's National Toxicity Rule and California Toxicity Rule, as well as other relevant and scientifically valid evidence.

References to Agriculture or AGR designations

In determining compliance with objectives including references to the AGR designated use, the Regional Board will refer to water quality goals and recommendations from sources such as the Food and Agriculture Organization of the United Nations, University of California Cooperative Extension, Committee of Experts, and McKee and Wolf's "Water Quality Criteria" (1963).

References to "Natural High Quality Waters"

The Regional Board generally considers "natural high quality water(s)" to be those waters with ambient water quality equal to, or better than, current drinking water standards. However, the Regional Board also recognizes that some waters with poor chemical quality may support important ecosystems (e.g., Mono Lake).

References to "10 Percent Significance Level"

A statistical hypothesis is a statement about a random variable's probability distribution, and a decision-making procedure about such a statement is a hypothesis test. In testing a hypothesis concerning the value of a population mean, the null hypothesis is often used. The null hypothesis is that there is no difference between the population means (e.g., the mean value of a water quality parameter after the discharge is no different than before the discharge.) First, a level of significance to be used in the test is specified, and then the regions of acceptance and rejection for evaluating the obtained sample mean are determined.

At the **10 percent significance level**, assuming normal distribution, the acceptance region (where one would correctly accept the null hypothesis) is the interval that lies under 90 percent of the area of the standard normal curve. Thus, a level of **significance of 10 percent** signifies that when the population mean is correct as specified, the sample mean will fall in the areas of rejection only 10 percent of the time.

If the hypothesis is rejected when it should be accepted, a Type I error has been made. In choosing a **10 percent level of significance**, there are 10 chances in 100 that a Type I error was made, or the hypothesis was rejected when it should have been accepted (i.e., one is 90 percent *confident* that the right decision was made.)

The **10 percent significance level** is often incorrectly referred to as the 90 percent significance level. As explained above, the significance level of a test should be low, and the confidence level of a confidence interval should be high.

References to "Means" (e.g., annual mean, log mean, mean of monthly means), "Medians" and "90th Percentile Values"

"Mean" is the arithmetic mean of all data. **"Annual mean"** is the arithmetic mean of all data collected in a one-year period. **"Mean of monthly means"** is the arithmetic mean of 30-day averages (arithmetic means). A logarithmic or **"log mean"** (used in determining compliance with bacteria objectives) is calculated by converting each data point into its log, then calculating the mean of these values, then taking the anti-log of this log transformed average. The **median** is the value that half of the values of the population exceed and half do not. The **average value** is the arithmetic mean of all data. For a **90th percentile value**, only 10% of data exceed this value.

Compliance determinations shall be based on available analyses for the time interval associated with the discharge. If only one sample is collected during the time period associated with the water quality objective, (e.g., monthly mean), that sample shall serve to characterize the discharge for the entire interval. Compliance based upon multiple samples shall be determined through the application of appropriate statistical methods.

Standard Analytical Methods to Determine Compliance with Objectives

Analytical methods to be used are usually specified in the monitoring requirements of the waste discharge permits. Suitable analytical methods are:

- those specified in 40 CFR Part 136, and/or
- those methods determined by the Regional Board and approved by the USEPA to be equally or more sensitive than 40 CFR Part 136 methods and appropriate for the sample matrix, and/or
- where methods are not specified in 40 CFR Part 136, those methods determined by the Regional Board to be appropriate for the sample matrix

All analytical data shall be reported uncensored with method detection limits and either practical quantitation levels or limits of quantitation identified. Acceptance of data should be based on demonstrated laboratory performance.

For **bacterial analyses**, sample dilutions should be performed so the range of values extends from 2 to 16,000. The detection method used for each analysis shall be reported with the results of the analysis. Detection methods used for coliforms (total and fecal) shall be those presented in *Standard Methods for the Examination of Water and Wastewater* (American Public Health Association et al.), or any alternative method determined by the Regional Board to be appropriate.

For **acute toxicity**, compliance shall be determined by short-term toxicity tests on undiluted effluent using an established protocol (e.g., American Society for Testing and Materials [ASTM], American Public Health Association, USEPA, State Board).

For **chronic toxicity**, compliance shall be determined using the critical life stage (CLS) toxicity tests. At least three approved species shall be used to measure compliance with the toxicity

objective. If possible, test species shall include a vertebrate, an invertebrate, and an aquatic plant. After an initial screening period, monitoring may be reduced to the most sensitive species. Dilution and control waters should be obtained from an unaffected area of the receiving waters. For rivers and streams, dilution water should be obtained immediately upstream of the discharge. Standard dilution water can be used if the above sources exhibit toxicity greater than 1.0 Chronic Toxicity Units. All test results shall be reported to the Regional Board in accordance with the "Standardized Reporting Requirements for Monitoring Chronic Toxicity" (State Board Publication No. 93-2 WQ).

Application of Narrative and Numerical Water Quality Objectives to Wetlands

Although not developed specifically for wetlands, many surface water **narrative objectives** are generally applicable to most wetland types. However, the Regional Board recognizes, as with other types of surface waters such as saline or alkaline lakes, that natural water quality characteristics of some wetlands may not be within the range for which the narrative objectives were developed. The Regional Board will consider site-specific adjustments to the objectives for wetlands (bacteria, pH, hardness, salinity, temperature, or other parameters) as necessary on a case-by-case basis.

The **numerical criteria** to protect one or more beneficial uses of surface waters, where appropriate, may directly apply to wetlands. For example, wetlands that actually are, or that recharge, municipal water supplies should meet human health criteria. The USEPA numeric criteria for protection of freshwater aquatic life, although not developed specifically for wetlands, are generally applicable to most wetland types. As with other types of surface waters, such as saline or alkaline lakes, natural water quality characteristics of some wetlands may not be within the range for which the criteria were developed. Adjustments for pH, hardness, salinity, temperature, or other parameters may be necessary. The Regional Board will consider developing site-specific objectives for wetlands on a case-by-case basis.

Variances from Water Quality Objectives

The USEPA allows states to grant variances from water quality standards under the narrow circumstances summarized below. Such variances must be "built into" the standards themselves, and thus variances cannot be granted in California without Basin Plan amendments.

According to the USEPA, variances from standards "are both discharger and pollutant specific, are time-limited, and do not forego the currently designated use." The USEPA recommends use of variances instead of removal of beneficial uses when the State believes that standards can ultimately be attained. Variances can be used with NPDES permits to ensure reasonable progress toward attainment of standards without violation of Clean Water Act Section 402(a)(1), which requires NPDES permits to meet applicable water quality standards.

The USEPA "has approved State-adopted variances in the past and will continue to do so if:

- each individual variance is included as part of the water quality standard;
- the State demonstrates that meeting the standard is unattainable based on one or more of the grounds outlined in 40 CFR 131.10 (g) for removing a designated use;
- the justification submitted by the State includes documentation that treatment more advanced than that required by sections 303(c)(2)(A) and (B) has been carefully considered, and that alternative effluent control strategies have been evaluated;
- the more stringent State criterion is maintained and is binding upon all other dischargers on the stream or stream segment;
- the discharger who is given a variance for one particular constituent is required to meet the applicable criteria for other constituents;
- the variance is granted for a specific period of time and must be rejustified upon expiration but at least every three years (Note: the 3-year limit is derived from the triennial review requirements of section 303(c) of the Act.);
- the discharger either must meet the standard upon the expiration of this time period or must make a new demonstration of "unattainability";
- reasonable progress is being made toward meeting the standards; and
- the variance was subjected to public notice, opportunity for comment, and public hearing. (See section 303(c)(1) and 40 CFR 131.20.) The public notice should contain a clear description of the impact of the variance upon

> achieving water quality standards in the affected stream segment."

(The "section" references in the quoted language above are to the Clean Water Act. As used in this language, "criteria" and "criterion" are equivalent to California's "water quality objective[s]".)

Table 3-1
ONE-HOUR AVERAGE CONCENTRATION FOR AMMONIA[1,2]

Waters Designated as COLD, COLD with SPWN, COLD with MIGR (Salmonids or other sensitive coldwater species present)

	Temperature, C						
pH	0	5	10	15	20	25	30
Un-ionized Ammonia (mg/liter NH_3)							
6.50	0.0091	0.0129	0.0182	0.026	0.036	0.036	0.036
6.75	0.0149	0.021	0.030	0.042	0.059	0.059	0.059
7.00	0.023	0.033	0.046	0.066	0.093	0.093	0.093
7.25	0.034	0.048	0.068	0.095	0.135	0.135	0.135
7.50	0.045	0.064	0.091	0.128	0.181	0.181	0.181
7.75	0.056	0.080	0.113	0.159	0.22	0.22	0.22
8.00	0.065	0.092	0.130	0.184	0.26	0.26	0.26
8.25	0.065	0.092	0.130	0.184	0.26	0.26	0.26
8.50	0.065	0.092	0.130	0.184	0.26	0.26	0.26
8.75	0.065	0.092	0.130	0.184	0.26	0.26	0.26
9.00	0.065	0.092	0.130	0.184	0.26	0.26	0.26
Total Ammonia (mg/liter NH_3)							
6.50	35	33	31	30	29	20	14.3
6.75	32	30	28	27	27	18.6	13.2
7.00	28	26	25	24	23	16.4	11.6
7.25	23	22	20	19.7	19.2	13.4	9.5
7.50	17.4	16.3	15.5	14.9	14.6	10.2	7.3
7.75	12.2	11.4	10.9	10.5	10.3	7.2	5.2
8.00	8.0	7.5	7.1	6.9	6.8	4.8	3.5
8.25	4.5	4.2	4.1	4.0	3.9	2.8	2.1
8.50	2.6	2.4	2.3	2.3	2.3	1.71	1.28
8.75	1.47	1.40	1.37	1.38	1.42	1.07	0.83
9.00	0.86	0.83	0.83	0.86	0.91	0.72	0.58

[1] To convert these values to mg/liter N, multiply by 0.822

[2] Source: U. S. Environmental Protection Agency. 1986. Quality criteria for water, 1986. EPA 440/5-86-001.

Table 3-2
ONE-HOUR AVERAGE CONCENTRATION FOR AMMONIA[1,2]

Waters designated WARM, WARM with SPWN, WARM with MIGR (Salmonids or other sensitive coldwater species absent)[3]

	Temperature, °C						
pH	0	5	10	15	20	25	30
Un-ionized Ammonia (mg/liter NH_3)							
6.50	0.0091	0.0129	0.0182	0.026	0.036	0.051	0.051
6.75	0.0149	0.021	0.030	0.042	0.059	0.084	0.084
7.00	0.023	0.033	0.046	0.066	0.093	0.131	0.093
7.25	0.034	0.048	0.068	0.095	0.135	0.190	0.190
7.50	0.045	0.064	0.091	0.128	0.181	0.26	0.26
7.75	0.056	0.080	0.113	0.159	0.22	0.32	0.32
8.00	0.065	0.092	0.130	0.184	0.26	0.37	0.37
8.25	0.065	0.092	0.130	0.184	0.26	0.37	0.37
8.50	0.065	0.092	0.130	0.184	0.26	0.37	0.37
8.75	0.065	0.092	0.130	0.184	0.26	0.37	0.37
9.00	0.065	0.092	0.130	0.184	0.26	0.37	0.37
Total Ammonia (mg/liter NH_3)							
6.50	35	33	31	30	29	29	20
6.75	32	30	28	27	27	26	18.6
7.00	28	26	25	24	23	23	16.4
7.25	23	22	20	19.7	19.2	19.0	13.5
7.50	17.4	16.3	15.5	14.9	14.6	14.5	10.3
7.75	12.2	11.4	10.9	10.5	10.3	10.2	7.3
8.00	8.0	7.5	7.1	6.9	6.8	6.8	4.9
8.25	4.5	4.2	4.1	4.0	3.9	4.0	2.9
8.50	2.6	2.4	2.3	2.3	2.3	2.4	1.81
8.75	1.47	1.40	1.37	1.38	1.42	1.52	1.18
9.00	0.86	0.83	0.83	0.86	0.91	1.01	0.82

[1] To convert these values to mg/liter, multiply by 0.822

[2] Source: U. S. Environmental Protection Agency. 1986. Quality criteria for water, 1986. EPA 440/5-86-001.

[3] These values may be conservative, however, if a more refined criterion is desired, USEPA recommends a site-specific criteria modification.

Table 3-3
FOUR DAY AVERAGE CONCENTRATION FOR AMMONIA[1,2]

Waters Designated as COLD, COLD with SPWN, COLD with MIGR (Salmonids or other sensitive coldwater species present)

	Temperature, °C						
pH	0	5	10	15	20	25	30
Un-ionized Ammonia (mg/liter NH_3)							
6.50	0.0008	0.0011	0.0016	0.0022	0.0022	0.0022	0.0022
6.75	0.0014	0.0020	0.0028	0.0039	0.0039	0.0039	0.0039
7.00	0.0025	0.0035	0.0049	0.0070	0.0070	0.0070	0.0070
7.25	0.0044	0.0062	0.0088	0.0124	0.0124	0.0124	0.0124
7.50	0.0078	0.0111	0.0156	0.022	0.022	0.022	0.022
7.75	0.0129	0.0182	0.026	0.036	0.036	0.036	0.036
8.00	0.0149	0.021	0.030	0.042	0.042	0.042	0.042
8.25	0.0149	0.021	0.030	0.042	0.042	0.042	0.042
8.50	0.0149	0.021	0.030	0.042	0.042	0.042	0.042
8.75	0.0149	0.021	0.030	0.042	0.042	0.042	0.042
9.00	0.0149	0.021	0.030	0.042	0.042	0.042	0.042
Total Ammonia (mg/liter NH_3)							
6.50	3.0	2.8	2.7	2.5	1.76	1.23	0.87
6.75	3.0	2.8	2.7	2.6	1.76	1.23	0.87
7.00	3.0	2.8	2.7	2.6	1.76	1.23	0.87
7.25	3.0	2.8	2.7	2.6	1.77	1.24	0.88
7.50	3.0	2.8	2.7	2.6	1.78	1.25	0.89
7.75	2.8	2.6	2.5	2.4	1.66	1.17	0.84
8.00	1.82	1.70	1.62	1.57	1.10	0.78	0.56
8.25	1.03	0.97	0.93	0.90	0.64	0.46	0.33
8.50	0.58	0.55	0.53	0.53	0.38	0.28	0.21
8.75	0.34	0.32	0.31	0.31	0.23	0.173	0.135
9.00	0.195	0.189	0.189	0.195	0.148	0.116	0.094

[1] To convert these values to mg/liter N, multiply by 0.822.

[2] Source: U. S. Environmental Protection Agency. 1992. Revised tables for determining average freshwater ammonia concentrations. USEPA Office of Water Memorandum, July 30, 1992.

Table 3-4
FOUR DAY AVERAGE CONCENTRATION FOR AMMONIA[1,2]

Waters designated WARM, WARM with SPWN, WARM with MIGR (Salmonids or other sensitive coldwater species absent)[3]

	Temperature, °C						
pH	0	5	10	15	20	25	30
Un-ionized Ammonia (mg/liter NH_3)							
6.50	0.0008	0.0011	0.0016	0.0022	0.0031	0.0031	0.0031
6.75	0.0014	0.0020	0.0028	0.0039	0.0055	0.0055	0.0055
7.00	0.0025	0.0035	0.0049	0.0070	0.0099	0.0099	0.0099
7.25	0.0044	0.0062	0.0088	0.0124	0.0175	0.0175	0.0175
7.00	0.0078	0.0111	0.0156	0.022	0.031	0031	0.031
7.75	0.0129	0.0182	0.026	0.036	0.051	0.051	0.051
8.00	0.0149	0.021	0.030	0.042	0.059	0.059	0.059
8.25	0.0149	0.021	0.030	0.042	0.059	0.059	0.059
8.50	0.0149	0.021	0.030	0.042	0.059	0.059	0.059
8.75	0.0149	0.021	0.030	0.042	0.059	0.059	0.059
9.00	0.0149	0.021	0.030	0.042	0.059	0.059	0.059
Total Ammonia (mg/liter NH_3)							
6.50	3.0	2.8	2.7	2.5	2.5	1.73	1.23
6.75	3.0	2.8	2.7	2.6	2.5	1.74	1.23
7.00	3.0	2.8	2.7	2.6	2.5	1.74	1.23
7.25	3.0	2.8	2.7	2.6	2.5	1.75	1.24
7.50	3.0	2.8	2.7	2.6	2.5	1.76	1.25
7.75	2.8	2.6	2.5	2.4	2.3	1.65	1.18
8.00	1.82	1.70	1.62	1.57	1.55	1.10	0.79
8.25	1.03	0.97	0.93	0.90	0.90	0.64	0.47
8.50	0.58	0.55	0.53	0.53	0.53	0.39	0.29
8.75	0.34	0.32	0.31	0.31	0.32	0.24	0.190
9.00	0.195	0.189	0.189	0.195	0.21	0.163	0.133

[1] To convert these values to mg/liter N, multiply by 0.822.

[2] Source: U. S. Environmental Protection Agency. 1992. Revised tables for determining average freshwater ammonia concentrations. USEPA Office of Water Memorandum, July 30, 1992.

[3] These values may be conservative, however, if a more refined criterion is desired, USEPA recommends a site-specific criteria modification.